DISSERTATION

THE PALLADIUM-CATALYZED ASYMMETRIC SYNTHESIS OF 4'-DISUBSTITUTED NUCLEOSIDE ANALOGS AND STUDIES TOWARDS THE TOTAL SYNTHESIS OF PLAKEVULIN A

Submitted by

Katherine L. Hervert

Department of Chemistry

In partial fulfillment of the requirements

For the Degree of Doctor of Philosophy

Colorado State University

Fort Collins, Colorado

Summer 2004

COLORADO STATE UNIVERSITY

July 6, 2004

WE HEREBY RECOMMEND THAT THE DISSERTATION PREPARED UNDER OUR SUPERVISION BY KATHERINE LEIGH HERVERT ENTITLED THE PALLADIUM-CATALYZED ASYMMETRIC SYNTHESIS OF 4'-DISUBSTITUTED NUCLEOSIDE ANALOGS AND STUDIES TOWARDS THE TOTAL SYNTHESIS OF PLAKEVULIN A BE ACCEPTED AS FULFILLING IN PART REQUIREMENTS FOR THE DEGREE OF DOCTOR OF PHILOSOPHY.

Committee on Graduate Work

Peter K. Dorhout

Ellen R. Fisher

Julia M. Inamine

Alan J. Kennan

Louis S. Hegedus / Advisor

Anthony K. Rappé / Department Head / Director

ABSTRACT OF DISSERTATION

THE PALLADIUM-CATALYZED ASYMMETRIC SYNTHESIS OF 4'-DISUBSTITUTED NUCLEOSIDE ANALOGS AND STUDIES TOWARDS THE TOTAL SYNTHESIS OF PLAKEVULIN A

4'-Substituted nucleoside analogues have been synthesized using palladium-catalyzed asymmetric allylic amination conditions. A kinetic discrimination between the diastereomeric lactol acetates afforded the desired aminated products and recovered α-acetate in high yields and <97:3 diastereoselectivity. Epimerization of the recovered lactol acetate produced a 60:40 α:β mixture which could be resubjected, in principle, to the palladium-catalyzed asymmetric allylic amination conditions.

Studies were conducted towards an enone intermediate for synthesis of plakevulin A. Progress was hindered by the discovery that the wrong regioisomer was obtained from a Lewis acid catalyzed sulfur ylide ring expansion reaction. NMR spectroscopy was utilized for a comparative analysis between model systems for structure elucidation of the product from the $BF_3 \bullet OEt_2$ catalyzed ethyl diazoacetate ring expansion reaction.

Katherine Leigh Hervert
Chemistry Department
Colorado State University
Fort Collins, CO 80523
Summer 2004

TABLE OF CONTENTS

LIST OF ABBREVIATIONS

AIBN	azobisisobutyronitrile
BOMCl	benzyloxymethyl chloride
BSA	N,O bis(trimethylsilyl)acetamide
Bz	benzoyl
COSY	correlation spectroscopy referring to the homonuclear proton-proton correlation
DBA	dibenzylidene acetone
DIBAL-H	diisobutyl aluminum hydride
DMDO	dimethyl dioxirane
DI	deionized
DMAP	4-dimethylamino pyridine
DME	1,2-dimethoxy ethane
DMF	N,N-dimethylformamide
dppe	diphenylphosphino ethane
dppf	1,1-bis(diphenylphosphino)ferrocene
EDA	ethyl diazoacetate
exact mass	calculations are based on the exact mass of only the most abundant isotopes for each element
FAB-HRMS	Fast Atom Bombardment-High Resolution Mass Spectrometry referring to the use of a Cs ion gun and can also be called FIB-HRMS

FCC	flash column chromatography
HMQC	Heteronuclear Multiple Quantum Coherence
HMPA	hexamethyl phosphoramide
m-CPBA	*meta*-chloro peroxybenzoic acid
IC_{50}	50% inhibitory concentration
KHMDS	potassium hexamethyldisilazane
LDA	lithium diisopropyl amide
MOM	methoxymethyl chloride
Ms	mesylate
molecular weight	calculations are based on the average of the exact masses for all naturally occurring isotopes weighted by their percent abundance for each element
NBS	N-bromosuccinimide
NFSI	*N*-fluorobenzenesulfonimide
NMO	N-methyl morpholine N-oxide
NMR	Nuclear Magnetic Resonance
PCC	Pyridinium chloro chromate
PMB	Paramethoxy benzyl
Rochelle's Salt	saturated, aqueous sodium potassium tartrate
SM	starting material
TBAF	tetrabutylammonium fluoride
TBDPS	*tert*-butyldiphenylsilane
Tf	trifluoromethyl sulfonate
TMS	trimethylsilyl
TsCl	4-methyl benzenesulfonyl chloride

ACKNOWLEDGEMENTS

I would like to thank the boss, Dr. Hegedus, for supporting me both financially and emotionally for the past five years. It would have been a more difficult road without an advisor who could follow my thought process, no matter how far in left field I sometimes might be. Past and present Hegedus group members also deserve a deal of gratitude, for without their help, I would have not have gained the authority and confidence that I have acquired through my years here. I would like to thank my friends and family who have been there for me since the beginning. Finally, I would like to thank Dr. Nathan Schnarr and his family who have been there to remind me of what I am capable of accomplishing and to calm down and relax once in a while, for everything is going to be all right.

PREFACE

Complex molecule synthesis in organic chemistry is an important area of research for scientists in both academia and the pharmaceutical industry. The need for innovative strategies in the synthesis of new biologically active compounds remains constant as new viruses and bacteria are encountered. These investigations allow for the development of new methodologies which can be applied towards new analogs for new classes of compounds. The first chapter of this thesis describes the investigations into the well-established palladium-catalyzed allylic alkylation reaction that was modified for the diastereoselective synthesis of compounds for potential HIV treatment. The second chapter of this thesis illustrates the studies towards the total synthesis of plakevulin A, as a DNA polymerase inhibitor.

The treatment for HIV, the virus that causes AIDS, has come a long way since its discovery in the mid-1980's, however, we are still far from any conceivable cure. Modern treatments focus on improving the condition and life expectancy of the patients with HIV while minimizing the detrimental side effects. Unfortunately, this virus exhibits considerable drug resistance, prompting an even greater need for the development of AIDS treatments. Nucleoside analogs have demonstrated success in the treatment of HIV cases; however, the perpetual virus mutations have made once effective analogs futile which has prompted investigations for new compounds. The synthesis of

several new nucleoside analogs is presented in the first chapter of this thesis. 4'-Disubstituted nucleoside analogs have been obtained through the use of a highly selective palladium-catalyzed allylic alkylation reaction involving a diastereomeric mixture of acetates with nucleoside bases. The diastereoselective manner in which the nucleoside base is attached is important due to an increase in biological activity demonstrated when in the β-position [chapter 1, ref. 5]. The 4'-substituent can greatly influence the HIV inhibitory activity and toxicity against retroviruses [chapter1, ref. 5], thus making the nucleoside analogs synthesized in this project of significant synthetic interest.

The attempts towards synthesis of plakevulin A are presented in the second chapter of this thesis. Plakevulin A has exhibited inhibitory activity against DNA polymerases α and γ. The initial synthetic route to plakevulin A was designed to be relatively straightforward, readily yielding the desired material in only a few steps. This chapter presents the intricacies associated with total synthesis. Quite often, when a particular outcome is highly desired, one can overlook subtle or sometimes glaring evidence against the observed result. In this work, the ring expansion step proved to be extremely challenging, providing an undesired product on every occasion. This however, is part of the research process and hopefully future obstacles may be avoided through careful scrutiny of the acquired data.

CHAPTER ONE

THE ASYMMETRIC SYNTHESIS OF 4'-ETHOXY-2', 3'-DIDEHYDRO-2', 3'-DIDEOXYNUCLEOSIDES BY PALLADIUM-CATALYZED KINETIC DISCRIMINATION BETWEEN DIASTEREOISOMERIC LACTOL ACETATES

I. Introduction and Background

Investigation into novel treatments for viral diseases has increased dramatically since the explosion in cases of human immunodeficiency virus (HIV), herpes simplex virus (HSV) and human papillomavirus (HPV). This epidemic has pushed scientists to improve the current treatments for these diseases, including the modification of proven antiretroviral agents such as nucleoside analogs. New nucleoside analogs can allow the modern AIDS patient to experience improvements in their condition and an increased life expectancy without substantial detrimental side effects. Unfortunately, the emergence of drug-resistant viruses can make certain drugs ineffective which has prompted an even greater need for the development of new nucleoside analogs.

Nucleoside analogs structurally resemble natural nucleosides which are vital components in the management and transfer of genetic information for virtually all biological processes.[1] The natural nucleoside's intimate involvement at the cellular level makes them ideal candidates for the investigation of analogs

which can disrupt antiviral activity. Nucleosides undergo phosphorylation at the 5′ position to produce the corresponding nucleotides (Figure 1.1). Once phosphorylated, nucleotides can become potent agents against retroviral diseases and have demonstrated significant antitumor, anticancer, and antifungal activity.[1] Structural variation through modifications to the ring structure and/or nucleoside base can modify the biological activity and stability of these nucleoside analogs.

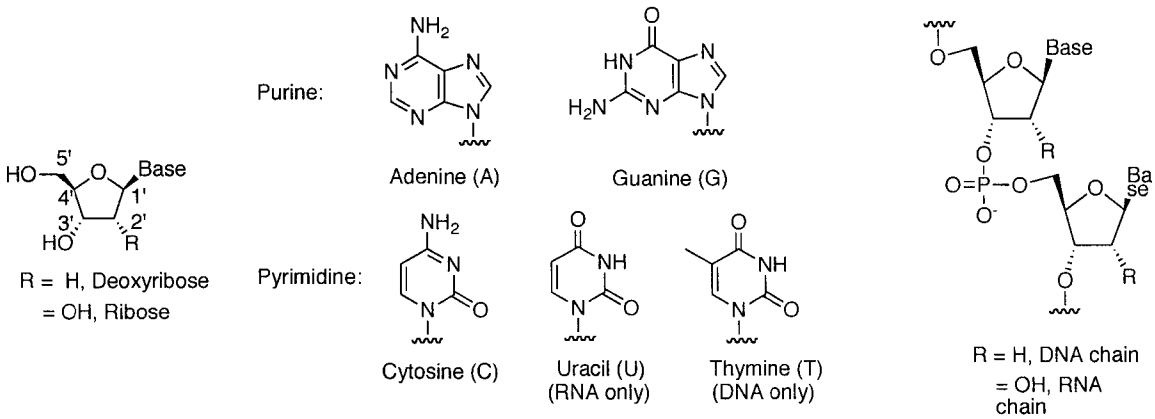

Figure 1.1 Natural Nucleosides

Several nucleoside analogs have been utilized in the treatment of retroviral diseases. C-BVDU (**3**) contains an altered nucleoside base which has aided in its effectiveness against herpes simplex virus (HSV). The removal or replacement of unnatural substituents at the 2′-, 3-′, and 4′- positions can increase their drug efficacy. Also, the furanose oxygen of the nucleoside core can be replaced with a methylene group to produce a carbocyclic nucleoside analog. The furanose oxygen weakens the 1′ N-C bond facilitating its cleavage by phosphorylases and hydrolases. Thus, some carbocyclic nucleoside analogs have demonstrated an increased metabolic stability compared to their oxygen-containing counterparts.[2]

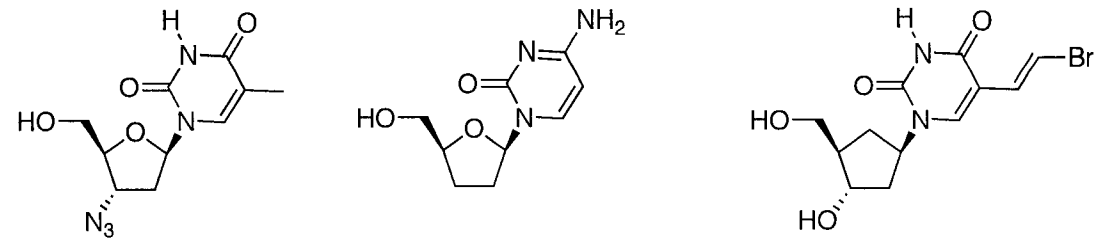

3'-Azido-3'-deoxythymidine
AZT (**1**)

2', 3'-Dideoxycytidine
ddC (**2**)

(E)-5-(2-Bromovinyl)-2'-deoxyuridine
C-BVDU (**3**)

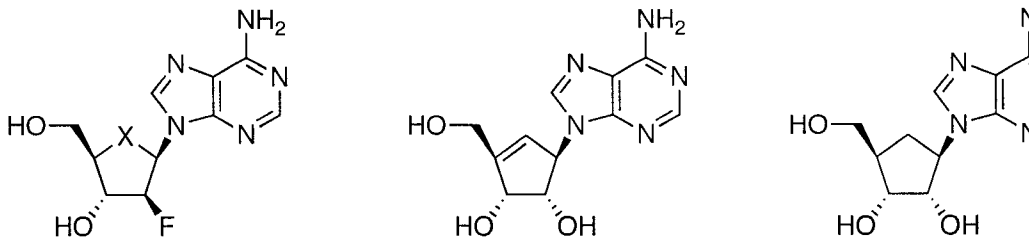

4: X = CH_2
5: X = O

Neplanocin A (**6**)

Aristeromycin (**7**)

Figure 1.2 Synthetic Nucleoside Analogs.

In 1983, scientists discovered that AIDS is caused by a retrovirus, which spawned immediate searches for antiviral agents. The first successful candidate was the nucleoside analog, AZT.[3] Retroviral infections begin with the incorporation of the virus into the host cell. Once the cell is penetrated, the viral RNA is reverse transcribed into a double-stranded DNA copy. AZT is incorporated into the growing viral DNA strand and acts as a chain terminator because it lacks the required 3'-hydroxyl group needed for chain elongation. The reverse transcriptase enzyme recognizes the phosphorylated AZT (AZT-TP) in place of the normal nucleotide triphosphate, deoxythymidine TP (dTTP) (Figure 1.3). Initial clinical studies showed that AZT was effective for the treatment of advanced stages of HIV, however the benefits were not permanent. After a year

or two of treatment, the patient's condition began to decline due to the development of drug-resistant viruses.

Mechanism of AZT incorporation into viral DNA

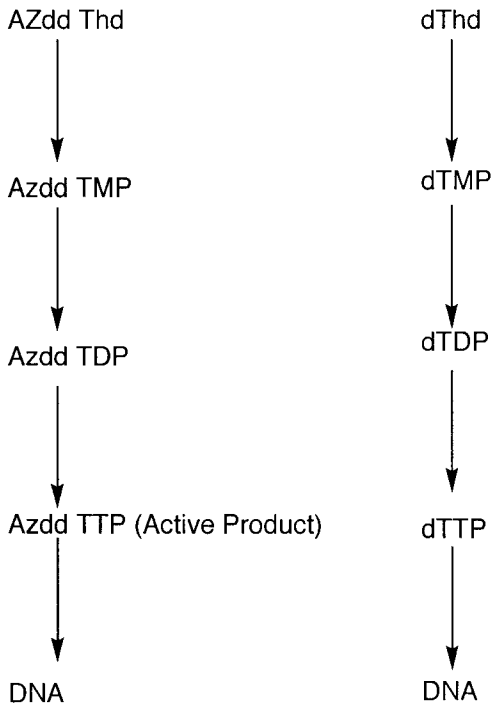

1. The triphosphate form of AZT is incorporated into the elongating nucleic acid by HIV reverse transcriptase. This incorporation blocks further elongation and causes DNA chain termination

2. The monophosphate dorm of AZT may block deoxythymidine kinase and decrease the production of normal dTTP or may block ribonuclease of the reverse transcriptase

Figure 1.3 The path of AZT incorporation into viral DNA

Investigations into effective nucleoside analogs led to the synthesis of 4'-disubstituted nucleoside analogs for antiretroviral treatments (**8-12**). Several nucleoside analogs in this class have demonstrated anti-HIV activity.[4,5] However, contrary to the traditional nucleoside analogs that act as chain terminators, the 3'-hydroxyl group is required for the biological activity of 4'-disubstituted

nucleoside analogues[6, 7, 8] This would suggest their mode of action would be inhibition of the reverse transcriptase enzyme

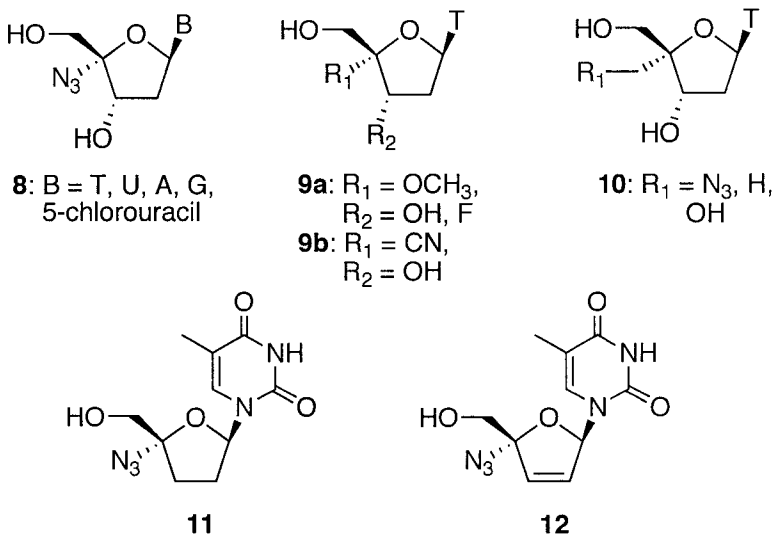

Figure 1.4 Synthetic 4'-Nucleoside Analogs.

In 1993, Prisbe and coworkers classified the structure-activity relationships among HIV inhibitory 4'-substituted nucleosides.[20] They found that in order to retain good biological activity, the 4'-substituted nucleoside must be a 2'-deoxy-β-D-*erythro* derivative. If these conditions are met, then none of the modifications to the nucleoside base result in a dramatic loss of activity. The 4'-substituent can greatly influence the HIV inhibitory activity and toxicity, which are roughly parallel (Figure 1.5).

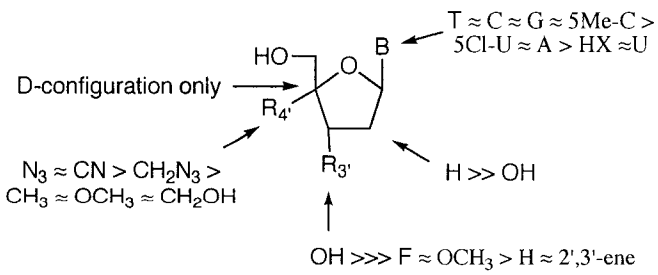

Figure 1.5 Structure/Activity Relationships of 4'-Disubstituted Nucleoside Analogs.

Traditionally, 4'-disubstituted nucleosides have been synthesized from existing nucleosides[9, 10, 11, 12] or carbohydrates[13, 14, 15, 16, 17] (Figure 1.6). These methods make it difficult to control the configuration at the 4'-position and are limited by the availability of naturally occurring starting materials. When non-nucleoside or carbohydrates are used to synthesize nucleoside analogs, the addition of the nucleoside base in a diastereoselective manner has proven to be a major synthetic challenge.

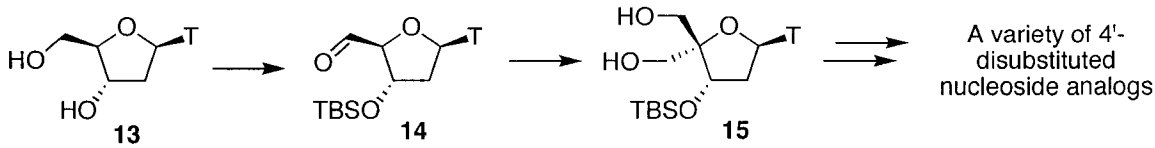

Figure 1.6 Traditional 4' -disubstituted nucleoside analog syntheses from natural nucleosides

Utilizing carbohydrates or other non-nucleoside substrates as the framework for 4'-disubstituted nucleoside analogs can make the addition of the nucleoside bases problematic because of the glycosidic bond formation. A traditional method for the addition of a nucleoside base is the Vorbrüggen coupling.[15] A Lewis acid is used to ionize compounds to form an oxonium ion, which upon addition of a silylated nucleoside bases, forms the glycosidic bond (Scheme 1.1). The silylated nucleoside base can be formed *in situ* or isolated as a silylated derivative to aid in its solubility in organic solvents.

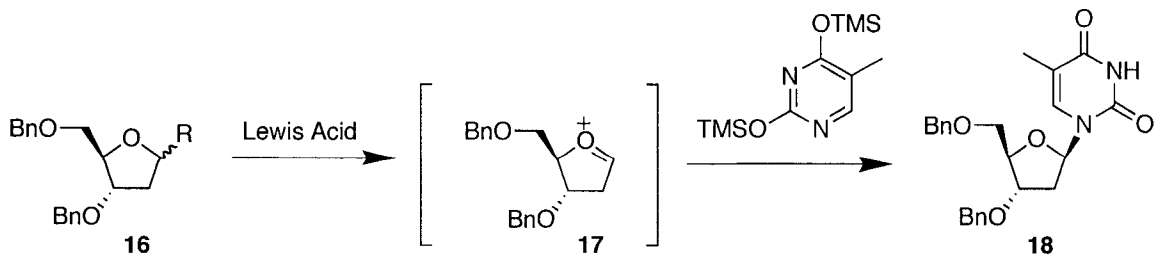

Scheme 1.1 R = Leaving group = Br, Cl, OAc, OCO_2Me, OBz, OTs, OMs, etc.

The Vorbrüggen coupling has been successful in the diastereoselective formation of only the β-anomer in selective nucleoside syntheses due to neighboring group participation. This occurs through the formation of the 1, 2-acyl oxonium species that effectively blocks the α-face of the sugar, producing only the β-anomer (Scheme 1.2).[18] In the synthesis of 2′-deoxy-, 2′, 3′-dideoxy-, and 2′, 3′-dideoxydidehydronucleoside analogs, Vorbrüggen coupling is nonselective, giving a 1:1 mixture of α:β anomers.

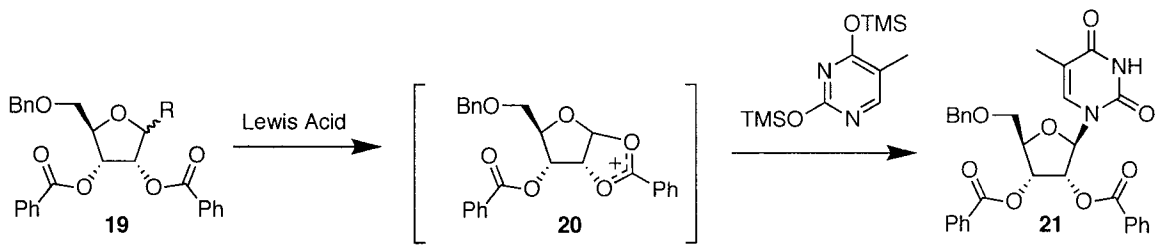

Scheme 1.2 R = Leaving group = Br, Cl, OAc, OCO_2Me, OBz, OTs, OMs, etc.

The use of palladium-assisted addition of nucleoside bases has become a powerful tool for nucleoside analog synthesis. The palladium (0)-catalyzed allylic alkylation of nucleophiles, the Tsuji-Trost reaction, is a powerful and versatile procedure for this transformation.[19] In 1988, Trost et al. reported the first example of direct substitution of a heterocyclic base on a carbocycle through a palladium-catalyzed substitution in the racemic synthesis of aristeromycin.[20] Monoepoxide **22** was an excellent substrate for palladium-catalyzed allylic alkylation by the nucleoside base, adenine, with $Pd(OAc)_2$ and $P(OiPr)_3$. Dihydroxylation and further elaboration of the aminated product produced (±)-aristeromycin in good yield (Scheme 1.3).[20]

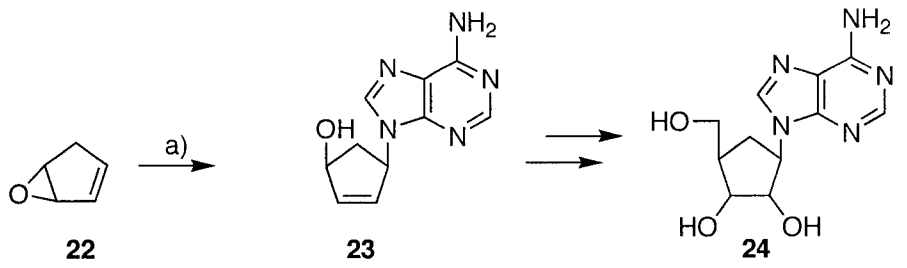

22 23 24

Scheme 1.3 (a) $Pd(OAc)_2$, 6 mol%(i-$C_3H_7O)_3P$, 1.2 mol%, n-C_4H_9Li, 1 equiv. of adenine, 1:1 THF/DMSO, 0°C to room temperature, 67%.

The mechanism of the palladium-catalyzed allylic alkylation reaction begins with initial complexation of the metal to the olefin (**26**).[21] Oxidative addition of the palladium species displaces the leaving group in an S_N2 type fashion to give an η^1-allylpalladium (II) with inversion of stereochemistry. The σ-complex is in equilibrium with an η^3-allylpalladium intermediate. Nucleophilic attack on the π–allylpalladium complex can occur at the less hindered terminus on the opposite face of the metal complex. Decomplexation of the metal regenerates palladium (0) and gives the substituted products. The palladium-catalyzed allylic alkylation reaction proceeds with a net retention of configuration and has proven to be a useful component in many organic syntheses.

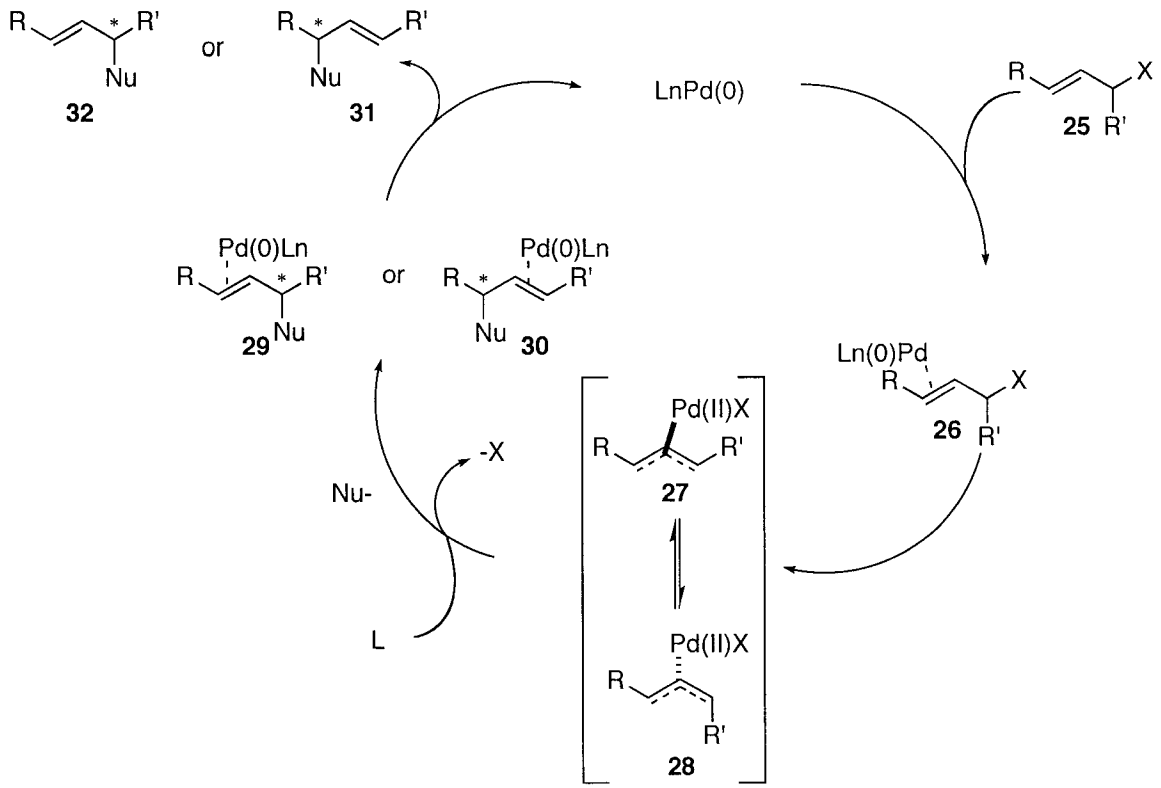

Scheme 1.4 The mechanism of the palladium catalyzed allylic alkylation reaction.

The use of chiral ligands has facilitated the introduction of asymmetry into the transition metal-catalyzed allylic alkylation reactions.[22] Trost and Shi demonstrated a facile synthesis of both the *l*-and *d*-enantiomeric series of nucleosides, depending on which chiral ligand was used with meso compound, *cis*-2, 5-diacyloxy-2, 5-dihydrofuran, **38**.[23] The differentiation between the prochiral leaving groups on **38**, furnished either enantiomeric product **41** or **42**. This desymmetrization of meso compound **38** through the use of Pd(0)-catalyzed reactions with chiral ligands efficiently produced L-nucleosides in 18% overall yield.

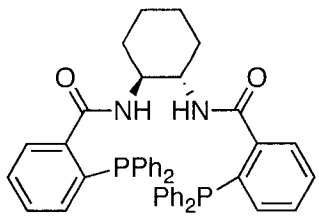

33

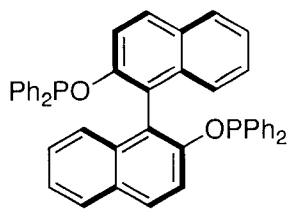

34

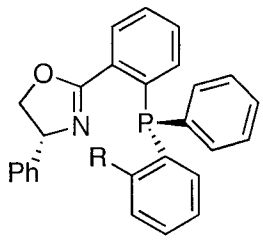

35

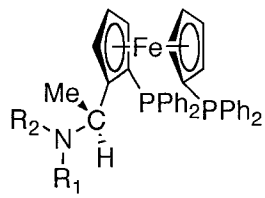

36 $R_1 = (CH_2)_4OH$, $R_2 = -(CH_2)_5$
37 $R_1 = Me$, $R_2 = CH(CH_2OH)_2$

Figure 1.7 Chiral ligands used in allylic alkylation reactions

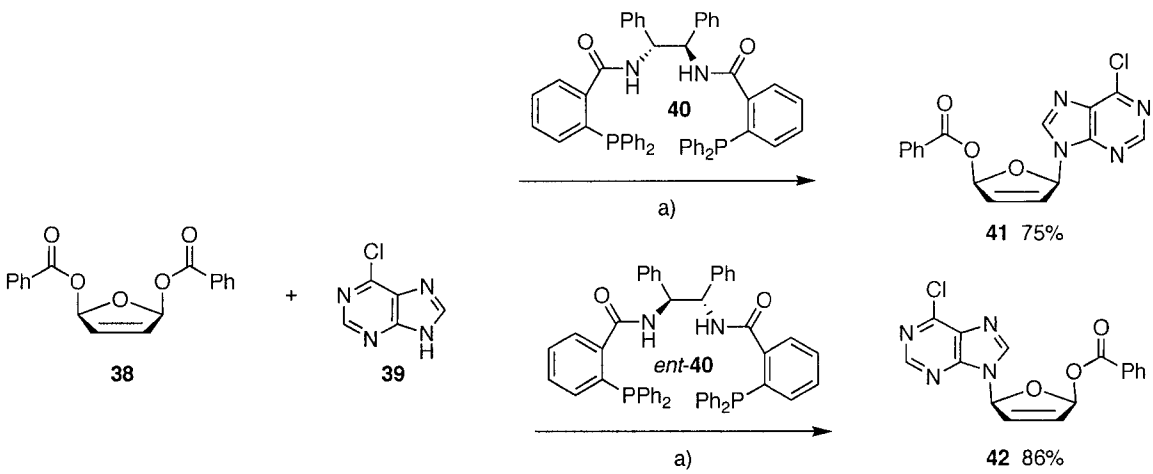

Scheme 1.5 1.1:1 ratio of **38:39**, $(C_3H_5)_3N$, THF, 2% **40** or *ent*-**40**, rt.

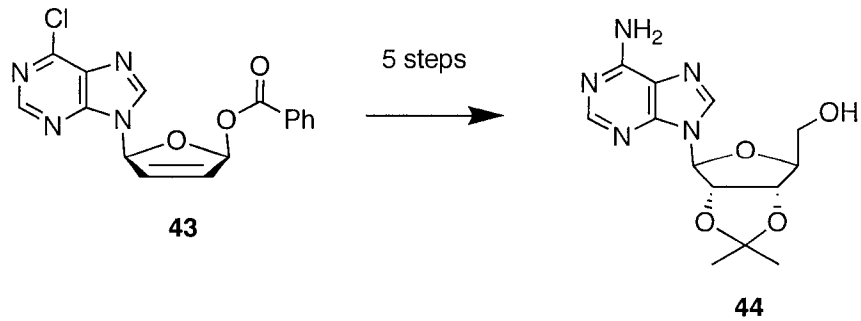

Scheme 1.6

Unfortunately, there are few examples of palladium-catalyzed allylic alkylation of 4-carboxybutenolides or 5-acyloxy-2(5H)-furanones. These compounds possess the allylic leaving group in the aldehyde oxidation state (Scheme 1.7). Trost has extensively studied allylic geminal dicarboxylates (acylals) as substrates for palladium-catalyzed nucleophilc attack and has obtained high asymmetric induction.[24] These are special cases in that the reacting allylic terminus is in the aldehyde oxidation state and bears two enantiotopic leaving groups.

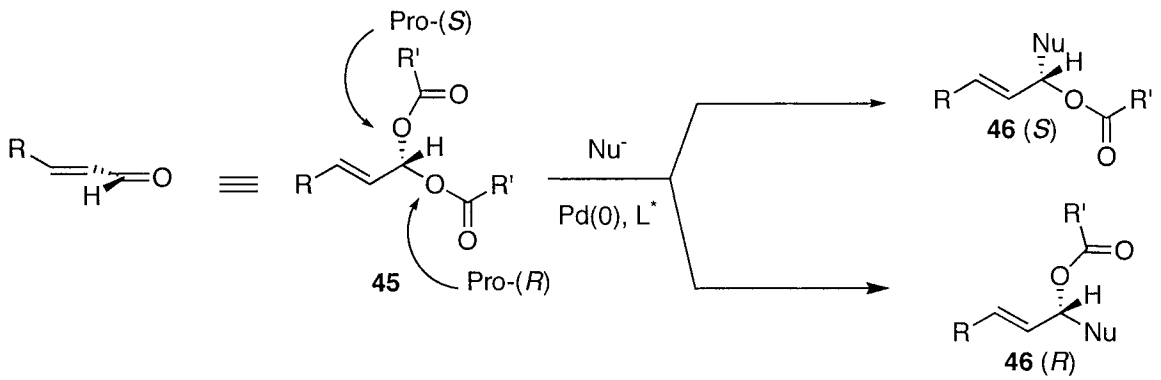

Scheme 1.7

Paquette has utilized the palladium-catalyzed allylic alkylation with lactol-acetate **47**.[25] Coupling of **47** with 6-chloropurine in the presence of $Pd_2(dba)_3$•$CHCl_3$, triphenylphosphine and triethylamine produced a 1:5 mixture of **48** and **49**. Elaboration of the protected nucleoside analog produced a variety of 4′-spirocyclic didehydrodideoxy nucleosides.

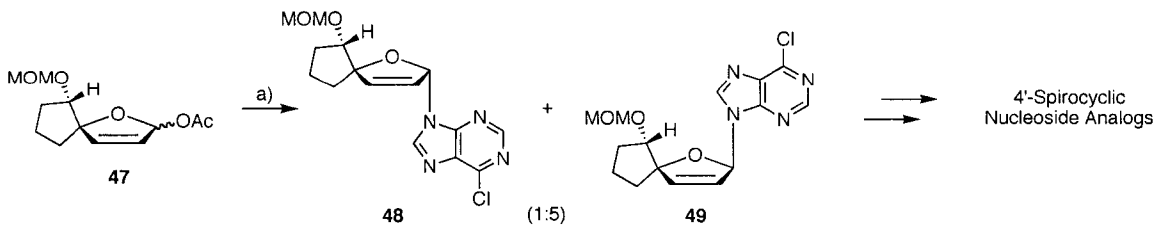

Scheme 1.8 a) Pd_2dba_3•$CHCl_3$, Ph_3P, Et_3N, THF 50%

Many 4′-disubstituted nucleoside analog syntheses use existing nucleosides or carbohydrates as the starting material. An influential paper published in 1959 by Schaffer first reported a mixed aldol reaction followed by a Cannizzaro reduction to synthesize 4′-bis(hydroxymethyl) ribose in 75% yield.[26] This reaction between aldehyde **50**, formaldehyde and aqueous sodium hydroxide has been utilized in many 4′-substituted nucleoside analog syntheses. Leland and Youssefyeh finished the synthesis by acetolysis of the 4′-bis(hydroxymethyl) ribose and coupling with a nucleoside base.[16, 17]

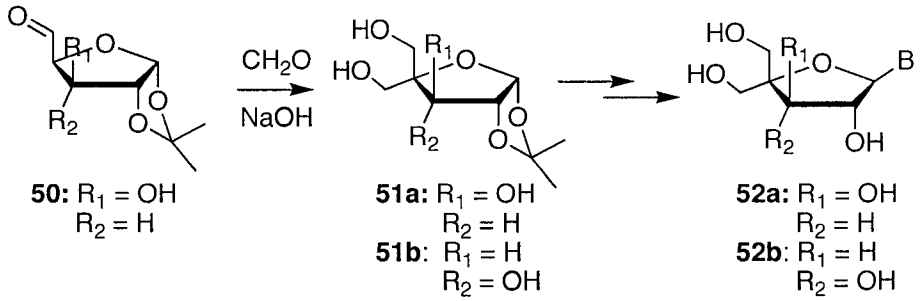

Scheme 1.9 B = adenine, 6-methoxyadenine, 6-methylthioadenine, 5-fluorouridine-6-aza-2-thiouracil, and 1,2,3-triazole-3-carboxamide

In 2003 Marx utilized this 4′-bis(hydroxymethyl) ribose core for the synthesis of 4′-alkylated nucleoside analogs to investigate the effects of steric demand of the 4′-substitutent.[27] Alcohol **53** was hydrogenated with Pd/C in the presence of Et_3N and subsequent cleavage of the silyl ethers produced the 4′-*C*-methylthymidine in good yield. An isopropyl group was successfully added to ketone **56** by means of a Wittig reaction and desilylation and hydrogenation of the aliphatic double bond.

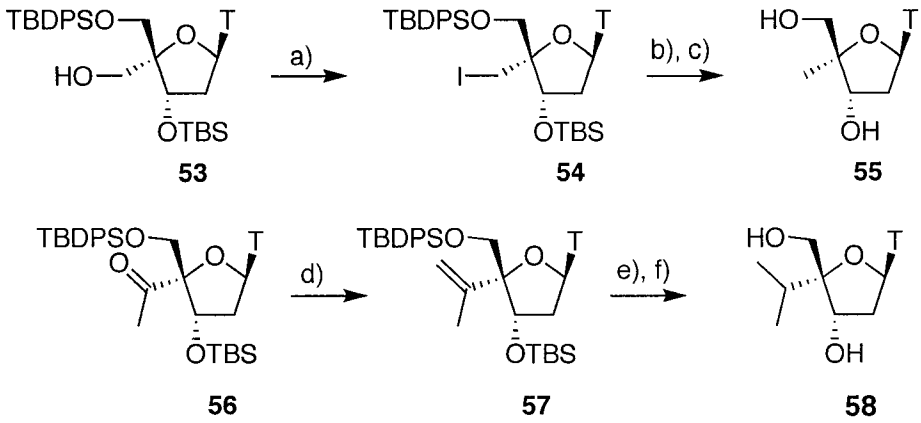

Scheme 1.10 (a) Ph_3P, I_2, imidazole, C_6H_6, 50°C, 85%; (b) Pd/C, H_2, EtOH, EtOAc, NEt_3; (c) TBAF, THF, 81% (over two steps); (d) CH_3PPh_3Br, *t*-BuOK, THF, 91%; (c) TBAF, THF; (d) Pd/C, H_2, CH_3OH, 99% (over two steps)

Secrist utilized a 5′-aldehyde nucleoside which enabled facile formation of 4′, 5′-enamine through alkylation with allyl halides (Scheme 1.11).[28] Alkylation of 4′, 5′-enamine at nitrogen followed by an aza-Claisen rearrangement produced the imine which was hydrolyzed to produce 4′-substituted aldehyde **62**. The newly installed olefin can easily be manipulated to yield protected 4'-disubstituted nucleosides **63** as shown.

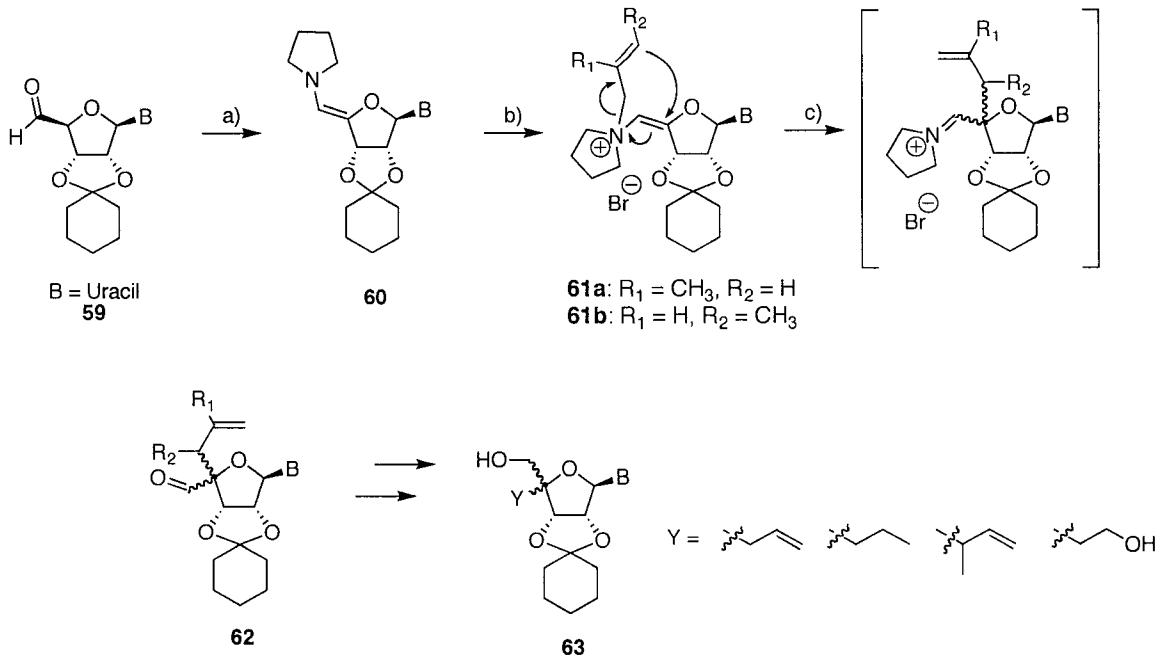

Scheme 1.11 (a) pyrrolidine, 1:1 benzene:acetonitrile, 50 °C, quant. yield; (b) allyl bromide, methylallyl bromide or crotyl bromide, 80 °C; (c) 80 °C, then aq. H^+.

In 2003, Haraguchi utilized the ring opening of 4′, 5′-epoxynucleosides with organosilicon reagents.[29] 3′-*O*-TBDMS-4′, 5′-unsaturated thymidine **64** was treated with an acetone solution of dimethyl dioxirane (DMDO) in CH_2Cl_2 at –30°C to produce 4′, 5′-epoxythymidine **65** as a single isomer. Reaction of the epoxythymidine product with (2-bromoallyl)trimethylsilane with $SnCl_4$ produced product **66** in 42% yield. Other organosilane reagents were used then the $SnCl_4$ assisted ring opening of the epoxynucleosides to produce the cyano, cyclopenten-3-yl, and allyl nucleoside analogs.[30]

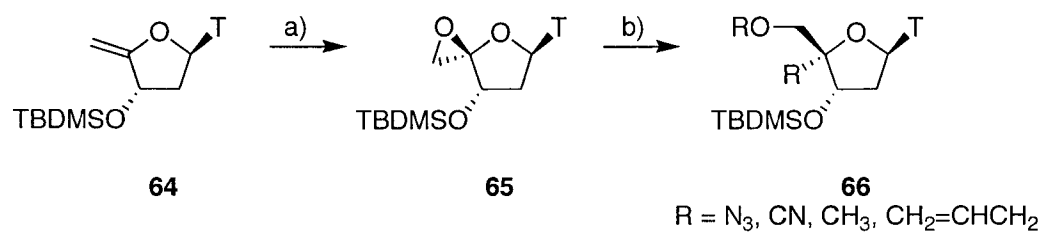

Scheme 1.12 (a) DMDO, CH_2Cl_2, -30°C; (b) Me_3Al (3 eq.), CH_2Cl_2, -30°C, 2 h.

Jung has reported the synthesis of 4′-disubstituted nucleoside analogs through an electrophilic addition to 5′-esters.[31] Treatment of nucleoside **67** with excess LDA, *tert*-butyllithium then an electrophile afforded the 4′-disubstituted product. The trapping can occur stereoselectively from either the α- or β-face depending on the electrophile. Phenylselenium chloride, allyl bromide and *N*-fluorobenzenesulfonimide (NFSI) predominantly gave the β-anomers.

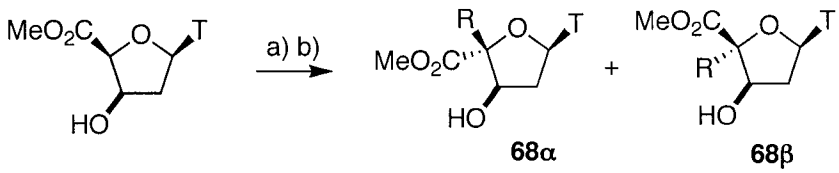

67	R-X =	PhSeCl	**a** 62%	(9.3:1)
		Me-I	**b** 22%	(7.3:1
		Allyl-Br	**c** 58%	(8.7:1)
		NFSI	**d** 30%	(1:0)

Scheme 1.13 a) LDA, *t*BuLi b) R-X

De novo syntheses of 4′-disubstituted nucleoside analogues provide a greater degree of flexibility with respect to functionality and stereochemistry, producing both L- and D-nucleosides quite easily. Unfortunately, there are few *de novo* syntheses of 4′-disubstituted nucleoside analogues with variety in the substitutents at the 4′ position.

Crich began his *de novo* synthesis of methyl 5-*O*-benzyl-3-*O*-*tert*-butyldimethylsilyl-4α-methoxycarbonyl-2-deoxyribofuranoside from dimethyl *L*-tartrate (Scheme 1.14).[32] The dimethyl ester was converted to monoalkylated **71** by protection of the diol and addition of BOMCl to the enolate. DIBAL-H reduction of one dimethyl ester group followed by homologation using standard Wittig chemistry gave enol ether **73** as a separable 1:1 mixture of *E:Z* isomers. Treatment of **73** with methanolic mercuric acetate followed by borohydride

reduction produced acetal **74** which was readily hydrolyzed to ribofuranose **75**. Vorbrüggen coupling with several nucleoside bases gave protected 4'-carboxylic methyl ester nucleoside analogs as α:β mixtures.

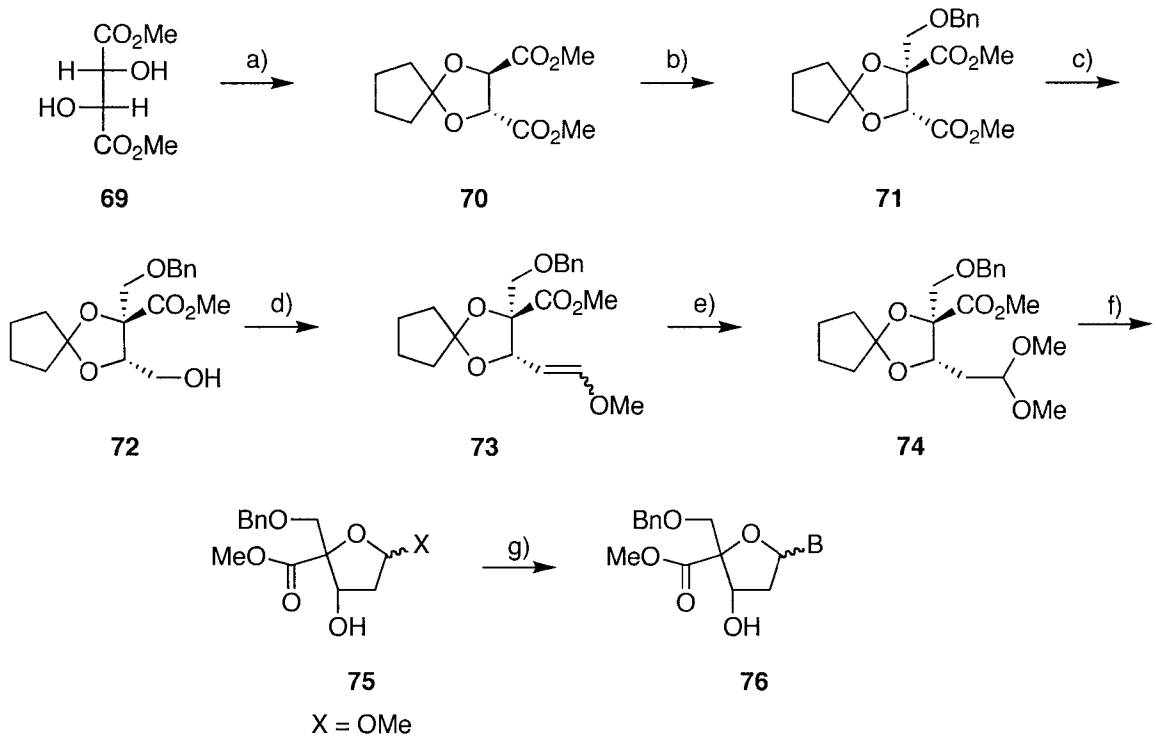

Scheme 1.14 Crich's Synthesis. a) cyclopentanone dimethyl acetal, TsOH, 90% yield; b) 1. LDA, THF/HMPA 2. BOMCl, 60% yield; c) 1. DIBAL-H, d) 1. Swern Ox., 60% yield; 2. $Ph_3P^+CH_2OMe$, LDA, 62% yield; e) 1. $Hg(OAc)_2$, MeOH 2. $NaBH_4$, 85% yield; f) 1. 3N HCl; 2. TsOH, MeOH, 85% yield over 2 steps; (h) TBDMSOTf, 96%; (i) nucleoside base, $SnCl_4$, MeCN, 40-90% yield. (B = Thymine, 4-*N*-Ac-C, 2-*N*-Ac-G, 6-*N*-BzA

Dulcere utilized a chemo- and regioselective cohalogenation of 1-*N*-vinylpyrimidinediones using *N*-bromosuccinimide in the presence of variously substituted propargylic alcohols.[33] Treatment of **77** with NBS in the presence of propargyl alcohols **78** and **81** respectively led to the β-bromo propargyl ethers **79** and **82**. Tri-*n*-butyltin hydride and AIBN promoted a radical carbocylization in the 5-*exo*-digonal mode to afford **80** and **83** in good yields.

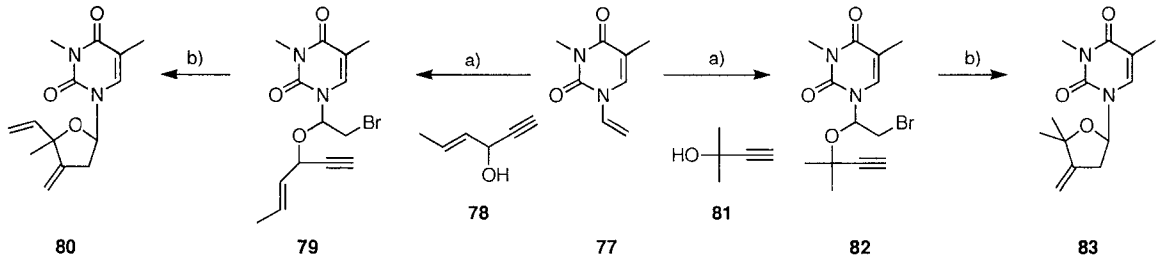

Scheme 1.15 a) NBS, -40°C (**79** 76%) (**82** 46%); b) 1.2 eq. Bu_3SnH, AIBN (cat.) 0.4 M Benzene (**80** 28%) (**83** 90%)

Recently published by the Hegedus group was the *de novo* synthesis of several 4′-ethoxy nucleoside analogs.[34] Butenolide **84** served as an optically active template for the *de novo* synthesis of 4′-disubstituted nucleoside analogues. Reduction of the butenolide followed by in situ acylation gave acetate **85** as a 1:1 mixture of C-1 anomers. Vorbrüggen coupling with silylated thymine produced the protected 4′-ethoxy-2′, 3′-dideoxydidehydrothymine derivative **86** in good yield, but as a mixture of diastereomers. Reduction with Pearlman's catalyst both debenzylated the 5′ position and reduced the double bond, giving 4′-ethoxy-2′, 3′-dideoxythymine **87** in excellent yield as an inseparable 1:1 mixture of C-1 anomers. The 4′-ethoxy-2′, 3′-dideoxydidehydrothymindine species was also synthesized in excellent yield utilizing a TES protected alcohol at the 5′ position.

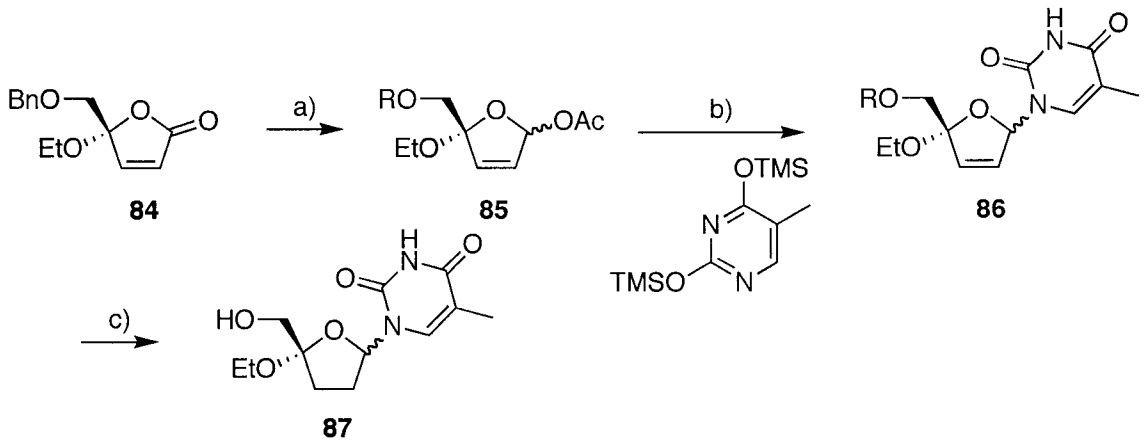

Scheme 1.16 a) 1. DIBAL, -78°C, 2. Ac_2O, Pyr, DMAP, 85% dr 1:1; b) $SnCl_4$, MeOH, 63% dr 1:1; c) $Pd(OH)_2/C$, H_2, MeOH, 88%

II. Rationale

4′ -Disubstituted nucleoside analogs may be synthesized in a diastereoselective manner through the use of novel and well-established methodology. Highly functionalized cyclobutanone **93** may provide a useful template for their synthesis. These cyclobutanones have been successfully synthesized via photolysis of hetereoatom-stablized chromium carbene complex **94** and electron-rich olefin **95**. These highly strained cyclobutanones can easily be modified to provide an intermediate for the synthesis of nucleoside analogs. Lactol acetate **92** could be subjected to well-established palladium catalyzed allylic alkylation chemistry to install the nucleoside base to produce a variety of 4′-disubstituted nucleoside analogs.

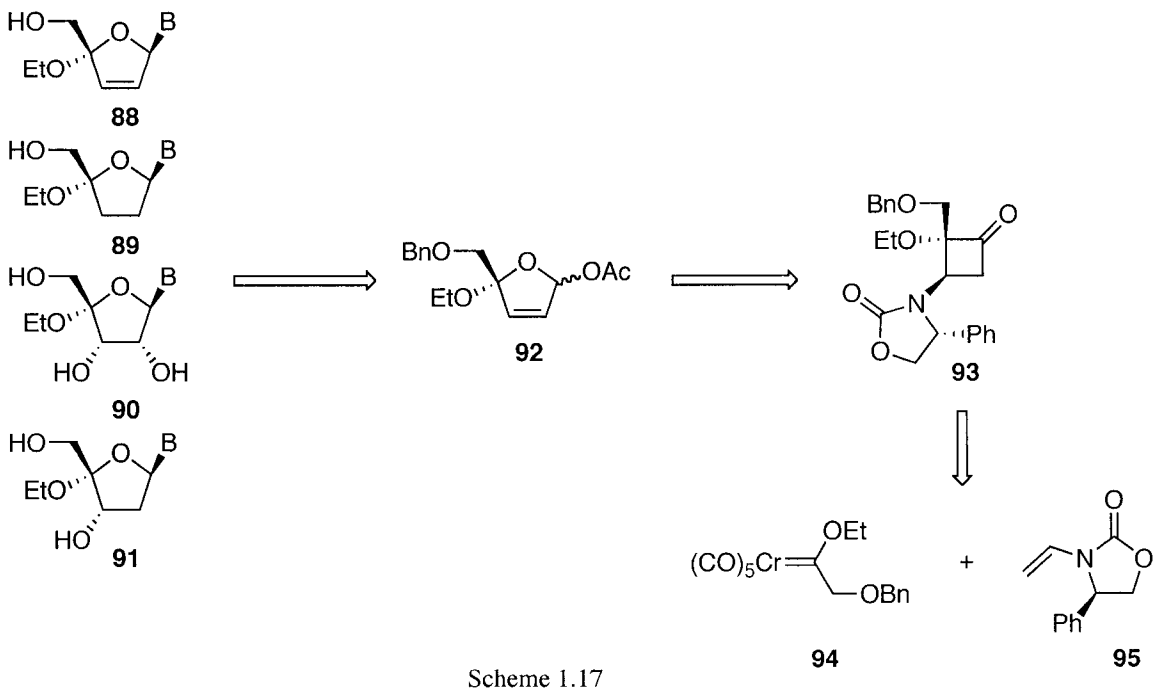

Scheme 1.17

Heteroatom-stabilized chromium carbene complexes can be obtained through several synthetic routes. Nucleophilic attack on a CO ligand in chromium hexacarbonyl (**96**) by an alkyllithium reagent (**97**) provides an anionic lithium acyl intermediate **98**. The acyl oxygen can be alkylated with a "hard" alkylating agent such as methyl trifluoromethylsulfonate (triflate),[35] or triethyloxonium tetrafluoroborate to yield the corresponding alkoxycarbene complex **103**. Alternatively, the formation of the tetramethylammonium salt, followed by addition of pivaloyl chloride forms a mixed anhydride. Subsequent addition of an alcohol can also produce the alkoxycarbene complex **103**. An alternative path to the chromium carbene complex involves the reduction of chromium hexacarbonyl with a potassium graphite intercalate **99** or a sodium napthalenide complex. The dianionic $(CO)_5Cr^{2-}$ intermediate (**101**) can react

with a variety of acyl transfer agents (**102**) to produce an anionic acyl intermediate. This intermediate also undergoes *O*-alkylation with a hard alkylating agent to produce an alkoxycarbene complex **103**.

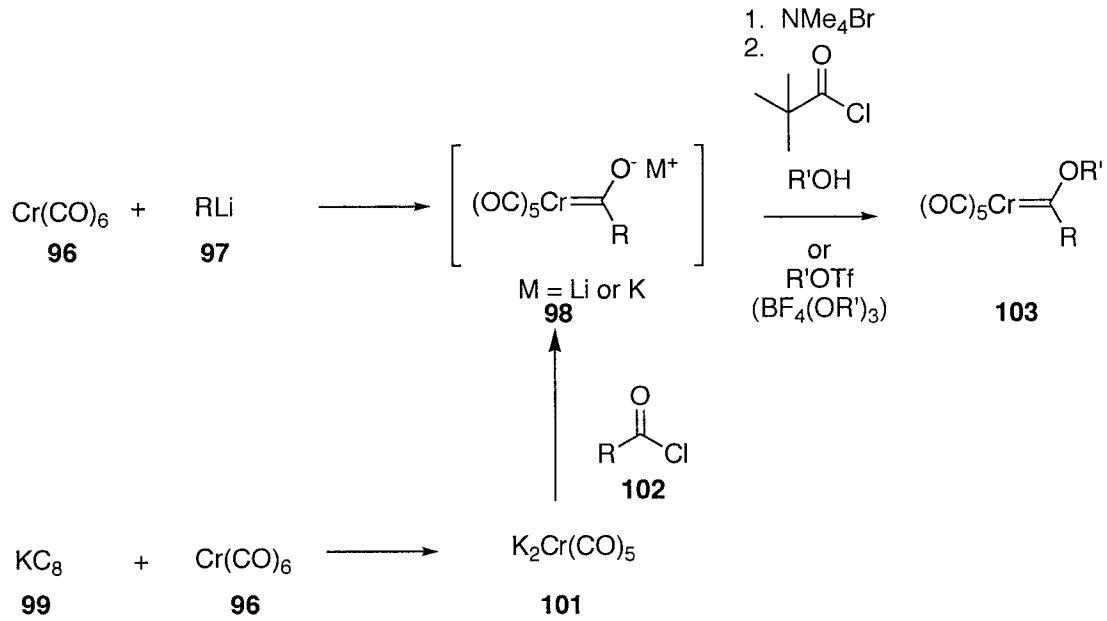

Scheme 1.18

Chromium carbene complexes are brightly colored crystalline solids which absorb in the visible spectrum around 350-450 nm. This absorption has been spectroscopically assigned to be a metal-to-ligand charge transfer (MLCT) band.[36] Irradiation into the MLCT band promotes an electron from a metal d-centered HOMO to a π^* -carbene-carbon centered LUMO, resulting in a formal oxidation of the metal center.[37] Irradiation into the MLCT band of chromium carbene complexes promotes a reversible insertion of one of the four *cis*-CO ligands into the chromium-carbon double bond, producing a metallocyclopropanone **105** or a metal-bound ketene **106**.[38]

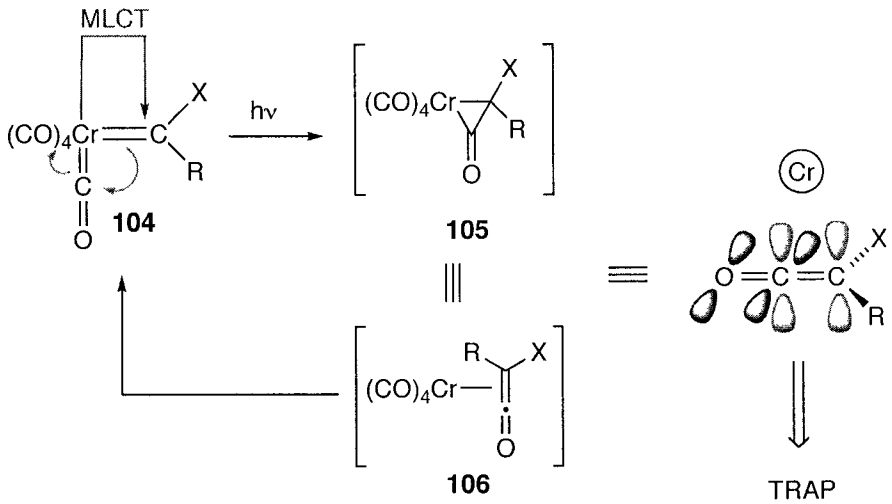

Scheme 1.19

Although the metal-bound ketenes have never been isolated, their structures are inferred by their demonstrated "ketene-like" reactivity.[39] Metal-bound ketenes are produced in low concentrations which do not display unwanted side effects, such as dimerization, associated with classical ketene reactions.

Ketenes undergo highly stereoselective [2+2] cycloadditions with electron-rich olefins to give cyclobutanones.[40] Similarly, the photolysis of chromium alkoxycarbene complexes in the presence of electron-rich olefins efficiently produces highly functionalized cyclobutanones. When certain optically active olefins are used, cyclobutanones can be produced in high diastereoselectivity and in high yields.[41] The stereochemistry can be rationalized by steric constraints in the transition state, with the alkene attacking over the smaller ketene substituent and the chiral auxiliary oriented to reduce unfavorable interactions **(112).**

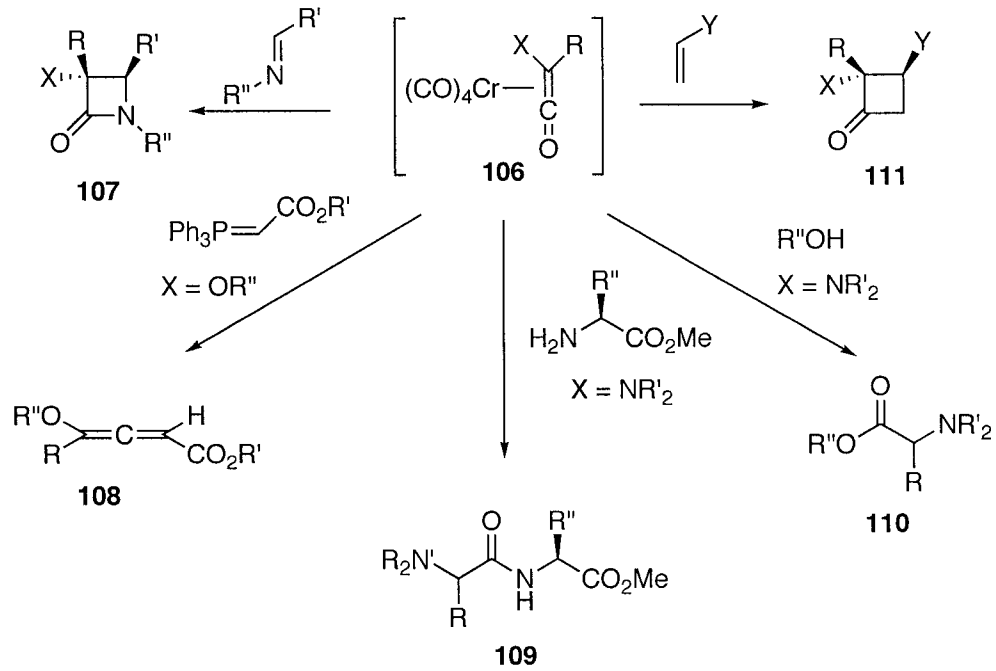

Scheme 1.20

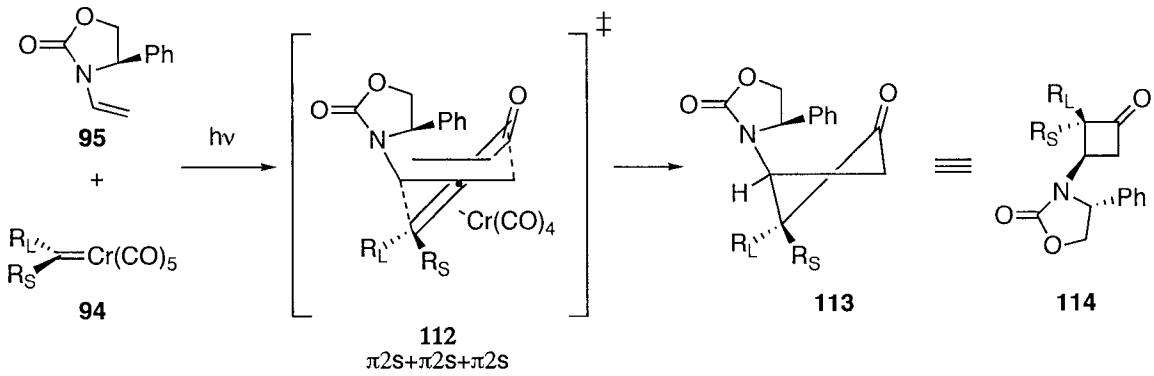

Scheme 1.21

Cyclobutanones can serve as an effective intermediate for the synthesis of nucleoside analogs (Scheme 1.22). Utilizing methodology developed in the Hegedus group, highly functionalized cyclobutanones can be easily obtained from the photolysis of a chromium alkoxycarbene complex and optically active ene carbamate **95**. The cyclobutanone can be obtained as a single stereoisomer,

creating a quaternary carbon center with the appropriate configuration for D-nucleoside analogs.

Elaboration of the highly strained cyclobutanone ring could produce a diastereomeric mixture of lactol acetates. The lactol acetate mixture could be subjected to well-established palladium allylic alkylation reaction conditions to diastereoselectively introduce the nucleoside base. This would produce a single stereoisomer of a 4'-disubstituted nucleoside analog.

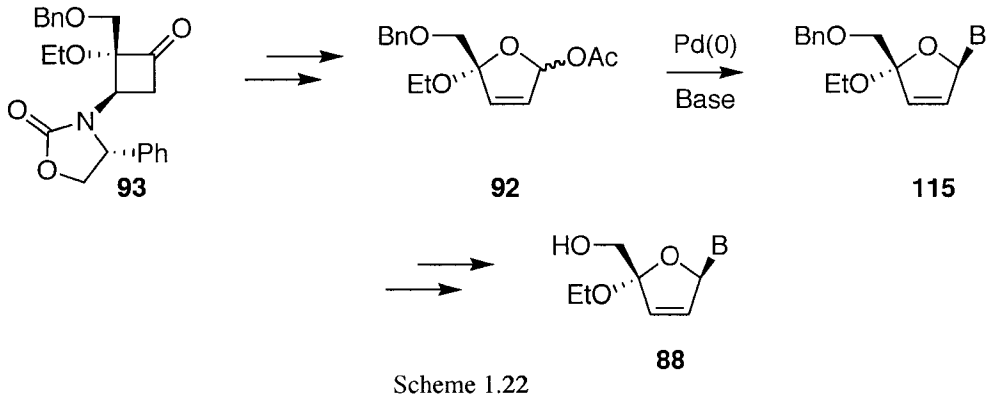

Scheme 1.22

III. Results and Discussion

Synthesis of the heteroatom stablized chromium carbene complex began with the reduction of $Cr(CO)_6$ with a potassium-graphite intercalate. This produced a dianionic chromium intermediate which reacted with an acyl chloride **116** species to give an anionic acyl potassium intermediate. Alkylation of the acyl oxygen with the hard aklyating agent, triethyloxonium tetrafluoroborate, gave chromium carbene complex **94** in 80% yield. Photolysis of the carbene complex in the presence of the chiral auxiliary (R)-vinyl carbamate **95** around 390 nm at –30°C for 7 days promoted a formal 2+2 cycloaddition reaction to give the highly functionalized cyclobutanone (**93**) as a single stereoisomer.

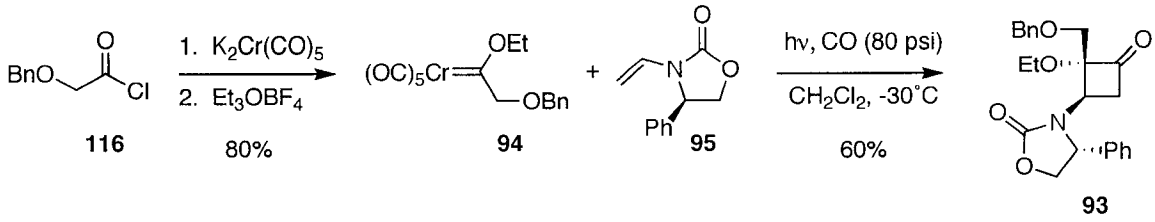

Scheme 1.23

The highly strained cyclobutanone underwent a Baeyer Villiger oxidation reaction via migration of the more substituted carbon bond to give lactone **117** in 98% yield with retention of configuration. Elimination of the chiral auxiliary with TBAF afforded optically active butenolide **118** species in 90% yield.[42]

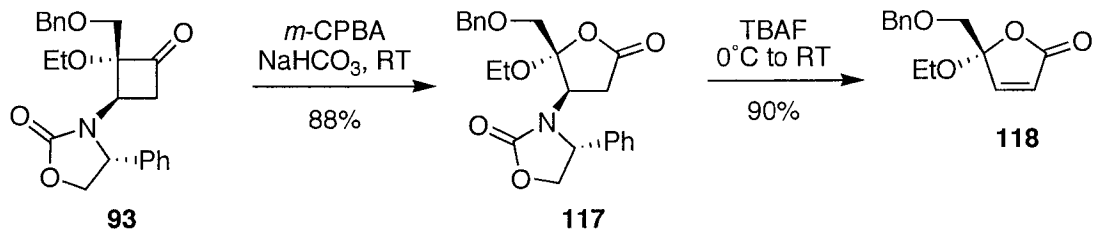

Scheme 1.24

Reduction of butenolide **118** with diisobutylaluminum hydride (DIBAL-H) produced an unstable hemi-acetal that contained an OEt- leaving group in the 4′-position, therefore the lactol intermediate **119** must be trapped *in situ* to prevent ring opening. A procedure developed by Rhychnovsky[43] was utilized to trap the intermediate at a low temperature with acetic anhydride in the presence of pyridine and 4-dimethylamino pyridine (DMAP). The reduction produced an approximately 1:1 diastereomeric mixture of lactol acetates **92**, without a diastereoselective influence from the 4′ chiral center. The diastereomeric mixture was inseparable via flash column chromatography. Therefore, diastereoselective methodology would be needed to install the nucleoside base.

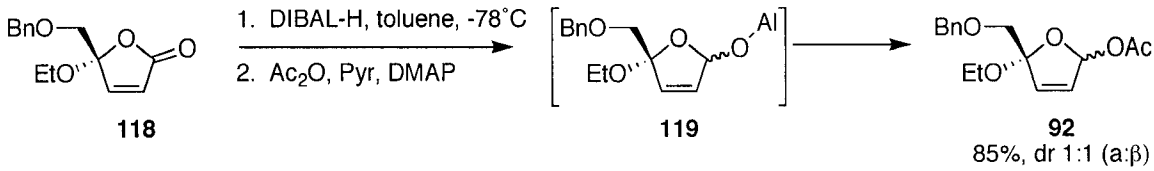

118 119 92

85%, dr 1:1 (a:β)

Scheme 1.25

The general reactivity of the lactol acetate toward π-allylpalladium chemistry was initially probed with the highly reactive nucleophile, dimethyl malonate. The π-allylpalladium complex of the lactol acetate was formed via addition of 5.5 mol % $(\eta^3\text{-}C_3H_5Cl_2Pd)_2$ and 15.6 mol % of diphenylphosphino ethane (dppe) to **92**. In a second flask, the sodium salt of dimethyl malonate was prepared and was transferred to the π-allylpalladium complex. Examination of the crude reaction mixture showed that elimination of the extremely acidic α-proton occurred. This resulted in the loss of the 4'-ethoxy substitutent and formation of aldehyde **119**.

Elimination of the α-proton was prevented through the use of dimethyl methyl malonate as the nucleophile. The lactol acetate was successfully alkylated with dimethyl methyl malonate producing the product **120** in 82% yield.

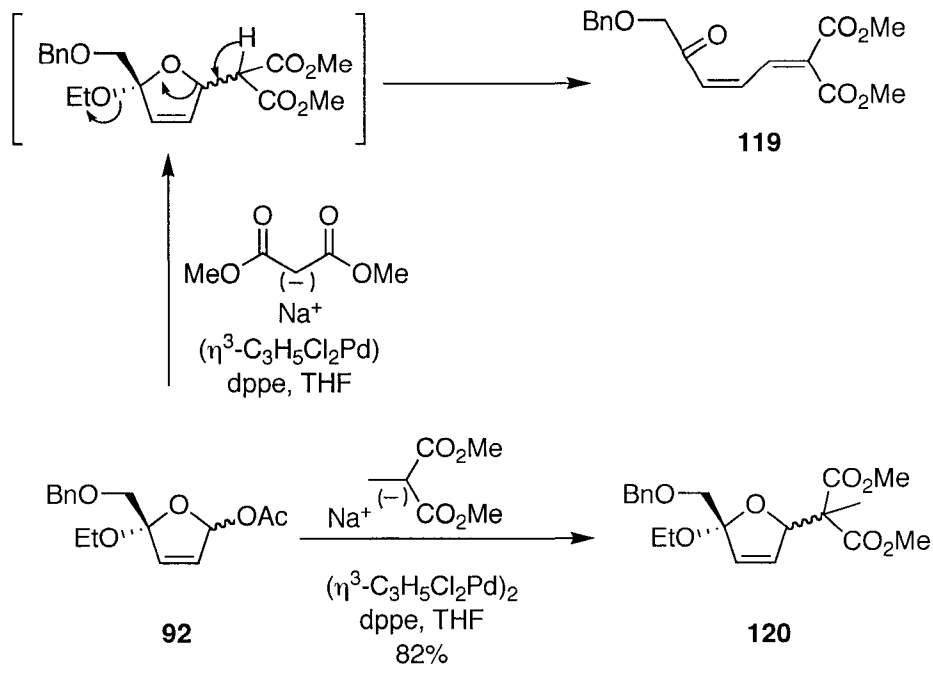

Scheme 1.26

Next, the viability of nucleoside bases as nucleophiles for allylic amination of the lactol acetate was investigated. The solubility of nucleoside bases in most organic solvents is extremely poor; therefore, they were silylated *in situ* with N,O bis(trimethylsilyl)acetamide (BSA), then released by the introduction of a fluoride source from tetrabutylammonium fluoride (TBAF).

Investigations into the effect of the resident chiral quaternary center on selectivity between the two diastereoisomeric α and β acetates was explored by using the achiral ligand 1,1'-bis(diphenylphosphino)ferrocene (dppf). The diastereomeric lactol acetates were aminated with the silylated thymine base with 5 mol % $Pd_2(dba)_3 \bullet CH_3Cl$ and 10 mol % of the achiral ligand dppf. The reaction was stopped after 6 hours and the aminated product **121** was isolated with a d.r. of 55:45 (α:β) and the recovered starting material **92** had a d.r. of 65:35 (α:β). These results showed that the distant, resident chiral center did not influence the diastereoselectivity of the reaction, and there was no intrinsic

preference for one diastereomer over the other. Since both diastereomeric mixtures of the starting material and aminated products are inseparable, asymmetry would have to be introduced into the palladium-catalyzed allylic alkylation reaction to allow formation and isolation of the desired β-thymine product.

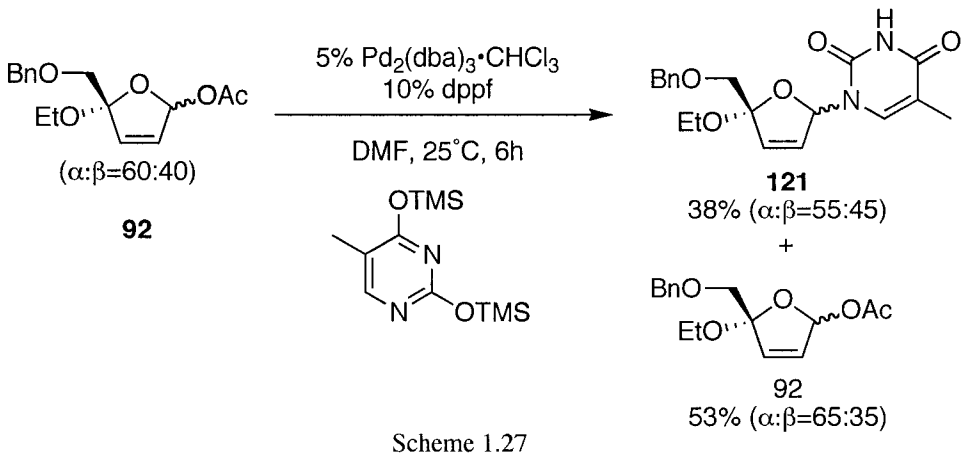

Scheme 1.27

The discrimination between the lactol acetates could occur through a kinetic resolution. A kinetic resolution is the separation of enantiomers due to a difference in the rate of reaction between the two enantiomers with a non-racemic, chiral reagent. In a kinetic resolution, the degree of separation or enantiomeric excess of the starting material and the product depends on how different the rates of reaction are for the two enantiomers of the starting material. If the rates differ by 1000, then after 50% of the starting material has reacted, the composition of the product and the remaining starting material might each contain 100% enantiomeric excess (Scheme 1.28).[44]

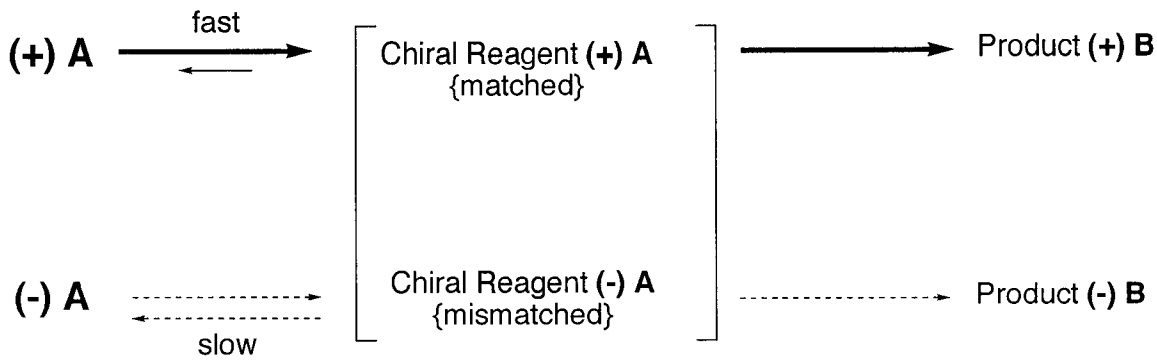

Scheme 1.28

In an enantioselective process, two enantiomers of a chiral product are produced in unequal amounts through the addition of a chiral auxiliary or ligand. The lactol acetates, however, are a mixture of diastereomers, and therefore the kinetic resolution must be performed diastereoselectively.

Executing a diastereoselective reaction would require introducing some element of asymmetry into the palladium-catalyzed allylic alkylation reaction by utilizing a chiral ligand on palladium that could discriminate between diastereomers. By doing this, a chiral ligand on palladium would create diastereotopic transition states that are unequal in energy, resulting in different reaction rates of the starting diastereomers. The resulting diastereomeric products can be produced in unequal amounts depending on which ligand is used. This method to induce diastereoselectivity through the use of chiral catalysts in metal-catalyzed transformations is a highly active field with frequent reports in the literature of new ligands. The incorporation of a chiral ligand on palladium would result in a kinetic resolution between diastereomeric lactol acetates by favoring the β-diastereomer over the α diastereomer (Scheme 1.29).

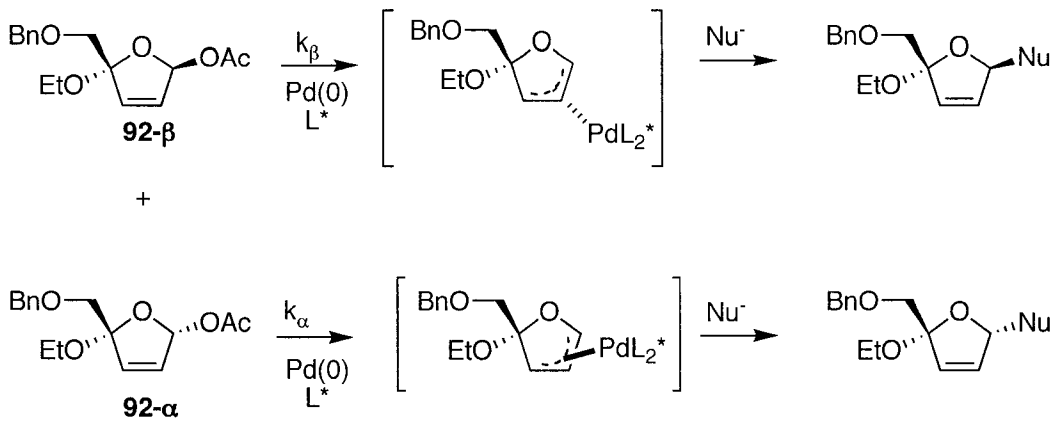

Scheme 1.29

The kinetic resolution of the diastereomeric lactol acetates began with one of the most extensively studied and broadly used ligands the *trans*-1, 2-cyclohexanediamine based ligands, developed by Trost[45] and $(\eta^3\text{-}C_3H_5\ Cl_2Pd)_2$ as the catalyst. Optimization of the reaction conditions was achieved and the *S, S* ligand proved to be a successful match with the β-acetate. The aminated product **121** was isolated in 36% yield with a d.r. 93:7 (β:α) and the starting material was recovered as a single stereoisomer in 45% with a d.r. of >97:3 (α:β) (Table 1.1, entry 5).

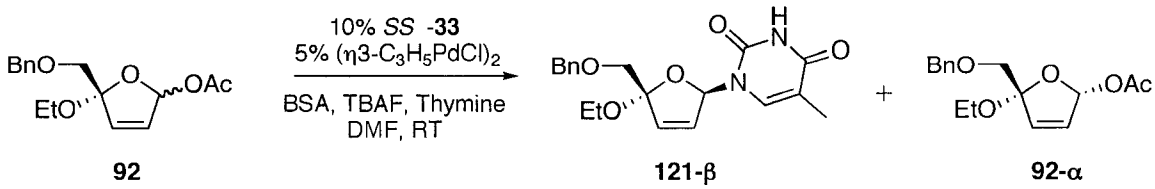

92 121-β 92-α

Table 1.1 Allylic Amination Attempts with Thymine, *SS* -**33**, and $(\eta^3\text{-}C_3H_5PdCl)_2$

Entry	BSA (eq.)	TBAF (eq.)	Thymine (eq.)	Time (days)	d.r. (**121** β:α)	Yield (**121**β)	d.r. (**92**α:β)	Yield (**92**α)
1	0.65	1.0	1.25	2	89:11	34%	>97:3	38%
2	1.25	2.0	1.25	5	86:14	40%	71:29	51%
3	1.25	2.0	1.25	3	81:19	43%	>97:3	26%
4	1.30	2.0	0.65	2	86:14	30%	>97:3	38%
5	1.25	2.0	2.50	3	93:7	36%	>97:3	45%

Although these results were encouraging, there was a slight formation of α-**121**. Unfortunately the diastereomeric products are inseparable, therefore, the reaction conditions had to be optimized to prevent conversion of the α acetate to the corresponding thymine product. The most significant increase in the d.r. of the product was seen using $Pd_2(dba)_3 \bullet CHCl_3$ as the palladium source.

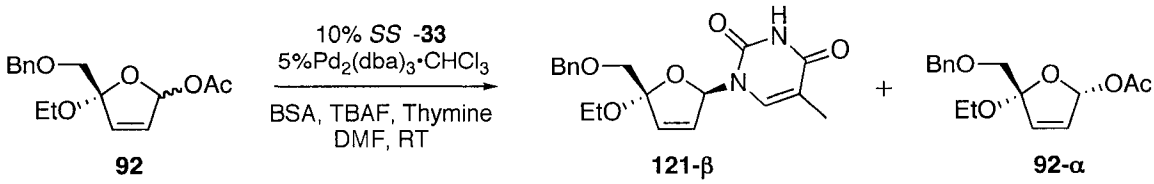

Table 1.2 Allylic Amination Attempts with Thymine, *SS* -**33**, and$Pd_2(dba)_3$•$CHCl_3$

Entry	BSA (eq.)	TBAF (eq.)	Thymine (eq.)	Time (hours)	d.r. (**121** β:α)	Yield (**121**-β)	d.r. (**92**α:β)	Yield (**92**α)
1	0.65	1.0	1.25	16	>97:3	47%	>97:3	49%
2	0.5	1.0	0.5	16	>97:3	32%	>97:3	59%

Once thymine was successfully added with the optimized reaction conditions, other purine and pyrimidine bases were examined. Adenine, cytosine, and uracil were utilized to produce β-4'substituted nucleoside analogs. Excellent yields of **92**-α were also obtained (Table 1.3). In most cases, both the aminated products (Table 1.3, entries 1-4) and recovered starting materials **92**-α were found to be diastereoisomerically pure by ^1H NMR spectroscopy. Only guanine failed to react effectively and produced an inseparable mixture of several products. Uracil was by far the most reactive, converting some of the **92**-α starting material to α-**124** in five hours at room temperature. At 0°C, only the β product was isolated from the reaction mixture.

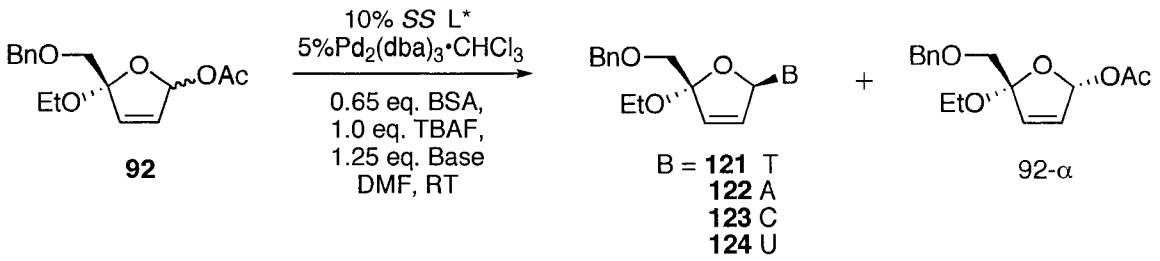

Table 1.3 Allylic Amination Attempts with Other Nucleoside Bases, *SS* -**33**, and $Pd_2(dba)_3 \cdot CH_3Cl$

Entry	Base	Time (hours)	d.r. (β:α)	Yield (β)	d.r. (**92** α:β)	Yield (**92**α)
1	T	16	>97:3	**121** 49%	>97:3	41%
2	A	16	>97:3	**122** 38%	>97:3	39%
3	C	16	>97:3	**123** 51%	>97:3	44%
4	U	5	>97:3	**124** 49%	>97:3	44%

The effective kinetic resolution of the diastereomeric mixture of lactol acetates prompted the inquiry into whether the *R, R*-chiral ligand would mirror the results from the *S, S*-series. Specifically, would the *R, R*-ligand be selective towards the α-acetate, leaving the β-acetate untouched? The lactol acetate mixture contains two diastereomers; however, the opposite enantiomeric ligand did not result in selective conversion of the α-acetate to the α-thymine product **92**-α. Before full consumption of **92**-α occurred, **92**-β began to react, giving a mixture of α– and β- **121** (Scheme 1.31).

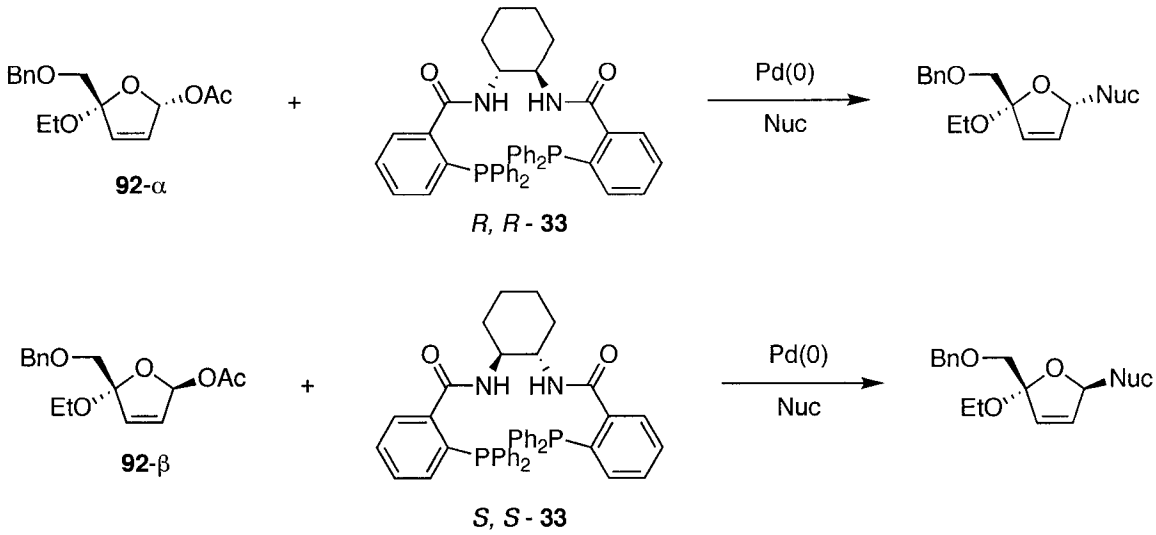

Scheme 1.30

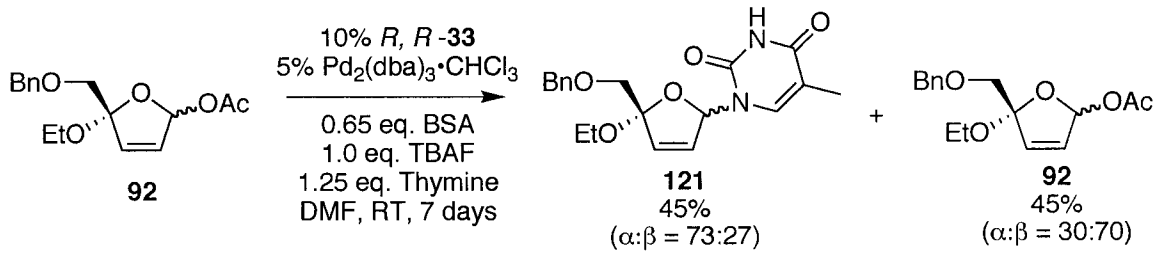

Scheme 1.31

In a successful kinetic resolution, there is a maximum 50% conversion of one stereoisomer to the product which leaves the remaining unreacted starting material enantioenriched. If a dynamic kinetic resolution could be employed, then the entire diastereomeric mixture could be converted to a single diastereoisomer of the product. A dynamic kinetic resolution involves the epimerization of the reactive stereocenter under the reaction conditions so that the enantiomeric center that does not react can be transformed into the one that does. This epimerization must occur rapidly to ensure conversion of the more reactive substrate to the product giving a possible theoretical yield of 100%. Also, the epimerization reaction must not interfere with the resolution process.[46]

A dynamic kinetic resolution is an example of a Curtin-Hammett system in which the product mixture is controlled by the free energies of the transition states and not the composition of the starting materials. The rates of the competing reactions along with the rate of racemization are extremely important in the overall resolution process. Figure 1.7a demonstrates an ideal dynamic kinetic resolution which possesses 100% conversion to a 100% enantiomerically enriched product where $k_{inv}>>k_R>k_S$.[47] If k_{inv} were closer or slower than k_R, then the *ee* of the product would be lowered because the amount of R in solution would not be produced fast enough to make k_S negligible.

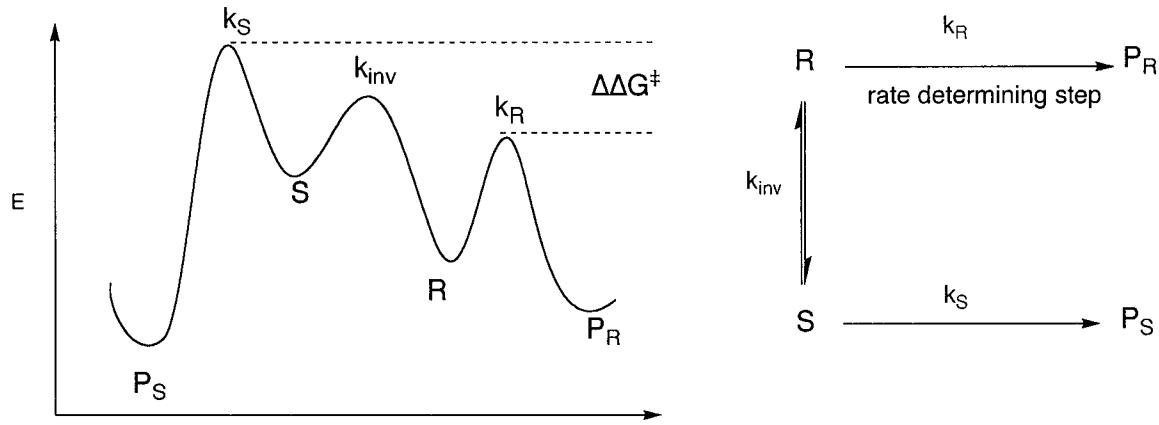

Figure 1.7 (a) The Potential Energy Diagram of a Dynamic Kinetic Resolution
(b) A Dynamic Kinetic Resolution Process

Investigations into the epimerization of the α-acetate began independently of the palladium-catalyzed allylic alkylation reaction. Palladium is known to racemize allylic acetates,[48] and for the dynamic kinetic resolution to be successful, the epimerization conditions must be compatible with the allylic alkylation reaction conditions. Palladium catalysts were screened,[49] alone at first, then with a variety of additives within the reaction mixture, but unfortunately these

attempts were unsuccessful. Lewis acid mediated epimerizations[50] were investigated next. The addition of zinc acetate to the α diastereomer (**92-α)** in acetic acid was found to be successful in producing a diastereomeric mixture of **92**.

The equilibration of the α diastereomer (**92-α)** of the lactol acetate with zinc acetate in acetic acid produced a 60:40 diastereomeric mixture of α and β anomers of **92**. This mixture of anomers could be, in principle, resubjected to the palladium-catalyzed allylic amination reaction procedure to produce more b-nucleosides, eventually producing a complete conversion of a 1:1 mixture of α - and β -**92** to the β-nucleoside.

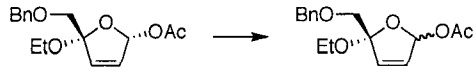

92-α 92

Table 1.4 Epimerization Attempts of **92-α**

Entry	Catalyst	Ligand	Solvent	Lewis Acid	Counter Ion	Time (hrs)	Temp.	Result
1	$Pd_2(dba)_3$ •$CHCl_3$	dppf	DMF	-	CsOAc	16	r.t.	SM
2	$Pd_2(dba)_3$ •$CHCl_3$	dppf	DMF	-	Bu_4NCl	16	r.t.	SM
3	-	-	CH_2Cl_2	$Sc(OTf)_3$	-	8	r.t.	SM
4	-	-	CH_2Cl_2	$Sc(OTf)_3$	LiOAc	8	r.t.	Decomposition
5	-	-	CH_2Cl_2	$Sc(OTf)_3$	NaOAc	8	r.t.	Decomposition
6	-	-	CH_2Cl_2	BF_3•OEt_2	NaOAc	7	0°C	Decomposition
7	-	-	THF	-	HOAc	48	r.t.	92:8 (α:β)
8	-	-	THF	-	HOAc	36	r.t.	SM
9	$PdCl_2(MeCN)_2$	-	CH_2Cl_2	-	NaOAC	7	r.t.	SM
10	-	-	CH_2Cl_2	BF_3•OEt_2	HOAc	1	-78°C	SM
11	$(Ph_3P)_4Pd$	-	THF	-	-	1	55°C	SM
12	-	-	$CHCl_3$	BF_3•OEt_2	-	1	0°C	Decomposition
13	$Pd_2(dba)_3$ •$CHCl_3$	dppe	DMF	-	CsOAc	96	r.t.	SM
14	-	-	THF	-	TFA	24	r.t.	Decomposition
15	-	-	CH_2Cl_2	$SnCl_4$	-	0.5	0°C	Decomposition
16	-	-	CH_2Cl_2	$SnCl_4$	Bu_4NOAc	0.2	0°C	Decomposition
17	-	-	CH_2Cl_2	TMSCl	Bu_4NOAc	1	0°C	Decomposition
18	-	-	CH_2Cl_2	TMSBr	Bu_4OAc	1	0°C	Decomposition
19	-	-	CH_3CN	TMSOTf	Bu_4NOAc	1	0°C	Decomposition
20	-	-	HOAc	ZnOAc	-	72	r.t.	70 : 30 (α:β)
21	-	-	HOAc	ZnOAc	-	2	35°C	60:40 (α:β) 92%

IV. Conclusion

4′-Ethoxy-2′, 3′-unsaturated nucleoside analogues have been synthesized using palladium-catalyzed asymmetric allylic amination conditions. A kinetic discrimination between diastereomeric lactol acetates produced the desired aminated products and recovered the α-acetate in high yields and high

diastereoselectivity when the *S, S* -**33** ligand was used. Unfortunately, attempts at a dynamic kinetic resolution were unsuccessful, however, the independent epimerization of the recovered lactol acetate with zinc acetate in acetic acid gave a 60:40 (α:β) diastereomeric mixture from a single stereoisomer.

V. Experimental Section

General Methods and Materials. THF was distilled from sodium-benzophenone ketyl, and DMF was distilled from $MgSO_4$. Commercially available reagents were used as received. ^1H NMR (300 MHz) and ^{13}C NMR (75 MHz) spectra were recorded in $CDCl_3$ unless otherwise noted and chemical shifts are given in ppm relative to $CDCl_3$ (7.27 ppm for ^1H NMR and 77.23 ppm for ^{13}C NMR). Column chromatography was performed with ICN 32-66 nm, 60 Å silica gel using flash column techniques. All reactions were performed in flame-dried glassware under an atmosphere of Ar unless otherwise noted.

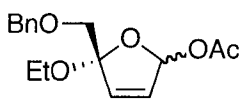

92

$C_{16}H_{20}O_5$
Exact Mass: 292.13
Mol. Wt.: 292.33
C, 65.74; H, 6.90; O, 27.37

(*S*)-5-((benzyloxy)methyl)-5-ethoxy-2,5-dihydrofuran-2-yl acetate 92. Butenolide (-)-**118** (66 mg, 0.27 mmol) was placed into a 100 mL round-bottom flask and dissolved in CH_2Cl_2 (20 mL). The mixture was cooled to –78°C, and DIBALH (0.4 mL, 0. 4 mmol) was added dropwise via syringe. The reaction was stirred at -78 C for 1.5 h or until

the disappearance of starting material was noted by TLC (silica gel, 3:1 hexanes/ethyl acetate). Pyridine (0.06 mL, 0.8 mmol), DMAP (65 mg, 0.53 mmol) in a minimal amount of CH_2Cl_2, and acetic anhydride (0.1 mL, 1.0 mmol) were added respectively, and the solution was warmed to 0°C for 4 h. The reaction mixture was quenched with a saturated solution of Rochelle's salt (50 mL), extracted with CH_2Cl_2, dried with $MgSO_4$, and concentrated. The crude oil was purified by flash column chromatography (10:1 hexanes/ethyl acetate) to yield acetate **92** (66 mg, 0.23 mmol, 85%) as a clear oil and as a 1:1 mixture of diastereomers: R_f 0.46 (25% ethyl acetate in hexanes); IR (neat) ν1734 cm^{-1}; ^1H NMR δ 7.29 (m, 10H, both diast.), 6.84 (s, 1H), 6.66 (s, 1H), 6.11 (m, 4H, both diast.), 4.59 (s, 2H), 4.56 (s, 2H), 3.71 (m, 2H), 3.55 (m, 2H) 3.42 (m, 4H, both diast.), 2.06 (s, 3H), 1.99 (s, 3H), 1.15 (t, J = 6.9 Hz, 6H, both diast.); ^{13}C NMR δ 170.5, 170.1, 138.3, 138.1, 136.6, 134.4, 133.7, 130.2, 128.4, 128.4, 127.7, 127.6, 115.2, 114.1, 100.6, 99.0, 74.0, 73.9, 73.7, 73.5, 58.8, 58.4, 21.4, 15.6, 15.5.

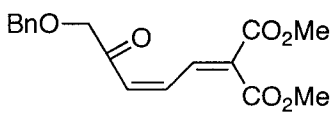

119
$C_{17}H_{18}O_6$
Exact Mass: 318.11
Mol. Wt.: 318.32
C, 64.14; H, 5.70; O, 30.16

Dimethyl 2-((*Z*)-5-(benzyloxy)-4-oxopent-2-enylidene)malonate 119. Dimethyl malonate (36 μL, 0.319 mmol) was added via syringe to a slurry of NaH (7.3 mg, 0.183 mmol, 60% in mineral oil) in THF (0.10 mL) in a 25 mL round-bottom flask. The suspension bubbled for 2 min and then subsided. Acetate **92** (30 mg, 0.103 mmol), allylpalladium chloride (2.1 mg, 0.006 mmol, 5.5%), 1,2-bis(diphenylphosphino)ethane (dppe) (6.4 mg, 0.016 mmol, 15.6%), and THF (0.1 mL) were placed into a second 25 mL flask and stirred for 5 min. The contents of

the second flask were transferred to the flask containing the NaH suspension via cannula needle, using THF (0.2 mL) to rinse. The yellow/orange mixture turned a dark orange after a few min. The reaction was monitored using TLC (silica gel, 4:1 hexanes/ethyl acetate) and was finished with the disappearance of starting material. After 3.5 h, the reaction solution was diluted with CH_2Cl_2 (10 mL) and then distilled H_2O (10 mL). The aqueous layer was extracted with CH_2Cl_2 (3 x 20 mL), and the organic layers were combined, dried with $MgSO_4$, and concentrated to give a brown oil. Analysis of the crude ^1H NMR spectrum showed no starting material present and no indication of the desired product.

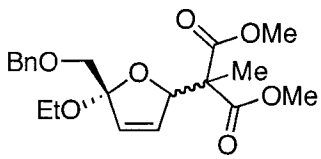

120

$C_{20}H_{26}O_7$
Exact Mass: 378.17
Mol. Wt.: 378.42
C, 63.48; H, 6.93; O, 29.60

Dimethyl 2-((*S*)-5-((benzyloxy)methyl)-5-ethoxy-2,5-dihydrofuran-2-yl)-2-methylmalonate (120). Dimethyl methylmalonate (23 μL, 0.172 mmol) was added via syringe to a slurry of NaH (7.0 mg, 0.287 mmol, 60% in mineral oil) in THF (0.10 mL) in a 25 mL round-bottom flask. After 5 min a mixture of the acetate **92** (25 mg, 0.086 mmol, d.r. 55:45, α:β), allylpalladium chloride (3.12 mg, 0.009 mmol, 10%), and dppe (6.8 mg, 0.017 mmol, 20%) in THF (0.3 mL) were transferred via cannula needle to the flask. The reaction mixture turned orange, and then dark red after 5 min. After being stirred at room temperature for 3 h, the reaction mixture was diluted with $CH_2Cl_2$and distilled H_2O. The layers were separated, and the aqueous layer was extracted with CH_2Cl_2 (3 x 25 mL). The combined organic layers were dried with $MgSO_4$, filtered, and concentrated. Flash column chromatography (10:1 hexanes/ethyl acetate) gave **120** as a clear oil as a 55:45 (α:β) mixture of

diastereomers (26 mg, 0.069 mmol, 82%.): R_f 0.42 (25% ethyl acetate in hexanes); IR (neat) ν 1734 cm^{-1}; ^1H NMR δ 7.34 (m, 10H, both diast.), 6.31 (dd, J = 6.0, 1.2 Hz, 1H), 6.26 (dd, J = 6.0, 1.2 Hz, 1H), 5.99 (dd, J = 6.3, 2.4 Hz, 1H), 5.91 (dd, J = 6.0, 2.4 Hz, 1H), 5.47 (dd, J = 2.4, 1.5 Hz, 1H), 5.29 (t, J = 2.1 Hz, 1H), 4.59 (m, 4H, both diast.), 3.78 (d, J = 5.1 Hz, 1H), 3.76 (d, J = 4.8 Hz, 1H), 3.72 (s, 12H, both diast.), 3.67 (d, J = 6.0 Hz, 1H), 3.65 (d, J = 4.2 Hz, 1H), 3.43 (m, 4H, both diast.), 1.45 (s, 3H), 1.34 (s, 3H), 1.19 (t, J = 6.9 Hz, 3H), 1.18 (t, J = 6.9 Hz, 3H); ^{13}C NMR δ 171.2, 170.1, 138.3, 134.4, 133.7, 130.2, 128.4, 128.4, 127.7, 127.6, 115.2, 114.1, 100.6, 99.0, 74.0, 73.9, 73.8, 73.5, 60.6, 58.8, 58.4, 21.4, 21.3, 15.6, 15.5, 14.4.

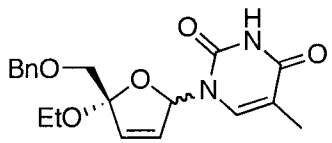

121

$C_{19}H_{22}N_2O_5$
Exact Mass: 358.15
Mol. Wt.: 358.39
C, 63.67; H, 6.19; N, 7.82; O, 22.32

(4′*S*)-5′-*O*-Benzyl-4′-ethoxy-2′,3′-dideoxy-didehydrothymidine (121). Tetra-*n*-butylammonium fluoride hydrate (TBAF·$3H_2O$) (21 mg, 0.068 mmol) was weighed into a 10 mL round-bottom flask and dried under vacuum for approximately 1 h. It was then dissolved in dry DMF (0.10 mL) and transferred via syringe to a 15 mL round-bottom flask containing 4 Å MS and stirred for 45 min at room temperature. A second 15 mL round-bottom flask was charged with the thymine base (11 mg, 0.085 mmol) and *N*,*O*-bis(trimethylsilyl)methane (BSA) (11 μL, 0.044 mmol) in DMF (0.10 mL) and stirred for 10 min. A 25 mL Schlenk tube was equipped with a stir bar and charged with tris(dibenzylideneacetone)-dipalladium(0)-chloroform adduct ($Pd_2(dba)_3$·$CHCl_3$) (3.5 mg, 0.0034 mmol, 5.0%) and 1,1-bis(diphenylphosphino)ferrocene (dppf) (3.8 mg, 0.0068 mmol, 10%). First, acetate **92** (15.4 mg, 0.068 mmol) in DMF (0.10 mL) was added to the

Schlenk tube via syringe. Next, the silylated base was transferred via syringe to the reaction tube. Last, the TBAF in DMF was transferred via syringe to the reaction flask. The reaction mixture was light yellow in color and gradually darkened to a deep red upon completion. The reaction's progress was monitored by the consumption of the starting material by TLC (silica gel, 3:1 hexanes/ethyl acetate) and of aliquots taken from the reaction mixture. After the reaction was completed, the DMF was removed under reduced pressure leaving a dark brown oil. The oil was taken up in ethyl acetate and washed with brine. The brine was extracted with ethyl acetate (3 x 50 mL). The organic layers were combined and washed with brine, dried with $MgSO_4$, and concentrated. The crude oil was purified by flash column chromatography (10:1 hexanes/ethyl acetate; 4:1 hexanes/ethyl acetate; 1:1 hexanes/ethyl acetate) to yield the allylated thymine product **121** as a 55:45 (α:β) mixture of diastereomers (7.0 mg, 38%) and as a white solid (mp 107-109°C). **121** was recovered as a 65:35 (α:β) mixture of diastereomers in 53% yield (8.2 mg, 0.028 mmol): Spectral data for **121**: R_f 0.45 (5% CH_3OH in CH_2Cl_2); IR (neat) ν 1695 cm^{-1}; ^1H NMR δ 8.01 (bs, 2H, both diast.), 7.53 (s, 1H), 7.32 (m, 11 H, both diast.), 7.11 (s, 1H), 6.91 (s, 1H), 6.39 (dd, J = 5.7, 1.5 Hz, 1H), 6.13 (s, 2H), 6.03 (dd, J = 5.7, 1.5 Hz, 1H), 4.60 (d, J = 2.4 Hz, 2H), 4.57 (s, 2H), 3.84 (d, J = 10.2 Hz, 1H), 3.75 (s, 2H), 3.62 (m, 2H), 3.50 (d, J = 10.2 Hz, 1 H), 3.41 (m, 2H), 1.92 (s, 3H), 1.27 (s, 3H) 1.20 (t, J = 6.9 Hz, 3H), 1.18 (t, J = 6.9 Hz, 3H); ^{13}C NMR δ 164.2, 151.3, 151.1, 137.7, 137.4, 136.5, 136.2, 135.4, 134.0, 131.3, 129.0, 128.7, 128.6, 128.2, 128.0, 127.9, 127.9, 114.2, 112.5, 111.4, 111.2, 88.7, 87.9, 73.7, 73.7, 72.9, 70.7, 58.9, 57.9, 15.5, 15.3, 12.6, 11.9. Anal. Calcd for $C_{19}H_{22}N_2O_5$: C, 63.67; H, 6.18; N, 7.82. Found: C, 63.62; H, 6.07; N, 7.58.

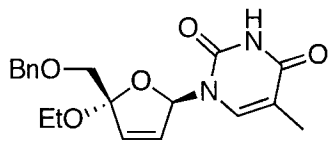

121-β

$C_{19}H_{22}N_2O_5$
Exact Mass: 358.15
Mol. Wt.: 358.39
C, 63.67; H, 6.19; N, 7.82; O, 22.32

(4′*S*)-5′-*O*-Benzyl-4′-ethoxy-2′,3′-dideoxy-β-didehydrothymidine (121-β). TBAF·$3H_2O$ (54 mg, 0.171 mmol) was weighed into a 5 mL round-bottom flask and dried under vacuum for approximately 1 h. The TBAF was dissolved in DMF (0.10 mL) and transferred via syringe to a 10 mL round-bottom flask containing 4 Å MS and was stirred for 45 min at room temperature. Thymine (27 mg, 0.214 mmol) and BSA (27 μL, 0.11 mmol) were placed in a 15 mL round-bottom flask and stirred for 10 min. $Pd_2(dba)_3$·$CHCl_3$ (8.9 mg, 0.0086 mmol, 5.0%) and *SS*-**33** (12 mg, 0.017 mmol, 10%) were weighed into a 15 mL Schlenk tube containing a stir bar. First, the contents of the flask containing silylated base were transferred via syringe to the reaction flask. The addition of acetate **92** (50.8 mg, 0.171 mmol) via syringe to the reaction tube followed. Last, the TBAF solution was transferred via syringe to the reaction tube. The reaction mixture was light yellow/orange in color and gradually darkened to a deep red upon completion. The reaction's progress was checked by the analysis of the crude 1H NMR spectrum of isolated aliquots. After 16 h the reaction was complete. The DMF was removed under reduced pressure leaving a dark brown oil. The oil was taken up in ethyl acetate and washed with brine. The brine was extracted with ethyl acetate (3 x 50 mL). The organic layers were combined and washed with brine, dried with $MgSO_4$, and concentrated. The crude oil was purified by flash column chromatography (20:1 hexanes/ethyl acetate to 1:1 hexanes/ethyl acetate) producing **121-β** as a white solid (mp 133-135°C), with a diastereomeric

ratio of <97:3 (β:α) in 49% (21 mg, 0.054 mmol) and recovering **92-α** with a diastereomeric ratio of <97:3 (α:β) in 41% (22 mg, 0.075 mmol): Spectral data for **121–β**: R_f 0.45 (5% CH_3OH in CH_2Cl_2); $[\alpha]_D$ +43 (*c* 0.9, $CHCl_3$); IR (neat) ν 1694 cm^{-1}; ^1H NMR δ 8.19 (bs, 1H), 7.54 (s, 1H), 7.32 (m, 5H), 7.11 (s, 1H), 6.13 (s, 2H), 4.58 (s, 2 H), 3.75 (s, 2H), 3.49 (m, 1H), 3.39 (m, 1H), 1.48 (s, 3H), 1.18 (t, *J* = 7.2 Hz, 3H); ^{13}C NMR δ 163.8, 151.0, 137.5, 136.6, 134.2, 131.2, 128.8, 128.3, 128.0, 114.3, 111.2, 88.8, 73.8, 73.0, 58.0, 15.4, 12.0. Anal. Calcd for $C_{19}H_{22}N_2O_5$: C, 63.67; H, 6.18; N, 7.82. Found: C, 63.48; H, 6.29; N, 7.76.

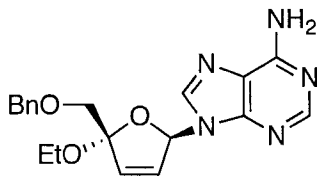

122-β

$C_{19}H_{21}N_5O_3$
Exact Mass: 367.16
Mol. Wt.: 367.4
C, 62.11; H, 5.76; N, 19.06; O, 13.06

(4′*S*)-5′-*O*-Benzyl-4′-ethoxy-2′,3′-dideoxy-β-didehydroadenine (122-β). TBAF·$3H_2O$ (60 mg, 0.190 mmol) was weighed into a 5 mL round-bottom flask and dried under vacuum for approximately 1 h. The TBAF was dissolved in DMF (0.10 mL) and transferred via syringe to a 10 mL round-bottom flask containing 4 Å MS which stirred for 45 min at room temperature. Adenine (32 mg, 0.238 mmol) and BSA (30 μL, 0.120 mmol) were placed in a 15 mL round-bottom flask and stirred for 45 min. $Pd_2(dba)_3$·$CHCl_3$ (9.8 mg, 0.0095 mmol, 5.0%) and *SS*-**33** (13 mg, 0.019 mmol, 10%) were weighed into a 15 mL Schlenk tube containing a stir bar. First, acetate **92** (55 mg, 0.190 mmol) was added to the reaction tube via syringe, followed by the flask containing the silylated base. Last, the addition of the TBAF solution via syringe was added to the reaction flask. The reaction mixture was light yellow/orange in color and gradually darkened to a deep red upon completion.

The reaction's progress was checked by the analysis of the crude 1H NMR spectrum of isolated aliquots. After 16 h the reaction was complete. The DMF was removed under reduced pressure leaving a dark brown oil. The oil was taken up in ethyl acetate and washed with brine. The brine was extracted with ethyl acetate (3 x 50 mL). The organic layers were combined and washed with brine, dried with $MgSO_4$, and concentrated. The crude oil was purified by flash column chromatography (20:1 hexanes/ethyl acetate to 1:1 hexanes/ethyl acetate then 1% CH_3OH/ CH_2Cl_2 to 3%) and produced **122-β** as a tan solid (mp 112-115°C) with a diastereomeric ratio of <97:3 (β:α) in 38% (21 mg, 0.057 mmol) and recovered **92-α** as a diastereomeric ratio of <97:3 (α:β) in 39% (21 mg, 0.072 mmol): Spectral data for **122-β**: R_f: 0.36 (5% CH_3OH in CH_2Cl_2); $[\alpha]_D$ +27 (*c* 0.8, $CHCl_3$); IR (neat) ν 1645, 1598 cm^{-1}; ^1H NMR δ 8.39 (s, 1H), 8.10 (s, 1H), 7.29 (m, 5H), 7.20 (s, 1H), 6.32 (d, *J* = 6.0 Hz, 1H), 6.22 (dd, *J* = 6.0, 1.8 Hz, 1H), 5.75 (bs, 2H), 4.58 (d, *J* = 12.0 Hz, 1H), 4.50 (d, *J* = 12.0 Hz, 1H), 3.72 (d, *J* = 10.2 Hz, 1H), 3.63 (d, *J* = 10.2 Hz, 1H), 3.58 (m, 1H), 3.44 (m, 1H), 1.20 (t, *J* = 6.9 Hz, 3H); ^{13}C NMR (100 MHz) δ 155.6, 153.3, 139.5, 134.3, 130.3, 128.7, 128.2, 115.1, 94.6, 87.2, 73.7, 72.8, 58.1, 29.9, 15.4; Anal. Calcd for $C_{19}H_{21}N_5O_3$: C, 62.11; H, 5.76; N, 19.06. Found: C, 61.99; H, 5.64; N, 18.94.

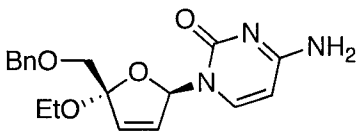

123-β

$C_{18}H_{21}N_3O_4$
Exact Mass: 343.15
Mol. Wt.: 343.38
C, 62.96; H, 6.16; N, 12.24; O, 18.64

(4′*S*)-5′-*O*-Benzyl-4′-ethoxy-2′,3′-dideoxy-β-didehydrocytosine (123-β). TBAF·$3H_2O$ (55 mg, 0.174 mmol) was weighed into a 5 mL round-bottom flask and dried under vacuum for approximately 1 h. The TBAF was dissolved in

DMF (0.10 mL) and transferred via syringe to a 10 mL round-bottom flask containing 4 Å MS which was stirred for 45 min at room temperature. Cytosine (24 mg, 0.218 mmol) and BSA (28 μL, 0.113 mmol) were placed in a 15 mL round-bottom flask and stirred for 40 min. $Pd_2(dba)_3 \cdot CHCl_3$ (12 mg, 0.017 mmol, 5.0%) and *SS*-**33** (9 mg, 0.0087 mmol, 10%) were weighed into a 15 mL Schlenk tube containing a stir bar. First, acetate **92** (51 mg, 0.174 mmol) was added to the reaction tube via syringe followed by the contents of the flask containing the silylated base. Last, the TBAF solution was transferred via syringe to the reaction tube. The reaction mixture was light yellow/orange in color and gradually darkened to a deep red upon completion. The reaction's progress was checked by the analysis of the crude 1H NMR spectrum of isolated aliquots. After 16 h the reaction was complete. The DMF was removed under reduced pressure leaving a dark brown oil. The oil was taken up in ethyl acetate and washed with brine. The brine was extracted with ethyl acetate (3 x 50 mL). The organic layers were combined and washed with brine, dried with $MgSO_4$, and concentrated. The crude oil was purified by flash column chromatography (20:1 hexanes/ethyl acetate to 1:1 hexanes/ethyl acetate then 1% CH_3OH/ CH_2Cl_2) and produced **123-β** as a white solid (mp 164-166 °C) with a diastereomeric ratio of <97:3 (β:α) in 51% (30 mg, 0.087 mmol)and recovered **92-α** as a diastereomeric ratio of <97:3 (α:β) in 44% (23.3 mg, 0.076 mmol): Spectral data for **123-β**: R_f 0.27 (5% CH_3OH in CH_2Cl_2); $[\alpha]_D$ +38 (c 0.9, $CHCl_3$); IR (neat) ν 2923, 2853, 1650 cm^{-1}; ^1H NMR δ 7.87 (d, J = 7.2 Hz, 1H), 7.31 (m, 5H), 7.24 (s, 1H), 6.19 (d, J = 5.7 Hz, 1H), 6.02 (dd, J = 6.0, 1.8 Hz, 1H), 5.30 (bs 2H) 5.15 (d, J = 7.5 Hz, 1H), 4.57 (d, J = 11.1 Hz, 1H), 4.52 (d, J = 11.1 Hz, 1H) 3.77 (s, 2H) 3.49 (m, 1H), 3.39 (m, 1H), 1.17 (t, J = 7.2 Hz, 3H);

^{13}C NMR (100 MHz) δ 165.8, 156.4, 142.5, 137.7, 132.6, 132.5, 128.7, 128.2, 128.1, 114.3, 94.4, 90.0, 73.8, 73.1, 57.8, 15.4; HRFABMS (M^+H) calculated for $C_{18}H_{22}N_3O_4$: 344.1622; found 344.1610.

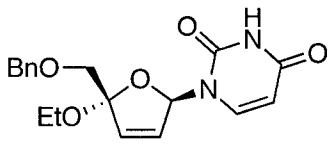

124-β

$C_{18}H_{20}N_2O_5$
Exact Mass: 344.14
Mol. Wt.: 344.36
C, 62.78; H, 5.85; N, 8.13; O, 23.23

(4′*S*)-5′-*O*-Benzyl-4′-ethoxy-2′,3′-dideoxy-β-didehydrouracil (124-β). TBAF·$3H_2O$ (55 mg, 0.171 mmol) was weighed into a 5 mL round-bottom flask and dried under vacuum for approximately 1 h. The TBAF was dissolved in DMF (0.10 mL) and transferred via syringe to a 10 mL round-bottom flask containing 4 Å MS which stirred for 45 min at room temperature. Uracil (24 mg, 0.218 mmol) and BSA (28 μL, 0.113 mmol) were placed in a 15 mL round-bottom flask and stirred for 10 min. $Pd_2(dba)_3$·$CHCl_3$ (12 mg, 0.017 mmol, 5.0%) and *SS*-**33** (9 mg, 0.0087 mmol, 10 %) were weighed into a 15 mL Schlenk tube containing a stir bar. The reaction tube was cooled to 0 C before the addition of acetate **92** (51 mg, 0.174 mmol) via syringe. Next, the silylated base was added to the reaction tube via syringe followed by the addition of TBAF via syringe. The reaction mixture was light yellow/orange in color and gradually darkened to a deep red upon completion. The reaction's progress was checked by the analysis of the crude 1H NMR spectrum of isolated aliquots. After 3 h the reaction was complete. The DMF was removed under reduced pressure leaving a dark brown oil. The oil was taken up in ethyl acetate and washed with brine. The brine was extracted with ethyl acetate (3 x 50 mL). The organic layers were combined and washed with brine, dried with $MgSO_4$

and concentrated. The crude oil was purified by flash column chromatography (20:1 hexanes/ethyl acetate to 1:1 hexanes/ethyl acetate then 1% CH_3OH/ CH_2Cl_2) and produced **124-β** as a white solid (mp 146-148°C) with a diastereomeric ratio of <97:3 (β:α) in 49% (29.6 mg, 0.086 mmol) and recovered **92-α** as a diastereomeric ratio of <97:3 (α:β) in 44% (22.5 mg, 0.077 mmol): Spectral data for **124-β**: R_f 0.55 (5% CH_3OH in CH_2Cl_2); $[\alpha]_D$ +17 (*c* 0.6, $CHCl_3$); IR (neat) ν 1694, 2359 cm^{-1}; ^1H NMR δ 8.38 (bs, 1H), 7.62 (d, *J* = 8.4 Hz, 1H), 7.25 (m, 5H), 7.02 (s, 1H), 6.05 (dd, *J* = 5.7, 1.8 Hz, 1H), 6.01 (d, *J* = 5.7 Hz, 1H), 5.03 (d, *J* = 8.1 Hz, 1H), 4.47 (d, *J* = 11.1 Hz, 1H), 4.41 (d, *J* = 10.8 Hz, 1H), 3.72 (d, *J* = 9.9 Hz, 1H), 3.67 (d, *J* = 10.2 Hz, 1H), 3.42 (m, 1H), 3.31 (m, 1H), 1.10 (t, *J* = 6.9 Hz, 3H); ^{13}C NMR δ 163.1, 150.9, 141.2, 137.3, 134.4, 131.0, 128.8, 128.5, 128.4, 114.5, 102.4, 88.8, 74.0, 73.1, 58.0, 15.4. Anal. Calcd for $C_{19}H_{20}N_2O_5$: C, 62.78; H, 5.85; N, 8.13. Found: C, 62.89; H, 5.65; N, 8.28.

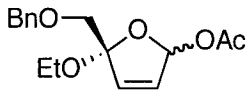

92

Epimerization of 92. A 10 mL round-bottom flask was equipped with a stir bar and dried under argon. **92-α** (21.1 mg, 0.072 mmol) was diluted with acetic acid (0.5 mL) and transferred via syringe to the reaction flask. Zinc acetate (13.2 mg, 0.072 mmol) was then added to the reaction flask. The reaction stirred at 35 °C for 12 h. The acetic acid was removed under reduced pressure, and the resulting yellow oil was dissolved with CH_2Cl_2. The crude mixture was washed with brine, and then the brine was extracted with CH_2Cl_2 (2 x 25 mL). The organic layers were combined, dried with $MgSO_4$, and concentrated. The crude oil was purified by

flash column chromatography (10:1 hexanes/ethyl acetate) to give **92** with a diastereomeric ratio of 60:40 (α:β) in 92% (19 mg, 0.065 mmol).

VI. References

[1] Stryer, L. *Biochemistry*; 4th ed.; W. H. Freeman and Co.:, 1995.
[2] White, E. L.; Parker, W. B.; Macy, L. J.; Shaddix, S. C.; McCaleb, G.; Secrist, J. A.; Vince, R.; Shannon, W. M. *Biochem. Biophys. Res. Commun.*, **1989**, *161*, 393.
[3] *AIDS Therapy*; Churchill Livingstone: Philadelphia, Penn, 1999.
[4] Maag, H.; Rydzewski, R. M.; McRoberts, M. J.;, Crawfordruth, D.; Verheyden, J. P. H.; Prisbe, E. J. *J. Med. Chem.*, **1992**, *35*, 1440.
[5] Prisbe, E. J.; Maag, H.; Verheyden, J. P. H.; Rydzewski, R. M. *Nucleosides and Nucleotides as Antitumor and Antiviral Agents*; Plenum Press: New York, 1993, pg. 101-113.
[6] Mitsuya, H.; Broder, S. *Proc. Natl. Acad. Sci. U.S.A.* **1986**, *83*, 1911.
[7] Nasr, M.; Litterst, C.; McGowan, J. *Antiviral Res.* **1990**, *14*, 125.
[8] Mahmoudian, M. *Pharm. Res.* **1991**, *8*, 43.
[9] Jones, G. H.; Taniguchi, M.; Tegg, D.; Moffatt, J. G. *J. Org. Chem.* **1979**, *44*, 1309.
[10] O-Yang, C.; Kurz, W.; Eugui, E. M.; McRoberts, M. J.; Verheyden, J. P. H.; Kurz, L. J.; Walker, K. A. M. *Tetrahedron Lett.*, **1992**, *33*, 41.
[11] Nomura, M.; Shuto, S.; Tanaka, M.; Sasaki, T.; Mori, S.; Shigeta, S.; Matsuda, A. *J. Med. Chem.* **1999**, *42*, 2901.
[12] Lamberth, C. *Organic Preparations and Procedures Int.* **1999**, *31*, 379.
[13] Kozak, J.; Johnson, C. R. *Nucleosides and Nucleotides* **1998**, *17*, 2221.
[14] Ohrui, H.; Kohgo, S.; Kitano, K.; Sakata, S.; Kodama, E.; Yoshimura, K.; Matsuoka, M.; Shigeta, S.; Mitsuya, H. *J. Med. Chem.* **2000**, *43*, 4516.
[15] Waga, T.; Nishizaki, T.; Miyakawa, I.; Ohrui, H.; Meguro, H. *Biosci. Biotech. Biochem.* **1993**, *57*, 1433.
[16] Leland, D. L.; Kotick, M. P. *Carbohydr. Res.* **1974**, *38*, C9-C11.
[17] Youssefyeh, R. D.; Verheyden, J. P. H.; Moffatt, J. G. *J. Org. Chem.* **1979**, *44*, 1301.
[18] Vorbrüggen, H.; Ruh-Pohlenz, C. *Handbook of Nucleoside Synthesis,* John Wiley & Sons, Inc.; New York, **2001**.
[19] Trost, B. M.; Li, L.; Guile, S. D. *J. Am. Chem. Soc.*, **1992**, *114*, 8745.
[20] Trost, B. M.; Kuo, G. H.; Benneche, T. *J. Am. Chem. Soc.*, **1988**, *110*, 621.
[21] Hegedus, L. S; *Transition Metals in the Synthesis of Complex Organic Molecules*; University Science Books; Mill Valley, **1994,** Chapter 4.
[22] Trost, B. M.; Van Vranken, D. L. *Chem. Rev.* **1996**, *96*, 395.
[23] Trost, B. M.; Shi, Z. *J. Am. Chem. Soc.*, **1996**, *118*, 3037.
[24] Trost, B. M.; Lee, C. B. *J. Am. Chem. Soc.*, **2001**, *123*, 3687; Trost, B. M.; Lee, C. B. *J. Am. Chem. Soc*, **2001**, *123*, 12191.
[25] Paquette, L. A. *Aus. J. Chem.*, **2004**, *57*, 7.
[26] Schaffer, R. *J. Am. Chem. Soc.*, **1959**, *81*, 5452.
[27] Marx, A.; Summerer, D.; Detmer, I. *Eur. J. Org. Chem.*, **2003**, 1837.
[28] Secrist, J. A., III; Winter, W. J. *J. Am. Chem. Soc.*, **1978**, *100*, 2554.
[29] Haraguchi, K.; Takeda, S.; Tanaka, H.; Nitanda, T.; Baba, M.; Dutschman, G. E.; Chen, Y. C. *Bioorg. & Med. Chem. Lett.*, **2003**, *13*, 3775.
[30] Haraguchi, K.; Takeda, S.; Tanaka, H. *Org. Lett.*, **2003**, *5*, 1399.
[31] Jung, M. E.; Toyota, A. *J. Org. Chem.*, **2001**, *66*, 2624.

[32] Crich, D.; Hao, X. L. *J. Org. Chem.*, **1999**, *64*, 4016.
[33] Baret, N.; Dulcere, J. P.; Rodriguez J.; Pons, J. M.; Faure, R. *Eur. J. Org. Chem.*, **2000**, *8*, 1507.
[34] Hegedus, L. S.; Geisler, L.; Riches, A. G.; Salman, S. S.; Umbricht, G. *J. Org. Chem.*, **2002**, *67*, 7649.
[35] Casey, C. P.; Cyr, C. R.; Bogga, R. A. *Synth. Inorg. Met. Org. Chem.*, **1973**, *3*, 249.; Harvey, D. F.; Brown, M. F. *Tetrahedron Lett.*, **1990**, *31*, 2529.
[36] Foley, H. C.; Strubinger, L. M.; Targos, T. S.; Geoffrey, G. L. *J. Am. Chem. Soc.*, **1983**, *105*, 3064.
[37] *Ab initio* study see: Nakatsuji, H.; Ushio, J.; Han, S.; Yonezawa, T.; *J. Am. Chem. Soc.*, **1983**, *105*, 426.
[38] Collman, J. P.; Hegedus, L. S.; Norton, J. R.; Finke, R. G., "Principles and Applications of Organotransition Metal Chemistry", University Science Books, Mill Valley, CA, **1987**, pp. 373-375.
[39] McGuire, M. A.; Hegedus, L. S. *J. Am. Chem. Soc.*, **1982**, *104*, 5538.
[40] Tidwell, T. T., "Ketenes", Wiley, New York, NY, 1995.
[41] Sierra, M. A.; Hegedus, L. S. *J. Am. Chem. Soc.*, **1989**, *111*, 2335.
[42] Miller, M; Hegedus, L. S. *J. Org. Chem.*, **1993**, *58*, 6779.
[43] Rhychnovsky, S, D.; Dahanukar, V. H. *J. Org. Chem.*, **1996**, *61*, 8317.
[44] Kagan, H. B.: Fiaud, J. C. *Top. Stereochem.*, **1985**, *18*, 249.
[45] Trost, B. M. *Acct. Chem. Res.* **1996**, *29*, 355.
[46] Noyori, R.; Tokunaga, M.; Kitamura, M. *Bull. Chem. Soc. Jpn.*, **1995**, *68*, 36; Kitamura, M.; Tokunaga, M.; Noyori, R. *J. Am. Chem. Soc.*, **1993**, *115*, 144.
[47] Hirsch, R.; Hoffmann, R. W. *Chem. Ber.* **1992**, *125*, 975.
[48] Bäckvall, J. E.; Granberg, K. L. *J. Am. Chem. Soc.*, **1992**, *114*, 6858; Bäckvall, J. E.; Byström, S. E.; Nordberg, R. E. *J. Org. Chem.*, **1984**, *49*, 4619.
[49] Pd(II) allyl acetate epimerizations: Henry, R. M. *J. Am. Chem. Soc.*, **1972**, *94*, 5200.
[50] Overman, L. E.; Knoll, F. M. *Tetrahedron Lett.*, **1979**, *4*, 321.

CHAPTER TWO

STUDIES TOWARD THE TOTAL SYNTHESIS OF PLAKEVULIN A

I. Introduction and Background

The marine sponges of the genus *Plakortis* have proven to be a rich source of unique oxylipins and peroxides[1,2,3] that are biosynthetically diverse natural products. These naturally occurring fatty acid derivatives all have the common structural features of a fully saturated 16-carbon alkyl chain and at least one methyl ester functionality. Their wide range of biological activity includes the inhibition of L1210 leukemia cells,[4] protein kinase C, and DNA polymerases α and γ,[5] and their structural complexity makes them interesting synthetic targets.

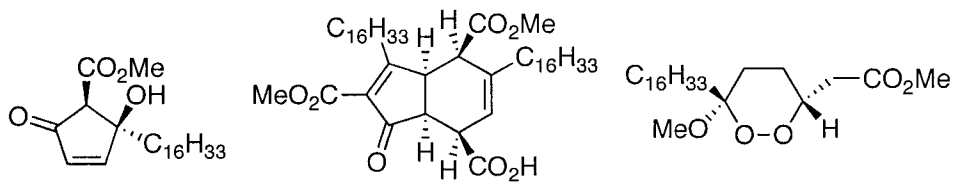

Untenone A(**122**) Manzamenone A (**123**) Plakorin (**124**)

Figure 2.1 Natural Products Isolated from the *Plakortis* Sponge

Plakevulin A (**125**), a new cytotoxic oxylipin isolated from an Okinawan *Plakortis* sponge, is an untenone A congener possessing a levulinyl ester. Untenone A (**122**) has been isolated as a racemate[6] and it is thought that a simple reduction and esterification can produce plakevulin A. Untenone A is thought to be a precursor to manzamenones A-F in the biosynthetic pathway.[7] Although

the manzamenones have demonstrated biological activity against protein kinase C, untenone A possesses potent anitproliferative activity (IC_{50} = 0.4 mg/mL) against L1210 leukemia.

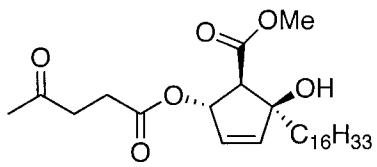

Plakevulin A (**125**)

Figure 2.2 Plakevulin A

Because of their interesting structural and biological activity, untenone A and the manzamenones have been the focus of several synthetic investigations. These syntheses have involved a variety of strategies that include a key [3+2] annulation, enantioselective deprotonation with a chiral lithium amide base, and a domino aza-Claisen/Mannich cyclization.

Takeda and coworkers reported the first synthesis of (±)-untenone A in 1994.[8] In five steps from β-(phenylthio)acryloylisilane, (±)-untenone A was synthesized utilizing a key [3+2] annulation of **129** with the lithium enolate of 2-octadecanone. β-(phenylthio)acryloyl trimethylsilane (E/Z mixture)[9] reacted with lithium enolate **127** to produce diastereomeric cyclopentenols **128** and **129**. Treatment of the diastereomeric mixture with *n*-Bu_4NF, followed by alcohol protection as a methoxymethyl (MOM) ether gave **130** in 89% yield. α-Methoxycarbonylation of **130** with LDA and methyl cyanoformate afforded the β-keto esters **131** in 50% yield as a 2:1 inseparable mixture of epimers. Treatment of **131** with acetic acid and *conc.* hydrochloric acid (50:1) at room temperature for 30 minutes gave (±)-untenone A (**122**) as a single diastereomer in 54% yield.

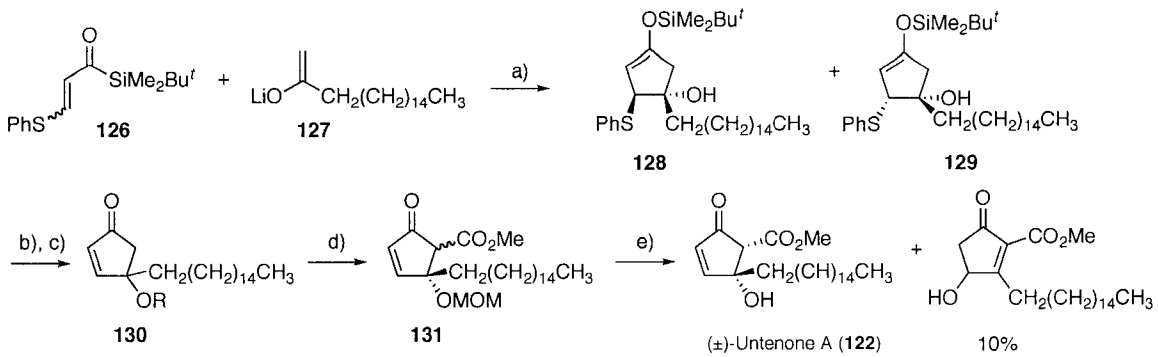

Scheme 2.1 (a) –80 to –30°C, THF, 56% (74% **7**, 89% **8**); (b) *n*-Bu_4NF, THF, CH_2Cl_2, r.t., 30 min.; (c) MOMCl, *i*-Pr_2NEt_2, CH_2Cl_2, 89%; (d) LDA, -80°C, 30 min. then $NCCO_2Me$, THF, HMPA, -80 to –50°C over 1h, 50%; (e) AcOH-*c*-HCL (50:1) r.t., 30 min. 54%

The first synthesis of (-)-untenone A was reported in 1995 by Asami and coworkers.[10] Utilizing the asymmetric transformation of *meso*-epoxides to allylic alcohols by enantioselective deprotonation with a chiral lithium amide base, Asami was able to obtain information about the absolute stereochemistry and optical purity of natural untenone A.

1-Hexadecyl-3-cyclopenten-1-ol was obtained in 62% yield by the addition of hexadecylmagnesium bromide with 3-cyclopentenone in the presence of $CeCl_3$. The *meso*-epoxide was obtained through the hydroxyl-directed epoxidation of **132** with *t*-butyl hydroperoxide and catalytic $VO(acac)_2$. Deprotonation of **133** with (*S*)-2-(pyrrolidin-1-ylmethyl)pyrrolidide[11] gave alcohol **134** in 75% yield with 89% *ee*. Oxidation with PCC, formation of the β-keto ester,[12] and removal of the silyl protecting group afforded (-)-untenone A **122** in 69% yield. The synthesized (-)-untenone A demonstrated a rather large specific rotation compared to the natural untenone A, which indicates that the isolated untenone A is likely to be almost racemic.

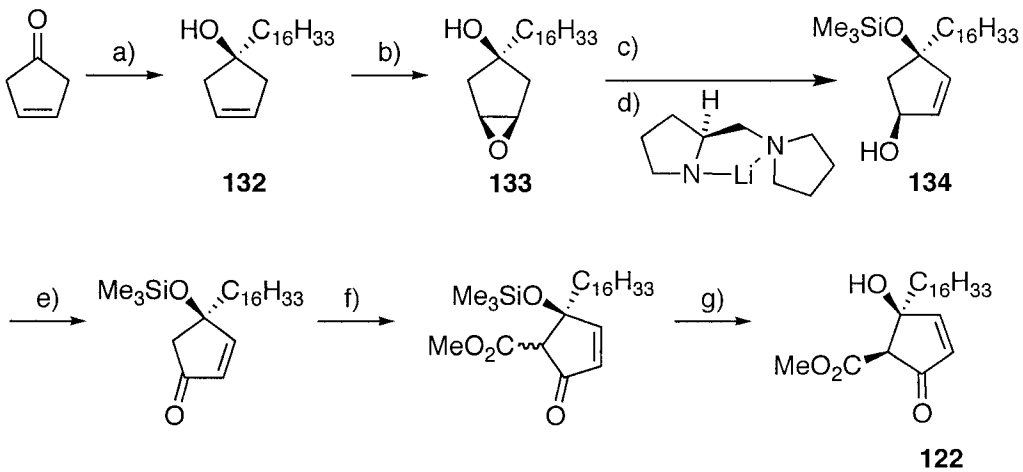

Scheme 2.2 (a) $C_{16}H_{33}MgBr$-$CeCl_3$, Et_2O, 0°C, 1 h, 62%; (b) *t*-BuOOH-$VO(acac)_2$, CH_2Cl_2, r.t., 15h, 86%; (c) TMSCl, imidazole, DMF, r.t., 2h, 91%; (d) toluene, 0°C, 5 h, 75%; (e) PCC, CH_2Cl_2, r.t., 5h, 67%; (f) 1.) LDA, -70°C, 1h, 2.) $CNCO_2Me$, -70° to –50°C, 1h, THF-HMPA; 65% (dr 5.5:1); (g) Dowex®, 50W-X8, MeOH, r.t., 2d; 69%.

Yamada and coworkers reported the syntheses of optically active (+)- and (-)-untenone A from (*S*)-4-[(*tert*-butyldimethylsilyl)oxyl]-2-cyclopentenone.[13] Addition of an alkylsamarium (III) reagent[14] to **135** produced alcohols **136** and **137** in 59% and 39% respectively. The diastereomers were separated at this stage and subjected to the same reaction procedures. Functional group manipulation, followed by formation of the β-keto esters with LDA and methyl cyanoformate produced **138** as a (3:2) diastereomeric mixture. Treatment of the β-keto esters with AcOH and concentrated HCl (50:1) gave (-)-untenone A as a single isomer. (+)-Untenone A was synthesized *via* enone **138** from alcohol **137**.

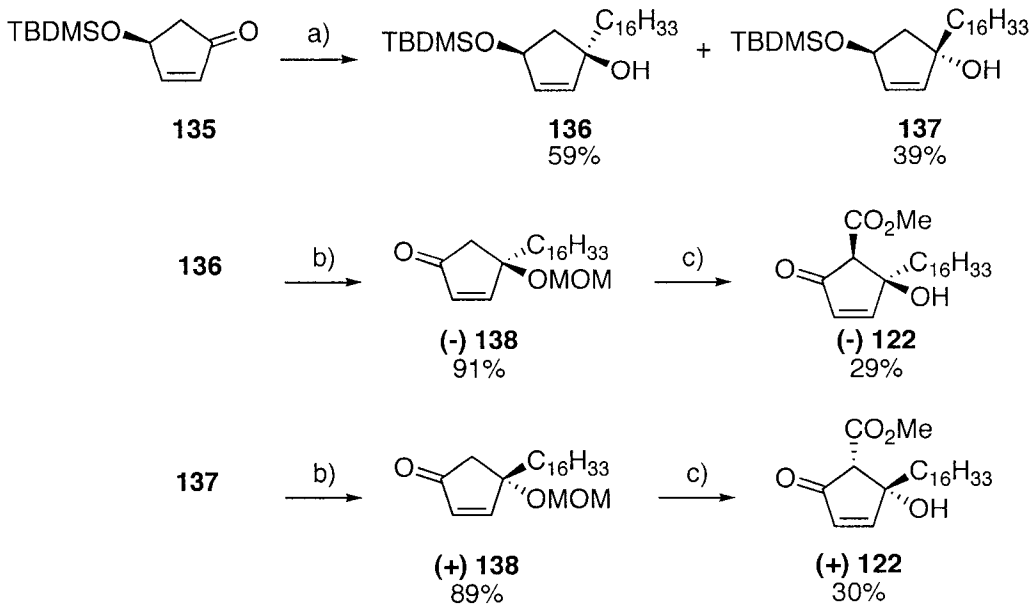

Scheme 2.3 (a) $CH_3(CH_2)_{14}CH_2SmI_2$, THF-HMPA, -78°C; (b) 1.) MOMCl, *i*-PrNEt, CH_2ClCH_2Cl, 50°C, 2.) Bu_4NF, THF, r.t., 3.) Jones Reagent, H_2CO, 0°C; (c) 1.) LDA, THF-HMPA, -78°C, then $NCCO_2Me$, -42°C, 2.) AcOH,-*c*.HCl (50:1).

A domino aza-Claisen/Mannich cyclization reaction from a chiral α-alkoxy enamine was utilized in Florent's formal total synthesis of (±)-untenone A.[15] Treatment of acrolein **139** with hexadecylmagnesium bromide gave the allylic alcohol **140** in 52% which was subsequently protected as its *p*-methoxymethyl ether. Oxidation to glycol **141**, followed by oxidation with lead tetraacetate gave **142** in 95% yield from **141**. Treatment of **142** with Florent's Claisen/Mannich reaction conditions gave cyclopentenone **143** in 38% yield, together with 12% of recovered starting material **142** and 19% of methoxymethyl ester **144**.

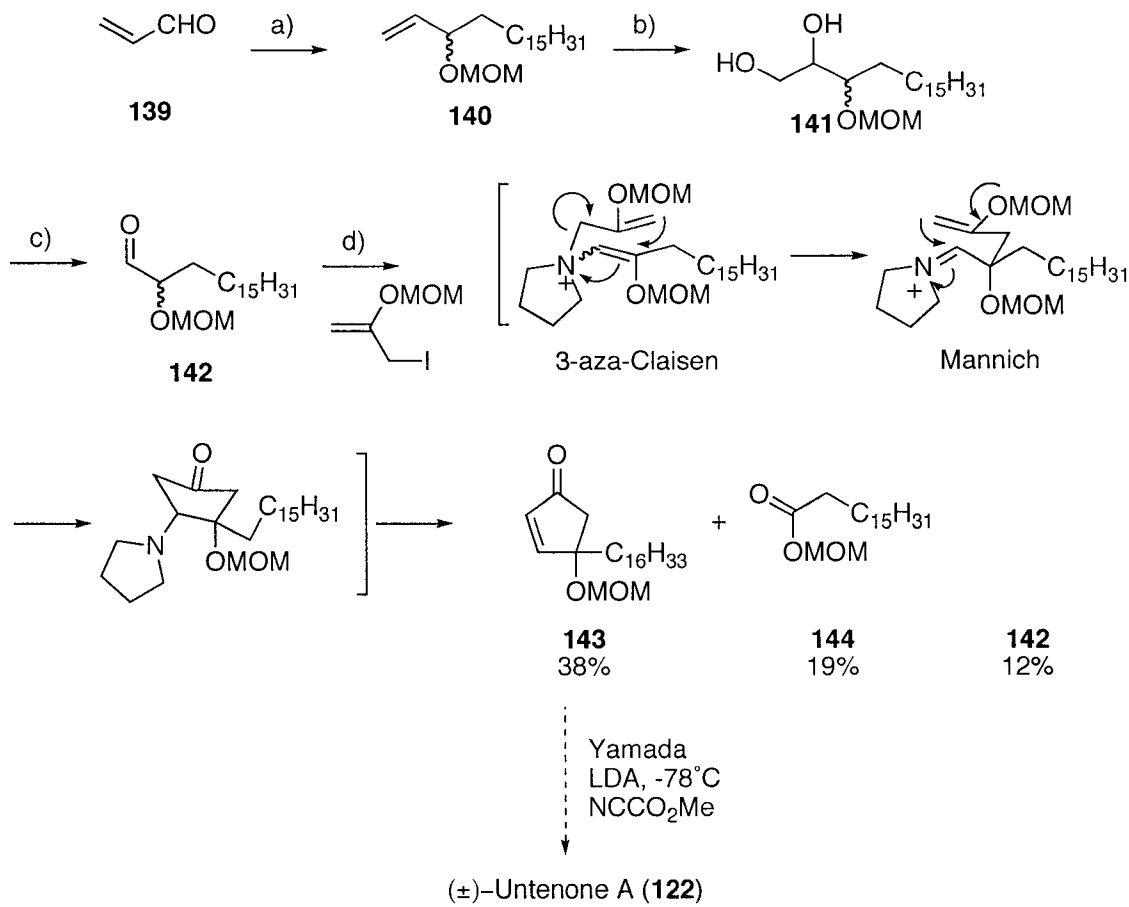

Scheme 2.4 (a) $C_{16}H_{33}MgBr$, Et_2O, 0°C; (b) MOMCl, $EtN(iPr)_2$, CH_2Cl_2, 0°C (c) OsO_4, NMO acetone/H_2O, 0°C to room temp.; (c) [$Pb(OAc)_4$], Benzene, 0°C to r.t.; (d) pyrolidine, MeCN/toluene, 50°C then CH_2=CH(MOM)-CH_2I

Whitehead believes that (±)-untenone A is a precursor in the 'predisposed' biosynthetic pathway towards the manzamenones. His investigations have led to a short, high yielding synthesis of (±)-untenone A (**122**) that is suitable for large-scale preparation and could be readily applied to the preparation of analogues of the natural material.

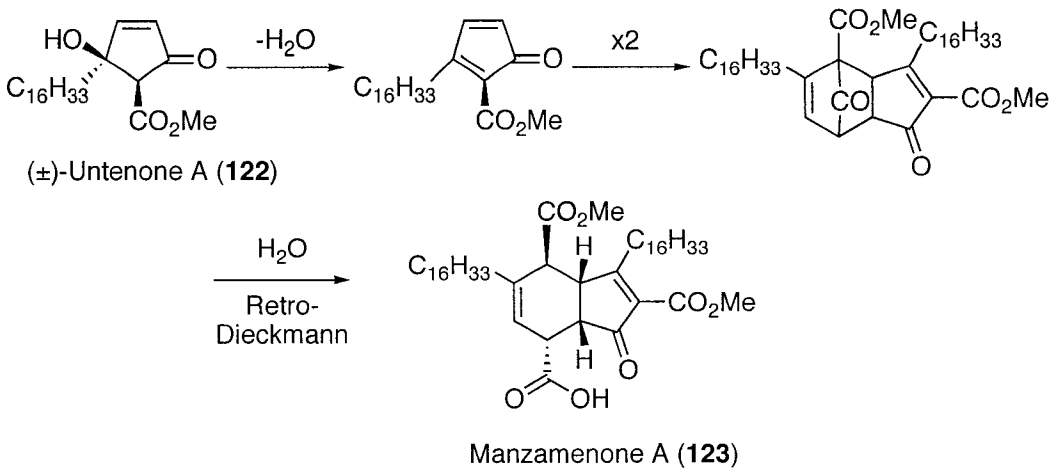

Scheme 2.5 Whitehead's 'predisposed' biosynthetic pathway towards Manzamenone A

Furan-2-ylacetonitrile **145** underwent a Friedel Crafts acylation with $C_{15}H_{31}COCl$ and $SnCl_4$ to produce acylfuran **146**. The Huang-Milon modification of the Wolff-Kishner reduction, followed by esterification with $TMSCHN_2$ gave ester **147** in 31% yield. Oxidation of the furan ring with bromine in methanol gave bis-acetal **148** as a 1:1 mixture of diastereomers in 96% yield. Acidic hydrolysis of **148** in aqueous dioxane followed by base treatment resulted in an 'aldol-type' cyclization to give the single diastereomer (±)-untenone A. Simple heating of a neat sample of (±)-untenone A (**122**) to just above its melting point for 24 hours resulted in the principle product in 26% yield.

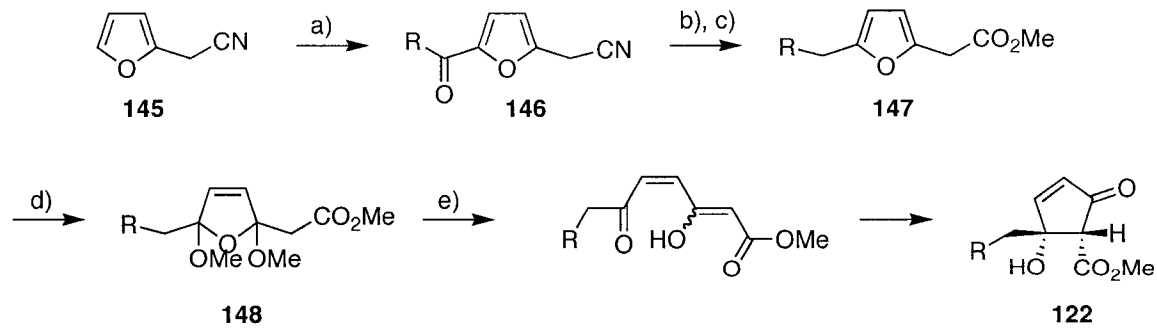

Scheme 2. 6 (a) R = $C_{15}H_{31}$; ROCl, $SnCl_4$, -5°C, 74%; (b) H_2NNH_2, NaOH, $HOCH_2CH_2OH$, Δ, 43%; (c) $TMSCHN_2$, MeOH, RT, 72%; (d) Br_2, MeOH, Na_2CO_3, -5°C to RT, 79%; (e) Dilute H_2SO_4 (aq.), dioxane, r.t., then 1.0 M $NaHCO_3$ 62%.

II. Rationale

The compounds isolated from the *Plakortis* sponge possess important biological activity as well as significant synthetic challenges due to their three contiguous stereogenic centers contained in the cyclopentene ring system. Untenone A, an important intermediate towards the synthesis of plakevulin A, might be obtained through well-established cyclobutanone chemistry developed by the Hegedus group. The proposed route involves formation of cyclobutanone **150** from the photocycloaddition reaction between chromium carbene complex **151** and chiral ene carbamate **152**. Cyclobutanone **150** could undergo a ring expansion, giving the desired cyclopentane core and the ester group in a single step. Elimination of the chiral auxiliary could provide the desired untenone A intermediate **148**. Subsequent hydrogenation/reduction and deprotection of the β-keto ester, followed by acylation with levelunic acid would give the desired plakevulin A **125**.

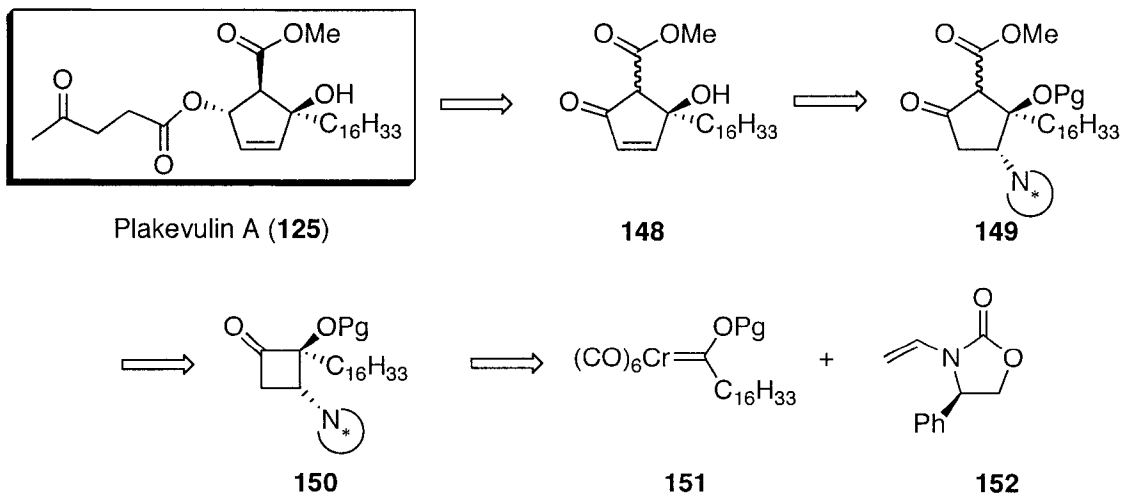

Plakevulin A (**125**) **148** **149** **150** **151** **152**

Scheme 2.7

The carbene synthesis began with investigations into the addition of a removable protecting group on the anionic acyl oxygen since the target contains a free hydroxyl group. Alkyllithium **154** ($C_{16}H_{33}Li$) was added to chromium hexacarbonyl **153** to form anionic acyl intermediate **155**. Addition of tetramethylammonium bromide to the ionic intermediate was expected to produce tetramethylammonium salt **156** which could form a mixed anhydride with pivalic chloride. A suitable protecting group could be installed through nucleophilic displacement of the mixed anhydride with an alcohol, thus giving protected alkoxychromium carbene complex **157**.

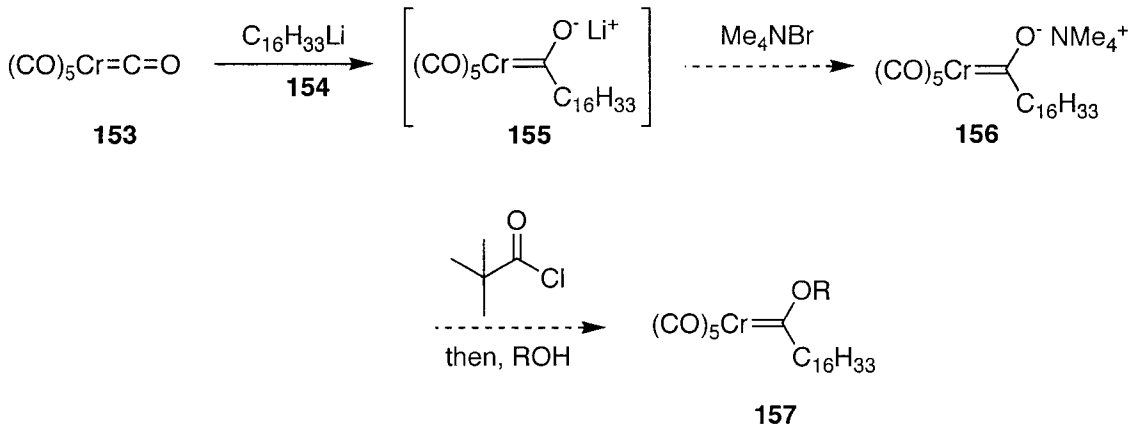

Scheme 2.8 Formation of an alkoxy chromium carbene complex

The addition of an alkyllithium to chromium hexacarbonyl produces lithiate **155** which contains a very tight ion pair between oxygen and lithium. This tight ion pair prevents O-acylation from occurring, therefore alkylation of **155** can only occur with extremely reactive alkylating agents or by forming the tetramethylammonium salts of the lithiate under phase transfer conditions.[16] Utilizing literature procedures, tetramethylammonium bromide was added to

lithiate **155**, but unfortunately, the desired tetramethylammonium salt **156** was not obtained. Instead, a tan precipitate, insoluble in organic solvents, was isolated and did not have any characteristics of carbene complexes.

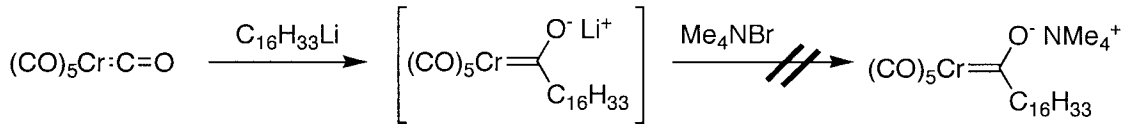

Scheme 2.9

Since the tetramethylammonium salt intermediate could not be obtained, an alternative route to the desired alkoxychromium carbene complex was investigated. Potassium could be used as a counter ion because potassium and oxygen possess a loose ion pair relative to lithium and oxygen. The weaker ion pair between potassium and oxygen would allow for O-alkylation with triflates[17] or sulfonium salts[18] which have demonstrated great success in the formation of alkoxychromium carbene complexes (Scheme 2.10).

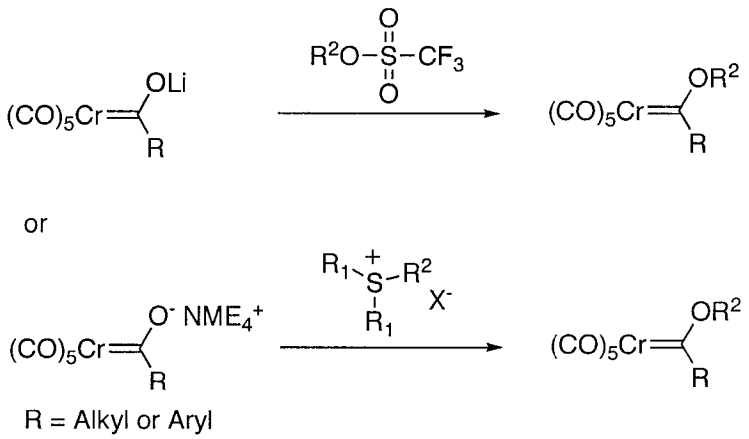

Scheme 2.10

The anionic acyl intermediate may be obtained through two general methods. The simplest involves the addition of an alkyllithium to chromium hexacarbonyl (Method 1). This gives lithium acyl intermediate **155** which can be alkylated with a triflate or sulfonium salt to provide alkoxychromium carbene complex **157**. Alternatively, chromium hexacarbonyl can be added to a potassium-graphite intercolate to produce dianion **158**. The addition of an acyl chloride species to **158** can give anionic intermediate **155** (Method 2). Again, formation of alkoxychromium carbene complex **157** can be obtained through addition of a hard alkylating agent to the anionic acyl intermediate **155** (Scheme 2.11).

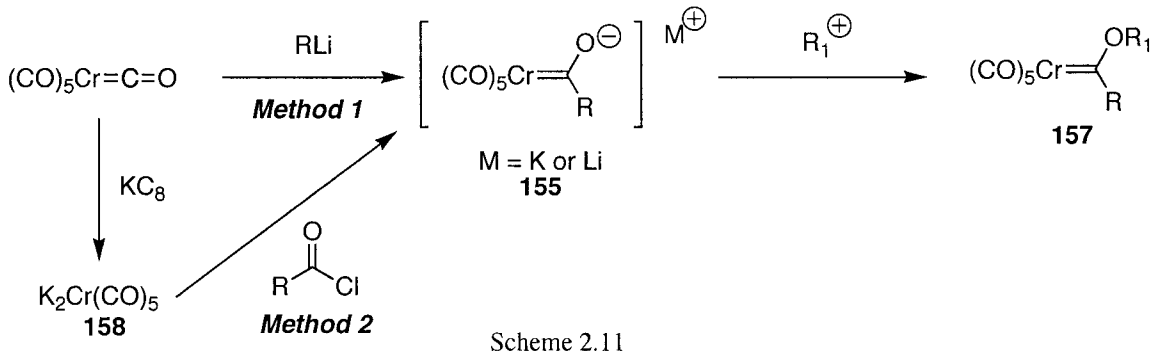

Scheme 2.11

Matusyama[18] has synthesized a variety of alkyldiarylsulfonium salts for the successful preparation of alkoxycarbene complexes via lithiate formation, followed by addition of tetramethylammonium bromide. Several sulfonium salts were prepared by reacting a large excess of Ph_2S or a dialkyl sulfide with alkyl halides in the presence of $AgBF_4$ or other counter ions.

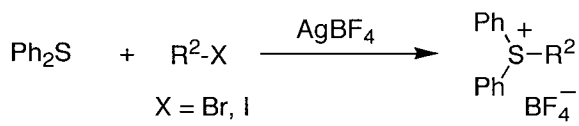

Scheme 2.12

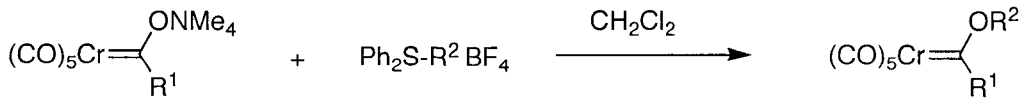

R^1 = Me, *n*-Bu, Ph

R^2 = Me, *i*Pr, $(CH_2)_7CH_3$, $(CH_2)_2OEt$, $(CH_2)_3CN$, $(CH_2)_3Cl$, $(CH_2)_3OH$, $CHCO_2Me$,

Scheme 2.13

Utilizing both methods of carbene preparation (Scheme 2.11), sulfonium salts were used in an attempt to alkylate the anionic acyl intermediate. Only entry 1 was successful in carbene formation.[19] Unfortunately, the low cyclobutanone yields from the subsequent photochemical cycloaddition and the substantial cost of silver tetrafluoroborate made the use of sulfonium salts as alkylating agents impractical for this synthesis.

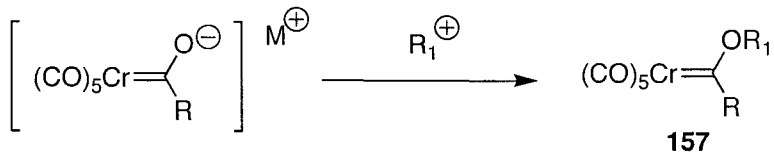

Method 1: M^+ = Li
Method 2: M^+ = K

155 **157**

Table 2.1 Alkylation attempts for the synthesis of alkoxy chromium carbene complex.

Entry	Method	R ⊕	Result
1	2	Me_2S^+PMB BF_4^-	20%
2	2	$Ph_2S^+CH_2Ph$ BF_4^-	9%
3	2	Me_2S^+PMB HSO_4^-	Recovered "ate" Complex
4	1	Me_2S^+PMB BF_4^-	Recovered "ate" Complex
5	1	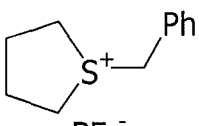 BF_4^-	Recovered "ate" Complex

Barluenga[20] and others[21] have reported the synthesis of alkoxychromium complexes via alkyllithium addition to chromium hexacarbonyl, followed by addition of benzyl and allyl triflates as alkylating agents (Scheme 2.14). They found that complexes bearing a benzyl group on oxygen quickly decomposed upon chromatographic purification, preventing their characterization. Utilizing literature procedures, [20] benzyl triflate was synthesized and transferred via a cannula into a flask containing the anionic acyl intermediate at –25°C. During removal of the solvent, the carbene began to decompose at room temperature. Additional attempts to synthesize benzyl protected alkoxychromium carbene complexes were pursued, however all were unsuccessful (Table 2.2).

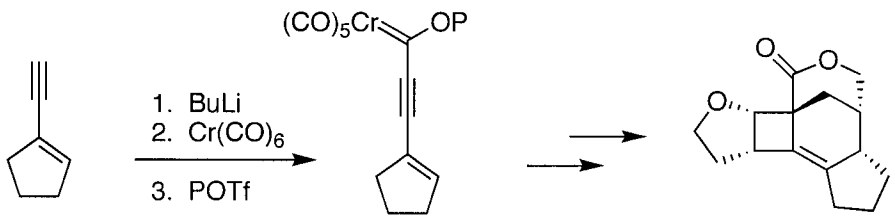

P = allyl, Benzyl

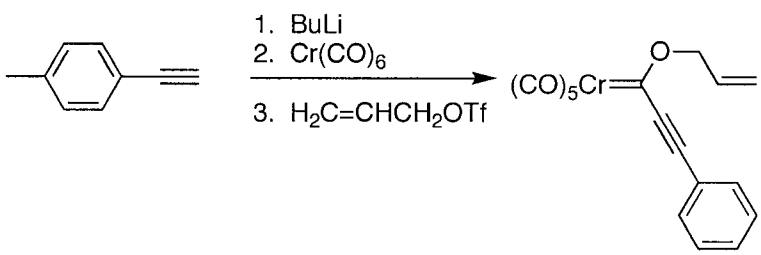

Scheme 2.14

48%

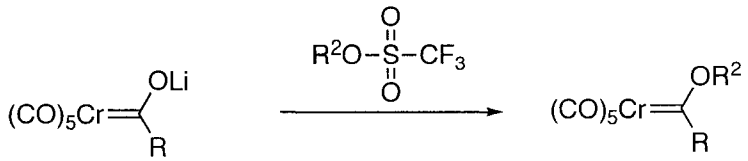

Table 2.2 Triflate addition to the anionic acyl intermediate

R =	R^2OTf	Result
$C_{16}H_{33}$	PMBOTf	Decomposition of PMBOTf
$C_{16}H_{33}$	BnOTf	Recovered "ate" Complex
C_4H_9	BnOTf	Decomposition of alkoxycarbene

Since a benzyl protected carbene complex could not be synthesized, studies with the O-ethyl analog were next pursued with the intent of deethylation at a later stage. The anionic acyl intermediate **155** was alkylated with Meerwein's reagent[22] to give alkoxychromium carbene complex **159** in 59% yield. Complex **159** underwent the photocycloaddition reaction with chiral ene carbamate **152** in 79% yield to give ethoxy-substituted cyclobutanone **160**.

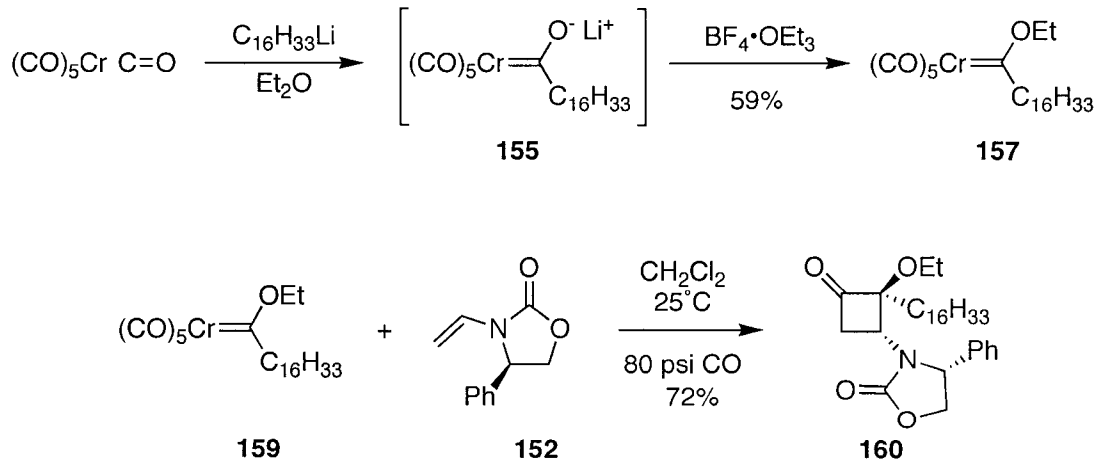

Scheme 2.15

The next step in the synthesis was to perform a ring-expansion reaction and installation of an ester moiety (Scheme 2.16). Many investigators have recognized cyclobutanones as an excellent source of cyclopentanones via one-carbon ring expansions. Five membered rings are ubiquitous in nature and therefore ring expansions of cyclobutanones to cyclopentanones provide a general approach to a variety of other cyclic structures. There are several general methods for the ring expansion of cyclobutanones reported in the literature. Gadwood[23] and Cohen[24] have described the expansion of several cyclobutanones to a variety of cyclopentanones using α-lithioalkyl aryl selenoxides and sulfoxides (Scheme 2.17). In 1987, Trost and Mikhail[25] developed a simple one-pot procedure for a ring-expansion of cyclic ketones with concomitant introduction of a α-methoxy group (Scheme 2.18).

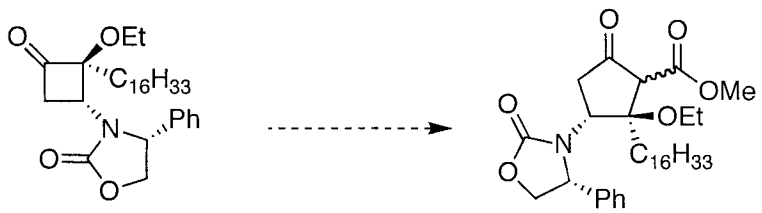

160 Scheme 2.16 **161**

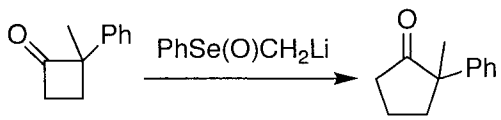

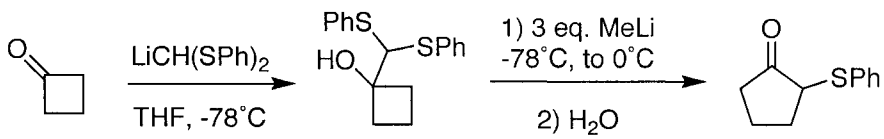

162

Scheme 2.17

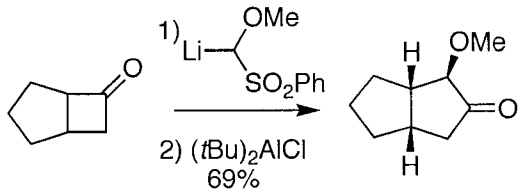

Scheme 2.18

Ring expansions of cyclobutanones with diazo compounds are also useful for the production of highly functionalized cyclopentanones. Hegedus et al. applied the regioselective ring expansion of β-substituted α-methyl-α-methoxy cyclobutanones with diazomethane to obtain valuable starting materials for butenolides.[26] The homologation of the functionalized cyclobutanone **163** led to a 97:3 mixture of regioisomeric cyclopentanones **164** and **165** in 89% yield.

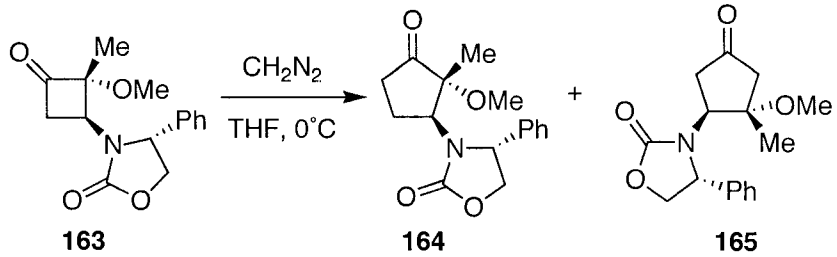

Scheme 2.19

From a synthetic view, the Lewis acid catalyzed ring expansion of cyclic ketones with diazoacetic esters is a very useful transformation for homologation and simultaneous formation of β-keto esters functionalities. Greene and coworkers[27] developed a regioselective ring enlargement of the cyclopentane-annelated cyclobutanones **166** to the bicyclo[3.3.0]octanone **167** with ethyl diazoacetate. A variety of Lewis acids were screened to investigate the regioselectivity of the expansion (Table 2.3) and they found that antimony pentachloride with ethyl diazoaceate produced **167** in 63% yield with a 98:2 mixture of regioisomeric products.

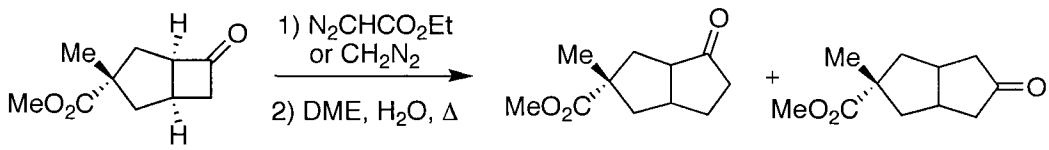

166 **167a** **167b**

Table 2.3 Conditions for diazo-mediated ring expansion of **166**.

Reagent	ring-expansion conditions	**167a** : **167b** ratio
CH_2N_2 (large excess)	C_2H_5O-CH_3OH (4:1) 0°C, 5 h	50 : 50
N_2CHCO_2Et (1.7 eq.)	$(C_2H_5)_2O$, BF_3•OEt_2(1.7 eq.) 0°C, 1 h	68 : 32
N_2CHCO_2Et (1.7 eq.)	CH_2Cl_2, $(C_2H_5)_3O^+BF_4^-$ (1.7 eq.), -30°C, 48 h	67 : 33
N_2CHCO_2Et (2.1 eq.)	CH_2Cl_2, $SbCl_5$, (0.44 eq.) -78°C, 2 h	98 : 2

Sulfur ylide chemistry has a rich history of successful carbocyclic ring expansions of cyclobutanones.[28] Previously, the Hegedus group reported the novel Lewis acid promoted one-pot ring-enlargement reaction of cyclobutanone **168** to cyclopentanone **169**.[29] The sulfur ylide was generated from trimethylsulfoxonium iodide ($Me_3S(O)I$) and sodium hydride. Using a catalytic amount of scandium triflate ($Sc(OTf)_3$) , the cyclopentanone **169** was obtained in 79% yield (Scheme 2.20).

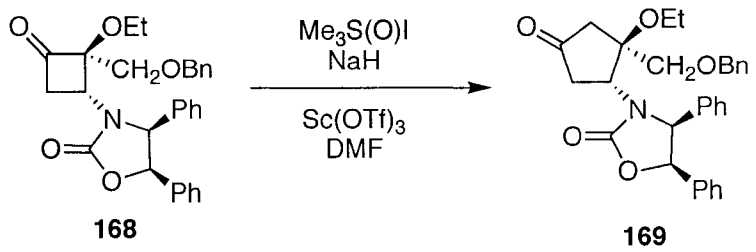

168 **169**

Scheme 2.20

Ring expansions of cyclobutanones with the formal insertion of simple methylenes possess the risk of competing epoxide formation as a side reaction. It was found that epoxide formation can be suppressed by the addition of a Lewis acid in ring homologation reactions. The addition of Lewis acids diminishes the amount of epoxide formation, thus promoting skeletal rearrangement over epoxidations[30] in a variety of sulfur-mediated ring expansion reactions.

Trost has added substituted α-lithiomethyl phenylsulfones to a variety of cyclobutanones that have produced the appropriate ring expanded products (Scheme 2.17). The observed regioselectivity of the products had migration of the more substituted carbon occurring when a cation-stabilizing substituent on the methylsulfone is present (e.g. OMe, SPh). The same methodology might be applied to cyclobutanone **160** by utilizing a sulfur ylide that contained a methyl ester moiety (Scheme 2.16). It is possible that the ester moiety would destabilize a positive charge if the reaction proceeded through a stepwise mechanism; therefore it was rationalized that the reaction would be concerted to avoid any unfavorable intermediates or formation of the epoxide.

Dimethyl(carbomethoxymethylene)sulfurane was prepared according to literature procedures[31] by the addition of methyl bromoacetate to dimethyl

sulfide to produce sulfonium salt **171**. A solution of 50 wt % sodium hydroxide was added to **171** to produce ylide **172** in near quantitative yield (Scheme 2.21).

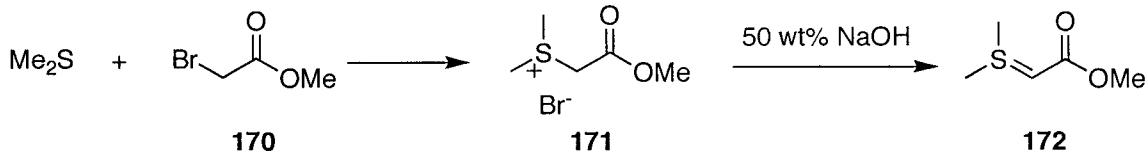

170 **171** **172**

Scheme 2.21

Ylide **172** was added to cyclobutanone **160** in CH_2Cl_2 in the presence of $Sc(OTf)_3$. After heating at reflux overnight, initial examination of the ^1H NMR spectrum of the crude reaction mixture showed that the starting material had been completely consumed to afford a new product. The data obtained from the ^1H NMR spectrum seemed to correspond to the desired ring-expanded product **161**. The α-methyne proton appeared at 3.72 ppm, which corresponded to estimated values from ChemNMR Pro compared to the other regioisomers (Figure 2.3). A ^1H-^1H COSY (correlated spectroscopy) provided a more detailed look at the proton relationships of compound **161** which supported the proposed structure. Also, the mass spectrometry data matched the proposed structure's molecular weight. Unfortunately, once the data from the ^{13}C experiment was obtained, it was found that compound **161** did not contain a ketone peak, but the ester and the carbamate peak were present at 168.7 and 157.9 ppm respectively.

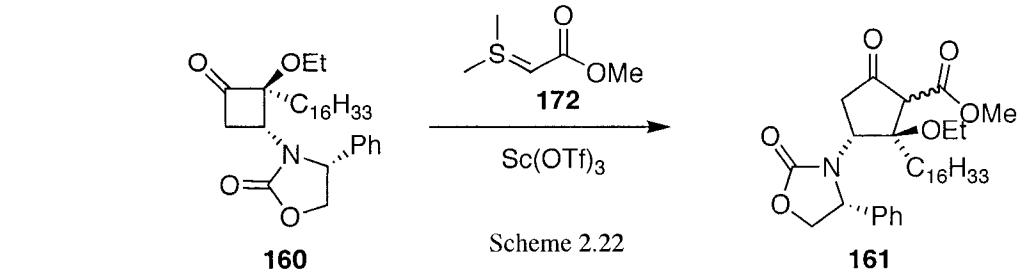

Scheme 2.22

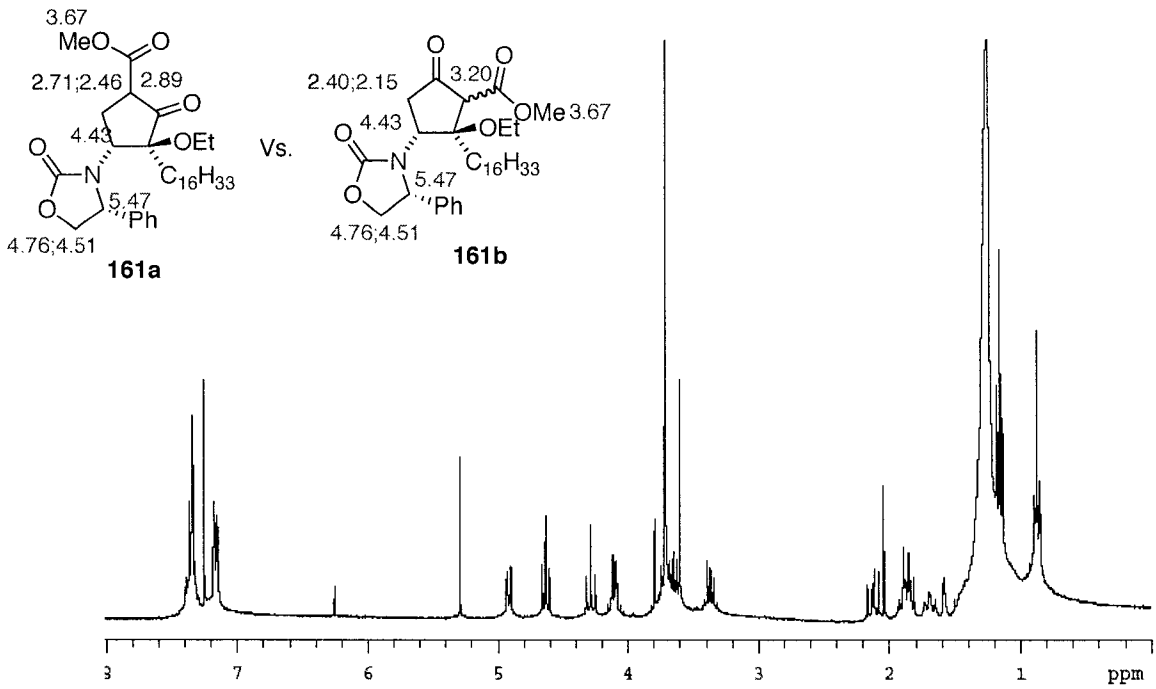

Figure 2.3 The ^{1}H NMR spectrum of **161**

Closer examination of all spectroscopic data for **170** led to the conclusion of another possible product that may be obtained from sulfur-mediated ring expansion reaction. Epoxides are a competitive side product that can occur instead of bond migration in the ylide ring expansion reaction. After assignment of the fully characterized data, epoxide **173** was assigned as the product of the sulfur ylide ring expansion reaction with cyclobutanone **160**.

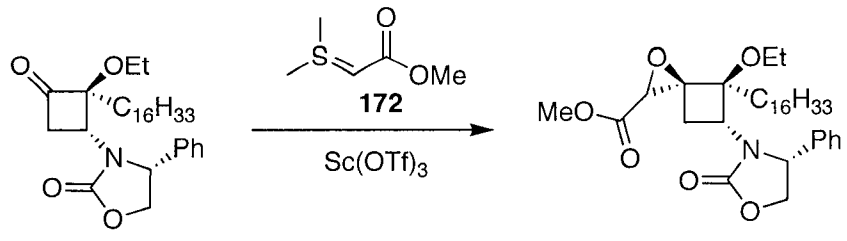

Scheme 2.23

Attention was shifted to the possible ring opening or isomerization of epoxide **173** to the desired cyclopentanone **161b**. Leriverend[32] and others[33,34] have reported the isomerization of spiroepoxides to cyclopentanones by the addition of lithium salts. Unfortunately, the rearrangement of epoxide **173** would have to go though an unfavorable carbocation α to an electron-withdrawing group during the bond migration step (Figure 2.4). Therefore, it was not surprising that when LiI and the Lewis acids were examined for skeletal rearrangement of epoxide **173** resulted in either decomposition or the epoxide remained unchanged (Table 2.4).

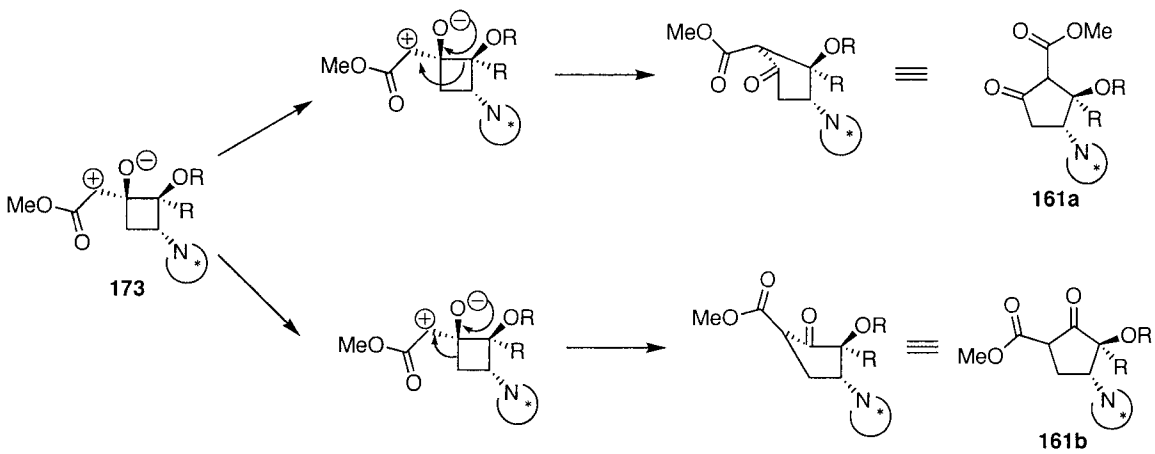

Figure 2.4 Rearrangement of epoxide **173** to cyclopentanone **161a** or **161b**.

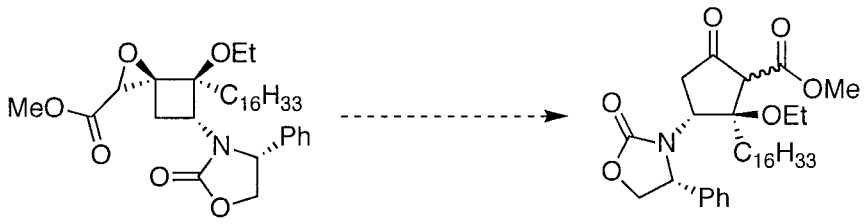

173 161a

Table 2.4 Attempts at epoxide rearrangement

Conditions	Result
LiI	NR
LiI, Δ	decomposition
$Sc(OTf)_3$	NR
$TiCl_4$	NR
TMSI	NR

Since the sulfur ylide chemistry did not produce the desired β-keto ester, a diazo-mediated ring expansion reagent was pursued next. There are a variety of diazo ring expansion reagents that have been quite successful to provided β-keto esters from cyclobutanones. The addition of ethyl diazoacetate (EDA) to ketones usually proceeds selectively in high yield under mild conditions, resulting in a synthetically useful β-keto ester moiety.[35] In general, EDA is not nucleophilic enough to attack carbonyl groups, however, in the presence of a Lewis acid catalyst, the addition product is formed quite readily.

Liu and Ogino have examined the regioselectivity of BF_3•OEt_2 catalyzed ethyl diazoacetate ring expansions of several bridged, bicyclic cyclobutanones.[36]

They found that the homologation is not regiospecific and usually gives a mixture of isomeric β-keto esters, but insertion occurs preferentially at the less substituted side of the carbonyl group. As shown previously, ethyl diazoacetate has been successful in the ring expansions of bicyclic cyclobutanones (Table 2.2), but few examples exist of isolated cyclobutanone ring expansions. With little literature precedent for solitary cyclobutanone homologations with EDA, it was thought that the product's regioselectivity would result in the more substituted carbon migrating due to its ability to stabilize a positive charge during the transition state. Following literature procedure,[37] $BF_3 \cdot OEt_2$ was slowly added to the reaction flask that contained cyclobutanone **160** and EDA. The reaction progress was monitored by the evolution of nitrogen and the formation of the β-keto ester spot by TLC that stained purple with $FeCl_3$. Analysis of the crude ^{1H} NMR spectrum showed an extremely complex mixture of products had formed (Figure 2.5).

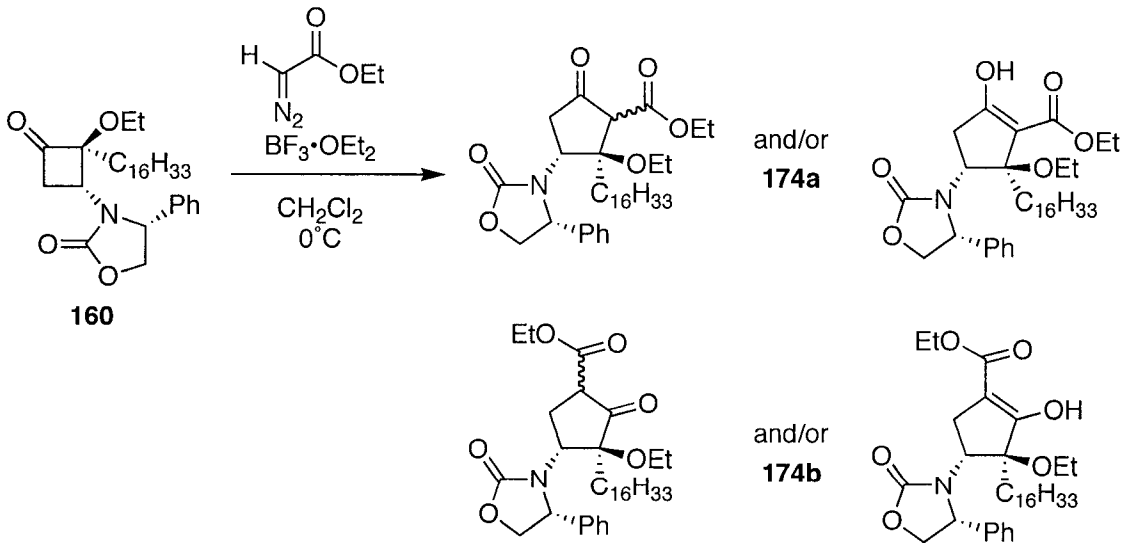

Scheme 2.24

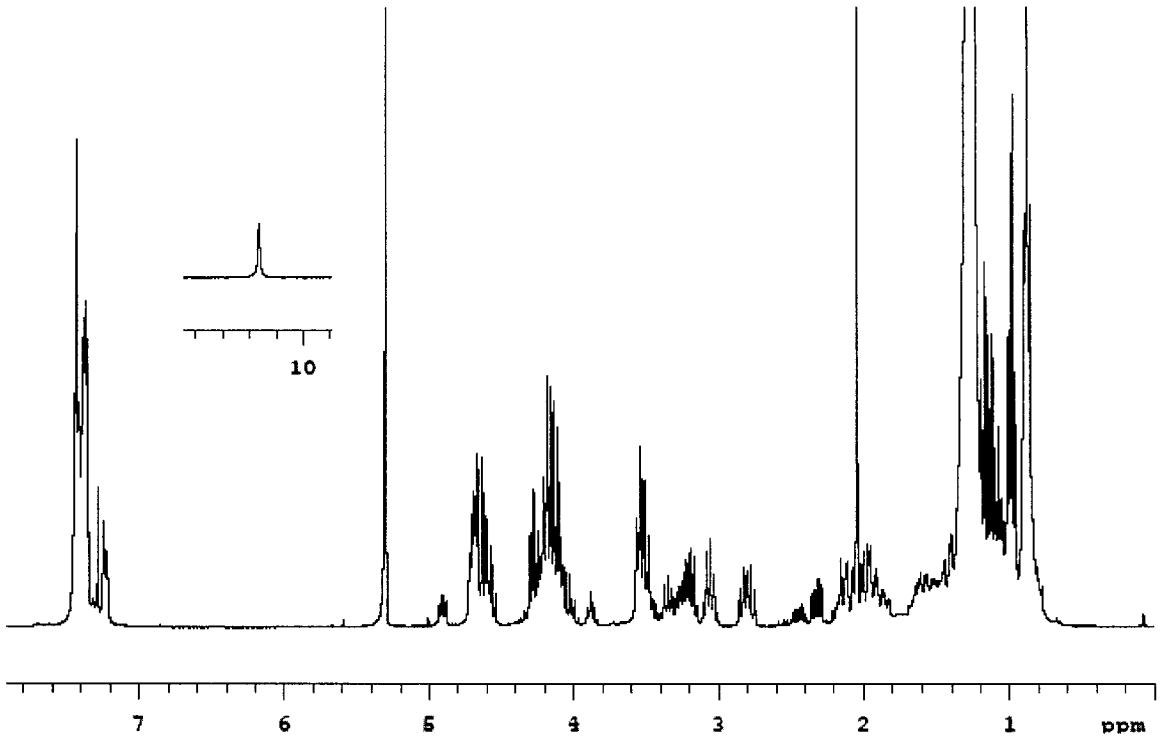

Figure 2.5 The ^{1}H NMR spectrum of **174.**

Since the isolated product mixture from the EDA ring expansion was so complex, a simpler model system was examined to try to aid in structure elucidation. Utilizing a literature procedure, [34] β-keto ester **176** was isolated in 60% yield as a 60:40 mixture of the keto and enol forms.[38] The crude ^{1}H NMR spectrum of the reaction mixture from cyclobutanone **175** was much more resolved than from **160**, yet it too was a mixture of products and therefore it did not provide any additional insight into the ring expansion reaction of cyclobutanone **160** (Figure 2.6).

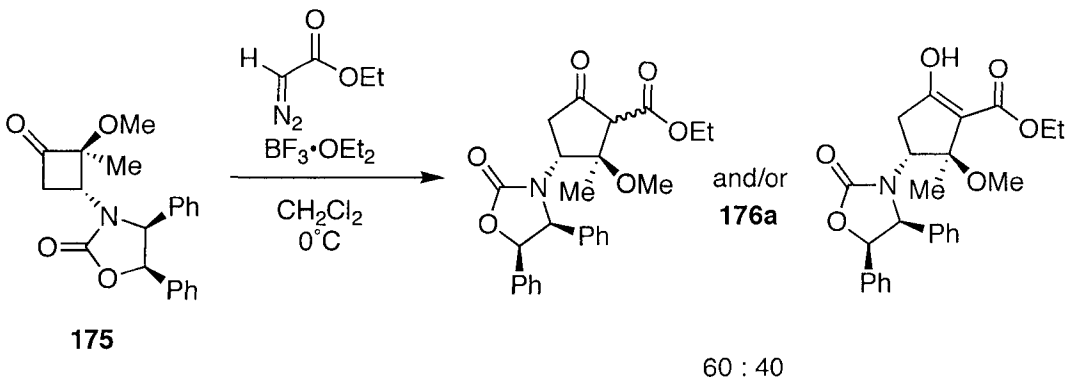

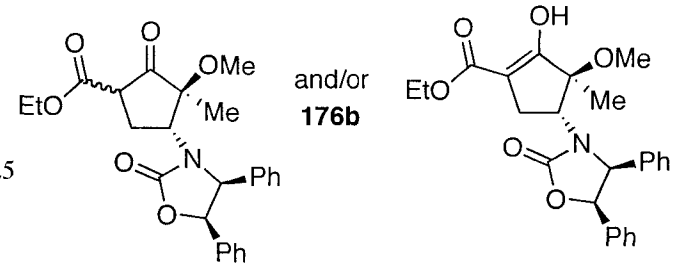

Scheme 2.25

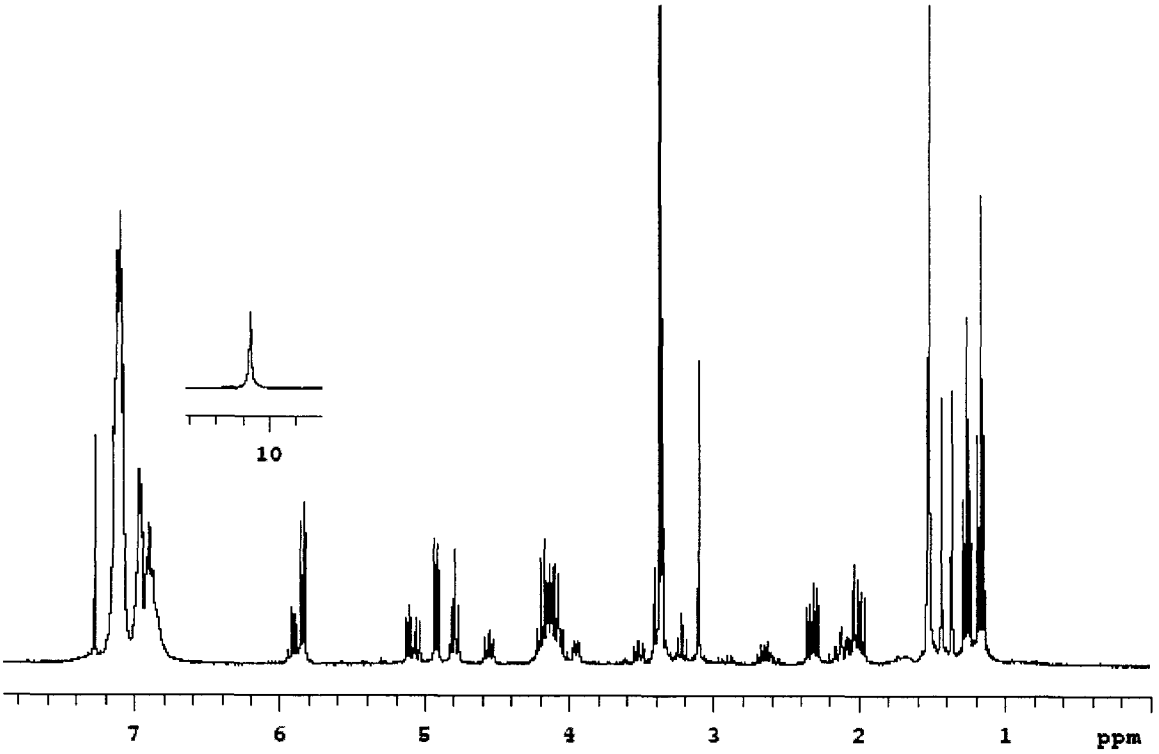

Figure 2.6 The 1H NMR spectrum of **176a/b**.

A variety of Lewis acids were screened in the ring expansion reaction of **160** in an attempt to simplify the product mixture (Table 2.5). In all cases, the same complex mixture was obtained. Unfortunately, all other spectroscopic techniques were ineffective for structure determination. In the infrared spectrum, the chiral auxiliary's carbamate stretch appeared at 1758 cm^{-1}, which masked any other carbonyl stretch that was present. The ^{13}C NMR spectrum also was inconclusive because diastereomeric β-keto esters, regioisomers, and tautomers could all be present in the mixture.

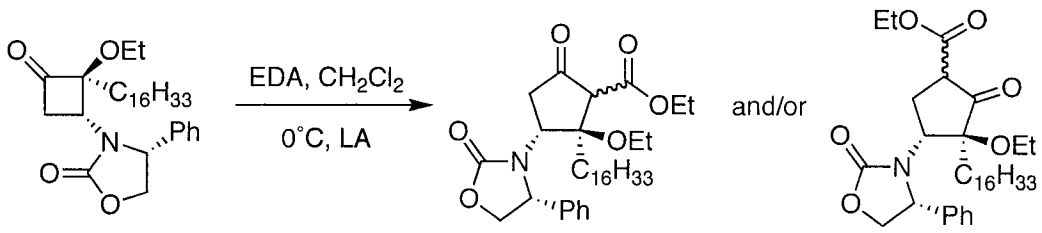

160 **174a** **174b**

Table 2.5 Lewis acid additions to the EDA ring expansion reaction

Conditions	Result
BF_3OEt_2, $SbCl_5$, BF_4OEt_3, $Sc(OTf)_3$, Me_3Al, $Yb(OTf)_3$	Mixture of Products

Structural elucidation of the product mixture from any of the Lewis acid catalyzed EDA ring expansion reaction proved to be futile. A portion of the complex mixture was due to the presence of enol tautomers of the products, and

it was postulated that if the formation these tautomers could be prevented by the removal of the enolizable α-proton, then it could be possible to elucidate the structure(s).

Yang and coworkers have reported the mild α-halogenation reactions of 1, 3-dicarbonyl compounds catalyzed by Lewis acids.[39] The Lewis acid forms a chelate to the two carbonyl groups of a β-keto ester substrate to promote enol formation, thus changing the electronic properties of the α-carbon. Utilizing *N*-bromosuccinimide as an electrophilic source of bromine and $Mg(ClO_4)_2$ as a Lewis acid, a mild and fast α-bromination of 1, 3-dicarbonyl compounds can occur.

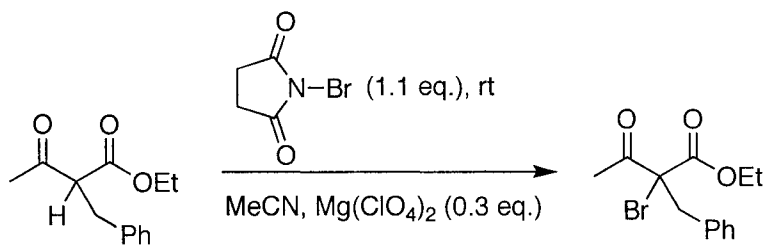

Scheme 2.26

98%

Employing this methodology, the crude β-keto ester mixture **174a/b** was subjected to the α-halogenation reaction conditions, which afforded the brominated β-keto ester **178** in 65% yield.[40] Analysis of the ^{1}H, ^{13}C, and HMQC NMR spectra of the product showed that the product of the EDA ring expansion reaction had produced a β-keto ester cyclopetanone moiety.

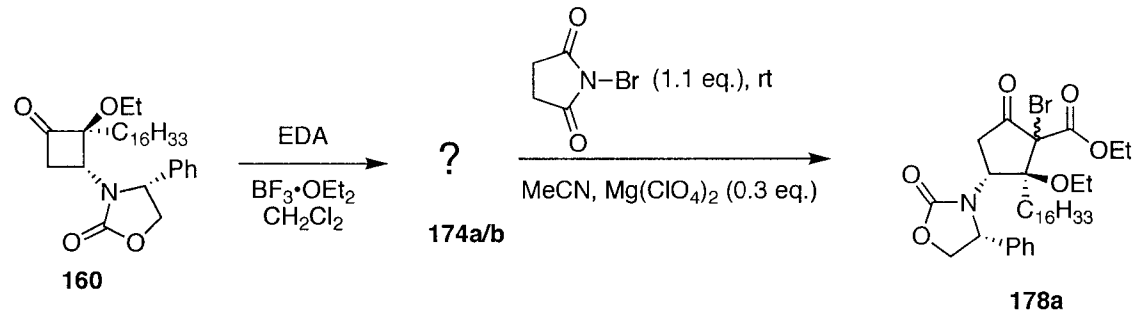

Scheme 2.27

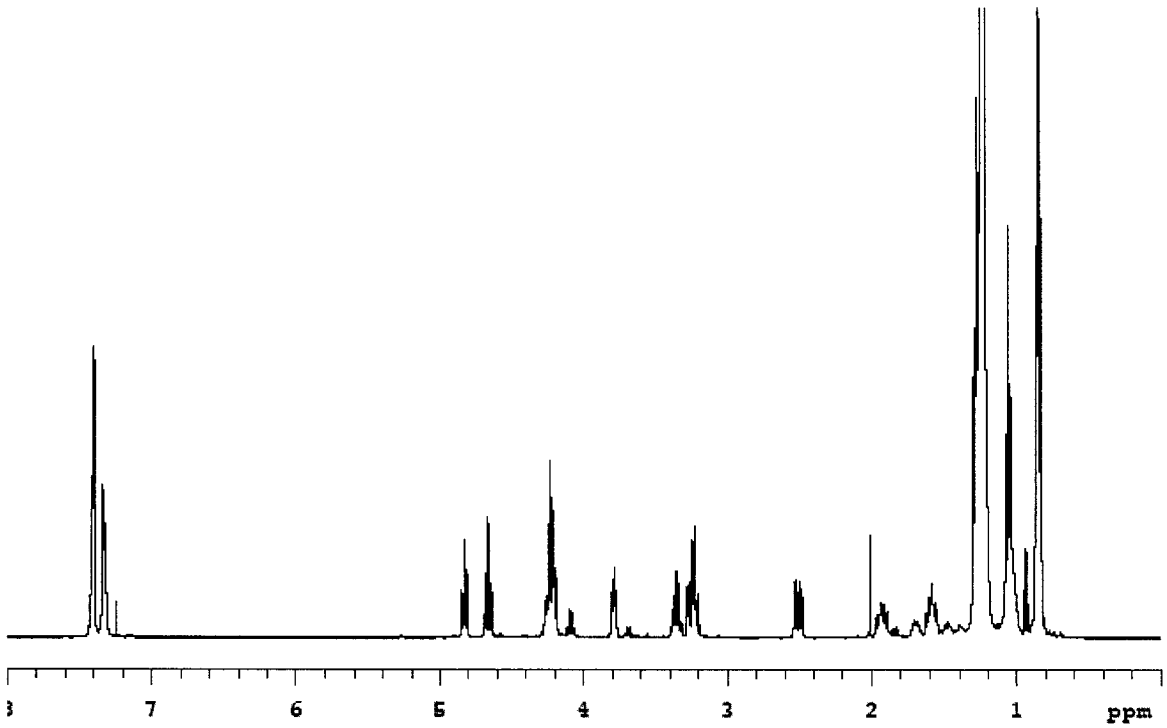

Figure 2.7 The ^{1}H NMR spectrum of **178a/b**.

The spectral data of **178** was examined further for some insight into for the correct structure. The information from the HMQC 2-D NMR experiment on **178** showed that the α-methylene protons at 3.27 ppm (m, 1H) and 2.53 ppm (dd, J =

7.2, 15.3 Hz, 1H) corresponded to a carbon at 38.6 ppm. The carbon chemical shifts matched the estimated values from ChemNMR Pro for structure **178a** better than the values for **178b** (Figure 2.8). Several other core carbons of the cyclopentanone structure were more consistent with structure **178a** than **178b**. The NMR spectroscopic similarities between the isolated compound **178** and the predicted values of **178a** led to the conclusion that the correct structure of **178** was isomer **178a**.

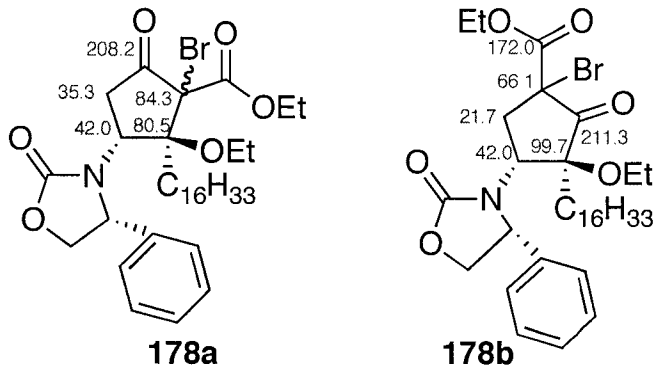

Figure 2.8 The estimated chemical shift values for **178a** and **178b**.

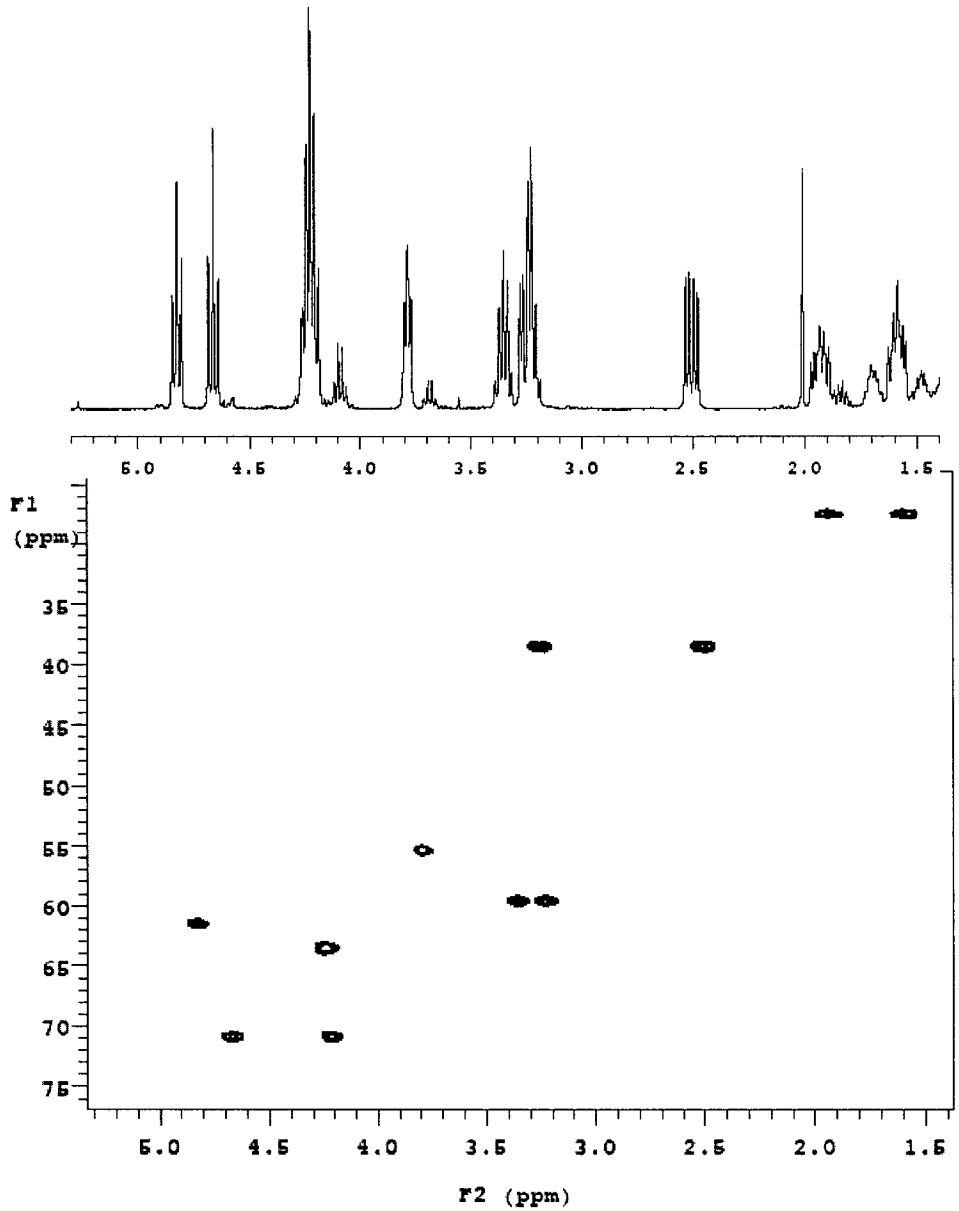

Figure 2.9 HMQC data for **178a/b**.

With the brominated β-keto ester in hand, investigations into the elimination of the chiral auxiliary began. An oxazolidinone, β to a carbonyl, would seem to be an excellent leaving group. The pK_a of an average α-proton is between approximately 19 – 20 pK_a units. If a halogen atom is present on the

other side of the carbonyl, then the α-proton should become more acidic, thus lowering the pK_a making its removal easier.

178

Scheme 2.28

A wide range of bases was examined and in all attempts the eliminated product was not observed (Table 2.6). In a few cases, a loss of bromine occurred which gave back β-keto ester **174**. The remainder of the elimination trials showed decomposition of the brominated β-keto ester had occurred.

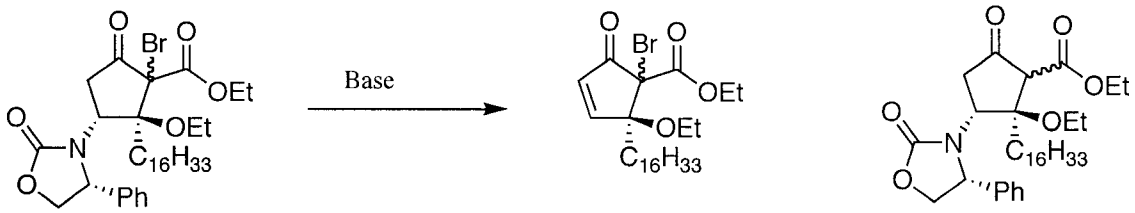

178 **179** **174**

Table 2.6 Attempts at oxazolidinone removal

Base	Result
TBAF	Recovered **174** & Decomposed product
KHMDS	Recovered **174** & Decomposed product
LDA	Recovered **174** & Decomposed product
Microwave	Starting Material
$NaH/BF_4•OEt_3$	Starting Material
t-BuLi	Recovered **174** & Decomposed product

The propensity for the removal of bromine led to the idea of utilizing the inherent reactivity that β-keto esters possess. In general, β-keto esters contain two very acidic sites. The first is the α-carbon between the two carbonyls and the second is the α-carbon next to the ketone carbonyl (Scheme 2.29). If two moles of base are used, then not only is the most acidic proton removed, but the second one is as well. Alkylation of the doubly charged anion then takes place at the less acidic position. Usually, the dianion of β-keto esters are made with one mole of sodium hydride, followed by one mol of *n*-butyllithium. Several investigators have reported the addition of *n*-butyllithium to the carbonyl group,[41] which can be avoided by using lithium diisopropyl amine (LDA) as the second base.

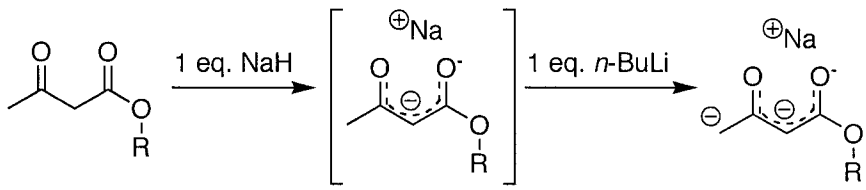

Scheme 2.29

Traditionally, dianion chemistry has only been used for alkylation at the second α-carbon and there are no reported cases of elimination to form an enone. Nevertheless, several combinations of the bases were examined for removal of the oxazolidinone of β-keto ester **178**. Unfortunately, the dianion chemistry was unsuccessful for auxiliary elimination and only starting material was recovered.

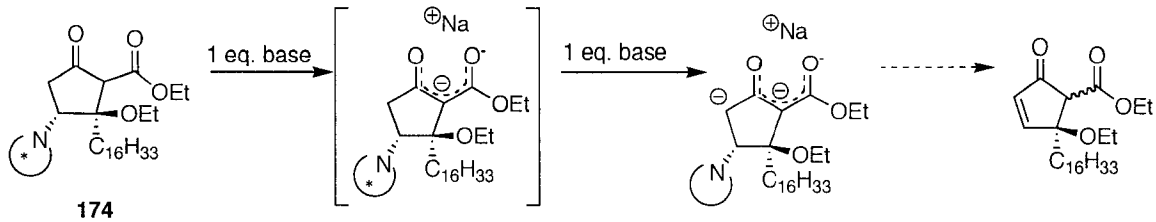

174

Table 2.7 Attempts at oxazolidinone removal with dianion chemistry

Base 1	Base 2	Result
LDA	LDA	No eliminated product found
NaH	*n*-BuLi	
NaH	*t*-BuLi	

Utilizing the Lewis basicity of the dicarbonyls, formation of a metal chelate, followed by the addition of a base might promote elimination of the oxazolidinone. Thallium (I) hydroxide or ethoxide have been used as chelating agents for 1, 3-dicarbonyl compounds[42] in several α-alkylation cases. Thallium ethoxide could be used to complex the two carbonyls in β-keto ester **178,** which could facilitate the elimination of the oxazolidinone. Unfortunately, analysis of the ^{1H} NMR spectrum of the crude reaction mixture showed that decomposition of the starting material had occurred.

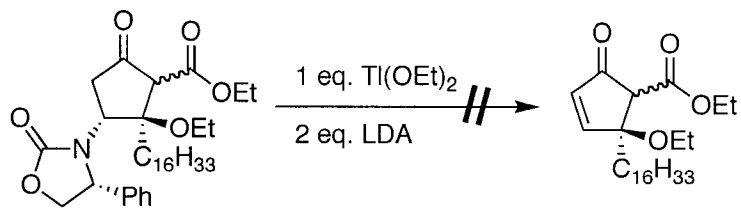

174 Scheme 2.30

The difficulty experienced with the oxazolidinone removal prompted an alternative plan of attack. The original chiral auxiliary used in the

photocycloaddition was ene carbamate **152**, which contained one phenyl group on C_1 (Scheme 2.31). If chiral auxiliary **180** was used, photolysis with chromium carbene complex **159** would yield cyclobutanone **181**. The β-keto ester could undergo hydrogenation to afford a primary amine **183** β to the carbonyl. The β-amine could be transformed into a more suitable leaving group through alkylation or acylation, or it could undergo a Hoffmann or Cope-type elimination with the appropriate modifications, to afford **185** (Scheme 2.31).

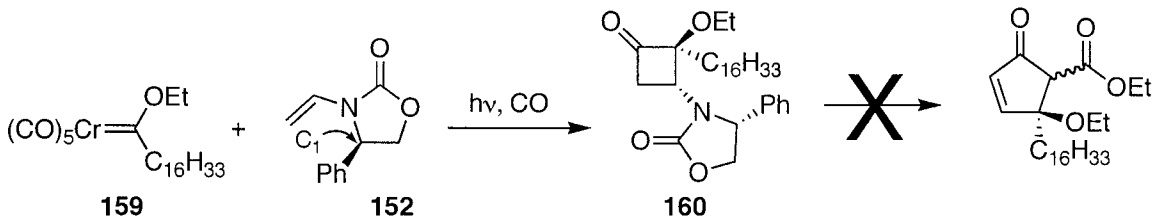

Scheme 2.31

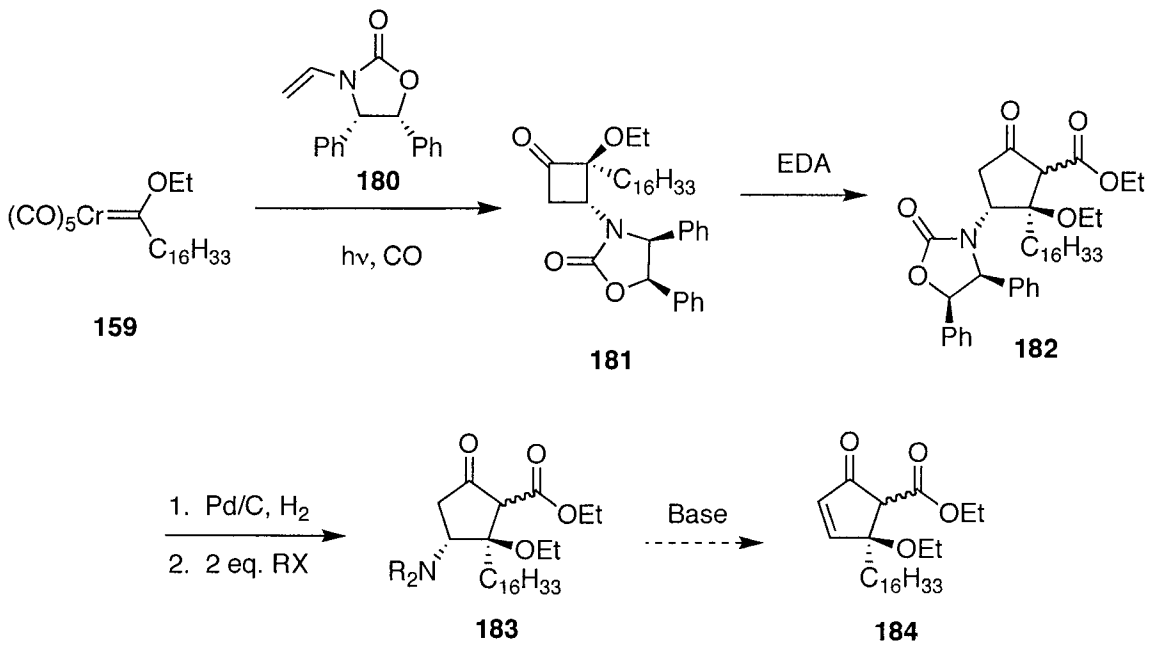

Scheme 2.32

Replacing chiral auxiliary **152** with auxiliary **180**, cyclobutanone **181** was synthesized using the same procedure used for cyclobutanone **160**. The ring expansion with EDA afforded the β-keto ester in 96% yield. Bromination with NBS gave brominated β-keto ester **186** in 64% yield. Hydrogenation of **186** with palladium on carbon in ethanol produced primary amine **187** in 86% yield.

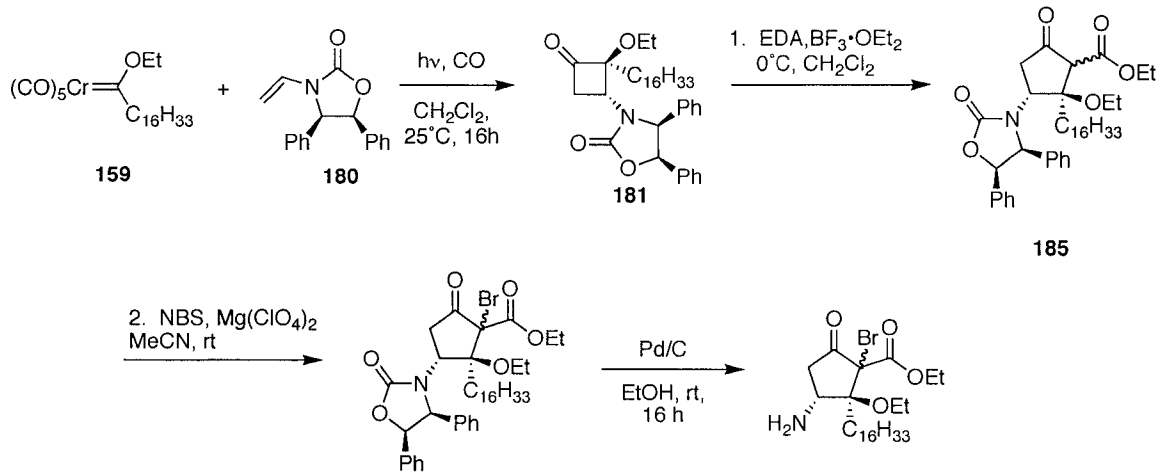

Scheme 2.33

Primary amines are extremely poor leaving groups[43], but their leaving group ability can greatly improve by conversion into a better leaving group such as a tosylate,[44] triflate, azide,[45] diazonium salt,[46] nitro compound[47, 48] or a tertiary amine. The primary amine **187** was converted into a variety of leaving groups and subjected to known β-elimination reaction conditions. In all cases, the leaving group failed to eliminate and provide the desired enone (Table 2.8).

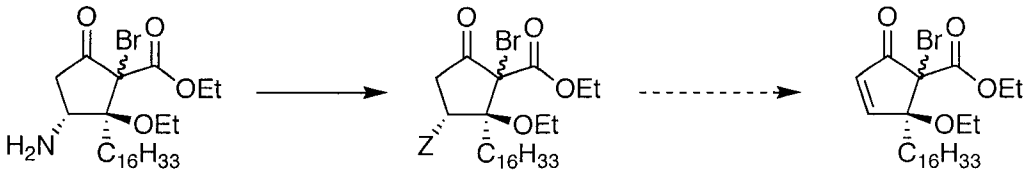

187 Proposed Structure Desired Enone

Table 2.8 Elimination attempts with a β-leaving group

Entry	Z	Conditions	Result
1	NTs_2	LDA 0°C to rt	Decomposition
2	NTf_2	0°C to rt	Decomposition
3	N_2	rt to reflux	Decomposition
4	N_3	Basic Al_2O_3 [a] NEt_3	Recovered Azide
5	NO_2	DBU NaH	Recovered Nitro Compound
6	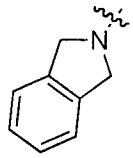	Δ	Recovered Starting Material

a.) reference 45

The numerous failed attempts to remove any group in the β-position supported the idea that the proposed structure for compound **187** was incorrect. This information would support a structure with a leaving group in the γ position instead of β (Figure 2.10), which would explain the extreme difficulty observed with the removal of any of the leaving groups.

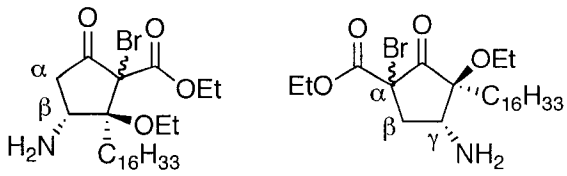

187a **187b**

Figure 2.10 Comparison of leaving group positions in **187a** and **187b.**

With the absolute structure of **187** unknown, there were several possibilities for structure elucidation. The simplest and most definitive method would be to obtain a crystal structure of **187**. However, the long, hydrophobic, alkyl side chain prevented crystallization of this compound. Efforts were shifted to **176**, which was prepared in the same manner as **187**, but possesses only a methyl substituent, which should aid in the crystallization attempts.

Concurrent with the crystallization attempts, a structural investigation began with a known cyclopentanone structure. Cyclobutanone **175** was utilized in these investigations due to its simplicity of substituents. Treatment of cyclobutanone **175** with diazomethane resulted in cyclopentanone **188**, with a migration of the less-substituted terminus predominating. The regioselectivity of cyclopentanone **188** was verified by an X-ray crystal structure of an elaborated compound by a previous Hegedus group member.[49] Cyclopentanone **188** contained the quaternary center next to the carbonyl moiety, which allowed acylation with ethyl chloroformate to give β-keto ester **189**. α-Halogenation with NBS and $Mg(ClO_4)_2$ afforded brominated β-keto ester **71** in good yield (Scheme 2.34).

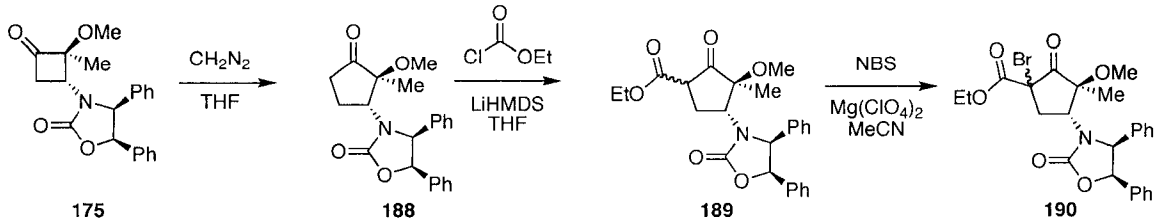

175 188 189 190

Scheme 2.34

The second model system was obtained using the synthetic route used for **186** (Scheme 2.35). Cyclobutanone **175** underwent the EDA ring expansion reaction, followed by bromination to provide β-keto ester **191**. With both brominated β-keto ester regioisomers available, comparative structural analysis experiments could be performed to elucidate the structure of **186**.

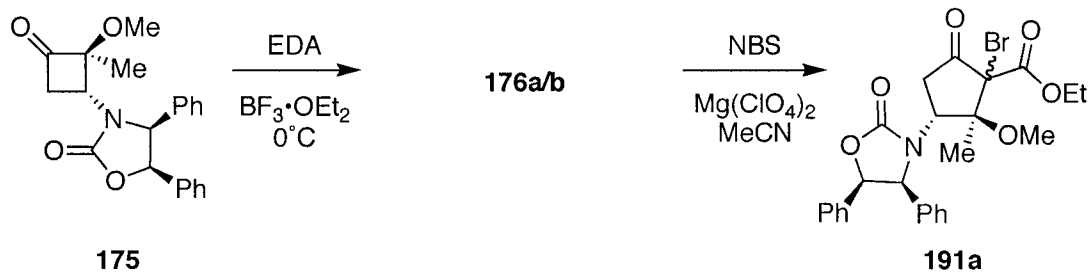

175 **176a/b** **191a**

Scheme 2.35

or

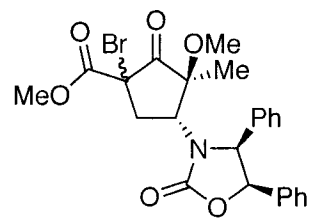

191b

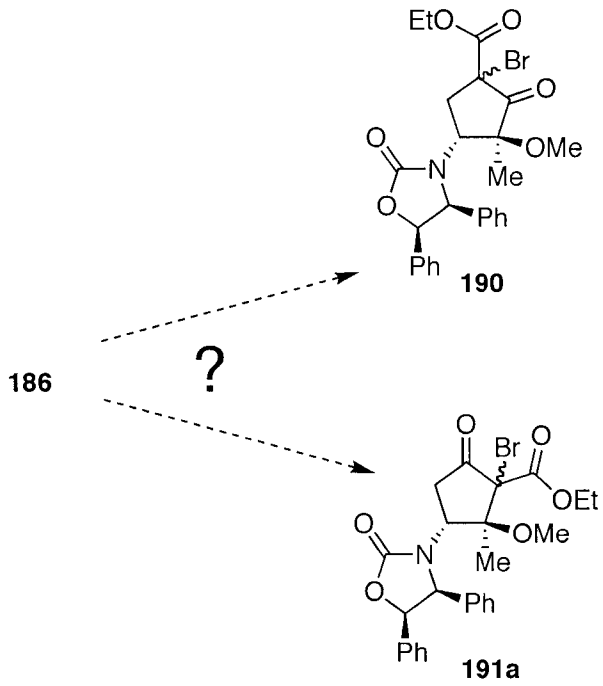

Scheme 2.36

In both cases, the CH_2 methylenes should possess the same splitting pattern, but their chemical shifts should be quite different. Cyclopentanone **190** contains a quaternary carbon α to the ketone carbonyl and a methylene β to both the ketone and ester moieties. Cyclopentanone **191** has its quaternary center β to the ketone and ester carbonyls and α to a carbon with a bromine substituent. Utilizing the tools available, initial analysis began with examination of the ^{1}H and ^{13}C NMR spectra for each compound. Next, a heteronuclear multiple quantum coherence (HMQC) experiment was performed so the ^{1}H and ^{13}C assignments could be cross-correlated to determine the carbon-hydrogen connectivity.

Initial examination of the ^{1}H NMR of **190** showed that the methylene protons at 2.82 ppm and 2.25 ppm (Figure 2.11). The methylene protons of **191** appeared at approximately 2.82 ppm and 2.25 ppm (Figure 2.12). The methylene

protons of **186** were almost identical to β-keto ester **191** and **190**, appearing at approximately 2.81 ppm and 2.19 ppm (Figure 2.13).

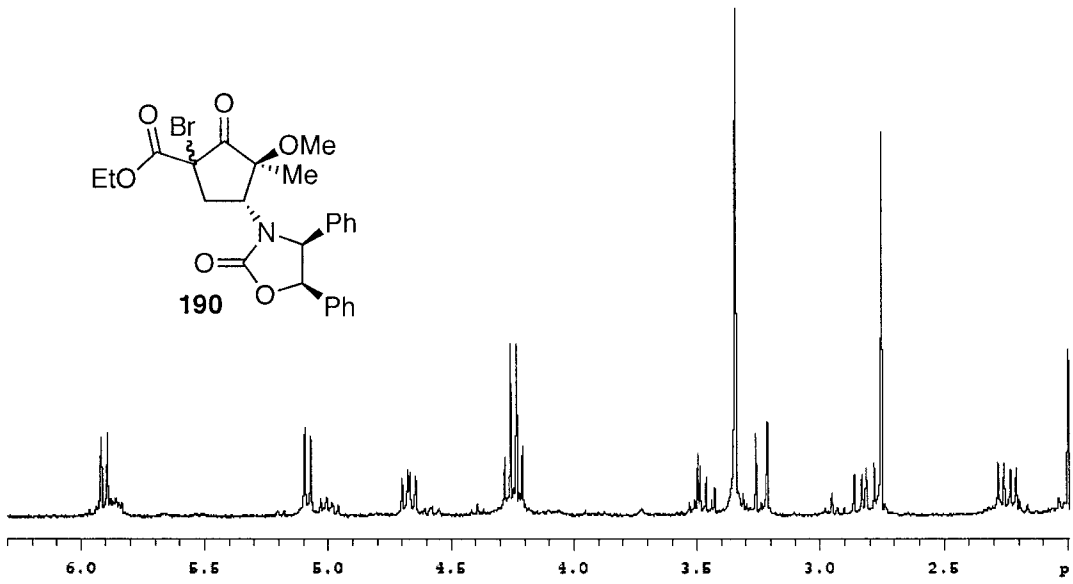

Figure 2.11 The ^{1}H NMR spectrum of compound **190**.

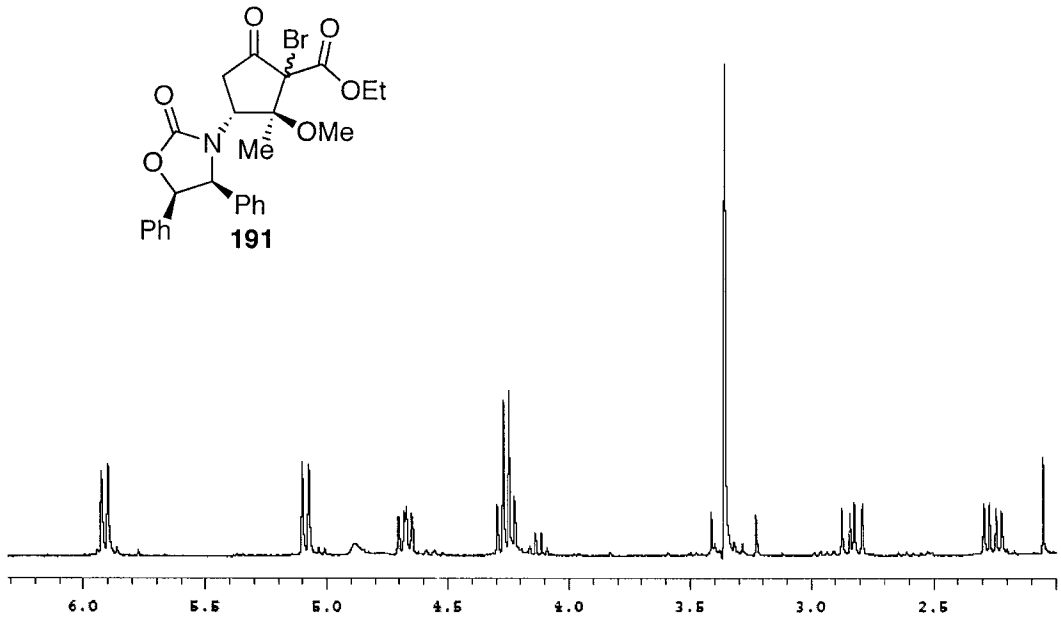

Figure 2.12 The ^{1}H NMR spectrum of compound **191**.

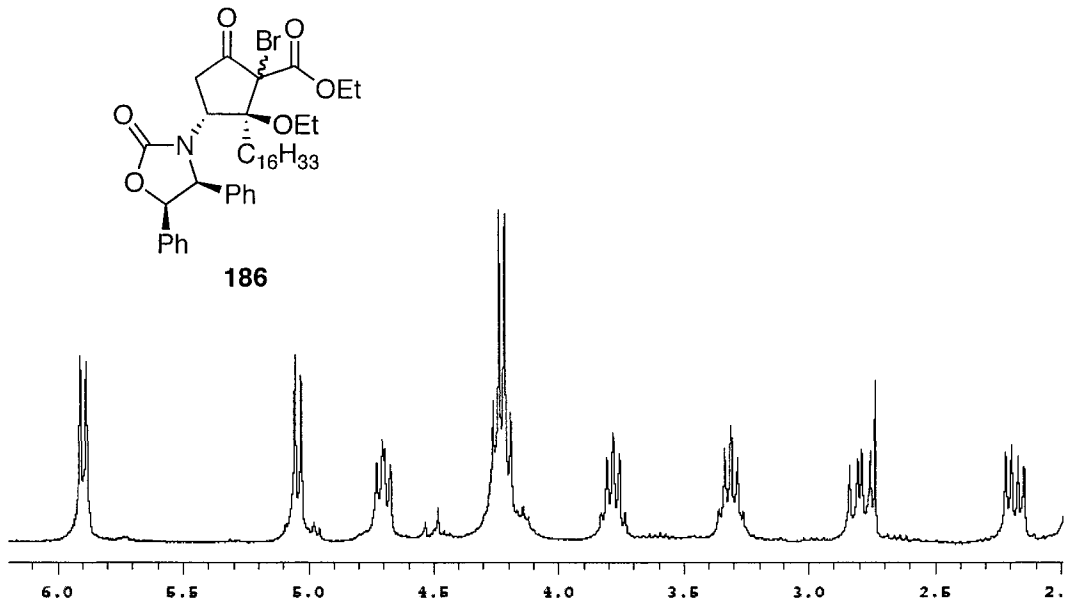

Figure 2.13 The ^{1}H NMR spectrum of compound **186**.

The data from the HMQC carbon-proton correlation experiment on **191** showed that the methylene α-carbon at 38.42 ppm corresponded to the two α–protons at 2.82 and 2.25 ppm (Figure 2.14). The methylene α-carbon of **186** appeared at 38.6 ppm and corresponded to the two α-protons at 2.81 and 2.19 ppm (Figure 2.15). Compound **190**'s α-protons at 2.82 ppm and 2.25 ppm belonged to a carbon appearing at 38.14 ppm (Figure 2.16).

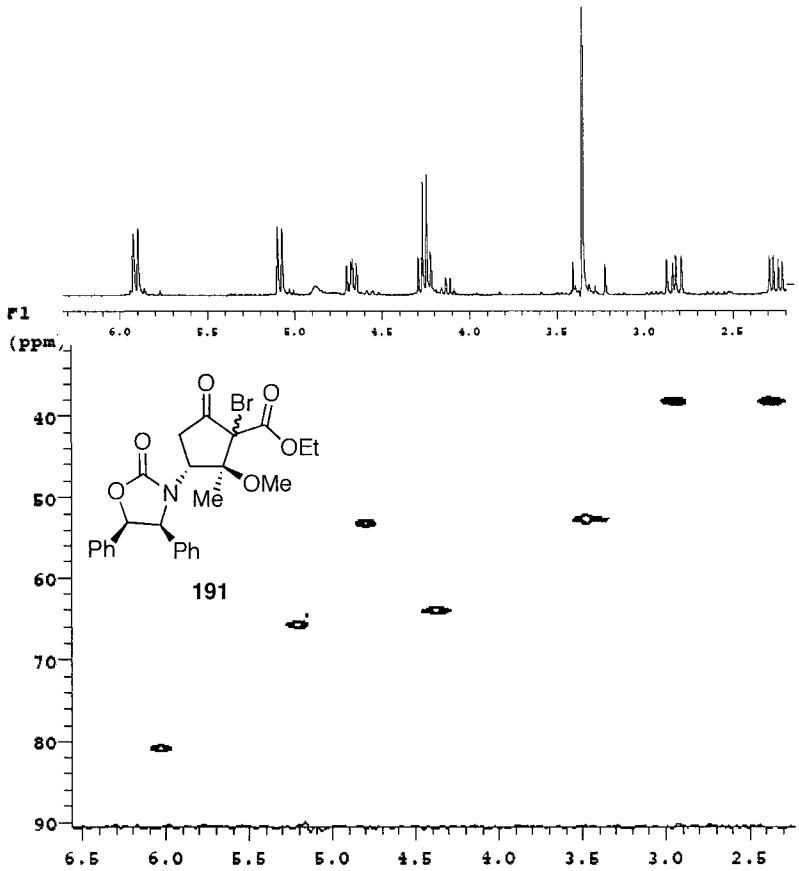

Figure 2.14 HMQC data for **191**.

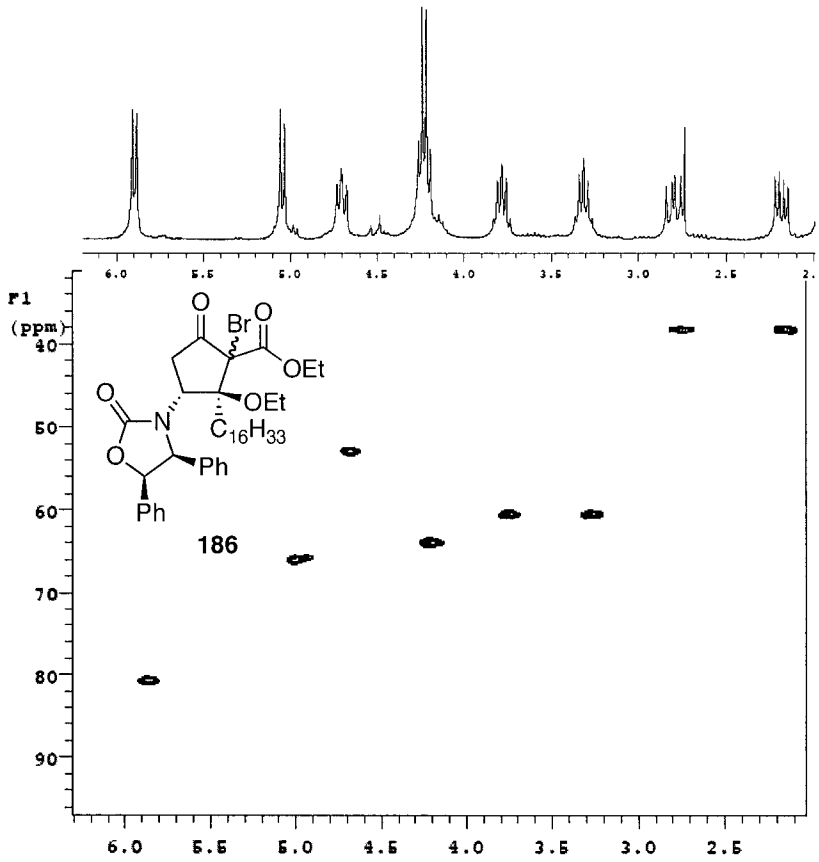

Figure 2.15 HMQC data of **186**

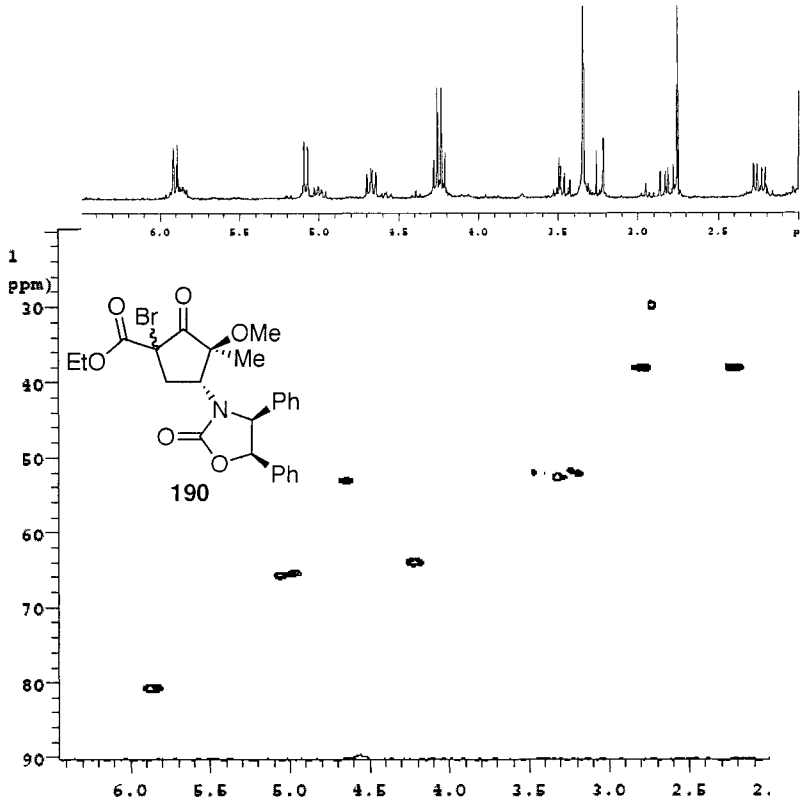

Figure 2.16 HMQC data for **190**.

The information gathered from the 1- and 2-D NMR experiments supported the idea that all three compounds, **186, 190,** and **191** have the same relative regiochemistry. Attempts to eliminate any type of β leaving group also supported this structural claim.

IV. Conclusion

The difficulties encountered with the ring expansion reactions with the cyclobutanones prevented successful advancement to plakevulin A **125** or to key enone intermediate, **148**. The structural ambiguity that exists in five-membered ring systems severely damaged the progress of the β oxazolidinone or

functionalized amine elimination attempts. Had the right regioisomer been obtained, the synthesis should not have encountered such difficulties as previously demonstrated. Utilizing a sulfur ylide that could stabilize a positive charge during bond-migration could be one way to obtain the correct regioisomer (Scheme 2.37). Alternatively, manipulations of cyclopentanone **188** could afford the desired β-keto ester regioisomer in several steps (Scheme 2.38).

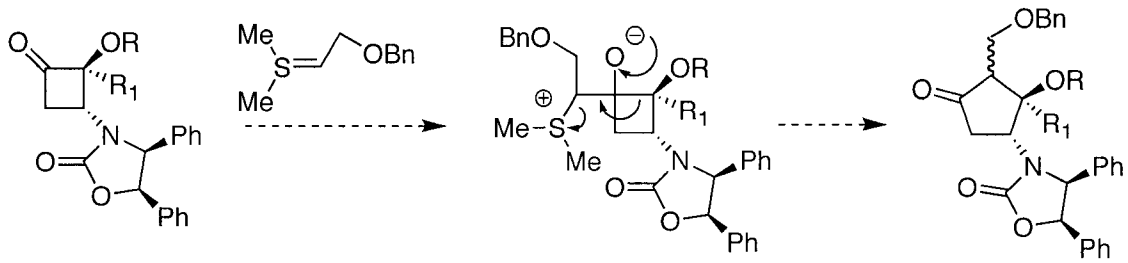

Scheme 2.37

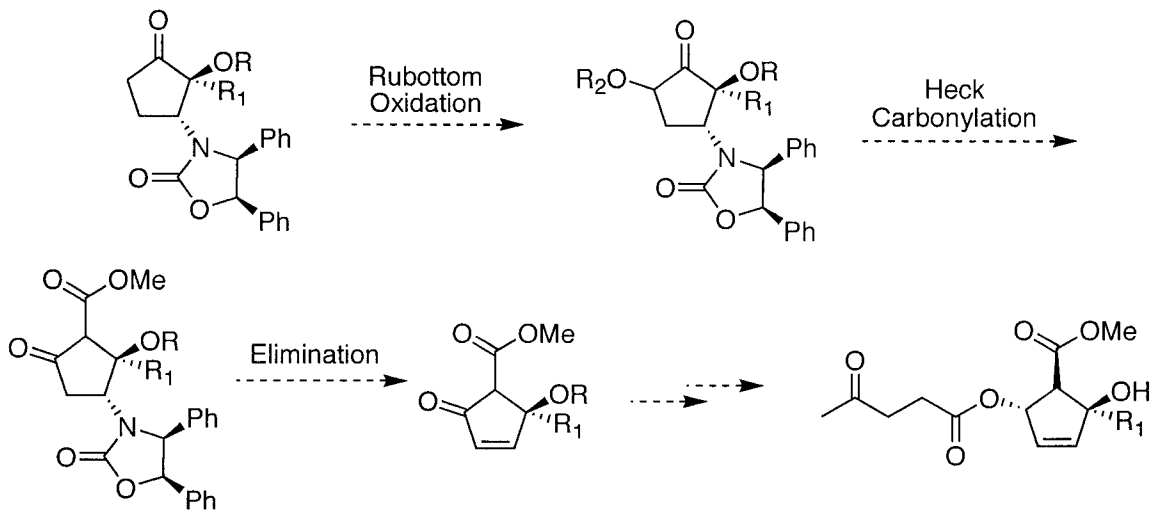

Scheme 2.38

V. Experimental Section

General Methods and Materials. THF was distilled from sodium-benzophenone ketyl, and DMF was distilled from $MgSO_4$. Commercially available reagents were used as received. ^1H NMR (300 MHz) and ^{13}C NMR (75 MHz) spectra were recorded in $CDCl_3$ unless otherwise noted and chemical shifts are given in ppm relative to $CDCl_3$ (7.27 ppm for ^1H NMR and 77.23 ppm for ^{13}C NMR). Column chromatography was performed with ICN 32-66 nm, 60 Å silica gel using flash column techniques. All reactions were performed in flame-dried glassware under an atmosphere of Ar unless otherwise noted.

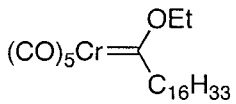

159
$C_{24}H_{38}CrO_6$
Exact Mass: 474.21
Mol. Wt.: 474.55
C, 60.74; H, 8.07; Cr, 10.96; O, 20.23

[(Ethoxy)(hexadecyl)carbene]pentacarbonylchromium(0) (159) Iodohexadecane (5.08g, 14.42 mmol) was dissolved in 144 mL of diethyl ether and cooled to –20°C. After equilibration, *tert*-butyllithium (17 ml, 28.84 mmol, 1.7M) was added quickly via syringe to the flask, turning the clear solution slightly yellow. The flask stirred at –20°C for 30 minutes and was then warmed to room temperature and let stir for 30 minutes. Chromium hexacarbonyl (3.18 g, 14.42 mmol) was loaded into a 250 mL round bottom flask with 30 mL of diethyl ether. 1-lithiohexadecane was transferred to the flask containing the $Cr(CO)_6$ via cannulae needle and the reaction progress was monitored by the disappearance of the $Cr(CO)_6$. The solvent was evaporated and 100 mL of distilled water was added to the flask followed by triethoxonium tetrafluoroborate (4.1 g, 21.63 mmol). The bright yellow solution was extracted with diethyl ether (3 X 30 mL) and the organic layers were

combined, washed with brine (50 mL), dried, and the solvent was removed. The crude carbene **159** was purified by flash column chromatography (100% hexanes) and the orange band was collected and the solvent was removed to yield carbene **159** (4.06 g, 8.56 mmol) 59% as an orange oil. Spectral data for **159**; ^{1}H NMR δ 5.07 (q, J = 6.9, 14.4 Hz, 2H), 3.28 (t, J = 7.2 Hz, 2H), 1.64 (t, J = 7.2 Hz, 3H), 1.45 (m, 2H), 1.27 (bs, 26H), 0.89 (t, J = 6.9 Hz, 3H).

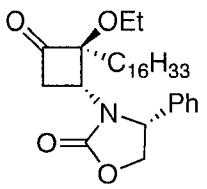

160

$C_{31}H_{49}NO_4$
Exact Mass: 499.37
Mol. Wt.: 499.73
C, 74.51; H, 9.88; N, 2.80; O, 12.81

Cyclobutanone 160. Chromium carbene complex **159** was dissolved in methylene chloride (11.1 ml, 0.3M) and transferred to a pressure tube via cannulae needle. Next, ene carbamate **152** (0.378 g, 2 mmol) was transferred to the pressure tube which was freezed, pumped, and thawed three times and then pressurized with carbon monoxide to 80 p.s.i. three times, purged with CO and placed in the 35°C photoreactor. 24 hours later, the tube was removed and the contents were transferred to a 250 mL round bottom flask. The solvent was removed and the $Cr(CO)_6$ was sublimed. The green oil was chromatographed (7:1 hexanes:ethyl acetate) to give cyclobutanone **160** in 79% yield (0.790g, 1.58 mmol); Spectral data for **160** R_f 0.43 (3:1 hexanes/ethyl acetate); IR (neat) ν 1786, 1751 cm^{-1}; ^{1}H NMR δ 7.40 (m, 2 H), 7.26 (m, 2H), 4.89 (m, 1H) 4.67 (t, J = 8.7 Hz, 1 H), 4.33 (t, J = 9.9 Hz, 1H), 4.20 (m, 1H), 3.48 (dd, J = 2.1, 7.2, 1 H), 3.30 (m, 2H), 2.52 (dd, J = 9.9, 18 Hz, 1H), 1.84 (t, J = 7.3, 1H), 1.49 (m, 1H), 1.22 (m, 29H), 1.04 (t, J = 6.9 Hz, 3H), 0.88 (t, J = 5.1 Hz, 3H); ^{13}C

NMR (100 MHz) δ 206.3, 157.9, 138.8, 129.6, 129.5, 126.7, 98.7, 81.1, 70.3, 62.1, 60.5, 48.2, 42.5, 30.3, 25.7, 25.6, 23.3, 15.6, 14.3.

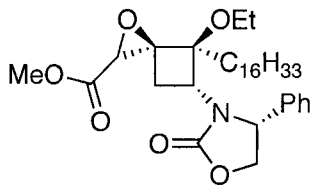

173

$C_{34}H_{53}NO_6$
Exact Mass: 571.39
Mol. Wt.: 571.79
C, 71.42; H, 9.34; N, 2.45; O, 16.79

Epoxide 173. Cyclobutanone **160** (0.134 g, 0.268 mmol) was dissolved in CH_2Cl_2 (0.01 M) in a 5 mL round bottom flask. Ylide **172** (0.360 g, 2.68 mmol) was dissolved in 0.2 mL CH_2Cl_2 and added to the flask via syringe. A spatula tip of $Sc(OTf)_3$ was added to the flask and the reaction mixture, which was allowed to reflux overnight. The reaction progress was monitored by TLC (3:1 hexane/ethyl acetate) and upon disappearance of starting material; the reaction flask was cooled and quenched with water (2 mL). The aqueous layer was extracted with CH_2Cl_2 (2 x 25 mL) and the organic layers were combined, washed with brine, dried, and the solvent was removed to afford a clear oil. The crude oil was purified via flash column chromatography (4:1 hexanes/ethyl acetate) to provide **173** in 94% yield (0.130 g, 0.228 mmol); Spectral data for **173**: R_f 0.68 (3:1 hexanes/ethyl acetate); IR (neat) ν 1754 cm^{-1}; ^1H NMR δ 7.35 (m, 2H), 7.18 (m, 2H), 4.93 (dd, J = 2.4, 8.1, 1H), 4.64 (t, J = 8.4, 1H), 4.30 (t, J = 9.9, 1H), 4.11 (dd, J = 2.4, 8.4, 1H), 3.72 (s, 3H), 3.61 (m, 1H), 3.38 (t, J = 8.4, 1H), 2.13 (m, 1H), 1.87 (m, 1H), 1.39 (m, 1H), 1.21 (s, 36H), 1.11 (t, J = 5.1, 3H), 0.83 (t, J = 4.8, 3H); ^{13}C NMR (100 MHz) δ 168.7, 157.9, 140.6, 129.8, 129.2, 125.6, 86.8, 70.5, 68.0, 59.9, 58.9, 53.3, 52.6, 52.4, 50.8, 32.1, 30.6, 29.9, 29.9, 29.6, 28.9, 27.5, 22.9, 22.6, 15.7, 14.3.

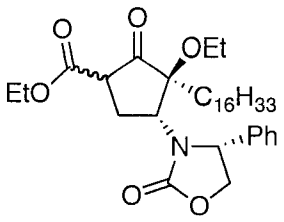

174

$C_{35}H_{55}NO_6$
Exact Mass: 585.4
Mol. Wt.: 585.81
C, 71.76; H, 9.46; N, 2.39; O, 16.39

β-Keto Ester 174. Cyclobutanone **160** (1.13 g, 1.96 mmol) was dissolved in methylene chloride (33 mL) and cooled to 0°C. Ethyl diazoacetate (1.0 M solution in CH_2Cl_2, 247 μL, 2.35 mmol) was added to the flask via syringe. Boron triflouride diethyl ethereate (248 μL , 1.96 mmol) was quickly added via syringe to the reaction flask. The reaction stirred at 0°C until bubbles ceased to form (approximately 15 minutes). The reaction was quenched by the addition of sodium bicarbonate (30 mL) and the mixture was extracted with methylene chloride (2 x 30 mL). The combined organic layers were washed with brine and dried with $MgSO_4$, and concentrated. The crude oil was purified by flash column chromatography (5:1 hexanes/ethyl acetate) to yield β-keto ester **174** (1.24 g, 1.87 mmol, 95%) as a clear oil and as a 1:1 mixture of diastereomers: R_f 0.53 (25% ethyl acetate in hexanes); IR(neat) ν 2924, 1754 cm^{-1}. ^1H and ^{13}C data is unavailable.

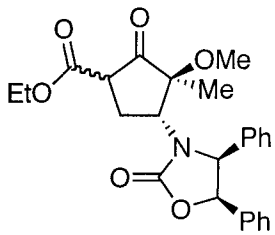

176

$C_{25}H_{27}NO_6$
Exact Mass: 437.18
Mol. Wt.: 437.48
C, 68.63; H, 6.22; N, 3.20; O, 21.94

β-Keto Ester 176. Boron trifluoride diethyl etherate (9 μL, 0.072 mmol) was added dropwise to a solution containing cyclobutanone **175** (100 mg, 0.285 mmol) and ethyl diazoacetate (1.0 M in CH_2Cl_2, 423 μL, 0.423 mmol) in CH_2Cl_2 (5 mL) at 0°C. The reaction stirred at 0°C until bubbles ceased to form (10 minutes). The reaction was quenched by the addition of saturated sodium bicarbonate (15 mL) and the

mixture was extracted with CH_2Cl_2 (2 x 25 mL). The organic layers were combined, washed with brine, dried, and the solvent was removed. The yellow oil was purified via flash column chromatography (3:1 hexanes/ethyl acetate) to afford β-keto ester **176** (82.4 mg, 66%) as a white solid. Spectral data for **176**: R_f 0.21; (3:1 hexanes/ethyl acetate) ; IR (neat) ν 1743 cm^{-1}; ^1H NMR δ 10.14 (s, 0.5H), 7.15-7.07 (m, 4H), 6.98-6.87 (m, 4H), 5.94 (d, J = 7.5 Hz, 0.25 H), 5.88 (d, J = 7.8 Hz, 0.75H), 5.15 (d, J = 7.2 Hz, 0.25H), 5.08 (d, J = 8.1 Hz, 0.25H), 4.95 (d, J = 7.2 Hz, 0.5H), 4.83 (t, J = 7.5 Hz, 0.5H), 4.59 (dd, J = 7.2, 9.9 H, 0.25H), 4.26-4.08 (m, 2H), 3.99 (dd, J = 3.6, 8.1 Hz, 0.25H), 3.56 (dd, J = 7.2, 2.4 Hz, 0.25H), 3.40 (s, 0.75H), 3.26 (t, J = 9.6, 0.25H), 3.14 (s, 0.75H), 2.69 (m, 0.25H), 2.36 (dd, J = 7.8, 14.4, 0.5H), 2.11 (dd, J = 3.9, 7.8 Hz, 0.25H), 2.04 (dd, J = 7.5, 14.4 Hz, 0.5H), 1.62 (s, 0.5H), 1.56 (s, 1.5H), 1.48 (s, 0.75H), 1.41 (s, 0.75H), 1.30 (t, J = 6.9 Hz, 1.5H), 1.21 (t, J = 7.2 Hz, 1.5H); ^{13}C NMR (100 MHz) δ 171.9, 168.8, 168.4, 158.8, 135.9, 135.5, 134.3, 134.2, 133.8, 129.0, 128.7, 128.6, 128.5, 128.4, 128.2, 128.1, 128.0, 127.2, 126.3, 126.2, 126.1, 100.0, 86.4, 83.2, 80.5, 66.0, 65.4, 65.2, 62.1, 61.8, 60.6, 57.4, 55.0, 53.9, 52.2, 52.1, 52.0, 51.6, 51.3, 28.0, 26.9, 25.9, 18.0, 16.1, 14.4, 13.7.

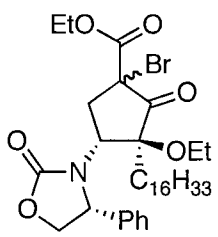

178

$C_{35}H_{54}BrNO_6$
Exact Mass: 663.31
Mol. Wt.: 664.71
C, 63.24; H, 8.19; Br, 12.02; N, 2.11; O, 14.44

Brominated β-Keto Ester 178. β-Keto ester **174** (1.18 g, 3.0 mmol) was dissolved in 60 mL of acetonitrile in a 100 mL round bottom flask. Next, $Mg(ClO_4)_2$ (201 mg, 0.9 mmol) was added to the flask and let stir for 5 minutes. *N*-Bromosuccinimide (0.587 g,

3.30 mmol) was added to the reaction flask in one portion and the reaction progress was monitored by the disappearance of the β-keto ester spot by TLC (approximately 5 minutes). The reaction was diluted with diethyl ether and quenched with distilled water. The water layer was extracted with diethyl ether (2 x 30 mL). The organic layers were combined, dried and the solvent was removed. The crude oil was purified by flash column chromatography (5:1 hexanes/ethyl acetate) and produced **178** as a yellow oil in 65% yield (1.30 g, 1..96 mmol); Spectral data for **178**: R_f 0.35 (3:1 hexanes/ethyl acetate) ; IR (neat) ν 1746 cm^{-1}; ^1H NMR δ 7.42 (m, 2H), 7.38 (m, 2H), 4.86 (t, J = 8.1 Hz, 1H), 4.69 (t, J = 9 Hz, 1H), 4.25 (m, 2H), 3.81 (dd, J = 5.1, 6.9, 1H), 3.37 (t, J = 7.8 Hz, 1H), 3.27 (m, 1H), 2.53 (dd, J = 7.2, 15.3 Hz, 1H), 1.94 (m, 1H), 1.62 (m, 1H), 1.28 (m, H), 1.08 (t, J = 6.9 Hz, 3H), 0.88 (t, J = 6.6 Hz, 3H); ^{13}C NMR (100 MHz) δ 197.7, 167.3, 159.1, 137.4, 129.9, 129.6, 127.8, 85.9, 63.6, 61.5, 59.6, 55.3, 54.6, 38.6, 34.9, 32.1, 31.8, 30.3, 29.9, 29.8, 29.6, 27.5, 25.5, 22.9, 22.8, 22.1, 20.9, 15.2, 14.3, 14.0.

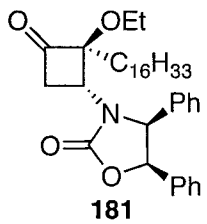

181

$C_{37}H_{53}NO_4$
Exact Mass: 575.40
Mol. Wt.: 575.82
C, 77.18; H, 9.28; N, 2.43; O, 11.11

Cyclobutanone 181. Chromium carbene complex **159** (1.5 g, 3.16 mmol) was dissolved in methylene chloride (11.1 ml, 0.3M) and transferred to a pressure tube via cannulae needle. Next, ene carbamate **180** (0.503 g, 1.89 mmol) was transferred to the pressure tube which was freezed, pumped, and thawed three times and then pressurized with carbon monoxide to 80 p.s.i. three times, purged with CO and placed in the 35°C photoreactor. 24 hours later, the tube was removed and the contents were transferred to a 250 mL round bottom

flask. The solvent was removed and the $Cr(CO)_6$ was sublimed. The green oil was chromatographed (7:1 hexanes:ethyl acetate) to give cyclobutanone **181** in 69% yield (1.255 g, 2.17 mmol); Spectral data for **181** R_f 0.55 (3:1 hexanes/ethyl acetate) ; IR (neat) ν1787, 1753 cm^{-1}; ^1H NMR δ 7.10 (m, 6H), 6.99 (m, 2H), 6.83 (m, 2H), 5.89 (d, J = 7.8 Hz, 1H), 5.04 (d, J = 7.8 Hz, 1H), 4.66 (t, J = 9.3 Hz, 1H), 3.59 (q, J = 6.6 Hz, 2H), 2.79 (dd, J = 9.3, 17.7 Hz, 1H), 2.46 (dd, J = 9.9, 18.0 Hz, 1H), 2.04 (m, 1H), 1.74 (m, 1H), 1.54 (s, 28H), 1.21 (t, J = 7.2 Hz, 3H), 0.88 (t, J = 6.3 Hz, 3H); ^{13}C NMR (100 MHz) δ 206.0, 158.5, 135.0, 133.7, 128.8, 128.5, 128.2, 127.2, 126.4, 98.7, 80.4, 66.2, 90.7, 48.3, 43.7, 32.1, 30.3, 30.1, 29.9, 29.8, 29.6, 23.4, 22.9, 15.7, 14.3.

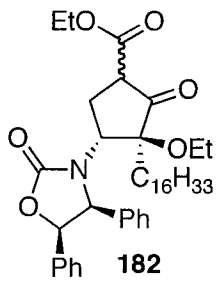

182

$C_{41}H_{59}NO_6$
Exact Mass: 661.43
Mol. Wt.: 661.91
C, 74.40; H, 8.98; N, 2.12; O, 14.50

β-Keto Ester 182. Cyclobutanone **181** (1.13 g, 1.96 mmol) was dissolved in 33 mL CH_2Cl_2 (0.06 M) and ethyl diazoacetate (1.0 M in CH_2Cl_2, 247 μL, 2.35 mmol) was added to the flask, which was cooled to 0°C. Boron triflouride diethyl ethereate (248 μL, 1.96 mmol) was added to the flask via syringe and soon bubbles began to form (N_2 evolution). Upon completion, the reaction was quenched by the addition of saturated sodium bicarbonate (15 mL) and the mixture was extracted with CH_2Cl_2 (2 x 25 mL). The organic layers were combined, washed with brine (50 mL), dried and the solvent was removed under reduced pressure. The yellow oil was purified by flash column chromatography (5:1 hexanes/ethyl acetate) to afford β-keto ester **182**

(1.24 g, 1.88 mmol) in 90% yield as a yellow oil. Spectral information is unavailable due to the complex mixture.

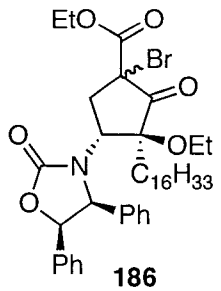

186

$C_{41}H_{58}BrNO_6$
Exact Mass: 739.345
Mol. Wt.: 740.806
C, 66.47; H, 7.89; Br, 10.79; N, 1.89; O, 12.96

Brominated β-Keto Ester 186. β-Keto ester **182** (0.754 g, 1.114 mmol) was dissolved in 22.8 mL MeCN (0.05 M). $Mg(ClO_4)_2$ (76 mg, 0.343 mmol) was added to the reaction flask and let stir for 5 minutes. *N*-bromosuccinimide was added next and the reaction stirred at room temperature for 5 minutes, or until the β-keto ester spot disappeared by tlc (3:1 hexanes:ethyl acetate; $FeCl_3$ stain). The reaction was quenched with 10 mL of Et_2O and 20 mL water. The aqueous layer was washed with Et_2O (2 X 20 mL) and the organic layers were combined, dried, and the solvent was removed to give a yellow oil. The crude oil was purified by flash column chromatography (5:1 hexanes/ethyl acetate) to give **186** as a yellow oil in 66% yield (0.556 g, 0.751 mmol). Spectral data for **186**: R_f 0.61 (3:1 hexanes/ethyl acetate; IR (neat) ν 1751 cm^{-1}; ^1H NMR δ 7.11 (m, 6H), 6.95 (m, 2H), 6.86 (m, 2H), 5.91 (d, J = 7.2 Hz, 1H), 5.35 (d, J = 7.2 Hz, 1H), 4.71 (q, J = 6.3, 9.3 Hz, 1H), 4.24 (q, J = 6.9, 12 Hz, 2H), 3.79 (m, 1H), 3.32 (m, 1H), 2.81 (dd, J = 9.6, 14.7 Hz, 1H), 2.19 (dd, J = 7.2, 15 1H), 1.88 (t, J = 9 Hz, 1H), 1.28 (s, 32H), 1.21 (t, J = 6.6, 3H), 0.88 (t, J = 6.3 Hz, 3H): ^{13}C NMR (100 MHz) δ 199.5, 166.4, 158.6, 134.9, 133.7, 128.9, 128.8, 128.6, 128.3, 128.0, 127.5, 126.2, 87.6, 80.6, 66.0, 63.8, 60.5, 56.8, 53.0, 38.3, 32.2, 30.45, 30.0, 29.6, 23.0, 22.2, 15.4, 14.4, 14.1.

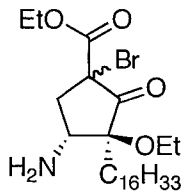

187

$C_{26}H_{48}BrNO_4$
Exact Mass: 517.28
Mol. Wt.: 518.57
C, 60.22; H, 9.33; Br, 15.41; N, 2.70; O, 12.34

Brominated amine 187. Bromo β-keto ester **186** (0.446 g, 0.602 mmol) was dissolved in 12 mL of absolute ethanol (0.05 M) and was loaded into a pressure tube with a stir bar. Palladium on carbon (0.323 g, 0.3 mmol) was transferred to the pressure tube, which was then pressurized and purged with H_2 3 times, and finally, pressurizing it to 80 psi. The reaction was stirred at room temperature until starting material disappeared by TLC (3:1 hexanes/ethyl acetate). When complete, the contents were filtered through celite and washed with CH_2Cl_2. The solvent was evaporated, leaving a clear oil. The crude oil was purified by flash column chromatography (5% CH_3OH in CH_2Cl_2 to 6:1 hexanes/ethyl acetate to give **187** as a clear oil in 86% yield (0.268 g, 0.52 mmol). Spectral data for **187**: R_f 0.38 (1:1 hexanes/ethyl acetate); IR (neat) ν 3396, 1756, 1727 cm^{-1}; ^1H NMR δ 4.20 (m, 2H), 3.61 (bs, 1H), 3.52 (bs, 1H), 3.42 (m, 2H), 3.35 (m, 1H), 3.21 (m, 2H), 2.76 (m, 1H), 2.63 (m, 1H), 2.05 (m, 1H), 1.86 (m, 1H), 1.25 (m, 28H), 1.10 (t, J = 5.1 Hz, 3H), 0.88 (t, J = 5.7 Hz, 3H); ^{13}C NMR (100 MHz) δ 207.5, 169.7, 85.6, 61.6, 60.6, 59.5, 59.1, 53.4, 50.9, 50.6, 32.1, 31.6, 30.6, 30.2, 29.9, 29.6, 26.5, 25.2, 24.5, 23.3, 22.9, 22.8, 22.5, 15.9, 15.5, 14.4, 14.3.

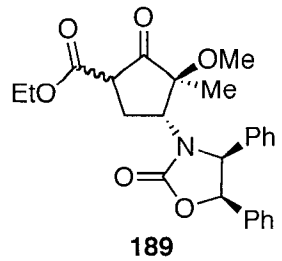

189

$C_{25}H_{27}NO_6$
Exact Mass: 437.18
Mol. Wt.: 437.48
C, 68.63; H, 6.22; N, 3.20; O, 21.94

β-Keto Ester 189. Diisopropyl amine (34 μL, 0.24 mmol) was dissolved into 0.1 mL THF and was cooled to –78°C. *N*-BuLi (0.24 mL, 0.24 mmol) was added to the DIA via syringe and the reaction was allowed to stir at –78°C for 30 minutes. The flask was warmed to room temperature and let stir for 15 minutes, before it was cooled down again to –78°C. Cyclopentanone **188** (73 mg, 0.20 mmol) in 0.1 mL THF was added to the reaction flask via cannula needle and the reaction stirred for 30 minutes at –78°C. Next, HMPA (35 μL, 0.20 mmol) and cyano ethylformate were added to the reaction flask via syringe. The reaction stirred at –78°C for 15 minutes, and then was slowly warmed to room temperature. The reaction's progress was monitored by TLC with the formation of the β-keto ester moiety. The reaction was quenched with water and diethyl ether and the aqueous layer was extracted with diethyl ether (2 X 20 mL). The organic layers were combined, washed with brine, dried and the solvent was removed to give a crude diastereomeric mixture of **189**. The yellow oil was purified via flash column chromatography (3:1 hexanes/ethyl acetate) to yield **189** as a yellow solid in 73% yield (64 mg, 0.146 mmol) Spectral data for **189**: R_f 0.21; (1:1 hexanes/ethyl acetate); IR (neat) ν 1750 cm^{-1}; ^1H and ^{13}C information is unavailable due to the complex NMR spectra.

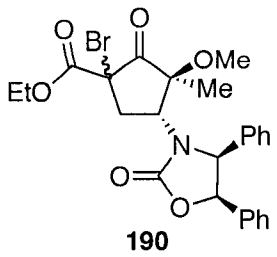

190

$C_{25}H_{26}BrNO_6$
Exact Mass: 515.09
Mol. Wt.: 516.38
C, 58.15; H, 5.08; Br, 15.47; N, 2.71; O, 18.59

Brominated β-Keto Ester 190. β-Keto ester **190** was dissolved in 1.7 mL of CH_3CN (0.05 M) and was loaded with $Mg(ClO_4)_2$ (6 mg, 0.026 mmol). After five minutes, NBS (17 mg, 0.093 mmol) was added to the reaction flask. The disappearance of the β-keto ester spot on TLC ($FeCl_3$ stain) marked the completion of the bromination and the reaction was quenched with water and diethyl ether. The aqueous layer was extracted with diethyl ether (2 x 10 mL) and the organic layers were combined and washed with brine, dried and the solvent was removed. Spectral data for **190**: R_f 0.35; (1:1 hexanes/ethyl acetate); IR (neat) ν 1750 cm-1; ^{1}H NMR δ 7.12 (m, 6H), 6.94 (m, 2H), 6.88 (m, 2H), 5.92 (d, J = 7.8 Hz, 1H), 5.09 (d, J = 7.8 Hz, 1H), 4.68 (dd, J = 6.9, 9.6 Hz, 1H), 4.25 (dd, J = 7.2, 14.1 Hz, 2H), 3.35 (s, 3H), 2.82 (dd, J = 9.3, 14.4 Hz, 1H), 2.25 (dd, J = 6.9, 15 Hz, 1H), 1.47 (s, 3H), 1.26 (s, 3H); ^{13}C NMR (100 MHz) δ 200.8, 166.4, 158.7, 135.0, 133.8, 129.0, 128.8, 128.6, 128.4, 128.2, 127.6, 126.2, 85.3, 65.7, 64.0, 56.2, 53.1, 52.6, 38.1, 29.9, 29.8, 29.6, 22.9, 17.3, 14.3, 14.1.

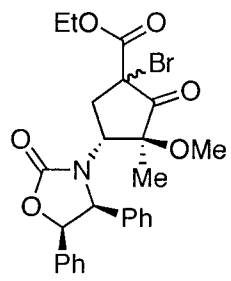

191

$C_{25}H_{26}BrNO_6$
Exact Mass: 515.094
Mol. Wt.: 516.381
C, 58.15; H, 5.08; Br, 15.47; N, 2.71; O, 18.59

Brominated β-Keto Ester 191. β-Keto ester **176** was dissolved in 0.1 mL of CH_3CN (0.05 M) and was loaded with $Mg(ClO_4)_2$ (3 mg, 0.011 mmol). After five minutes, NBS (7 mg, 0.039 mmol) was added to the reaction flask. The

disappearance of the β-keto ester spot on TLC ($FeCl_3$ stain) marked the completion of the bromination and the reaction was quenched with water and diethyl ether. The aqueous layer was extracted with diethyl ether (2 x 10 mL) and the organic layers were combined and washed with brine, dried and the solvent was removed. Spectral data for **191**: R_f 0.35; (1:1 hexanes/ethyl acetate); IR (neat) ν 1750 cm^{-1}; ^1H NMR δ 7.13 (m, 6H), 6.94 (m, 2H), 6.88 (m, 2H), 5.91 (d, J = 7.8 Hz, 1H), 5.09 (d, J = 7.8 Hz, 1H), 4.68 (dd, J = 6.9, 9.6 Hz, 1H), 4.26 (dd, J = 6.9, 13.8 Hz, 2H), 3.36 (s, 3H), 2.82 (dd, J = 9.3, 15 Hz, 1H), 2.25 (dd, J = 6.9, 15 Hz, 1H), 1.47 (s, 3H), 1.30 (s, 3H); ^{13}C NMR (100 MHz) δ200.8, 166.4, 158.7, 135.0, 133.8, 129.1, 128.9, 128.5, 128.2, 127.6, 126.3, 85.3, 80.82, 65.7, 64.0, 56.2, 53.1, 52.7, 38.1, 17.3, 14.1.

VI. References

[1] Tsukamoto, S.; Takeuchi, S.; Ishibashi, M.; Kobayashi, J. *J. Org. Chem.* **1992**, *57*, 5255.
[2] Kobayashi, J.; Tsukamoto, S.; Takeuchi, S.; Ishibashi, M.; *Tetrahedron,* **1993**, *49*, 5955.
[3] Akeuchi, S.; Kikuchi, T.; Tsukamoto, S.; Ishibashi, M.; Kobayashi J. *Tetrahedron,* **1995**, *51*, 5979.
[4] Ishibashi, M.; Takeuchi, S.; Kobayashi, J. *Tetrahedron Lett.,* **1993**, *34,* 3749(B) Kobayashi, J. *Kagaku To Seibutsu,* **1993**, *31*, 659.
[5] Tsuda, M.; Endo, T.; Perpelescu, M.; Yoshida, S.; Watanabe, K.; Fromont, J.; Mikami, Y.; Kobayashi, J. *Tetrahedron,* **2003**. *59,* 1137.
[6] Miyaoka, H.; Watanuki, T.; Saka, Y.; Yamada, Y. T*etrahedron,* **1995**, *51,* 8749.
[7] Al-Busafi, S.; Drew, M. G. B.; Sanders, T.; Whitehead, R. C. *Tetrahedron Lett.*, **1998**, *39*, 1647.
[8] Takeda, K.; Nakayama, I.; Yoshii, E. *Synlett,* **1994**, *3,* 178.
[9] Takeda, K.; Fujisawa, M.; Makino, T.; Yoshii, E.; Yamaguchi, K. *J. Am. Chem. Soc.,* **1993**, 115, 9351.
[10] Asami, M.; Ishizaki, T.; Inoue, S. *Tetrahedron Lett.*, **1995**, *36*, 1893.
[11] Asami, M. *Tetrahedron Lett.,* **1985**, *26,* 5803; Asami, M. *Bull. Chem. Soc. Jpn.,* **1990**, *63,* 1402; Asami, M.; Takahashi, J.; Inoue, S. *Tetrahedron:Asymmetry,* 1994, *5*, 649.
[12] Mander, L. N.;, Sethi, S. P.; *Tetrahedron Lett.*, **1983**, *24*, 5425.
[13] Miyaoka, H.; Watanuki, T.; Saka, Y.; Yamada, Y. *Tetrahedron,* **1995**, *51*, 8749.
[14] Wipf, P.; Venkatraman, S. *J. Org. Chem.*, **1993**, *58*, 3455.
[15] Kuhn, C.; Skaltsounis, L.; Monneret, C.; Florent, J. C. *Eur. J. Org. Chem.,* **2003**, *14*, 2585.
[16] Hoye, T. R.; Chen, K. J.; Vyvyan, J. R. *Organometallics,* **1993**, *12*, 2806.
[17] Casey, C. P.; Cyr, C. R.; Bogga, R. A. *Synth. Inorg. Met. Org. Chem.*, **1973**, *3*, 249.; Harvey, D. F.; Brown, M. F. *Tetrahedron Lett.*, **1990**, *31*, 2529.
[18] Matsuyama, H.; Nakamura, T.; Iyoda, M. *J. Org. Chem.,* **2000**, *65*, 4796.
[19] *Carbene formation was determined by cyclobutanone isolation after the photocycloaddition reaction with chiral auxiliary* ***33***.
[20] Barluenga, J.; Aznar, F.; Palomero, M. A. *J. Org. Chem.* **2003**, *68*, 537.
[21] Dötz, K. H.; Christoffers, J. *Organometallics*, **1994**, *13*, 4189.
[22] Semmelhack, M. F.; Lee, G. R. *Organometallics* **1987**, *6*, 1839.
[23] Gadwood, R. C.; Mallick, I. M.; DeWinter, A. J. *J. Org. Chem.,* **1987**, *52,* 774.
[24] Abraham, W. D.; Bhupathy, M.; Cohen, T. *Tetrahedron Lett.*, **1987**, *28*, 2203.
[25] Trost, B. M.; Mikhail, G. K. *J. Am. Chem. Soc.,* **1987**, *109*, 4124.
[26] Hegedus, L., S.; Reeder, L, R.; *J. Org. Chem.,* **1999**, *64*, 3306.
[27] Greene, A. E.; Luche, M. J.; Serra, A. A. *J. Org. Chem.,* **1985**, *50*, 3957.
[28] Wong, H. C. N. In *Houben-Weyl Methods of Organic Chemistry*; de Meijere, A., Ed.; Georg Thieme Verlag: Stuttgart, Germany, **1997**; Vol. E17e, pp 495-521.
[29] Brown, B.; Hegedus, L. S. *J. Org. Chem.,* **2000**, *65*, 1865.
[30] House, H. O.; Grubbs, E. J.; Gannon, W. F. *J. Am. Chem. Soc.*, **1960**, *82*, 4099.
[31] Johnson, A. W.; Amel, R. T. *J. Org. Chem.,* **1969**, *34*, 1240.
[32] Leriverend, M. L.; Leriverend, P. *Acad. Sci., Ser. C,* **1975**, *280*, 791.

[33] Trost, B. M.; Latimer, L. H. *J. Org. Chem.,* **1978**, *43*, 1031.
[34] Paquette, L. A.; Cox, O.; Oku, M.; Henzel, R. P. *J. Am. Chem. Soc.*, **1974**, *96*, 4892.
[35] Mock, W. L.; Hartman, M. E. *J. Org. Chem.,* **1977**, *42*, 466.
[36] Liu H. J.; Ogino, T., *Tetrahedron Lett.,* **1973**, *49*, 4937.
[37] Tai, T. W.; Warnhoff, E. W. *Can. J. Chem.,* **1964**, *42*, 1333.
[38] Ranslow, P. D. B. R. . *Ph.D. Dissertation, Colorado State University* **2003**.
[39] Yang, D.; Yan, Y. L.; Lui, B. *J. Org. Chem.* **2002**, *67*, 7429.
[40] *The absolute configuration of* ***56*** *has not been assigned.*
[41] Brieger, G.; Spencer, D. G. *Tetrahedron Lett.,* **1971**, *47*, 4585.
[42] Taylor, E. C.; Hawks, G. H.; Mckillop, A. *J. Am. Chem. Soc.,* **1968**, *90*, 2421; Hooz, J.; Smith, J. *J. Org. Chem.,* **1972**, *37*, 4200; Stratford, E. S.; Curley, R. W. *J. Org. Chem.,* **1980**, *45*, 2576.
[43] For a review of the deamination of amines, see Baumgarten, R. J.; Curtis, V. A. in Patai *The Chemistry of Functional Groups, Supplement F,* part 2, Wiley: NY, **1982**, p. 929.
[44] Muller, P.; Thi M. P. N. *Helv. Chim. Acta,* **1980**, *63*, 2168.
[45] Cavender, C. J.;, Shiner V. J. *J. Org. Chem.,* **1972**, *37*, 3567; Leighton J. L.; Jacobsen, E. N. *J. Org. Chem.,* **1996**, *61*, 389.
[46] Takamura, N.; Mizoguchi, T.; Koga, K.; Yamada, S. *Tetrahedron,* **1975**, *31*, 227; Fritschi, H.; Leutenegger, U.; Pfaltz, A. *Helv. Chim. Acta*, **1988**, *71*, 1553.
[47] Ono, N.; Miyake, H.; Tanikaga, R.; Kaji, A. *J. Org. Chem.,* **1982**, *47*, 5017.
[48] Gilbert, K. E.; Borden, W. T. *J. Org. Chem.,* **1979**, *44*, 659.
[49] Wen, X.; Norling, H.; Hegedus, L. S. *J. Org. Chem.,* **2000**, *65*. 2096.

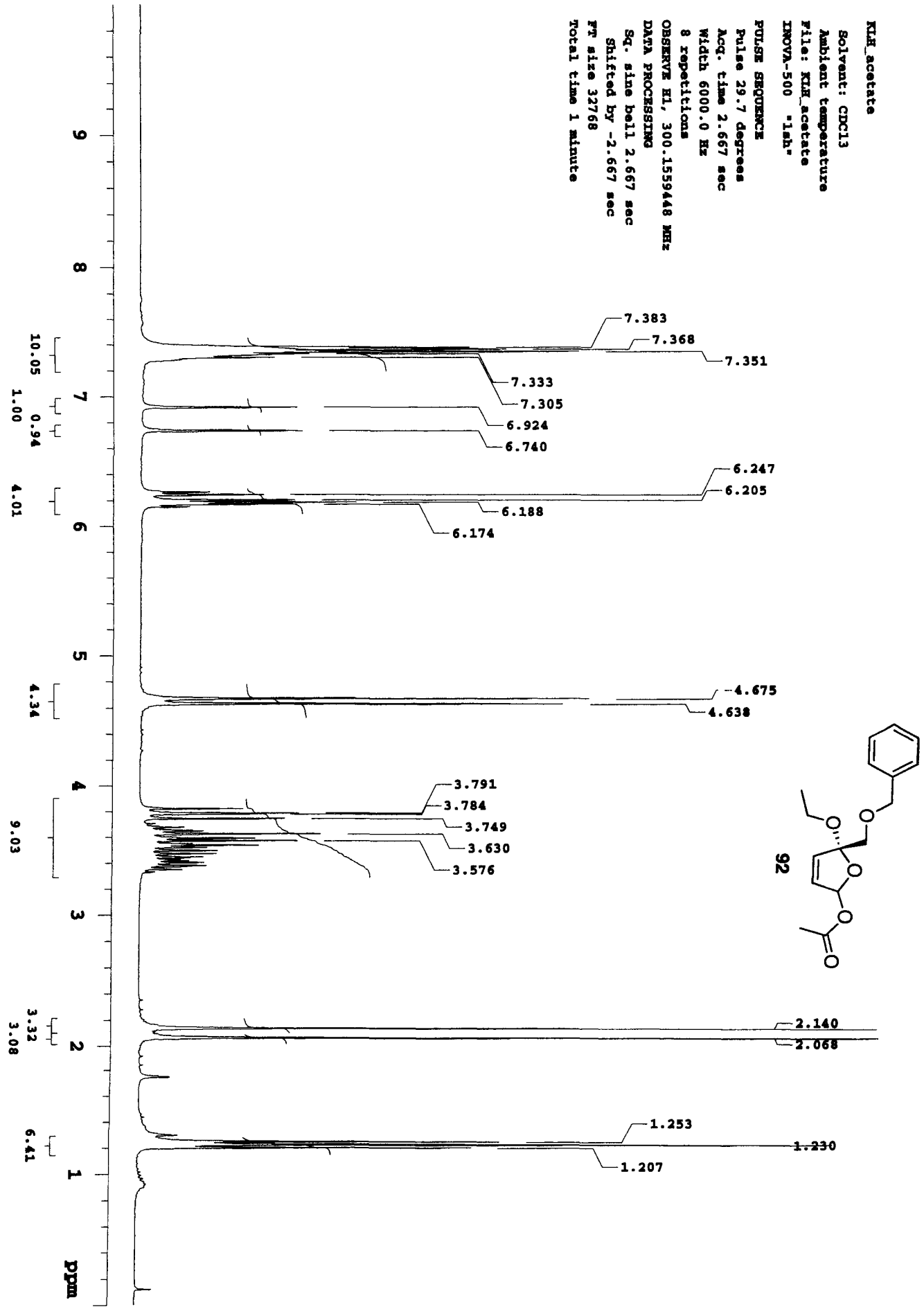

13C OBSERVE

Solvent: CDCl3
Ambient temperature
File: KLH_acetaeC
INOVA-500 "lsh"

PULSE SEQUENCE
Relax. delay 1.200 sec
Pulse 48.7 degrees
Acq. time 0.727 sec
Width 22000.0 Hz
80 repetitions
OBSERVE C13, 75.4742661 MHz
DECOUPLE H1, 300.1574402 MHz
Power 37 dB
continuously on
WALTZ-16 modulated
DATA PROCESSING
Line broadening 2.0 Hz
FT size 32768
Total time 2 minutes

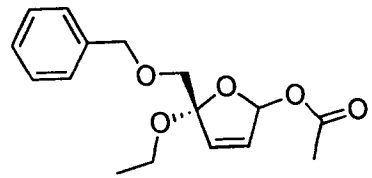

92

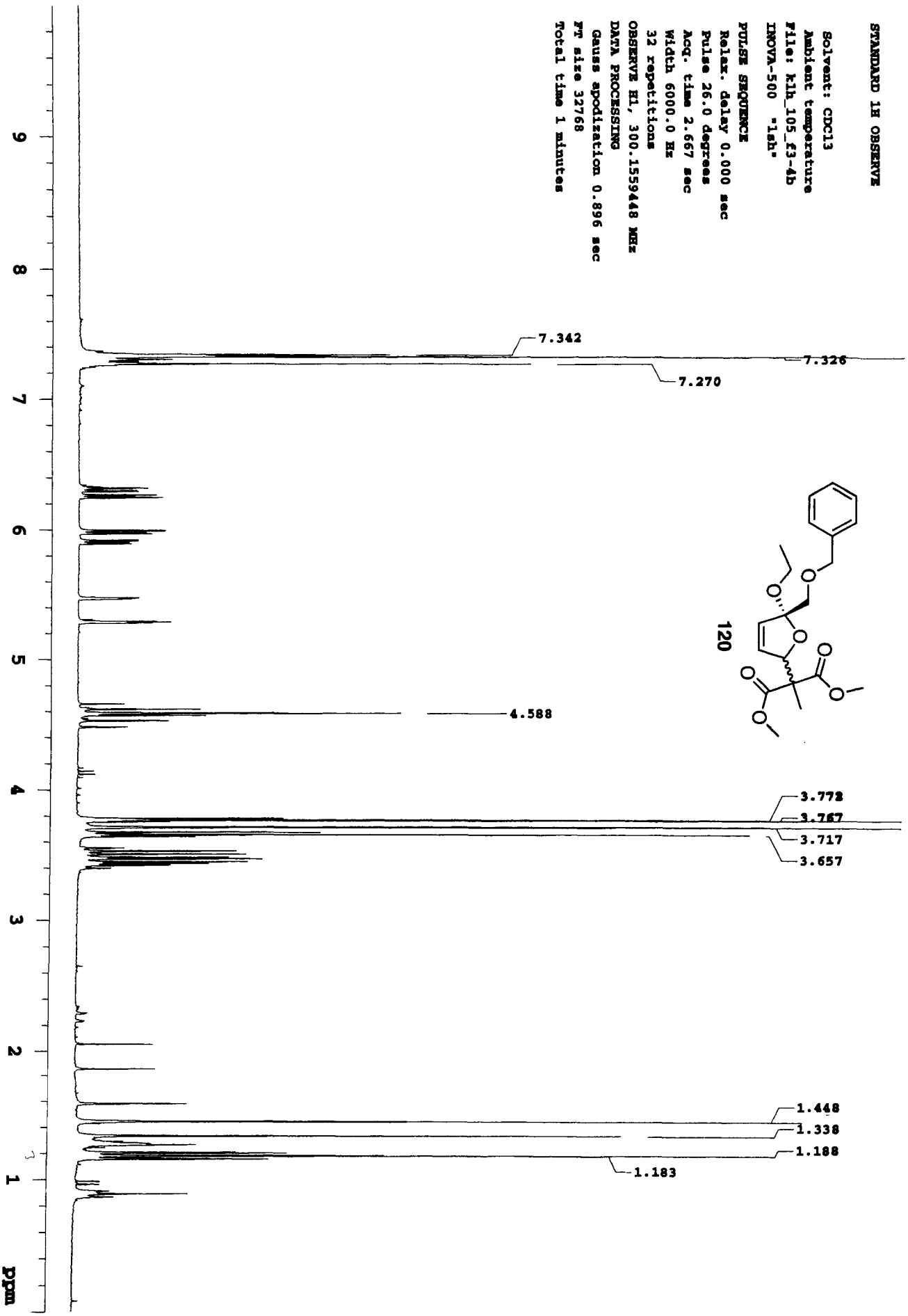

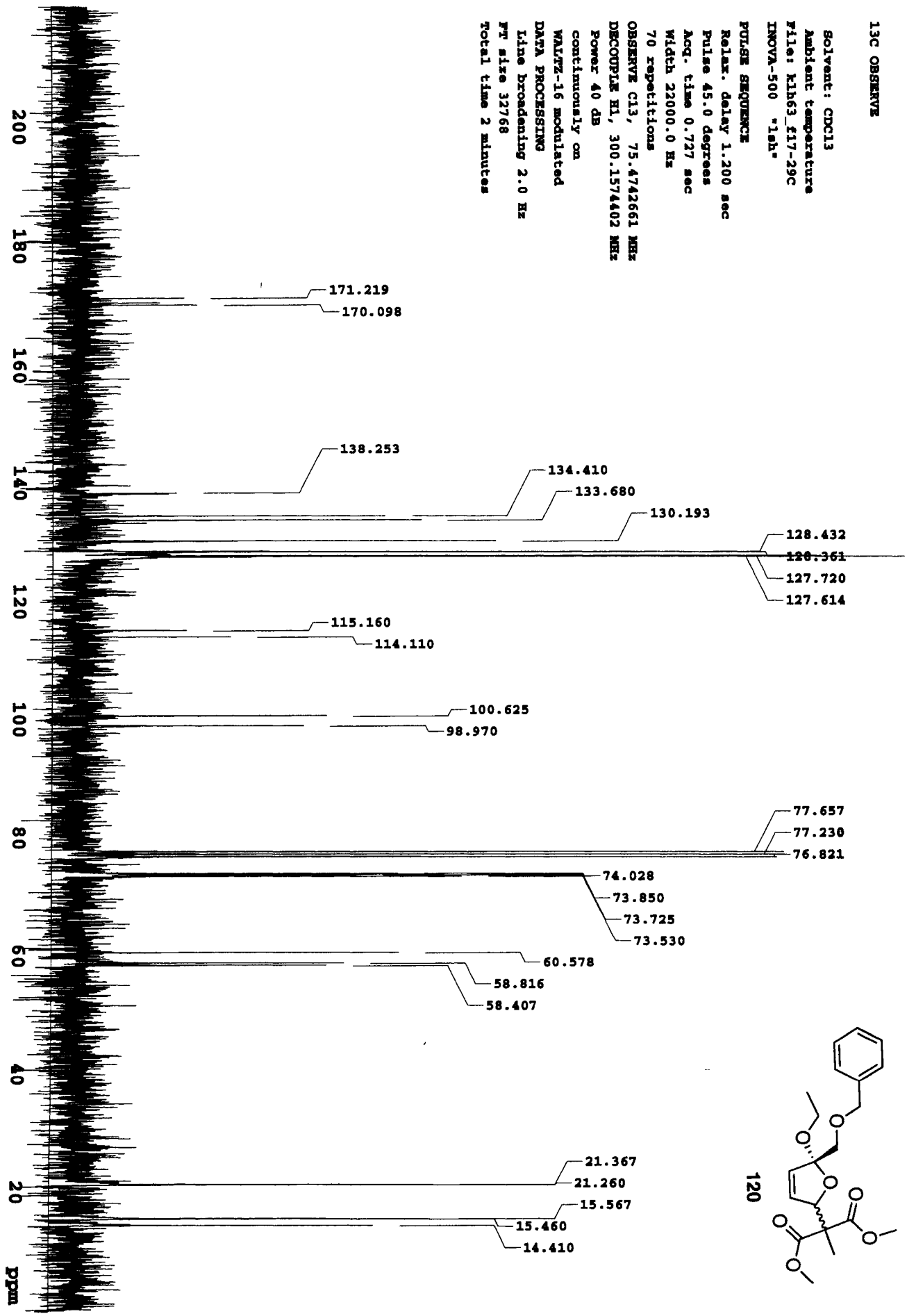

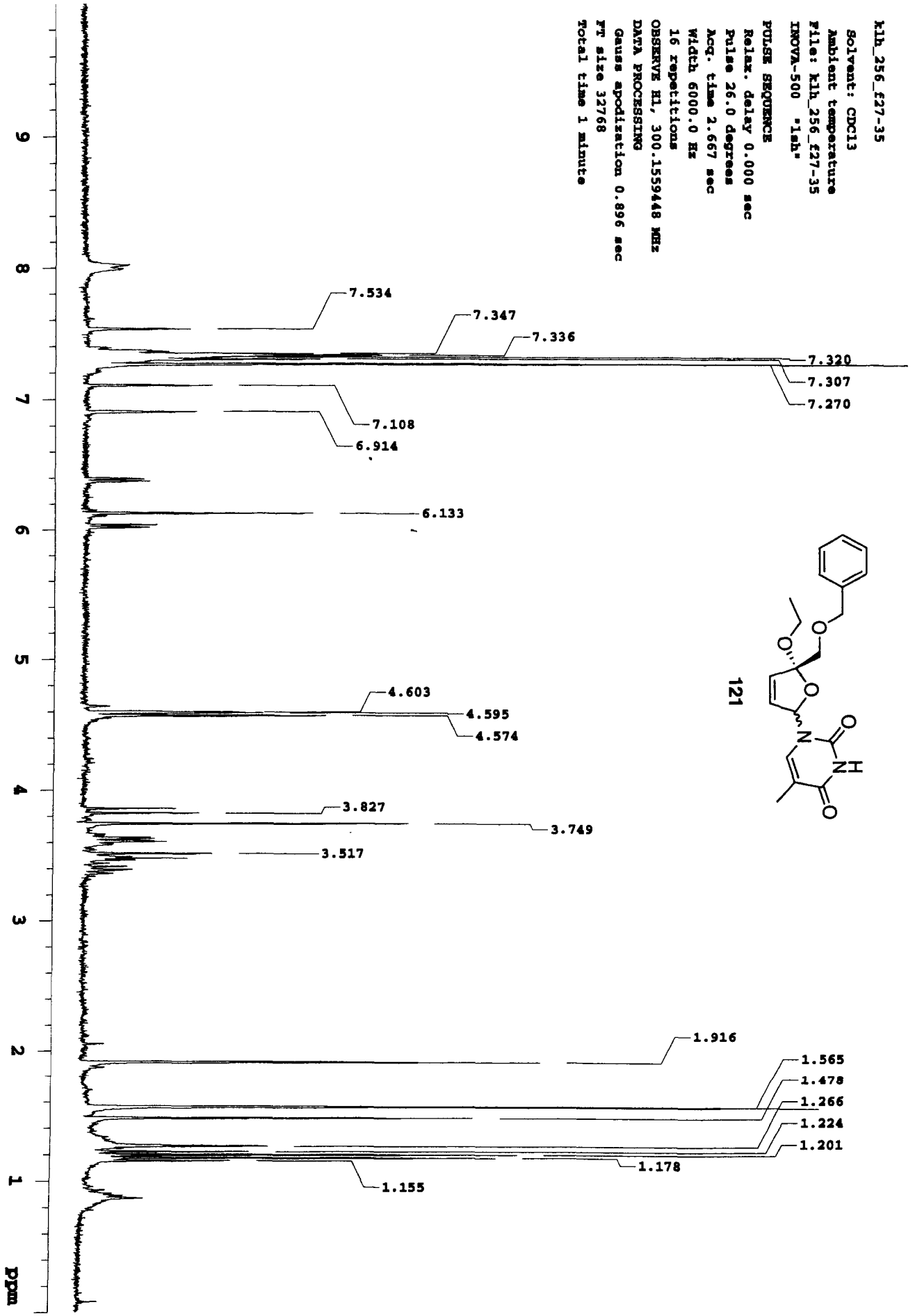

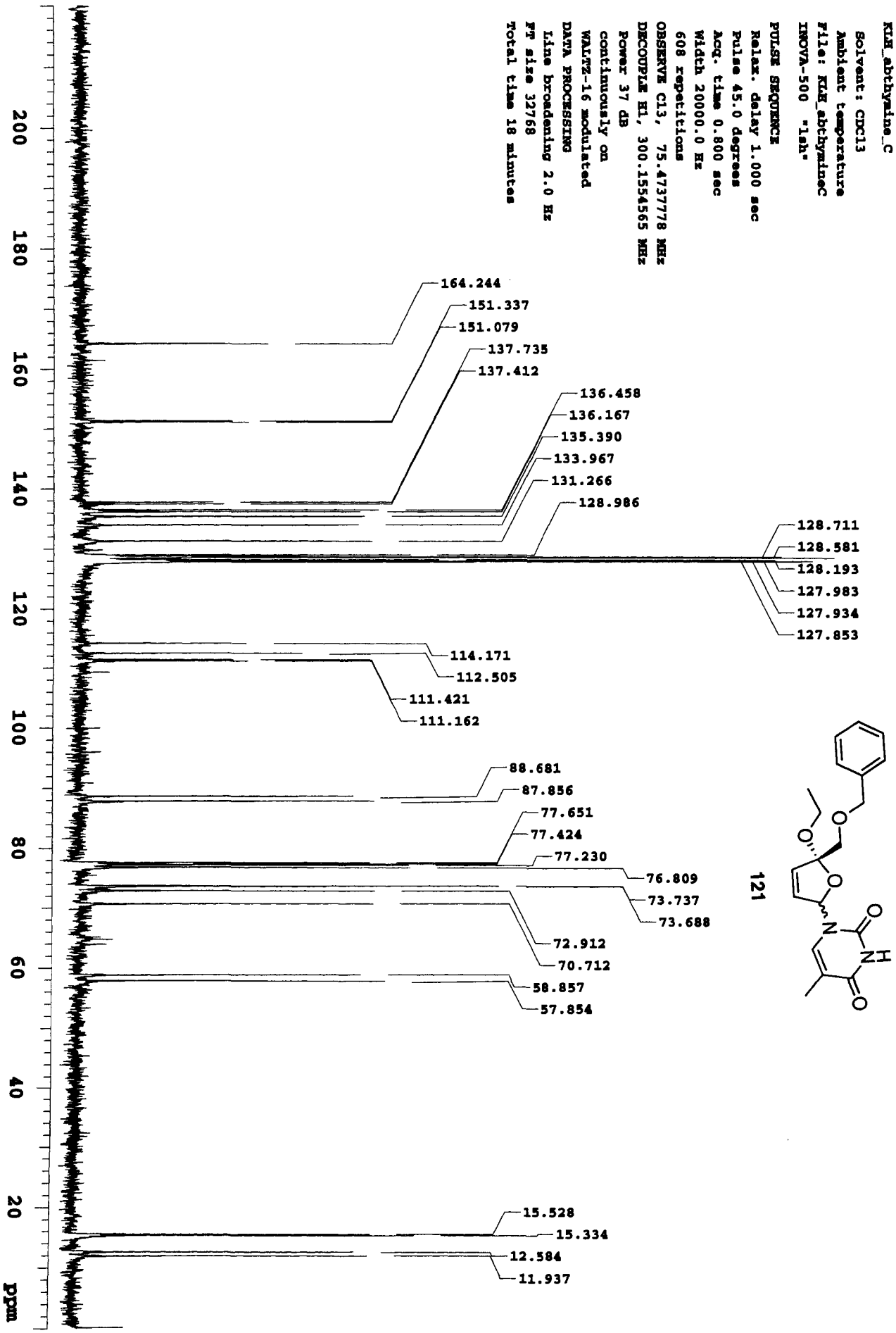

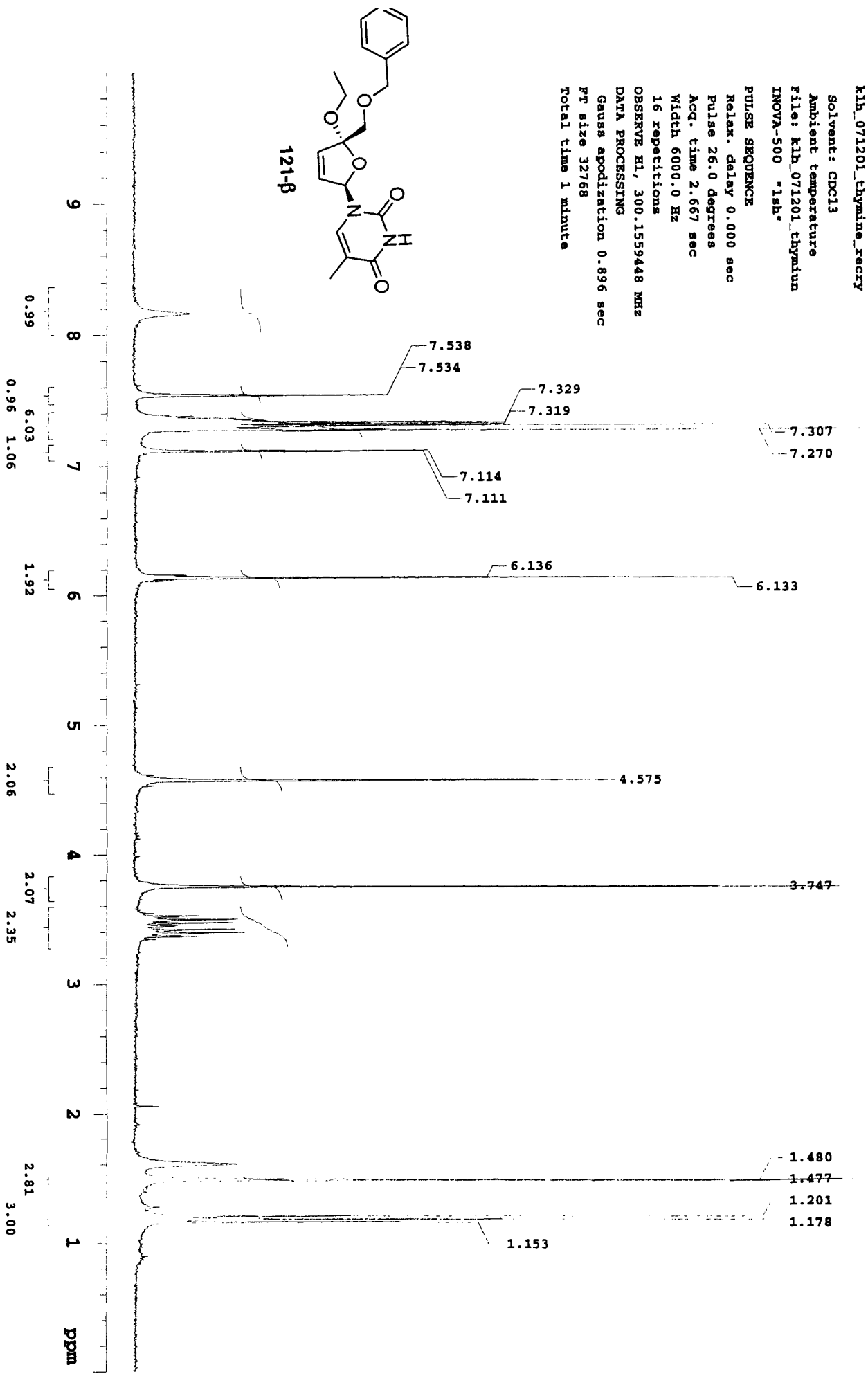

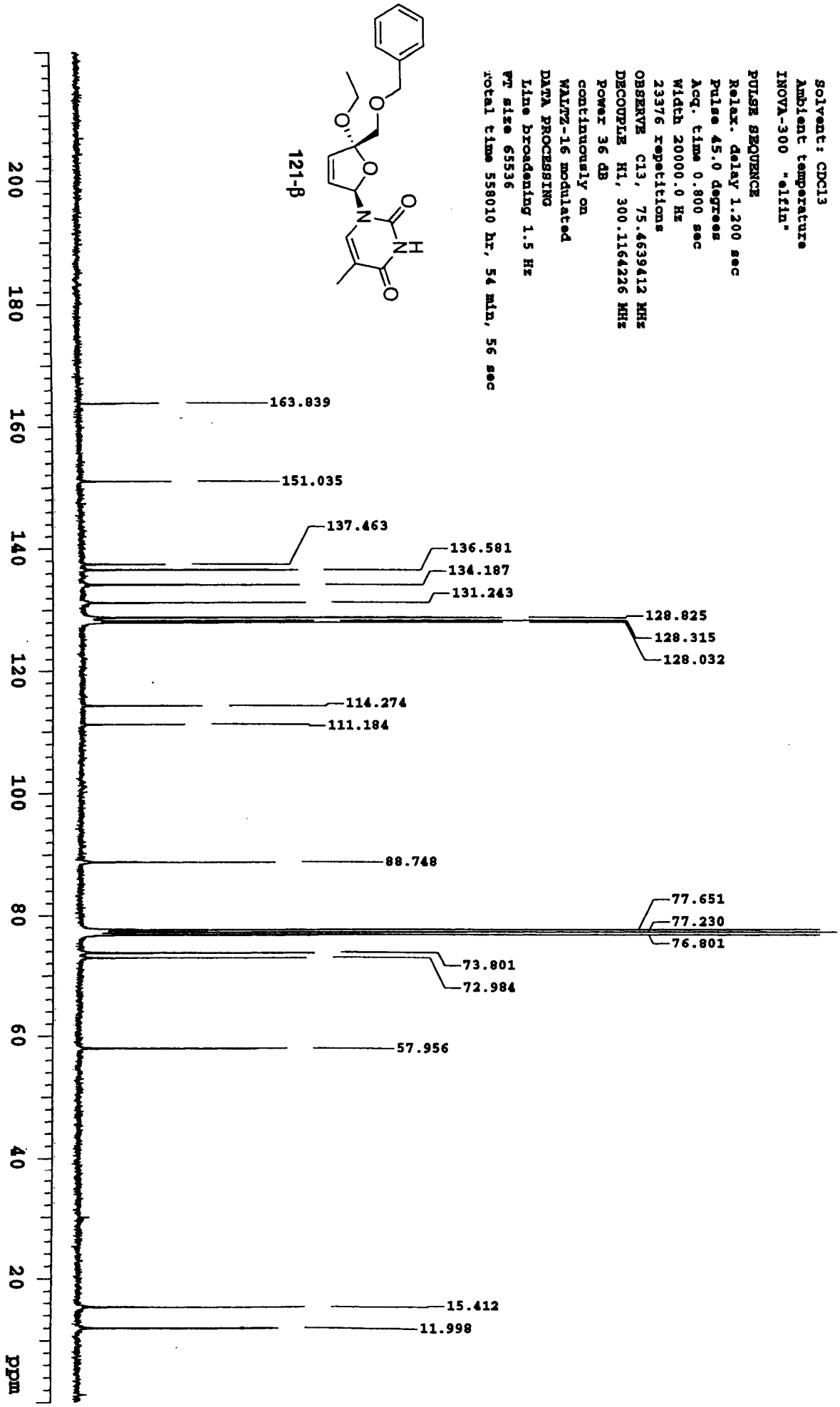

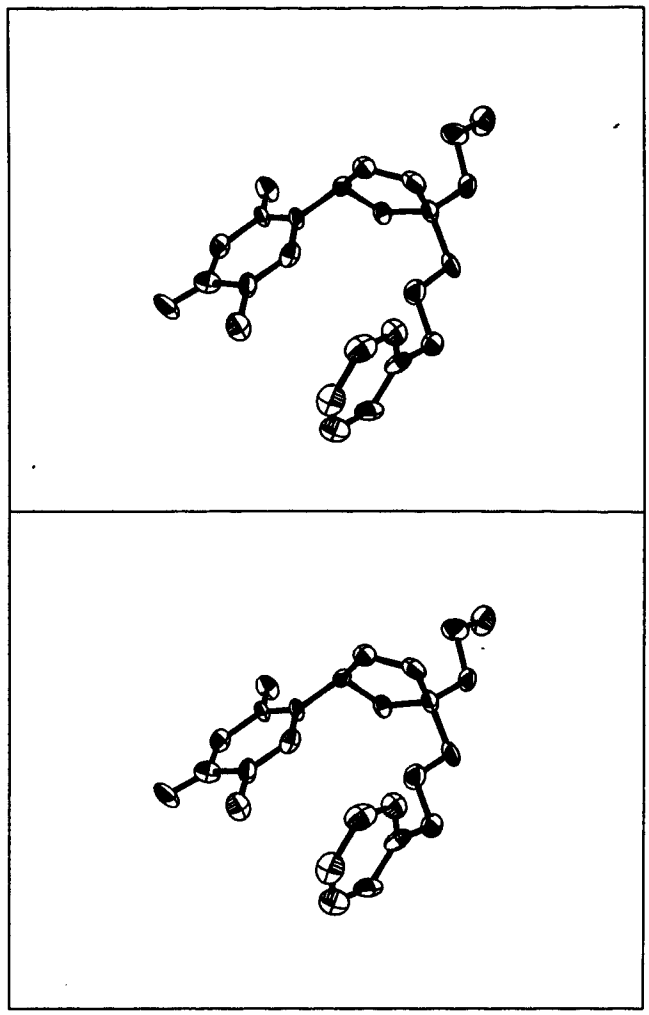

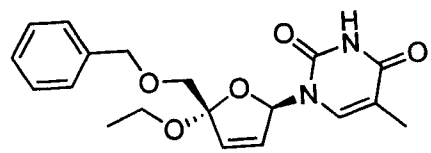

121-β

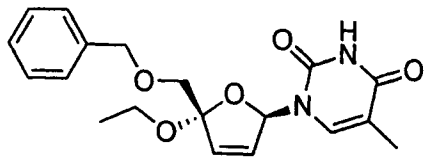

121-β

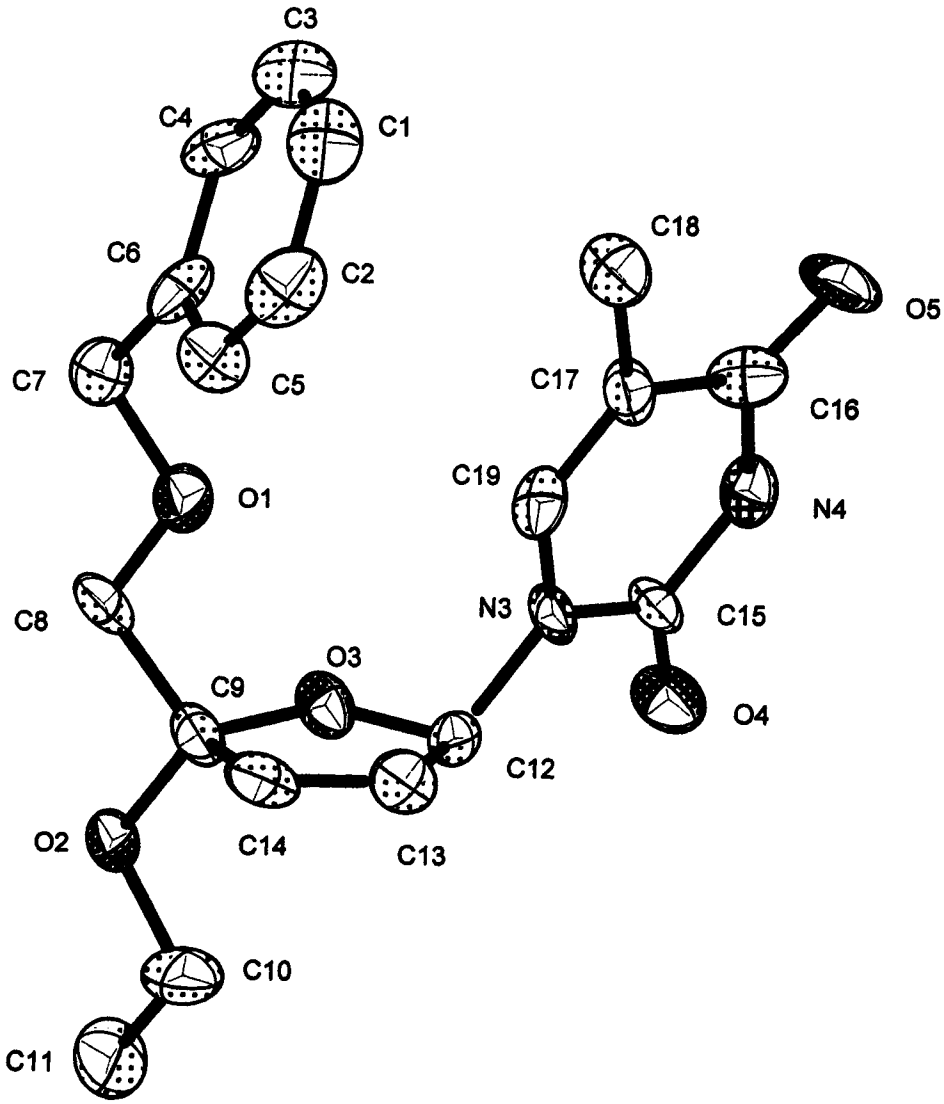

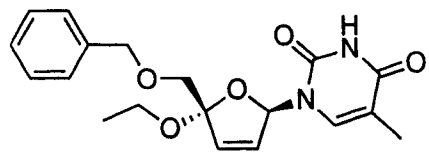

121-β

Table 1. Crystal data and structure refinement for lsh45.

Identification code	lsh451m	
Empirical formula	C19 H22 N2 O5	
Formula weight	358.39	
Temperature	293(2) K	
Wavelength	0.71073 Å	
Crystal system	Triclinic	
Space group	P1	
Unit cell dimensions	a = 5.9018(12) Å	α= 87.863(5)°.
	b = 9.814(2) Å	β= 80.098(5)°.
	c = 15.715(3) Å	γ = 85.539(5)°.
Volume	893.7(3) Å^3	
Z	2	
Density (calculated)	1.332 Mg/m^3	
Absorption coefficient	0.097 mm^{-1}	
F(000)	380	
Crystal size	0.08 x 0.08 x 0.30 mm^3	
Theta range for data collection	2.08 to 23.27°.	
Index ranges	-6<=h<=6, -10<=k<=10, -17<=l<=14	
Reflections collected	4211	
Independent reflections	3235 [R(int) = 0.0364]	
Completeness to theta = 23.27°	99.5 %	
Absorption correction	SADABS	
Refinement method	Full-matrix least-squares on F^2	
Data / restraints / parameters	3235 / 3 / 474	
Goodness-of-fit on F^2	0.825	
Final R indices [I>2sigma(I)]	R1 = 0.0492, wR2 = 0.0919	
R indices (all data)	R1 = 0.0887, wR2 = 0.1043	
Absolute structure parameter	-2(2)	
Extinction coefficient	0.0051(18)	
Largest diff. peak and hole	0.240 and -0.290 e.Å^{-3}	

Table 2. Atomic coordinates (x 10^4) and equivalent isotropic displacement parameters ($Å^2$x 10^3) for lsh45. U(eq) is defined as one third of the trace of the orthogonalized U^{ij} tensor.

	x	y	z	U(eq)
C(1)	12961(12)	1636(8)	4446(5)	45(2)
C(2)	13427(12)	2930(8)	4062(5)	46(2)
C(3)	11142(13)	990(7)	4281(5)	44(2)
C(4)	9763(12)	1589(7)	3704(5)	38(2)
C(5)	12013(13)	3500(8)	3497(5)	44(2)
C(6)	10179(11)	2851(7)	3313(4)	32(2)
C(7)	8750(11)	3520(7)	2696(4)	35(2)
C(8)	7042(12)	5741(6)	2381(4)	41(2)
C(9)	6589(11)	7118(7)	2779(4)	29(2)
C(10)	5387(13)	9401(7)	2370(5)	51(2)
C(11)	3814(13)	10078(7)	1795(4)	59(2)
C(12)	5368(11)	7579(6)	4260(4)	27(2)
C(13)	7864(10)	7857(6)	3996(4)	32(2)
C(14)	8486(11)	7608(6)	3180(4)	36(2)
C(15)	2856(11)	6699(7)	5516(4)	27(2)
C(16)	4175(11)	4673(7)	6365(5)	33(2)
C(17)	6252(12)	4584(7)	5727(4)	33(2)
C(18)	8018(11)	3399(7)	5850(4)	41(2)
C(19)	6564(11)	5484(7)	5079(4)	29(2)
C(20)	-3472(17)	12069(10)	8275(6)	61(3)
C(21)	-1573(18)	12709(9)	8390(6)	63(3)
C(22)	-4022(15)	10937(11)	8706(7)	70(3)
C(23)	-210(13)	12124(10)	8996(6)	67(3)
C(24)	-2808(15)	10363(9)	9264(5)	54(2)
C(25)	-935(13)	10916(8)	9442(5)	40(2)
C(26)	270(20)	10229(12)	10127(6)	145(6)
C(27)	913(12)	7831(8)	10305(5)	52(2)
C(28)	2579(12)	6582(7)	9977(4)	33(2)
C(29)	6239(11)	6495(6)	9204(4)	36(2)
C(30)	5025(11)	6753(6)	9976(4)	36(2)
C(31)	4673(11)	6258(7)	8599(4)	35(2)

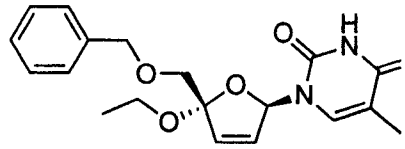

121-β

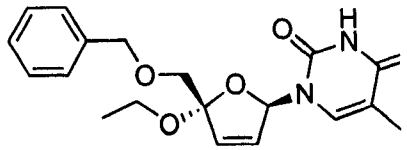

121-β

C(32)	6882(12)	7093(8)	7263(4)	34(2)
C(33)	3209(11)	8266(7)	7740(4)	34(2)
C(34)	3400(10)	9162(7)	7065(4)	32(2)
C(35)	1545(12)	10247(7)	6932(5)	48(2)
C(36)	5504(11)	9033(7)	6435(4)	33(2)
C(37)	2743(17)	4162(8)	10293(5)	75(3)
C(38)	4513(15)	3718(9)	10822(5)	80(3)
N(1)	4866(9)	7245(5)	7848(3)	30(1)
N(2)	7100(9)	7986(5)	6587(3)	33(2)
N(3)	4965(8)	6579(5)	4972(3)	25(1)
N(4)	2602(9)	5775(5)	6189(3)	32(1)
O(1)	7926(8)	4855(5)	3007(3)	45(1)
O(2)	5898(7)	7998(4)	2125(2)	37(1)
O(3)	4704(6)	7076(4)	3504(2)	29(1)
O(4)	1363(7)	7616(5)	5433(3)	37(1)
O(5)	3666(8)	3950(5)	7006(3)	49(1)
O(6)	1638(10)	8982(6)	9823(3)	76(2)
O(7)	2440(7)	6391(4)	9087(3)	40(1)
O(8)	8406(8)	6160(5)	7355(3)	41(1)
O(9)	5916(8)	9760(5)	5778(3)	44(1)
O(10)	1667(8)	5507(5)	10505(3)	59(1)

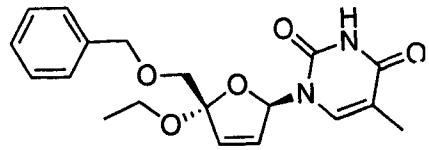

121-β

Table 3. Bond lengths [Å] and angles [°] for lsh45.

C(1)-C(3)	1.354(10)
C(1)-C(2)	1.411(10)
C(2)-C(5)	1.394(10)
C(3)-C(4)	1.403(9)
C(4)-C(6)	1.382(9)
C(5)-C(6)	1.374(9)
C(6)-C(7)	1.493(9)
C(7)-O(1)	1.435(8)
C(8)-O(1)	1.428(7)
C(8)-C(9)	1.496(9)
C(9)-O(2)	1.411(7)
C(9)-O(3)	1.452(7)
C(9)-C(14)	1.494(9)
C(10)-O(2)	1.438(7)
C(10)-C(11)	1.506(9)
C(12)-O(3)	1.429(7)
C(12)-N(3)	1.461(7)
C(12)-C(13)	1.504(8)
C(13)-C(14)	1.299(8)
C(15)-O(4)	1.229(7)
C(15)-N(4)	1.363(7)
C(15)-N(3)	1.383(7)
C(16)-O(5)	1.218(7)
C(16)-N(4)	1.420(8)
C(16)-C(17)	1.443(9)
C(17)-C(19)	1.321(8)
C(17)-C(18)	1.530(9)
C(19)-N(3)	1.399(7)
C(20)-C(22)	1.313(12)
C(20)-C(21)	1.368(12)
C(21)-C(23)	1.426(12)
C(22)-C(24)	1.309(11)
C(23)-C(25)	1.412(11)
C(24)-C(25)	1.344(10)

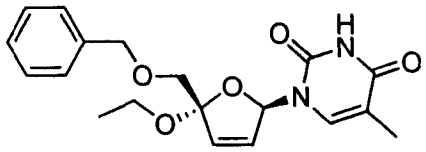

121-β

C(25)-C(26)	1.502(10)
C(26)-O(6)	1.461(10)
C(27)-O(6)	1.390(9)
C(27)-C(28)	1.555(9)
C(28)-O(10)	1.401(7)
C(28)-O(7)	1.436(7)
C(28)-C(30)	1.466(8)
C(29)-C(30)	1.321(8)
C(29)-C(31)	1.471(9)
C(31)-O(7)	1.405(7)
C(31)-N(1)	1.494(8)
C(32)-O(8)	1.255(7)
C(32)-N(2)	1.346(8)
C(32)-N(1)	1.374(8)
C(33)-C(34)	1.347(8)
C(33)-N(1)	1.372(7)
C(34)-C(36)	1.450(9)
C(34)-C(35)	1.503(9)
C(36)-O(9)	1.232(7)
C(36)-N(2)	1.382(7)
C(37)-O(10)	1.444(9)
C(37)-C(38)	1.474(11)

C(3)-C(1)-C(2)	120.2(7)
C(5)-C(2)-C(1)	118.4(7)
C(1)-C(3)-C(4)	119.9(7)
C(6)-C(4)-C(3)	121.4(7)
C(6)-C(5)-C(2)	122.1(8)
C(5)-C(6)-C(4)	117.9(6)
C(5)-C(6)-C(7)	119.2(7)
C(4)-C(6)-C(7)	122.9(7)
O(1)-C(7)-C(6)	107.9(5)
O(1)-C(8)-C(9)	106.0(5)
O(2)-C(9)-O(3)	109.1(5)
O(2)-C(9)-C(14)	114.4(5)
O(3)-C(9)-C(14)	102.6(5)

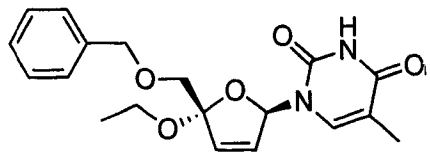

121-β

O(2)-C(9)-C(8)	105.0(5)
O(3)-C(9)-C(8)	109.5(5)
C(14)-C(9)-C(8)	116.2(5)
O(2)-C(10)-C(11)	108.3(6)
O(3)-C(12)-N(3)	110.1(5)
O(3)-C(12)-C(13)	105.1(5)
N(3)-C(12)-C(13)	113.4(5)
C(14)-C(13)-C(12)	108.7(6)
C(13)-C(14)-C(9)	113.0(6)
O(4)-C(15)-N(4)	122.0(6)
O(4)-C(15)-N(3)	122.9(6)
N(4)-C(15)-N(3)	115.0(6)
O(5)-C(16)-N(4)	119.0(6)
O(5)-C(16)-C(17)	128.5(6)
N(4)-C(16)-C(17)	112.5(6)
C(19)-C(17)-C(16)	120.8(6)
C(19)-C(17)-C(18)	123.1(6)
C(16)-C(17)-C(18)	116.1(6)
C(17)-C(19)-N(3)	123.2(6)
C(22)-C(20)-C(21)	120.9(9)
C(20)-C(21)-C(23)	118.5(8)
C(24)-C(22)-C(20)	122.5(10)
C(25)-C(23)-C(21)	117.1(8)
C(22)-C(24)-C(25)	121.7(9)
C(24)-C(25)-C(23)	119.2(7)
C(24)-C(25)-C(26)	118.0(10)
C(23)-C(25)-C(26)	122.8(10)
O(6)-C(26)-C(25)	112.2(7)
O(6)-C(27)-C(28)	108.4(5)
O(10)-C(28)-O(7)	111.5(5)
O(10)-C(28)-C(30)	115.0(6)
O(7)-C(28)-C(30)	104.5(5)
O(10)-C(28)-C(27)	102.7(6)
O(7)-C(28)-C(27)	108.3(5)
C(30)-C(28)-C(27)	114.9(6)
C(30)-C(29)-C(31)	109.5(6)

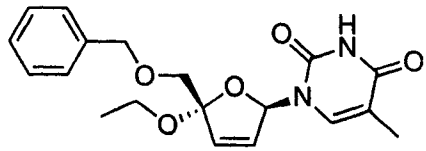

121-β

C(29)-C(30)-C(28)	110.1(6)
O(7)-C(31)-C(29)	105.6(5)
O(7)-C(31)-N(1)	110.1(5)
C(29)-C(31)-N(1)	113.2(5)
O(8)-C(32)-N(2)	122.5(7)
O(8)-C(32)-N(1)	121.3(7)
N(2)-C(32)-N(1)	116.2(6)
C(34)-C(33)-N(1)	123.6(6)
C(33)-C(34)-C(36)	117.1(6)
C(33)-C(34)-C(35)	123.5(6)
C(36)-C(34)-C(35)	119.4(6)
O(9)-C(36)-N(2)	119.2(6)
O(9)-C(36)-C(34)	124.7(6)
N(2)-C(36)-C(34)	116.1(6)
O(10)-C(37)-C(38)	112.9(7)
C(32)-N(1)-C(33)	120.8(6)
C(32)-N(1)-C(31)	115.3(6)
C(33)-N(1)-C(31)	123.8(6)
C(32)-N(2)-C(36)	126.2(6)
C(15)-N(3)-C(19)	120.3(5)
C(15)-N(3)-C(12)	117.4(5)
C(19)-N(3)-C(12)	122.3(5)
C(15)-N(4)-C(16)	128.0(6)
C(8)-O(1)-C(7)	114.0(5)
C(9)-O(2)-C(10)	114.4(5)
C(12)-O(3)-C(9)	110.4(5)
C(27)-O(6)-C(26)	112.3(7)
C(31)-O(7)-C(28)	109.6(5)
C(28)-O(10)-C(37)	115.5(5)

Symmetry transformations used to generate equivalent atoms:

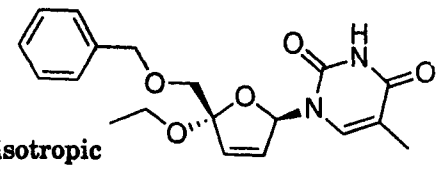

121-β

Table 4. Anisotropic displacement parameters ($Å^2 x\ 10^3$) for lsh45. The anisotropic displacement factor exponent takes the form: $-2\pi^2[\ h^2\ a^{*2}U^{11} + ...\ + 2\ h\ k\ a^*\ b^*\ U^{12}\ ]$

	U^{11}	U^{22}	U^{33}	U^{23}	U^{13}	U^{12}
C(1)	35(5)	56(6)	44(5)	-3(4)	-14(4)	15(4)
C(2)	33(5)	48(5)	57(5)	-14(5)	-3(4)	-10(4)
C(3)	45(5)	33(5)	52(5)	3(4)	-15(4)	22(4)
C(4)	38(5)	24(4)	53(5)	-8(4)	-4(4)	-9(4)
C(5)	55(5)	40(5)	37(5)	4(4)	-7(4)	-1(4)
C(6)	27(4)	29(5)	39(5)	-16(4)	-9(4)	8(3)
C(7)	35(4)	34(5)	32(4)	-2(4)	1(3)	2(3)
C(8)	60(5)	34(4)	23(4)	14(3)	0(3)	2(4)
C(9)	33(4)	33(4)	19(4)	6(3)	0(3)	-2(3)
C(10)	78(6)	27(5)	49(5)	6(4)	-22(4)	4(4)
C(11)	85(6)	51(5)	38(4)	4(4)	-21(4)	24(5)
C(12)	40(4)	22(4)	20(4)	-2(3)	-13(3)	1(3)
C(13)	34(4)	34(4)	32(4)	1(3)	-14(3)	-12(3)
C(14)	42(4)	28(4)	38(4)	11(3)	-10(4)	-9(3)
C(15)	38(5)	27(5)	17(4)	8(3)	-5(4)	-8(4)
C(16)	20(4)	28(5)	49(5)	1(4)	-8(4)	5(3)
C(17)	41(5)	36(5)	19(4)	1(4)	-3(3)	7(4)
C(18)	33(4)	44(5)	39(4)	5(4)	8(3)	15(4)
C(19)	20(4)	39(5)	26(4)	-8(4)	-2(3)	12(4)
C(20)	67(7)	54(7)	56(6)	-6(5)	-8(5)	35(6)
C(21)	75(7)	45(6)	53(6)	9(5)	33(5)	-3(6)
C(22)	45(6)	80(8)	86(8)	-28(7)	-12(6)	3(6)
C(23)	26(5)	87(8)	83(7)	-53(6)	11(5)	-6(5)
C(24)	51(6)	58(6)	50(6)	-5(5)	8(5)	-17(5)
C(25)	43(5)	40(5)	36(5)	-4(4)	-13(4)	16(4)
C(26)	212(12)	143(10)	63(7)	-20(7)	-42(8)	141(10)
C(27)	40(5)	67(6)	45(5)	-21(4)	4(4)	2(4)
C(28)	36(4)	42(5)	20(4)	0(4)	0(3)	-12(4)
C(29)	25(4)	38(4)	40(4)	9(3)	0(3)	7(3)
C(30)	45(5)	36(4)	31(4)	4(3)	-10(3)	-11(3)
C(31)	37(5)	39(5)	29(4)	1(4)	-2(4)	-7(4)

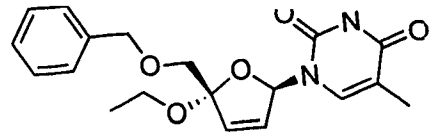

121-β

C(32)	35(5)	38(5)	28(4)	-3(4)	-3(4)	0(4,
C(33)	33(4)	39(5)	27(4)	-4(4)	-3(3)	8(4)
C(34)	22(4)	36(5)	34(4)	-5(4)	0(3)	6(4)
C(35)	51(5)	36(5)	52(5)	3(4)	-2(4)	11(4)
C(36)	37(5)	28(5)	31(4)	-2(4)	-6(4)	7(4)
C(37)	145(9)	52(6)	30(5)	-3(4)	4(5)	-59(6)
C(38)	114(8)	64(6)	63(6)	-1(5)	-29(6)	5(6)
N(1)	32(4)	30(4)	26(3)	4(3)	1(3)	-3(3)
N(2)	31(4)	39(4)	23(3)	10(3)	6(3)	9(3)
N(3)	26(3)	30(3)	16(3)	5(3)	6(3)	1(3)
N(4)	23(3)	40(4)	27(3)	-6(3)	6(3)	-1(3)
O(1)	66(3)	37(3)	27(3)	-1(2)	-8(2)	14(3)
O(2)	57(3)	32(3)	20(2)	2(2)	-9(2)	6(2)
O(3)	24(2)	35(3)	25(2)	4(2)	1(2)	1(2)
O(4)	29(3)	38(3)	40(3)	9(2)	0(2)	7(2)
O(5)	57(4)	33(3)	47(3)	21(3)	6(3)	10(3)
O(6)	106(5)	64(4)	42(3)	10(3)	9(3)	52(4)
O(7)	39(3)	55(3)	23(3)	2(2)	-2(2)	-9(2)
O(8)	42(3)	41(3)	32(3)	7(2)	3(2)	15(3)
O(9)	41(3)	47(3)	39(3)	14(3)	-2(2)	9(3)
O(10)	76(4)	60(4)	39(3)	0(3)	5(3)	-34(3)

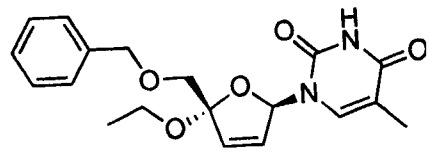

121-β

Table 5. Hydrogen coordinates (x 10^4) and isotropic displacement parameters ($Å^2$x 10^3) for lsh45.

	x	y	z	U(eq)
H(1)	13905	1225	4813	54
H(2)	14648	3391	4183	55
H(3)	10809	152	4549	53
H(4)	8543	1128	3583	46
H(5)	12321	4347	3235	53
H(7A)	9670	3592	2124	41
H(7B)	7460	2981	2660	41
H(8A)	5630	5421	2249	49
H(8B)	8158	5779	1851	49
H(10A)	6801	9865	2305	61
H(10B)	4642	9445	2969	61
H(11A)	4536	9993	1201	88
H(11B)	3518	11028	1929	88
H(11C)	2386	9645	1887	88
H(12)	4459	8437	4423	32
H(13)	8806	8157	4358	38
H(14)	9959	7722	2877	43
H(18A)	7345	2547	5816	62
H(18B)	8468	3456	6406	62
H(18C)	9349	3450	5406	62
H(19)	7912	5386	4675	35
H(20)	-4386	12441	7885	73
H(21)	-1179	13507	8081	76
H(22)	-5323	10528	8612	84
H(23)	1099	12522	9094	80
H(24)	-3254	9551	9544	65
H(26A)	1271	10857	10310	174
H(26B)	-870	10005	10625	174
H(27A)	-649	7675	10238	62
H(27B)	931	7962	10912	62

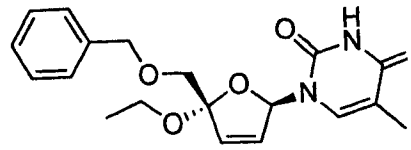

121-β

H(29)	7839	6467	9065	43
H(30)	5634	7006	10450	44
H(31)	4991	5324	8387	42
H(33)	1880	8344	8155	40
H(35A)	914	10046	6431	72
H(35B)	2188	11120	6850	72
H(35C)	346	10267	7430	72
H(37A)	3449	4163	9688	90
H(37B)	1567	3509	10375	90
H(38A)	5627	4391	10775	119
H(38B)	5268	2859	10621	119
H(38C)	3796	3615	11415	119
H(2A)	8350	7895	6215	40
H(4A)	1334	5870	6551	38

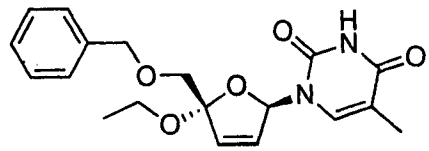

121-β

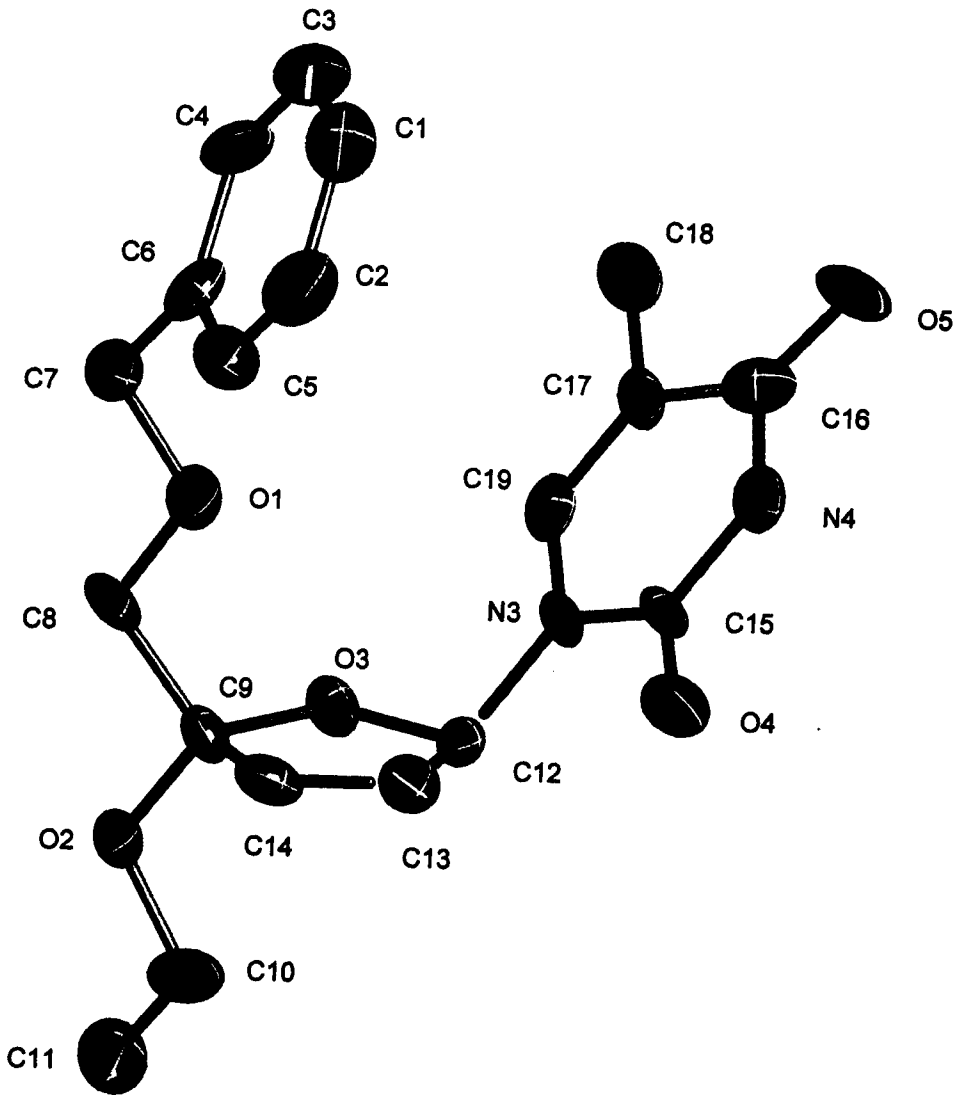

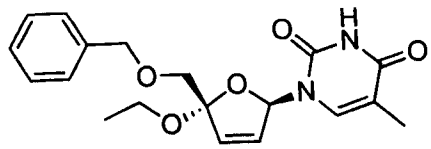

121-β

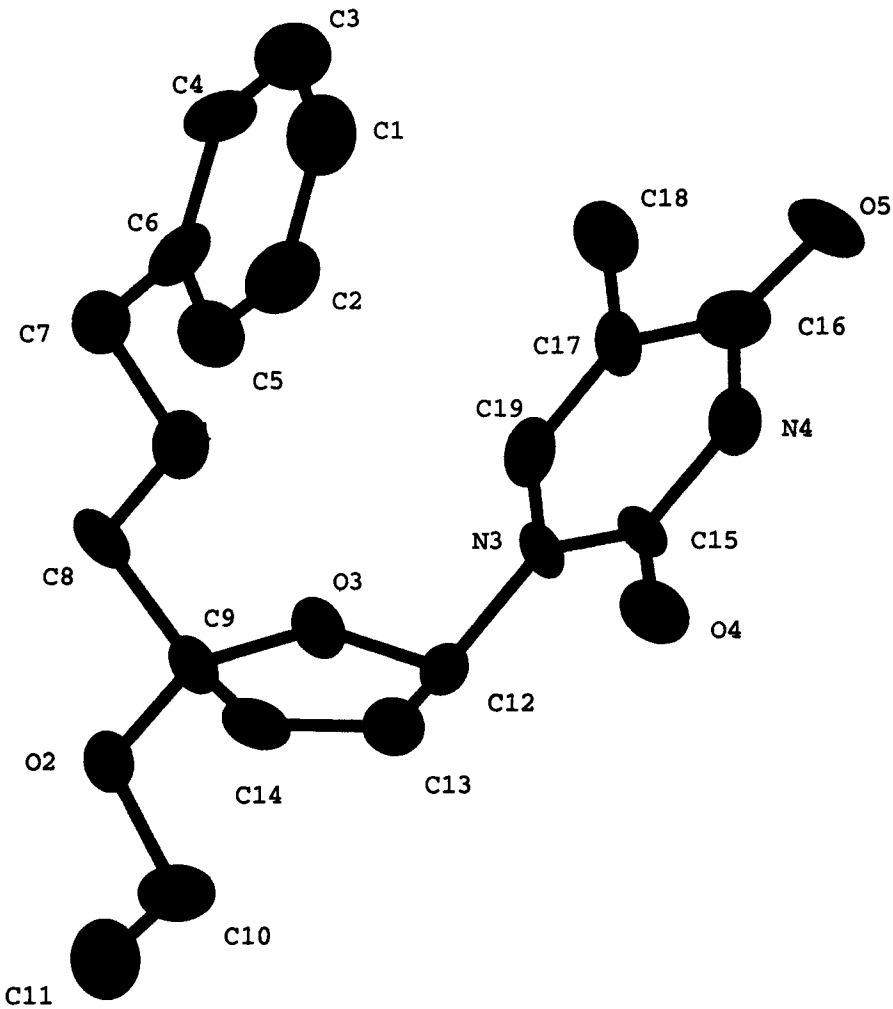

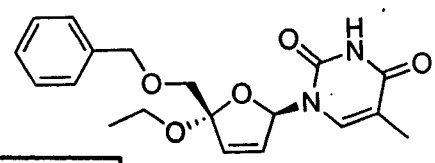

121-β

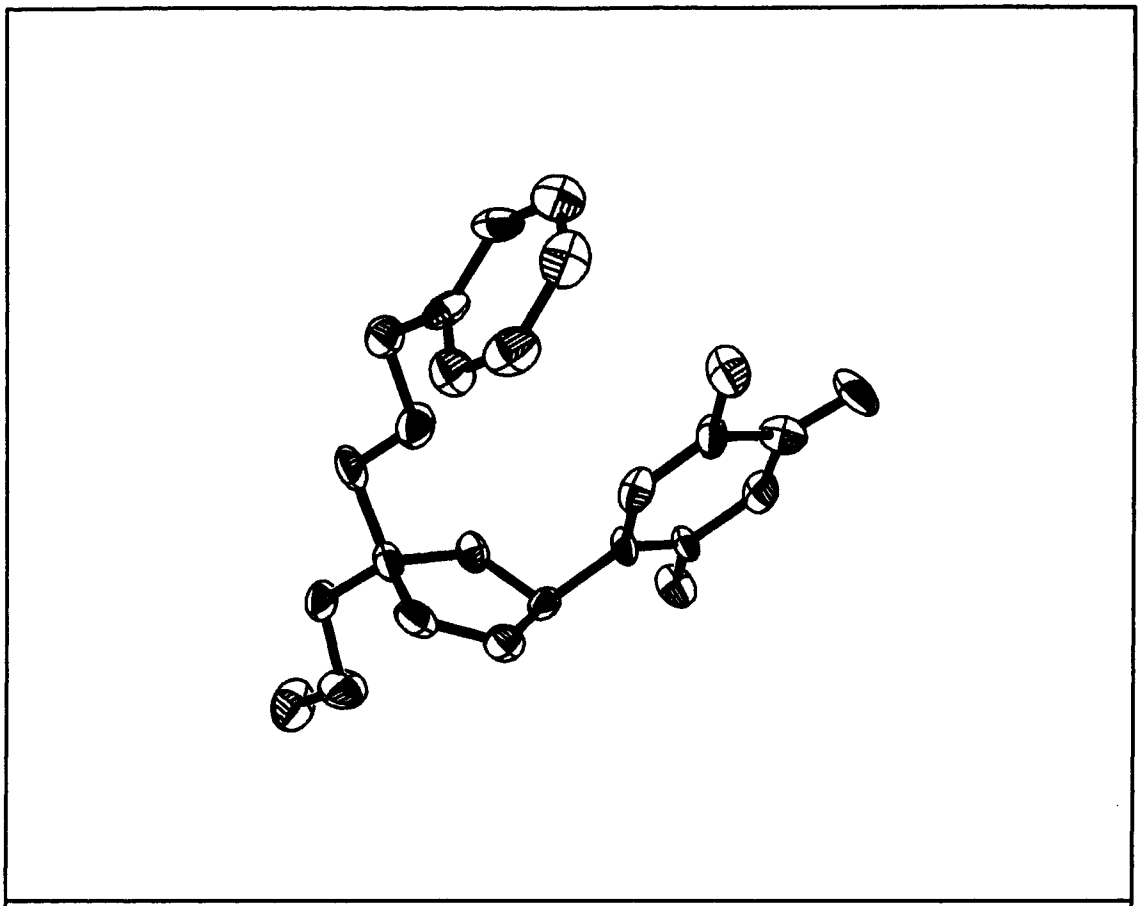

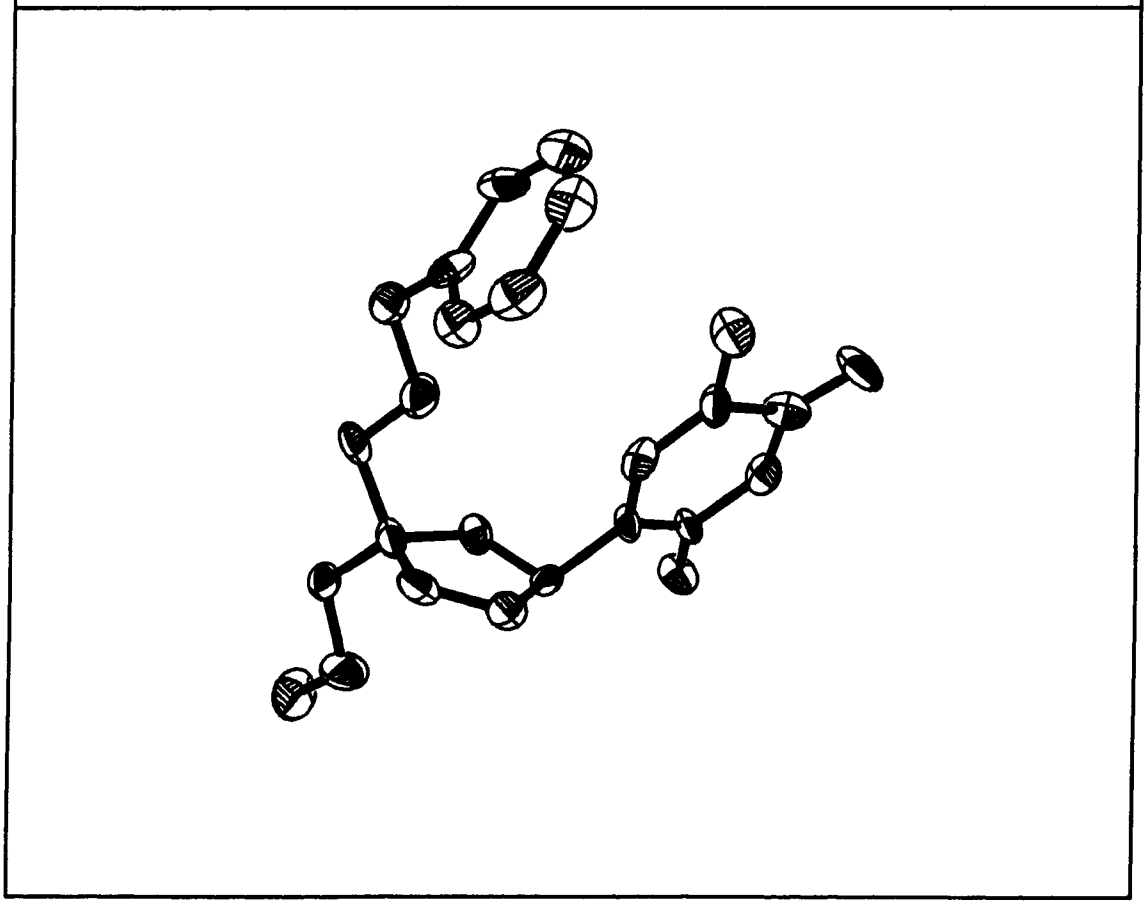

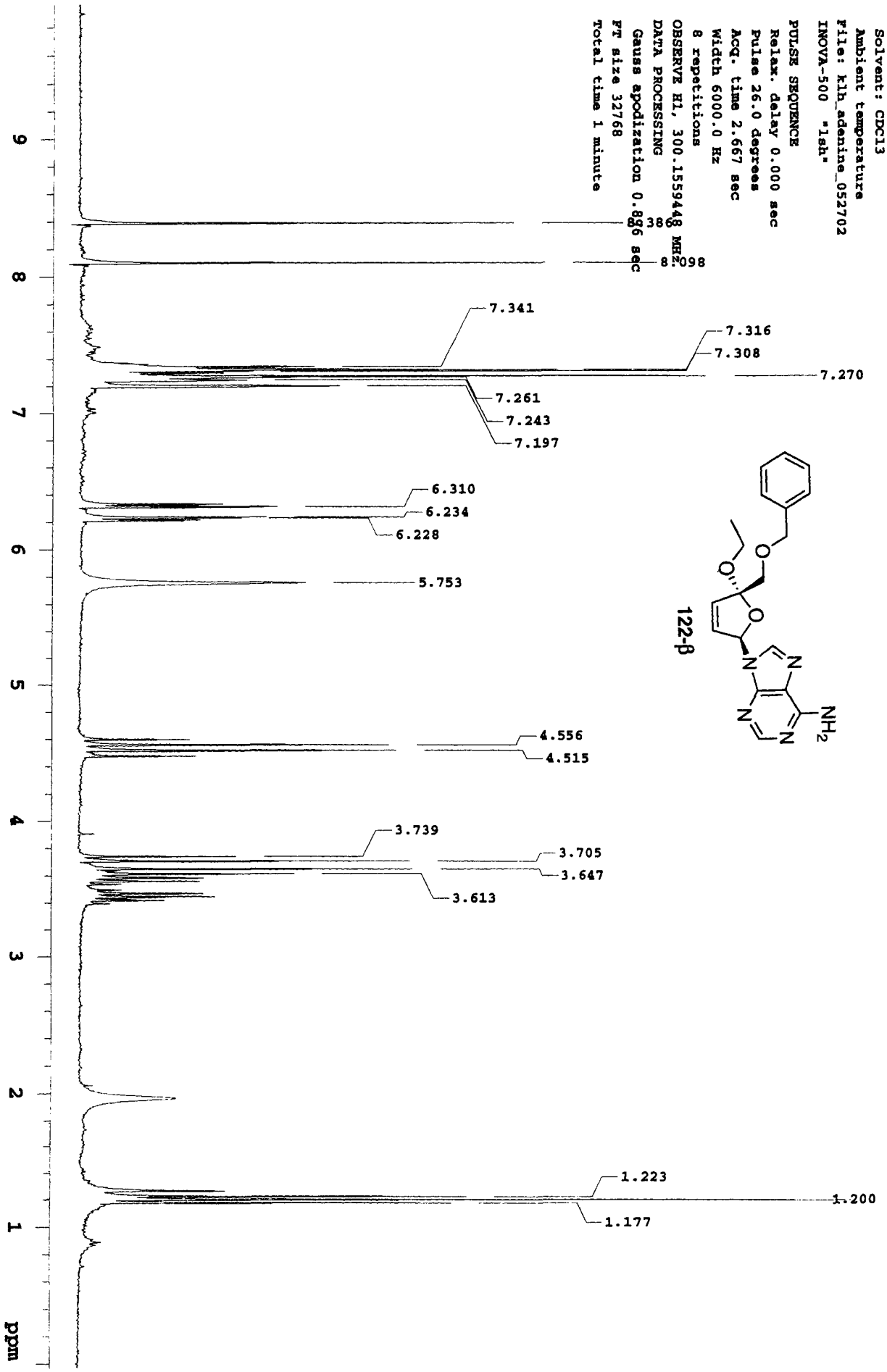

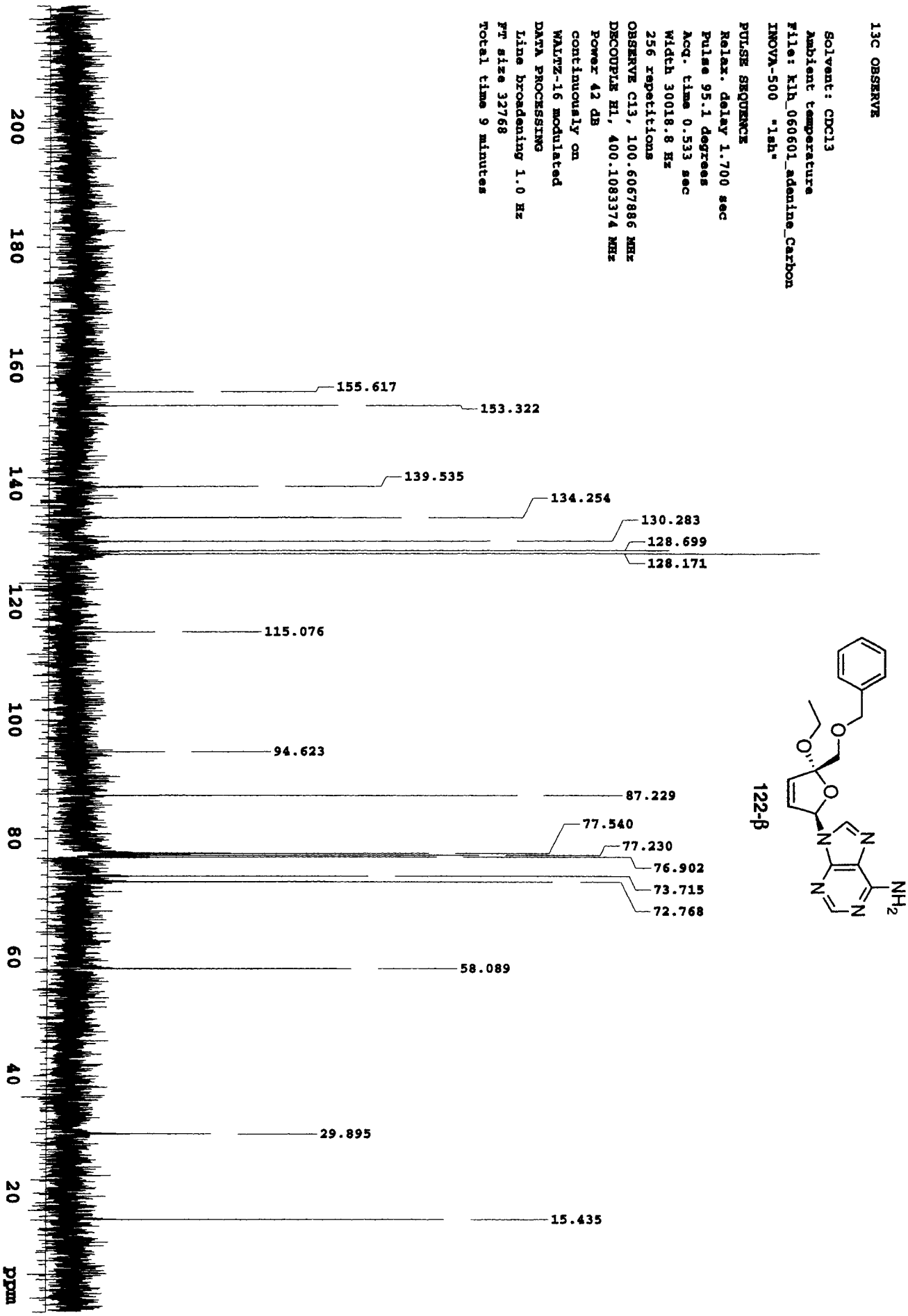

. 1h_060601_adenine

Pulse Sequence: gHMQC

Solvent: CDCl3

Ambient temperature

INOVA-400 "narnia"

Relax. delay 1.000 sec

Acq. time 0.147 sec

Width 6982.6 Hz

2D Width 17105.0 Hz

16 repetitions

2 x 128 increments

OBSERVE H1, 400.1063260 MHz

DECOUPLE C13, 100.6143372 MHz

Power 36 dB

on during acquisition

off during delay

GARP-1 modulated

DATA PROCESSING

Gauss apodization 0.068 sec

F1 DATA PROCESSING

Gauss apodization 0.014 sec

FT size 2048 x 2048

Total time 1 hr, 22 min, 39 sec

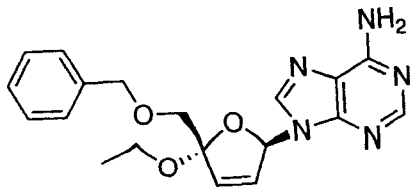

122-β

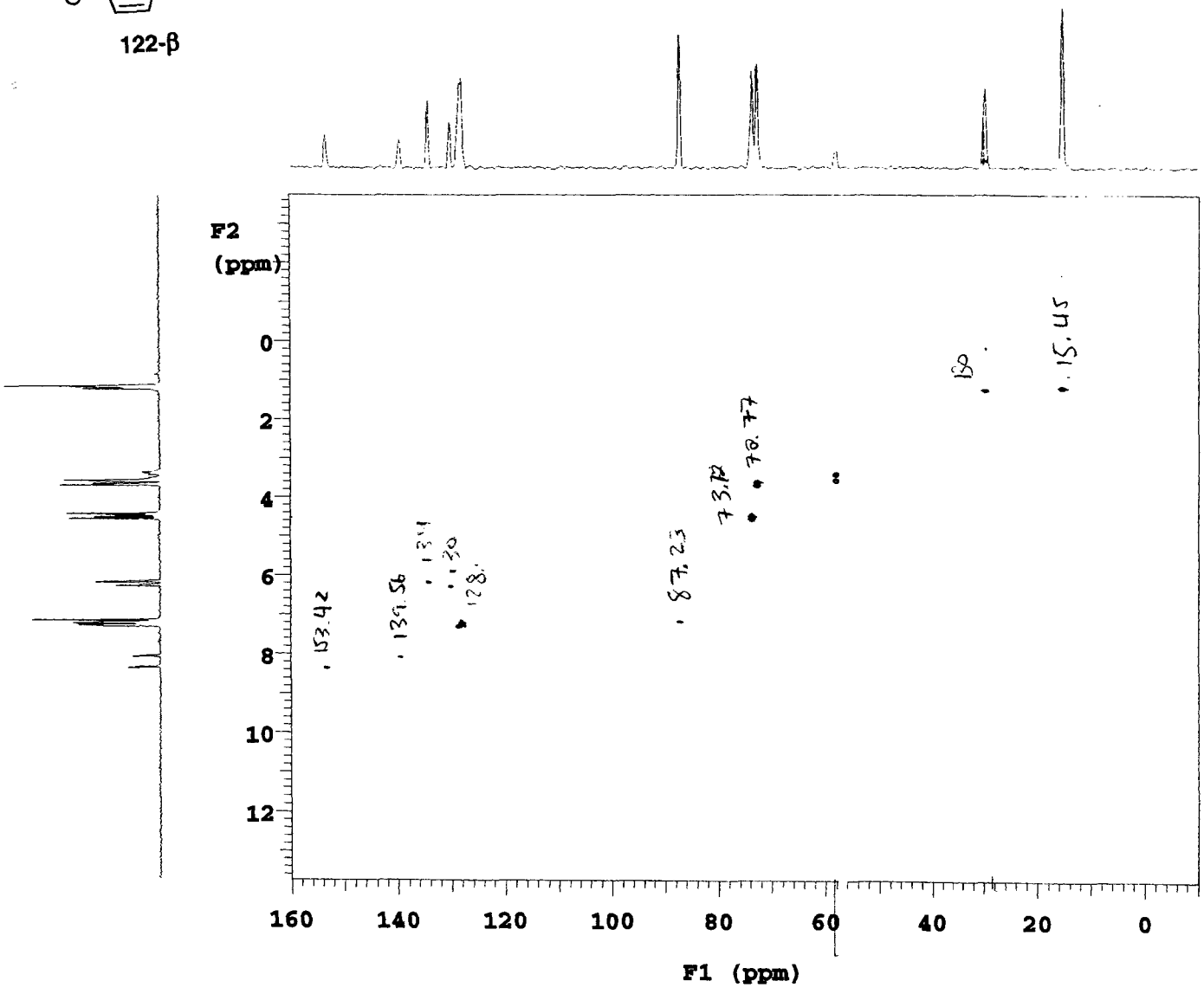

klh_060601_adenine

Pulse Sequence: gHMQC

Solvent: CDCl3
Ambient temperature
INOVA-400 "narnia"

Relax. delay 1.000 sec
Acq. time 0.147 sec
Width 6982.6 Hz
2D Width 17105.0 Hz
16 repetitions
2 x 128 increments
OBSERVE H1, 400.1063260 MHz
DECOUPLE C13, 100.6143372 MHz
Power 36 dB
on during acquisition
off during delay
GARP-1 modulated
DATA PROCESSING
Gauss apodization 0.068 sec
F1 DATA PROCESSING
Gauss apodization 0.014 sec
FT size 2048 x 2048
Total time 1 hr, 22 min, 39 sec

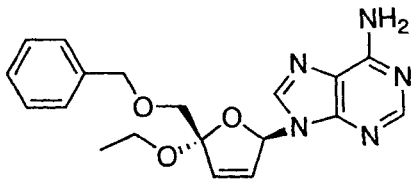

122-β

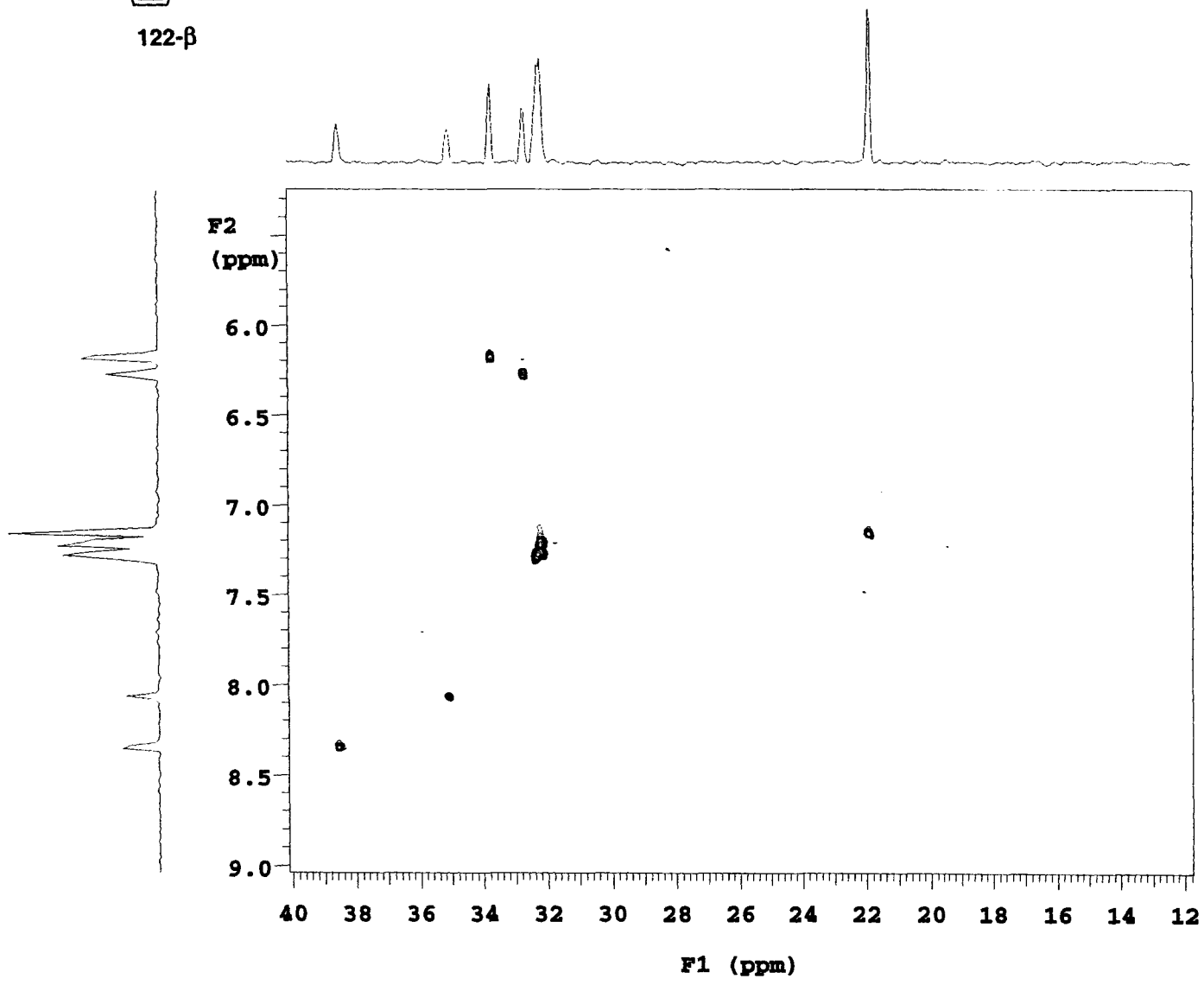

klh_060601_adenine

Pulse Sequence: gHMQC

Solvent: CDCl3
Ambient temperature
INOVA-400 "narnia"

Relax. delay 1.000 sec
Acq. time 0.147 sec
Width 6982.6 Hz
2D Width 17105.0 Hz
16 repetitions
2 x 128 increments
OBSERVE H1, 400.1063260 MHz
DECOUPLE C13, 100.6143372 MHz
Power 36 dB
on during acquisition
off during delay
GARP-1 modulated
DATA PROCESSING
Gauss apodization 0.068 sec
F1 DATA PROCESSING
Gauss apodization 0.014 sec
FT size 2048 x 2048
Total time 1 hr, 22 min, 39 sec

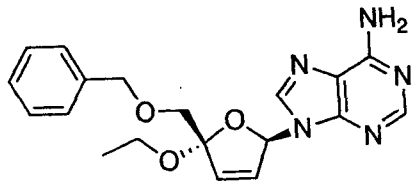

122-β

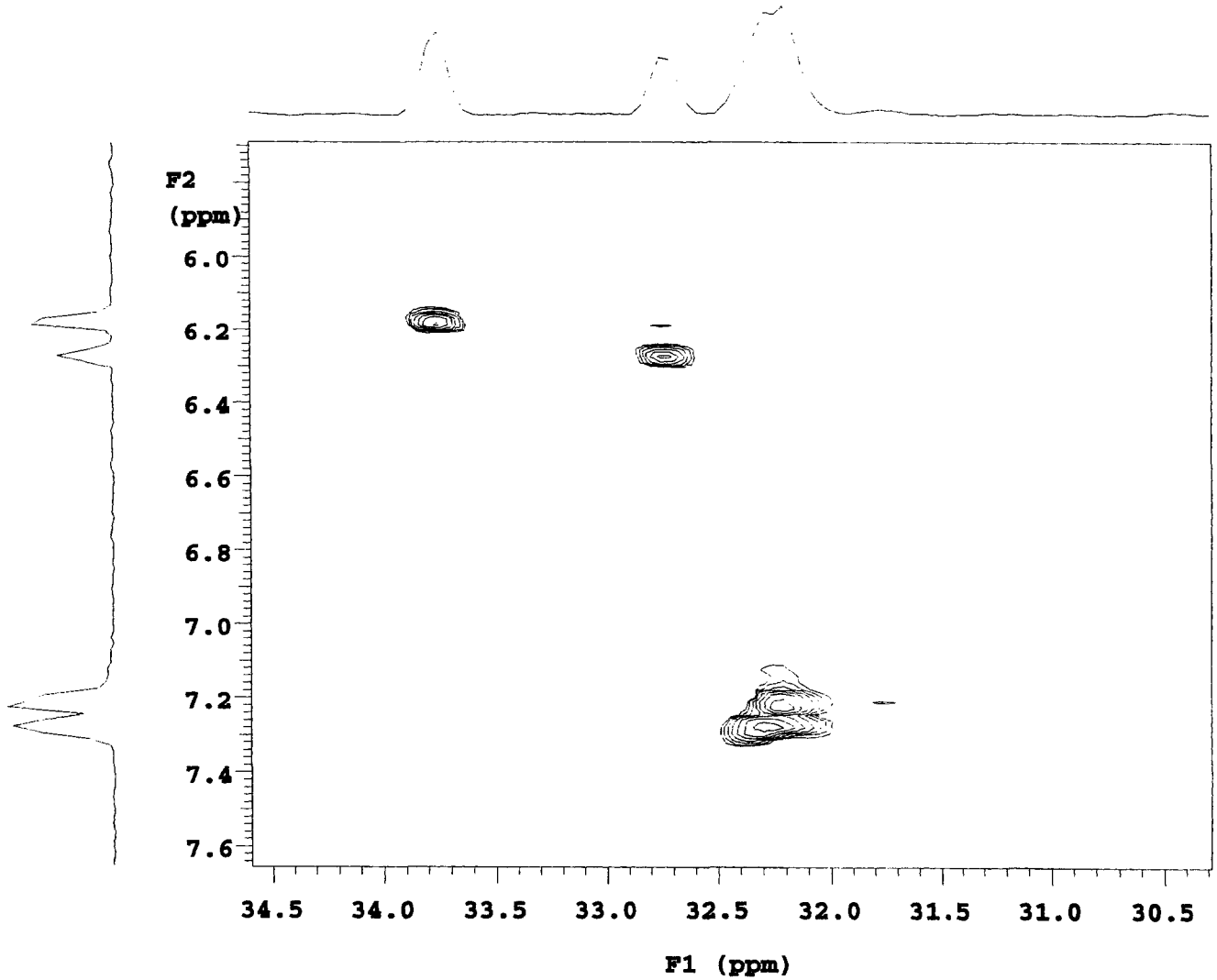

klh_060601_adenine

Pulse Sequence: gHMQC

Solvent: CDCl3
Ambient temperature
INOVA-400 "narnia"

Relax. delay 1.000 sec
Acq. time 0.147 sec
Width 6982.6 Hz
2D Width 17105.0 Hz
16 repetitions
2 x 128 increments
OBSERVE H1, 400.1063260 MHz
DECOUPLE C13, 100.6143372 MHz
Power 36 dB
on during acquisition
off during delay
GARP-1 modulated
DATA PROCESSING
Gauss apodization 0.068 sec
F1 DATA PROCESSING
Gauss apodization 0.014 sec
FT size 2048 x 2048
Total time 1 hr, 22 min, 39 sec

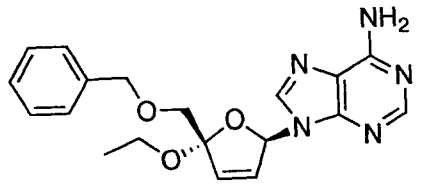

122-β

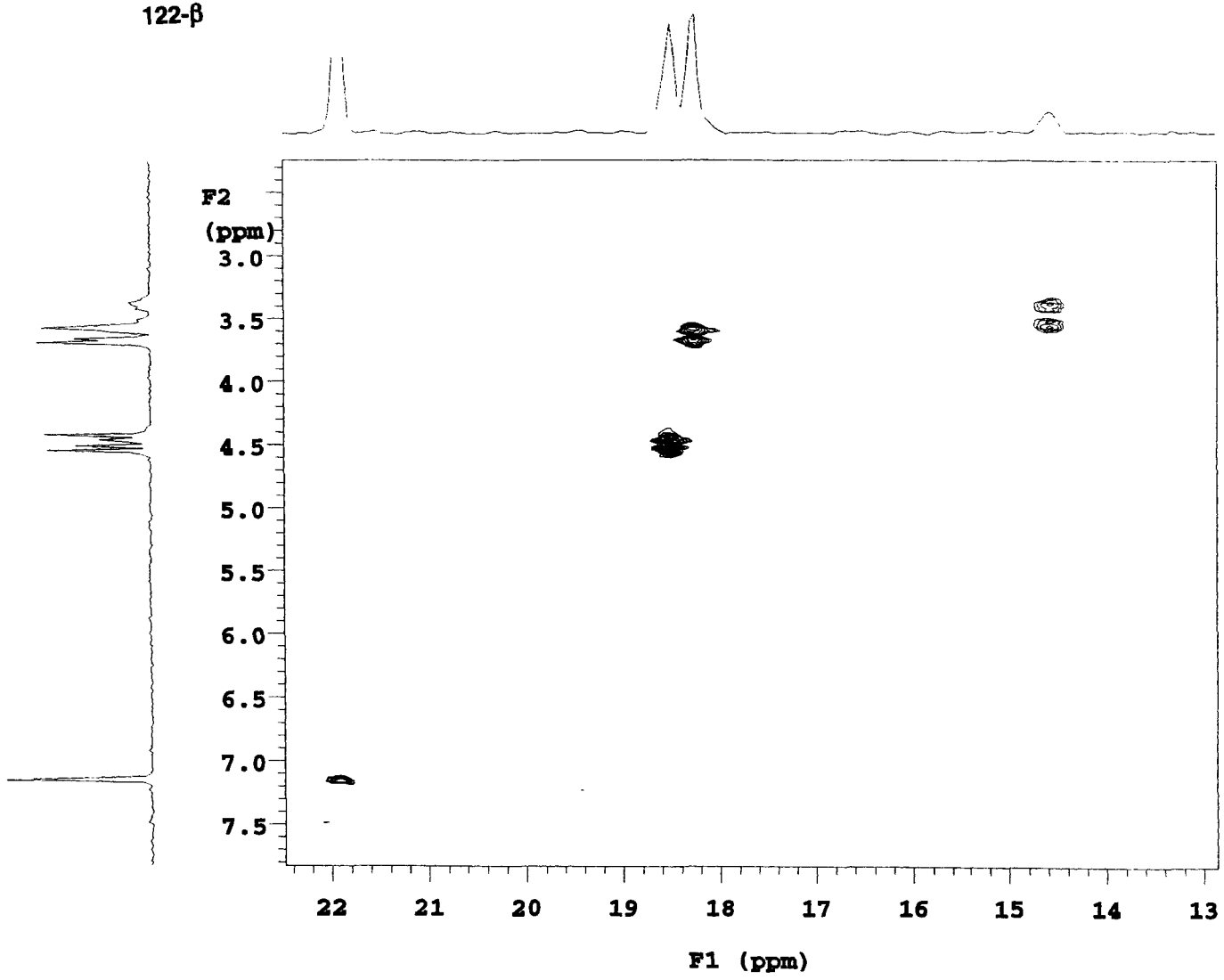

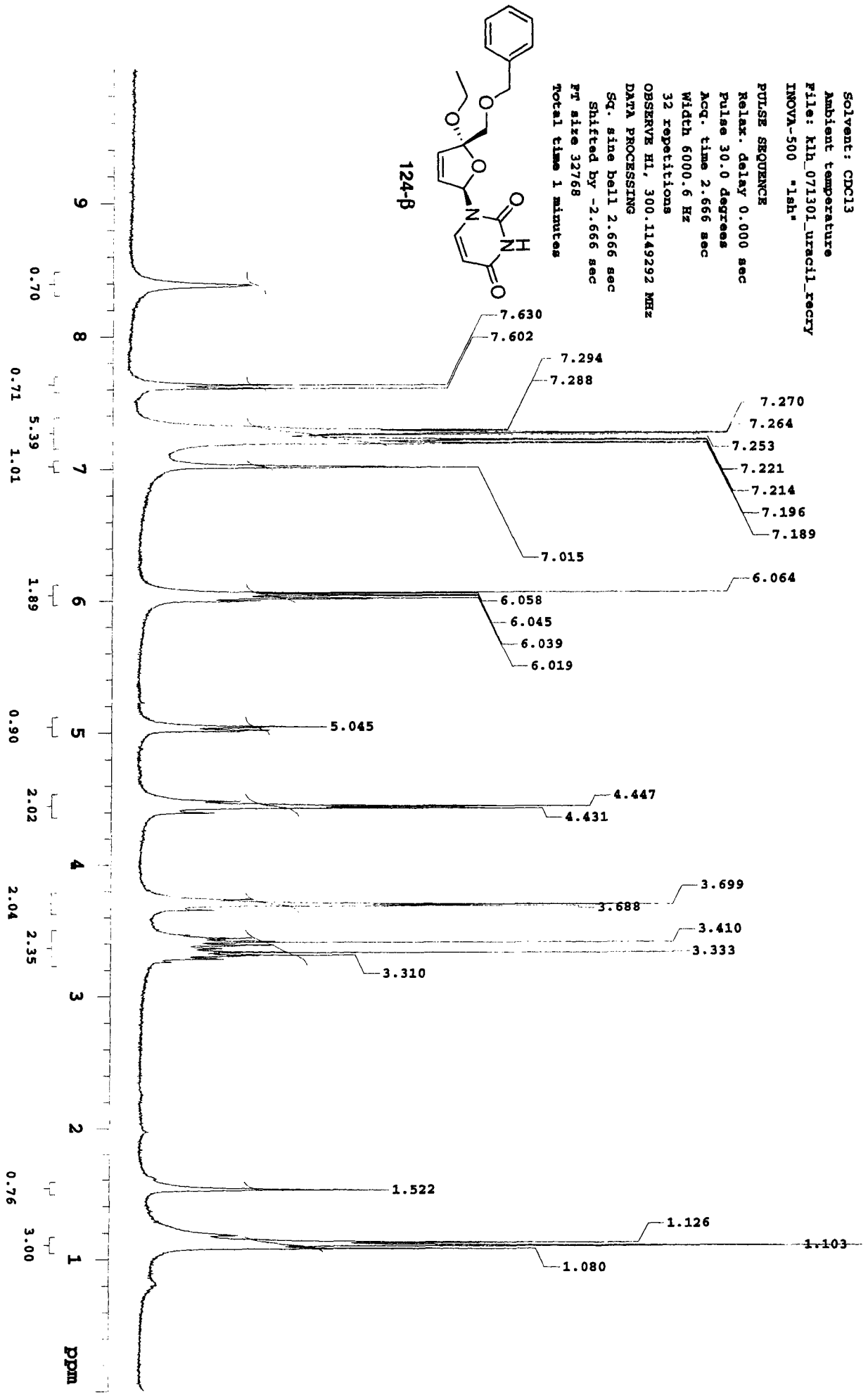

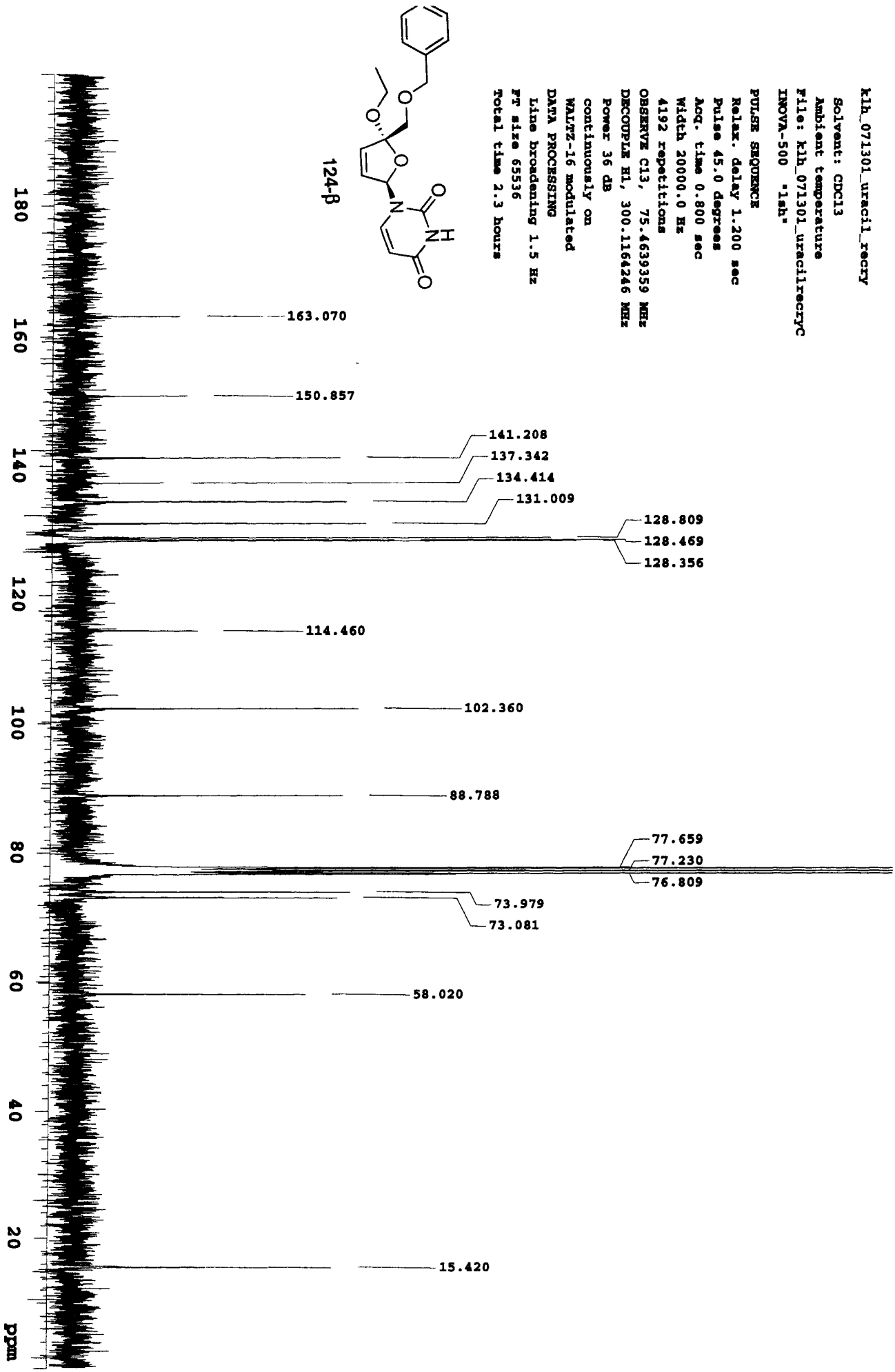

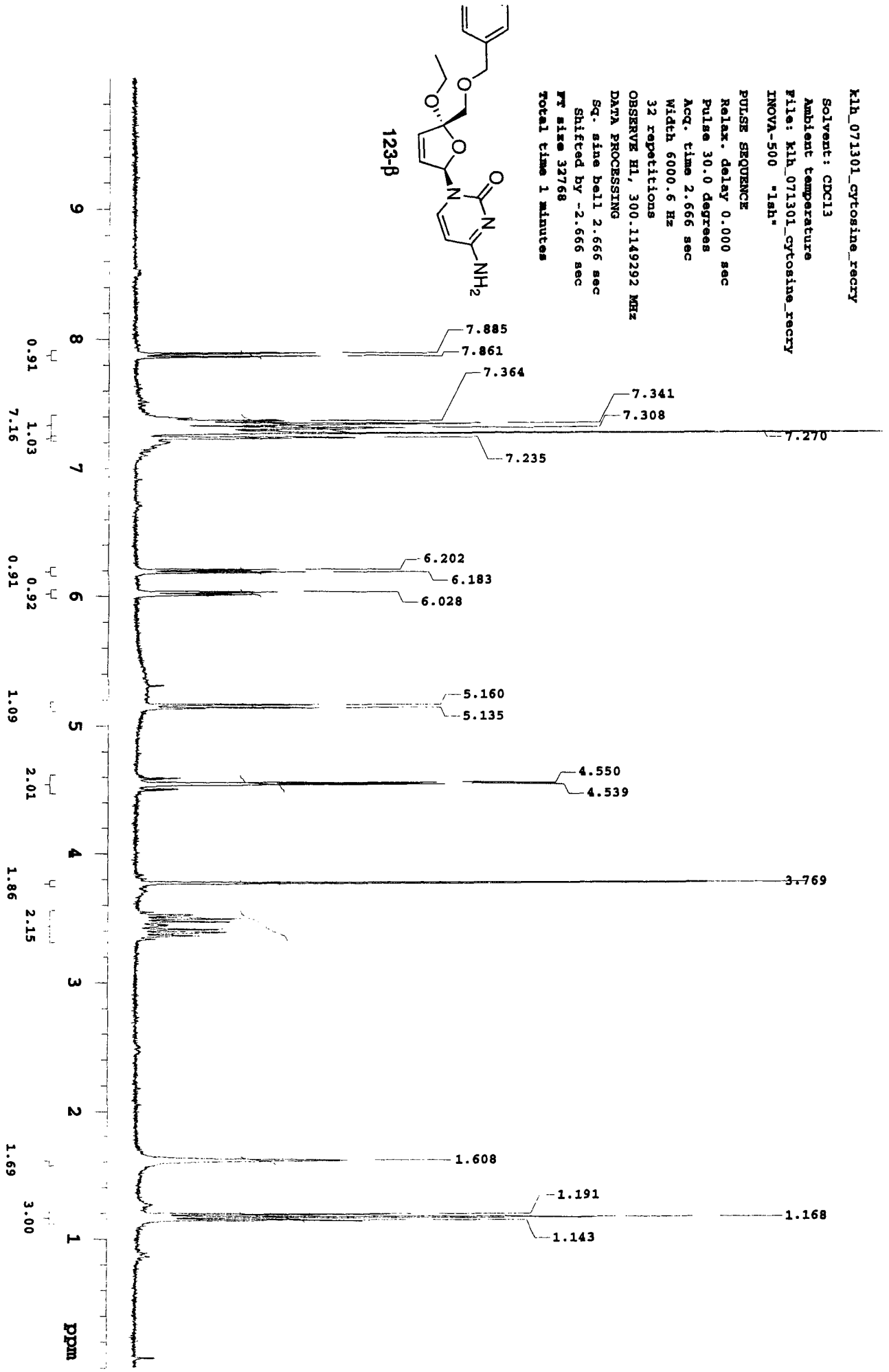

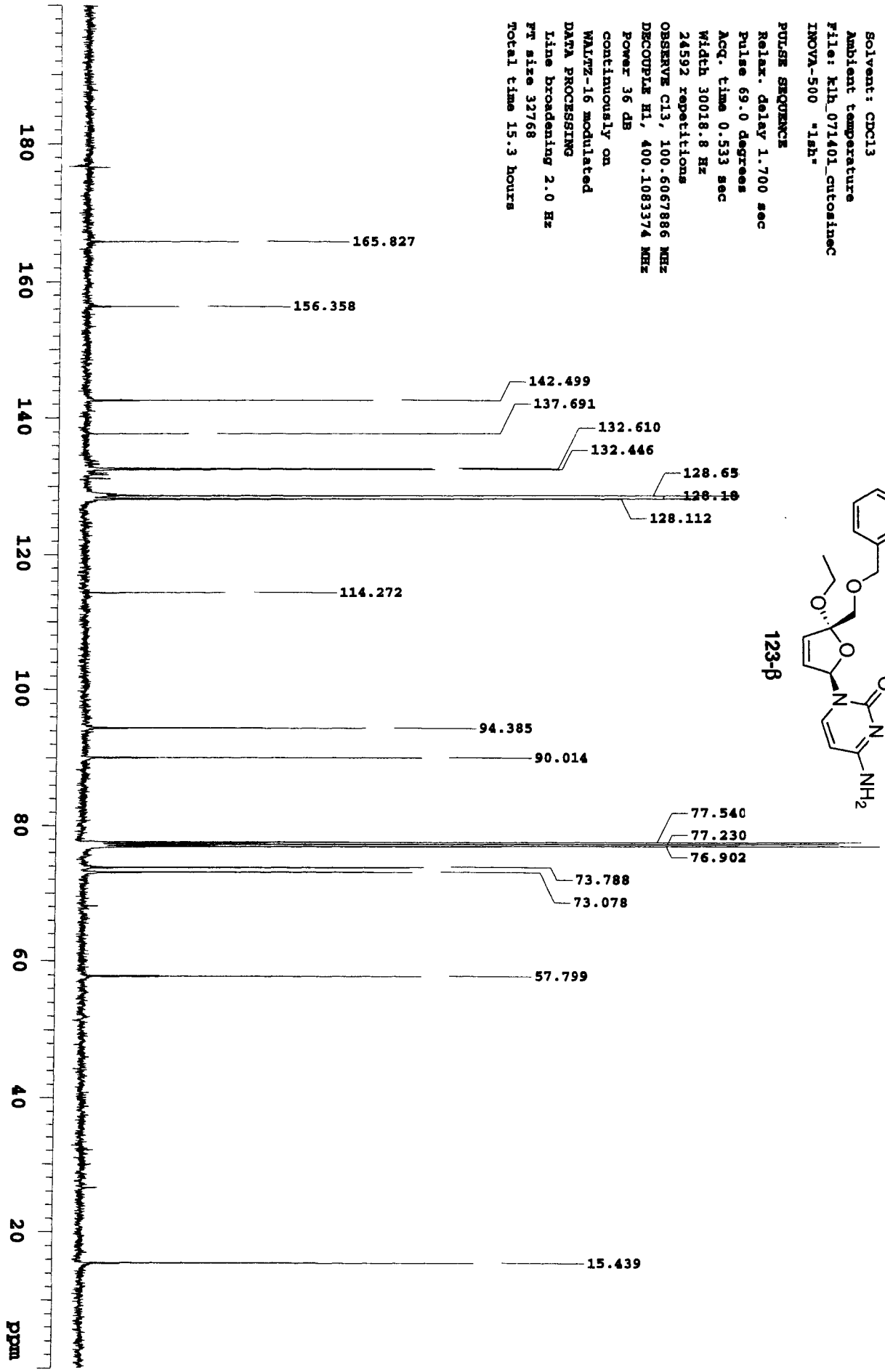

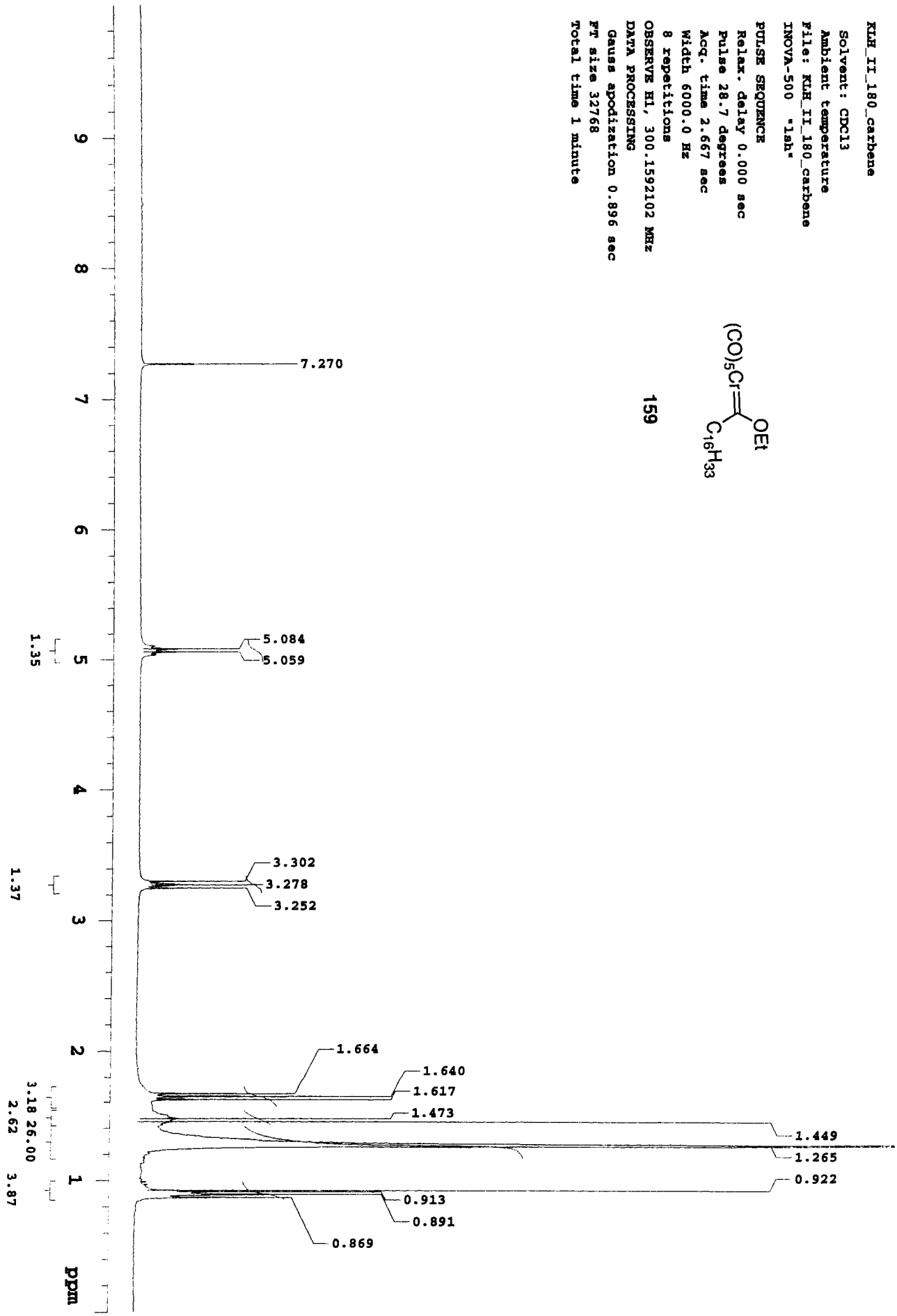

KLH_II_229_f74-96

Solvent: CDCl3
Ambient temperature
File: KLH_II_229_f74-96
INOVA-500 "lsh"

PULSE SEQUENCE
Relax. delay 0.000 sec
Pulse 28.7 degrees
Acq. time 2.667 sec
Width 6000.0 Hz
8 repetitions
OBSERVE H1, 300.1592102 MHz
DATA PROCESSING
Gauss apodization 0.896 sec
FT size 32768
Total time 1 minute

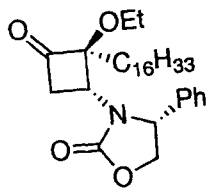

160

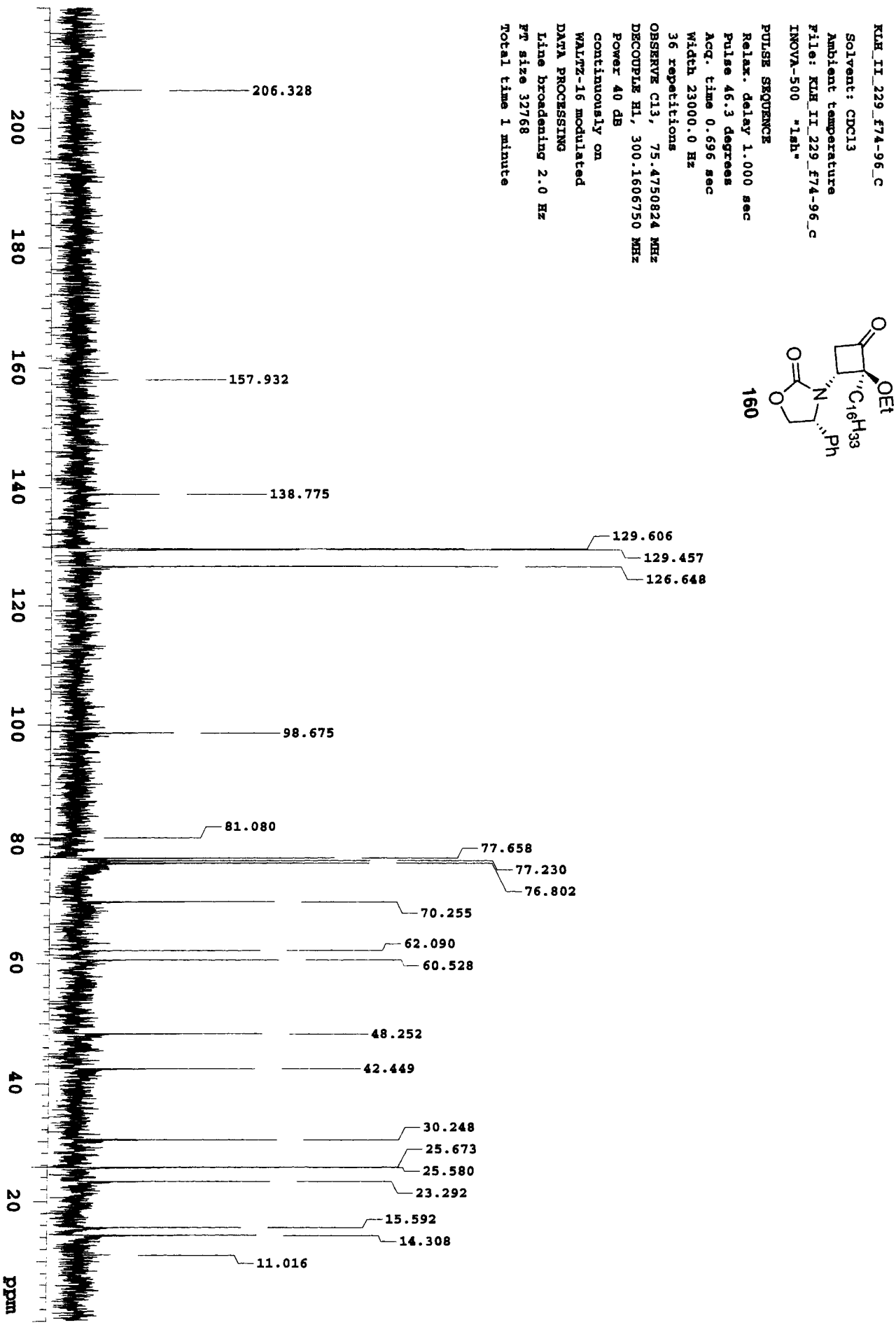

STANDARD 1H OBSERVE

Solvent: CDCl3
Ambient temperature
File: KLH_II_279_H
INOVA-500 "lsh"

PULSE SEQUENCE
Pulse 30.8 degrees
Acq. time 2.291 sec
Width 6982.6 Hz
16 repetitions
OBSERVE H1, 400.1063232 MHz
DATA PROCESSING
Gauss apodization 0.971 sec
FT size 65536
Total time 1 minute

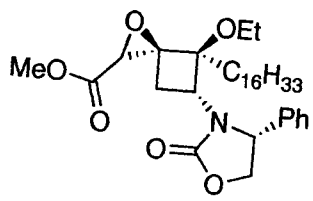

173

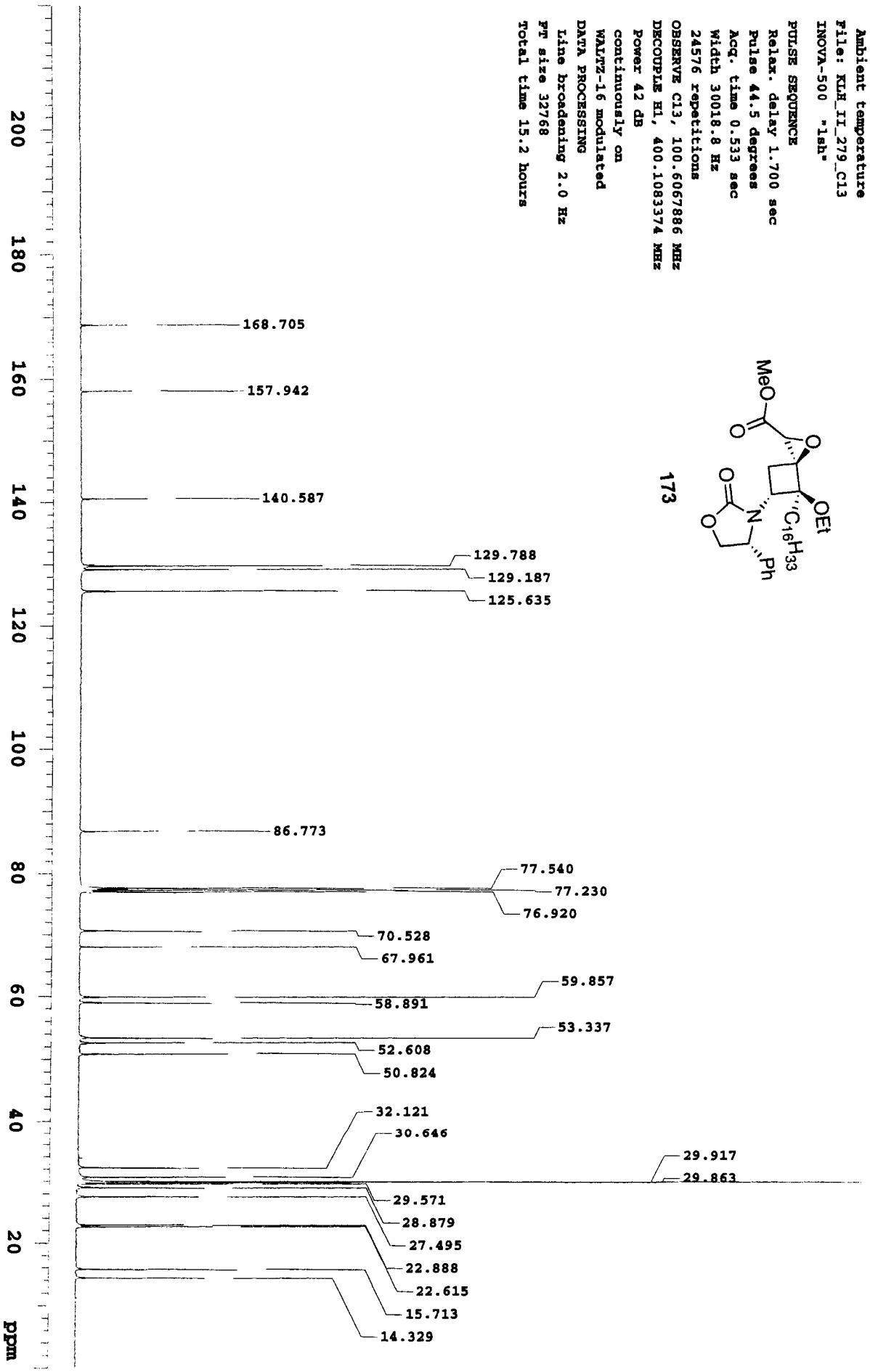

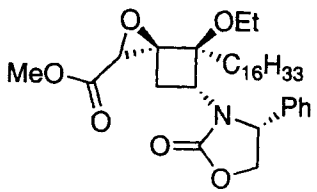

173

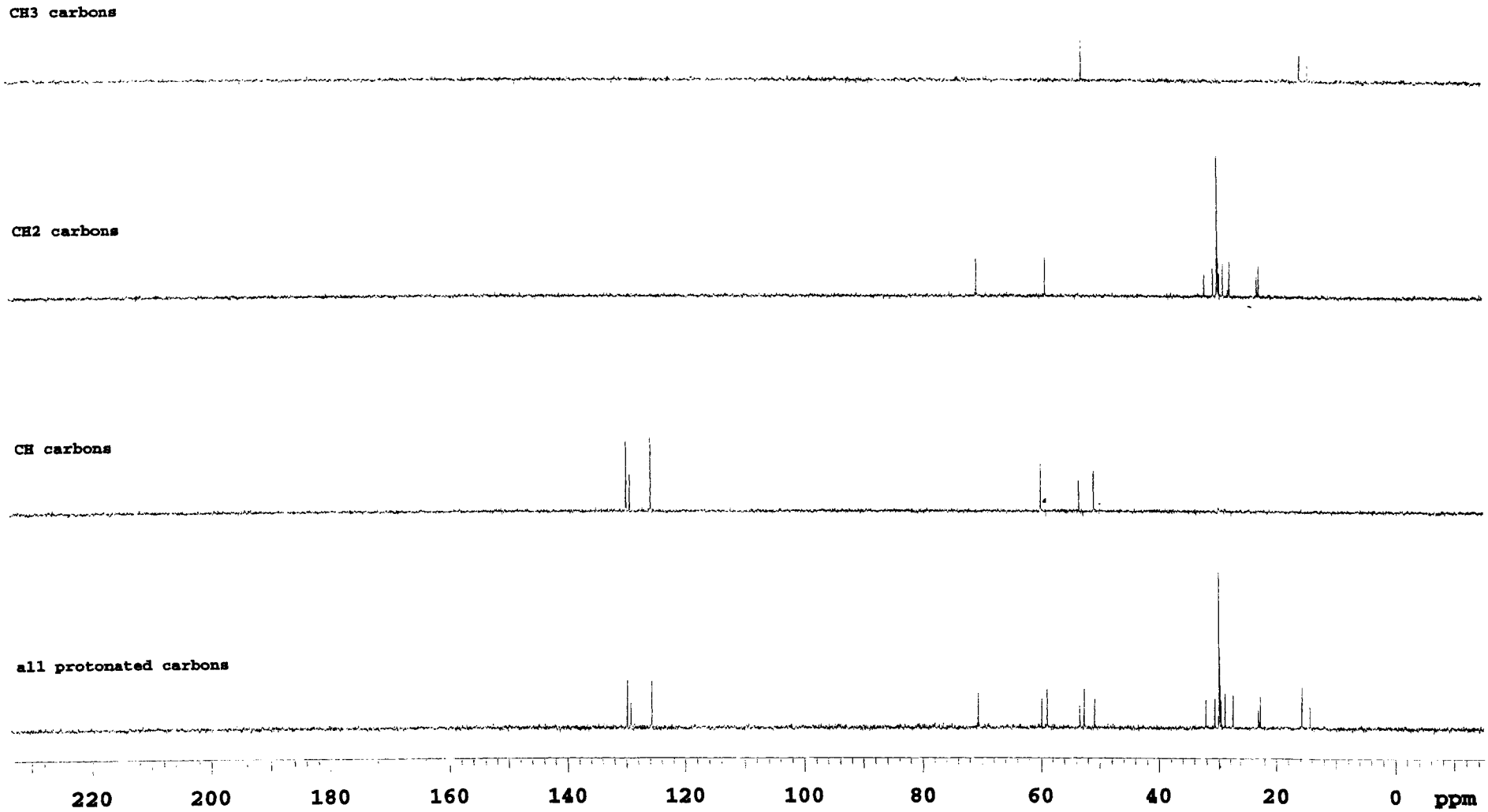

STANDARD 1H OBSERVE

Pulse Sequence: gCOSY

Solvent: CDCl3
Ambient temperature
File: KLH_II_262_COSY
INOVA-500 "strmcld"

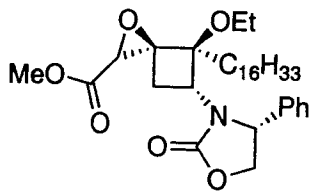

173

Relax. delay 1.000 sec
Acq. time 0.147 sec
Width 6982.6 Hz
2D Width 6982.6 Hz
4 repetitions
128 increments
OBSERVE H1, 400.1063260 MHz
DATA PROCESSING
Sq. sine bell 0.073 sec
F1 DATA PROCESSING
Sq. sine bell 0.018 sec
FT size 2048 x 2048
Total time 10 min, 16 sec

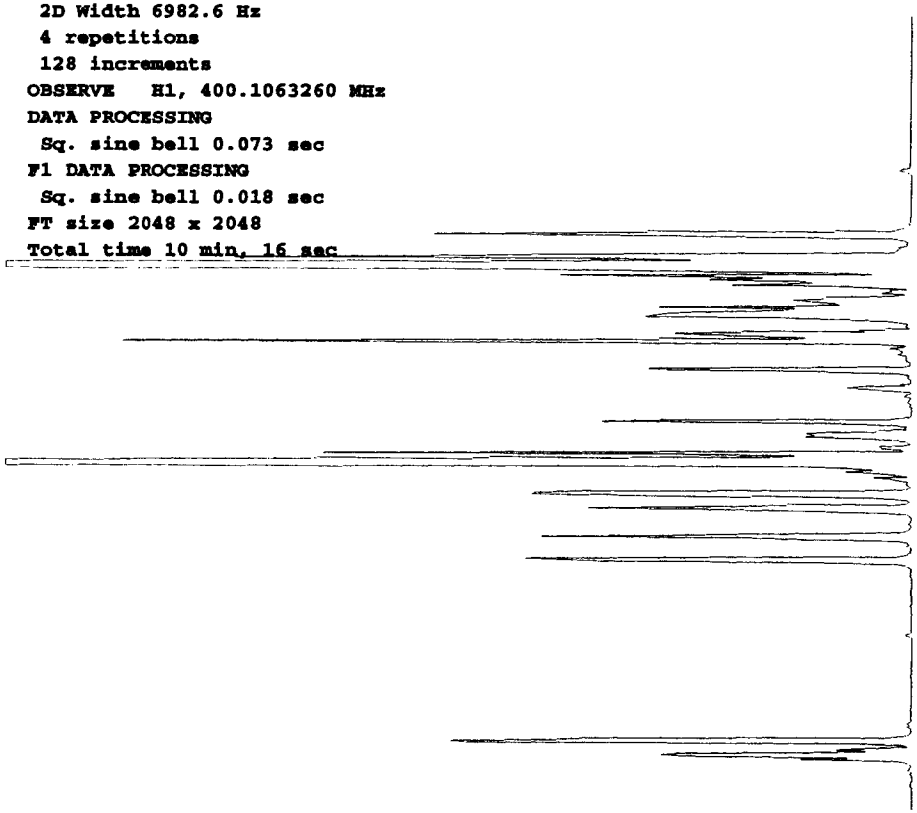

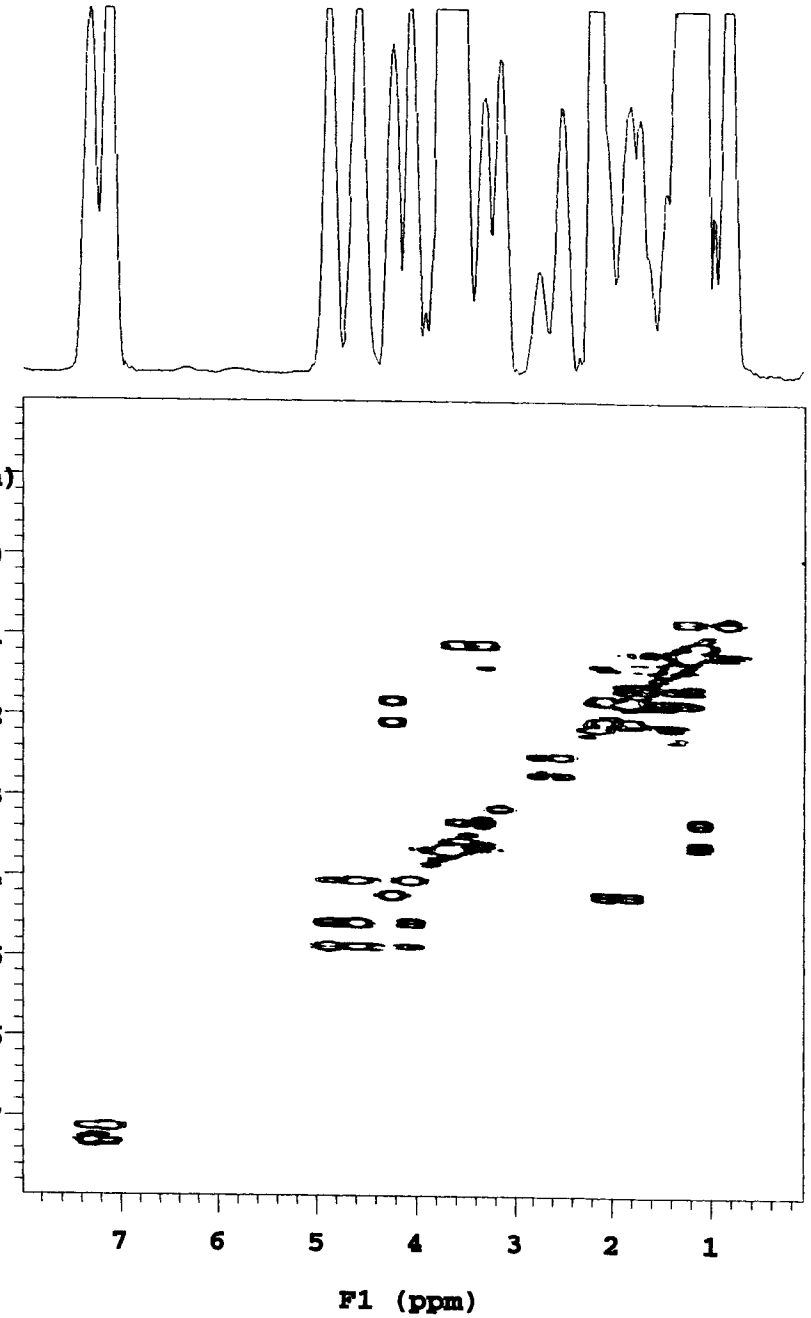

STANDARD 1H OBSERVE

Pulse Sequence: gCOSY
Solvent: CDCl3
Ambient temperature
File: KLH_II_262_COSY
INOVA-500 "strmcld"

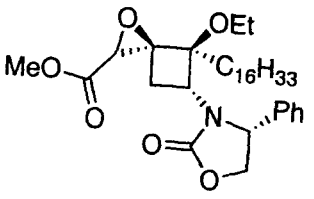

173

Relax. delay 1.000 sec
Acq. time 0.147 sec
Width 6982.6 Hz
2D Width 6982.6 Hz
4 repetitions
128 increments
OBSERVE H1, 400.1063260 MHz
DATA PROCESSING
Sq. sine bell 0.073 sec
F1 DATA PROCESSING
Sq. sine bell 0.018 sec
FT size 2048 x 2048
Total time 10 min, 16 sec

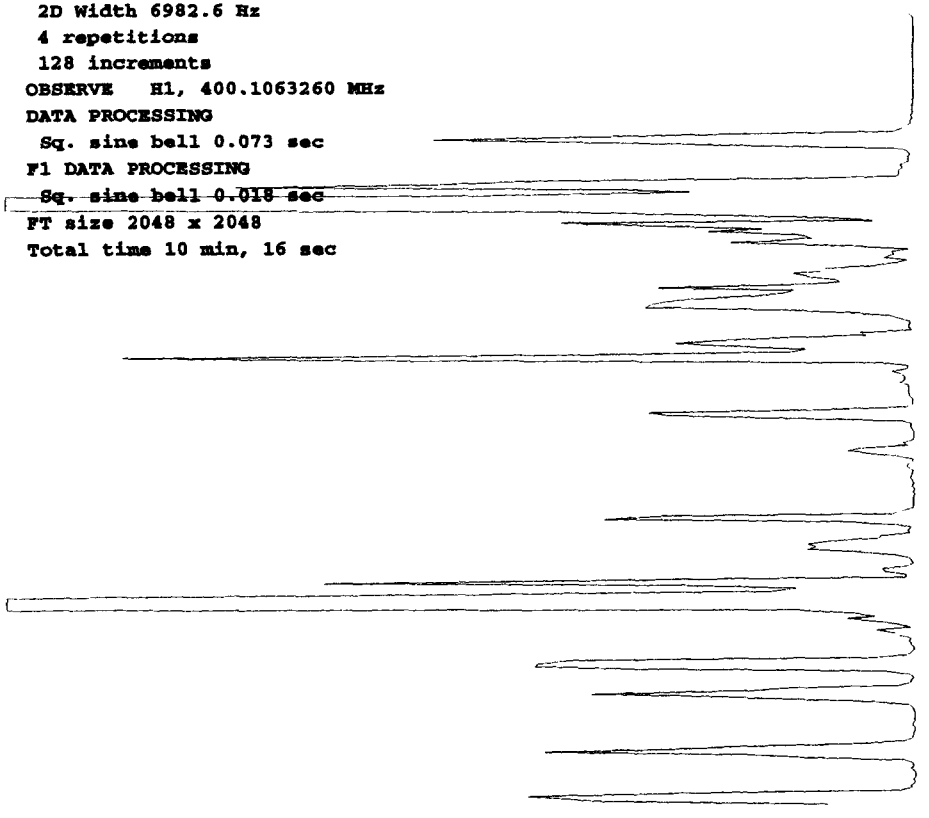

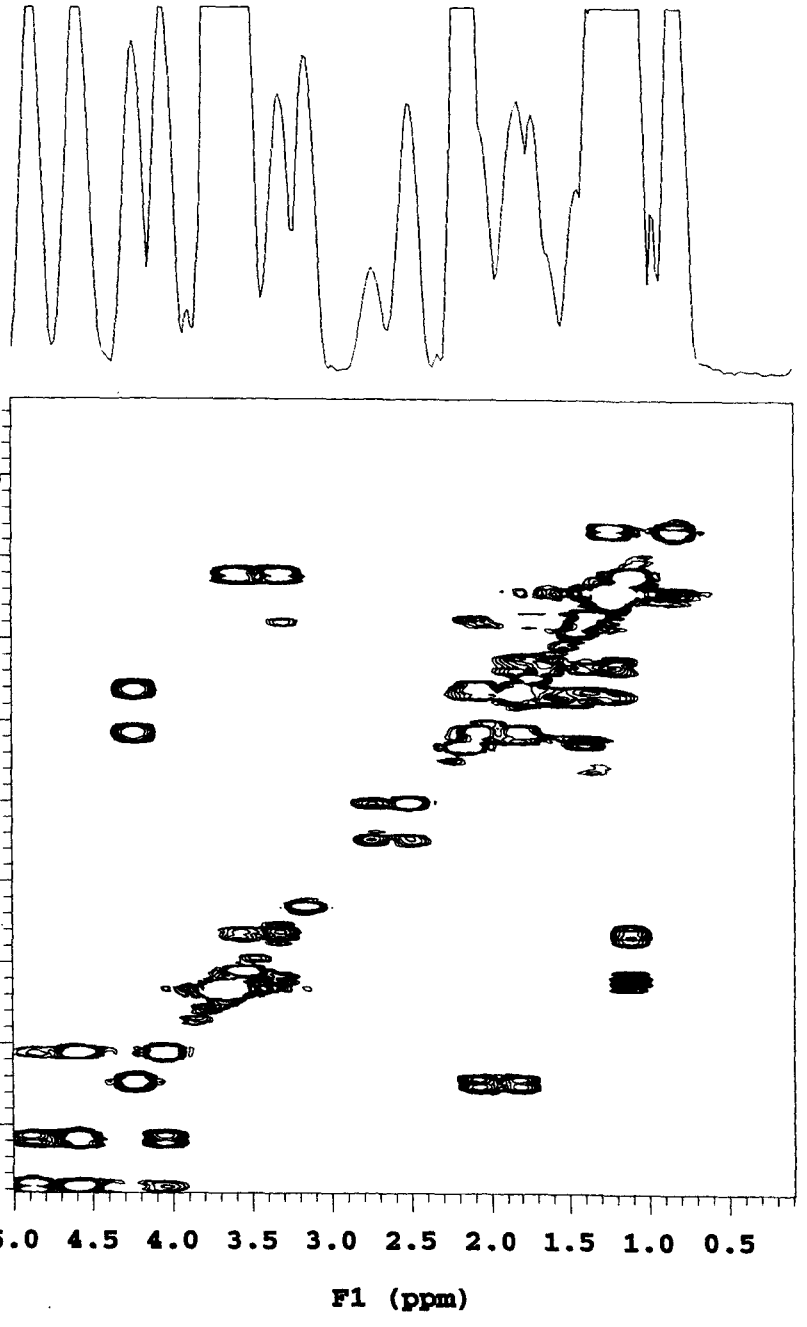

STANDARD 1H OBSERVE

Pulse Sequence: gCOSY

Solvent: CDCl3
Ambient temperature
File: KLH_II_262_COSY
INOVA-500 "strmcld"

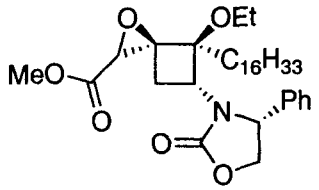

173

Relax. delay 1.000 sec
Acq. time 0.147 sec
Width 6982.6 Hz
2D Width 6982.6 Hz
4 repetitions
128 increments
OBSERVE H1, 400.1063260 MHz
DATA PROCESSING
Sq. sine bell 0.073 sec
F1 DATA PROCESSING
Sq. sine bell 0.018 sec
FT size 2048 x 2048
Total time 10 min, 16 sec

KLH_II_262_HMQC

Pulse Sequence: gHMQC

Solvent: CDCl3
Ambient temperature
File: KLH_II_262_HMQC
INOVA-500 "strmcld"

Relax. delay 1.000 sec
Acq. time 0.147 sec
Width 6982.6 Hz
2D Width 17105.0 Hz
16 repetitions
2 x 128 increments
OBSERVE H1, 400.1063260 MHz
DECOUPLE C13, 100.6143372 MHz
Power 38 dB
on during acquisition
off during delay
GARP-1 modulated
DATA PROCESSING
Gauss apodization 0.068 sec
F1 DATA PROCESSING
Gauss apodization 0.014 sec
FT size 2048 x 2048
Total time 1 hr, 22 min, 39 sec

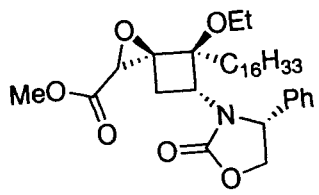

173

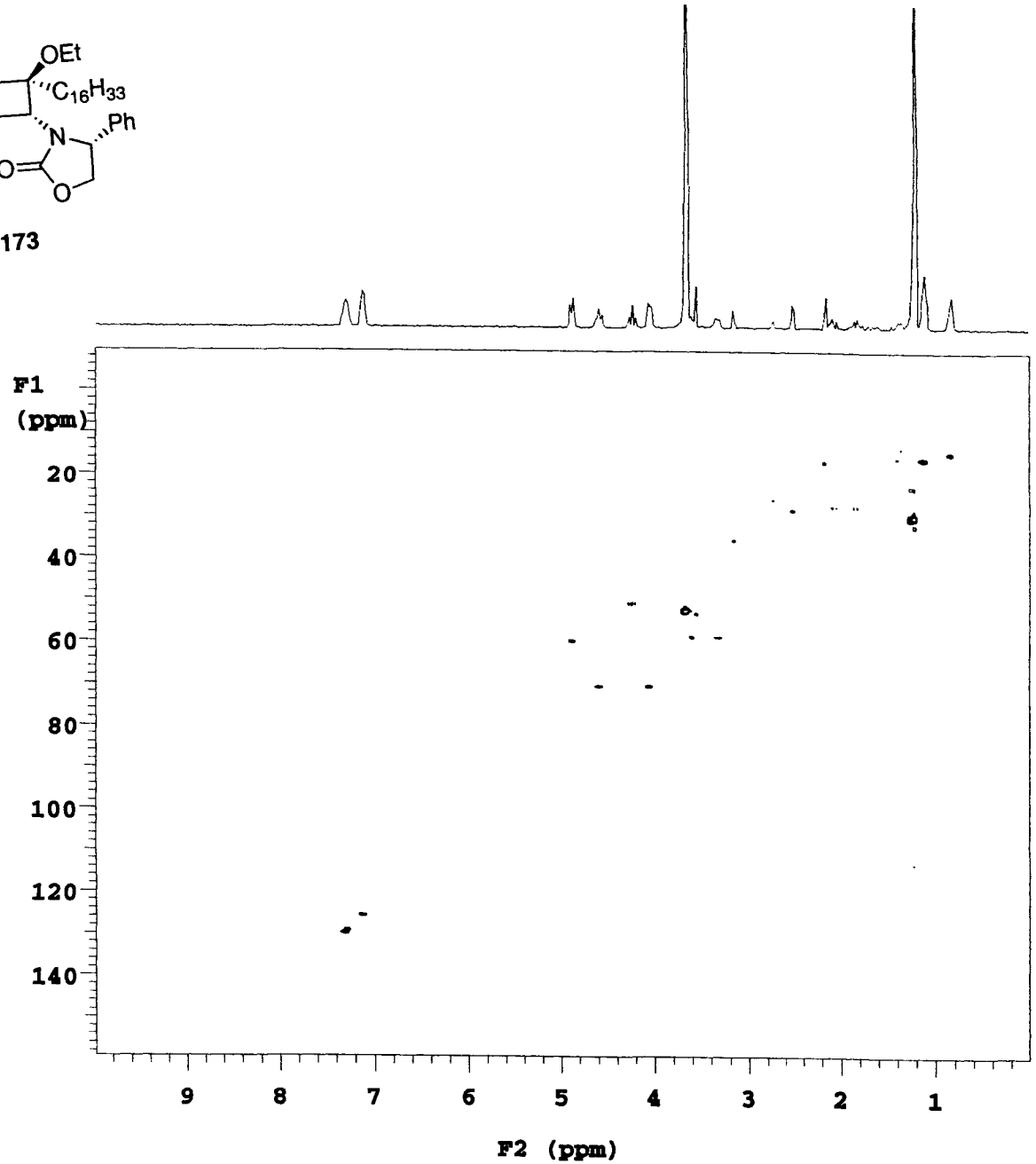

KLH_II_262_HMQC

Pulse Sequence: gHMQC

Solvent: CDCl3
Ambient temperature
File: KLH_II_262_HMQC
INOVA-500 "strmcld"

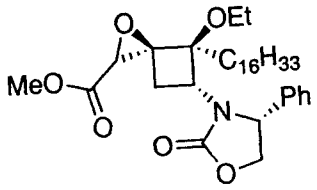

173

Relax. delay 1.000 sec
Acq. time 0.147 sec
Width 6982.6 Hz
2D Width 17105.0 Hz
16 repetitions
2 x 128 increments
OBSERVE H1, 400.1063260 MHz
DECOUPLE C13, 100.6143372 MHz
Power 38 dB
on during acquisition
off during delay
GARP-1 modulated
DATA PROCESSING
Gauss apodization 0.068 sec
F1 DATA PROCESSING
Gauss apodization 0.014 sec
FT size 2048 x 2048
Total time 1 hr, 22 min, 39 sec

KLH_II_315_f24-45

Solvent: CDCl3
Temp. 23.0 C / 296.1 K
File: KLH_II_315_f24-45
INOVA-500 "lsh"

PULSE SEQUENCE
Relax. delay 1.000 sec
Pulse 38.9 degrees
Acq. time 2.732 sec
Width 6000.6 Hz
16 repetitions
OBSERVE H1, 300.1149292 MHz
DATA PROCESSING
Gauss apodization 0.824 sec
FT size 65536
Total time 1 minute

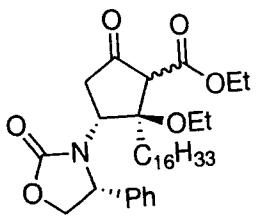

174

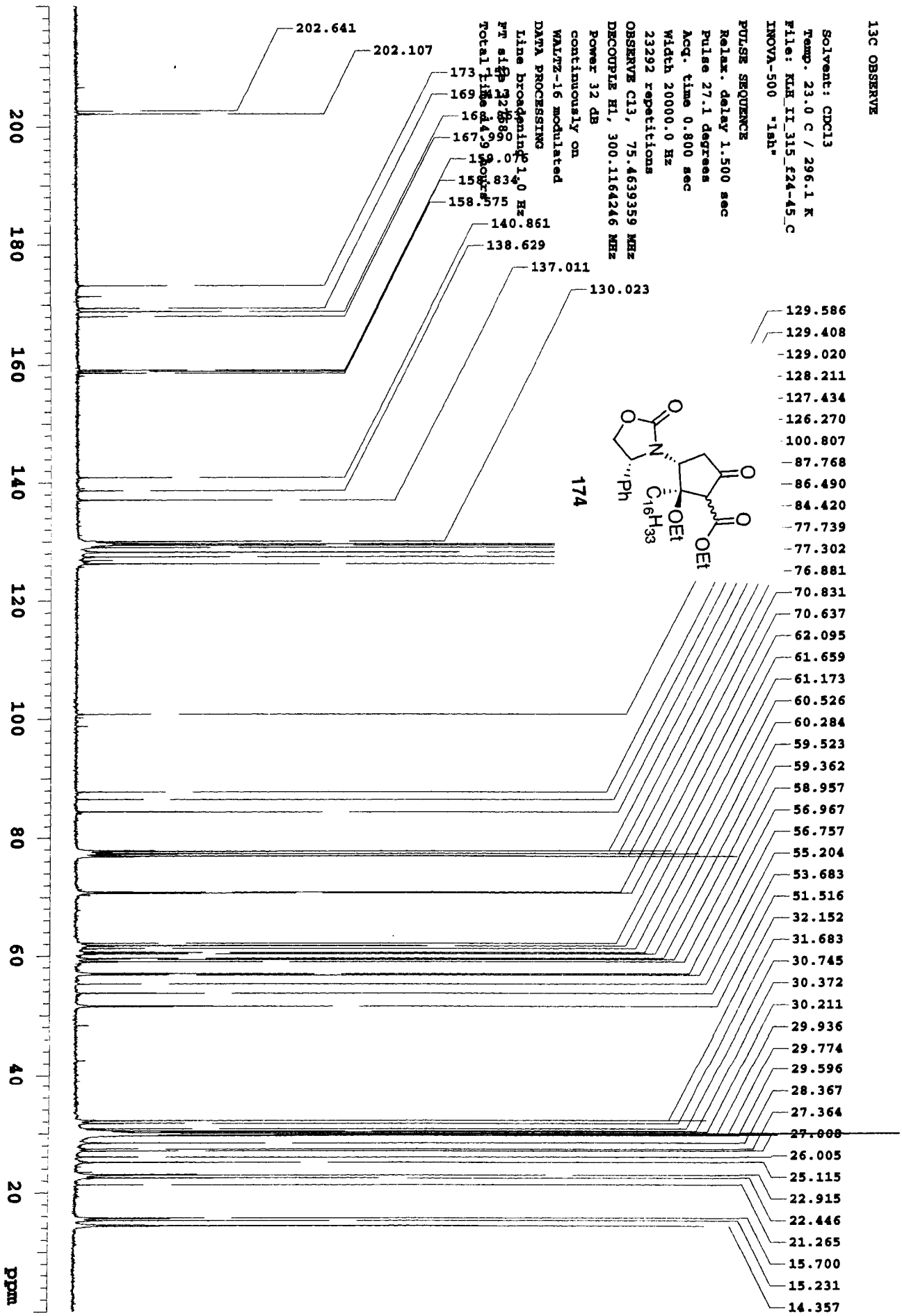

KLH_II_407_SM

Solvent: CDCl3
Ambient temperature
File: KLH_II_407_SM
INOVA-500 "lsh"

PULSE SEQUENCE
Relax. delay 0.000 sec
Pulse 28.7 degrees
Acq. time 2.667 sec
Width 6000.0 Hz
16 repetitions
OBSERVE H1, 300.1592102 MHz
DATA PROCESSING
Gauss apodization 0.896 sec
FT size 32768
Total time 1 minute

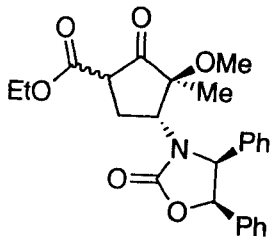

176

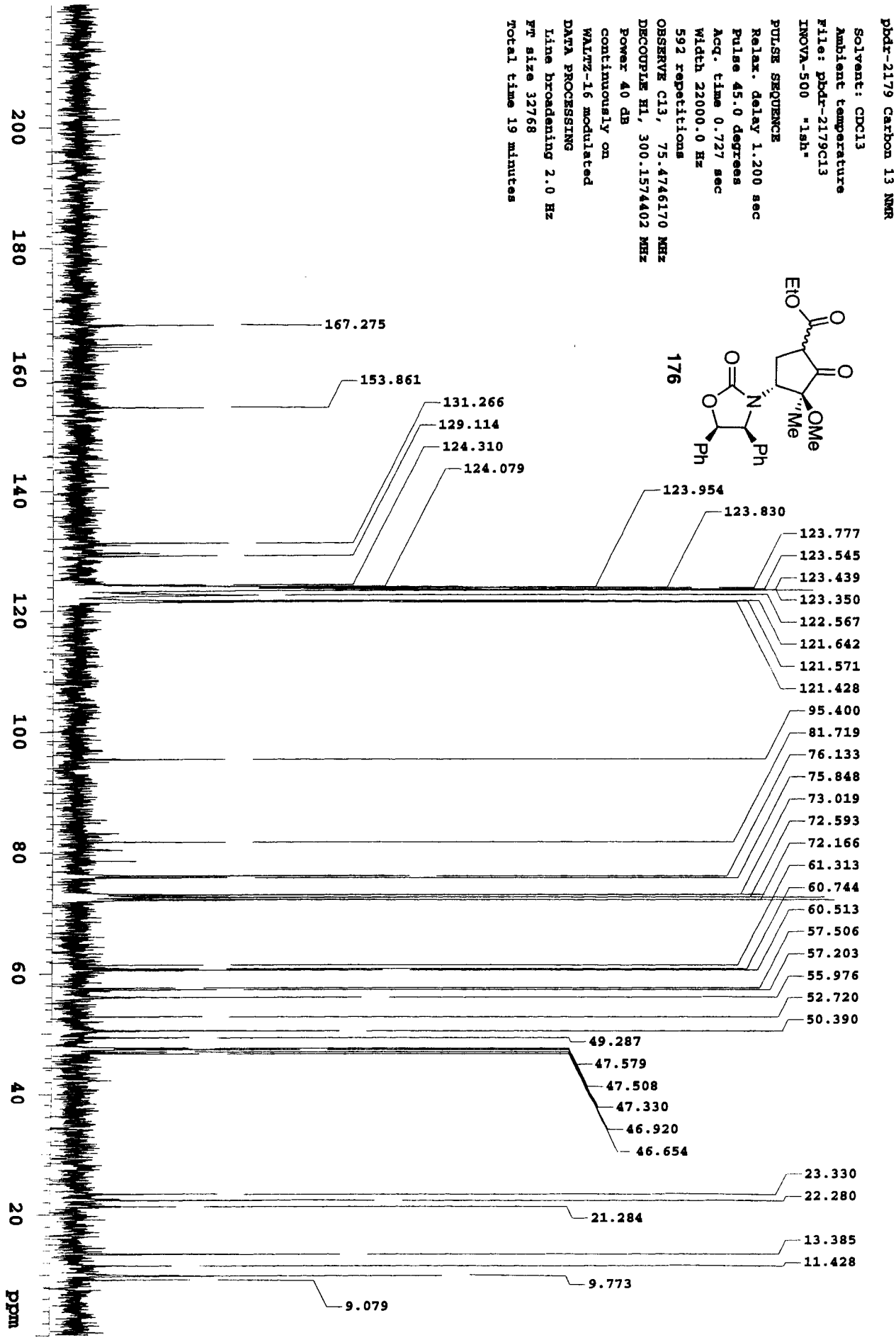

KLH_II_326_f20-29

Solvent: CDCl3
Ambient temperature
File: KLH_II_326_f19-29
INOVA-500 "lsh"

PULSE SEQUENCE
Relax. delay 0.000 sec
Pulse 28.7 degrees
Acq. time 2.667 sec
Width 6000.0 Hz
8 repetitions
OBSERVE H1, 300.1592102 MHz
DATA PROCESSING
Gauss apodization 0.896 sec
FT size 32768
Total time 1 minute

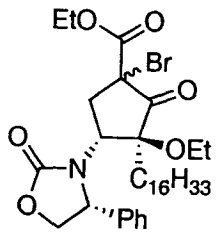

178

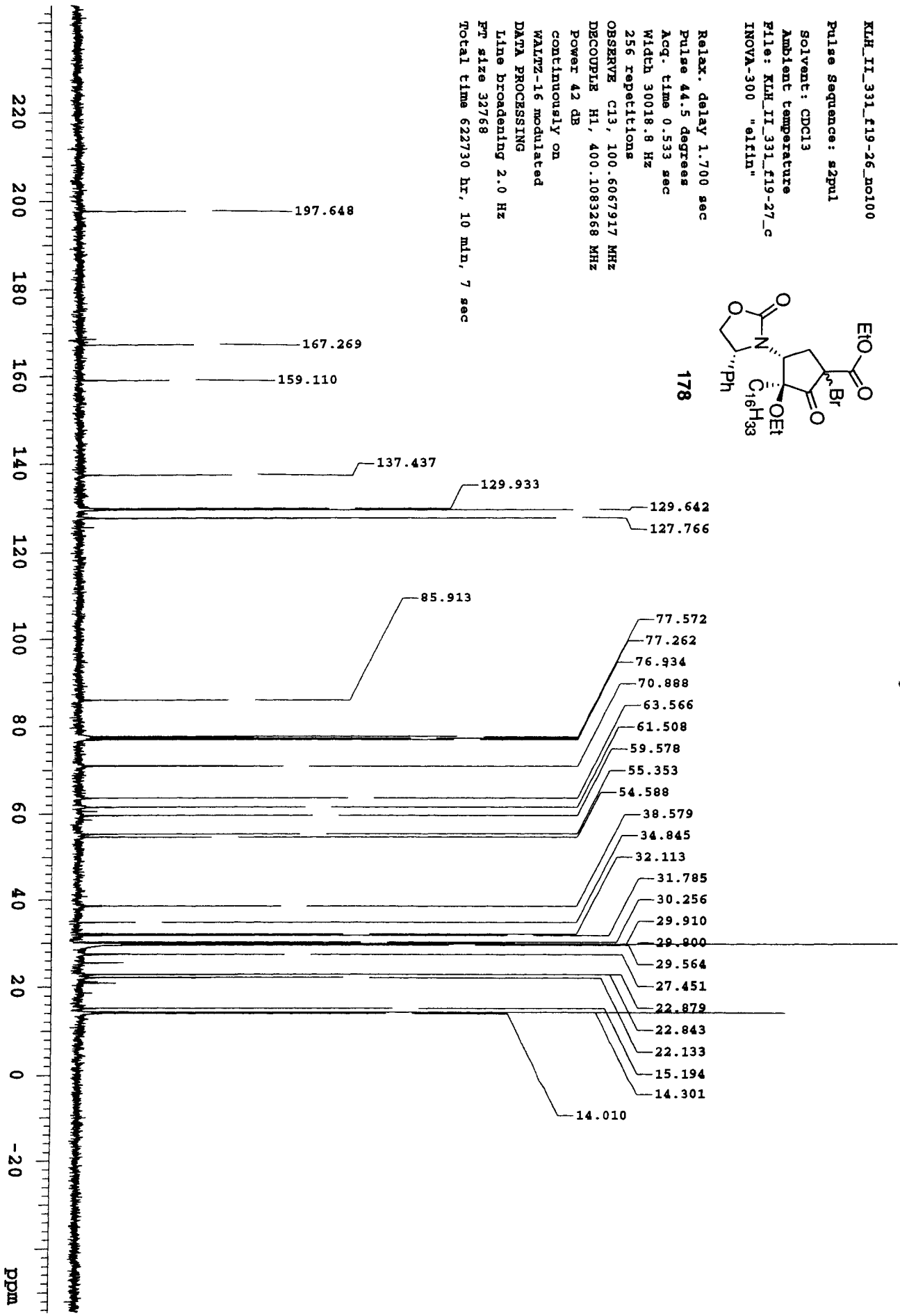

STANDARD 1H OBSERVE

Pulse Sequence: HMQC

Solvent: CDCl3
Ambient temperature
File: KLH_II_331_f19-27_HMQC
INOVA-500 "strmcld"

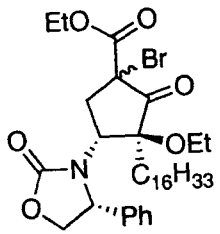

178

Relax. delay 1.000 sec
Acq. time 0.147 sec
Width 6982.6 Hz
2D Width 17105.0 Hz
8 repetitions
2 x 128 increments
OBSERVE H1, 400.1063260 MHz
DECOUPLE C13, 100.6143372 MHz
Power 38 dB
on during acquisition
off during delay
GARP-1 modulated
DATA PROCESSING
Gauss apodization 0.068 sec
F1 DATA PROCESSING
Gauss apodization 0.014 sec
FT size 2048 x 2048
Total time 40 min, 59 sec

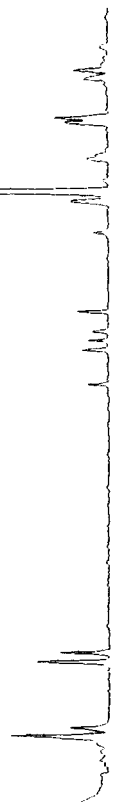

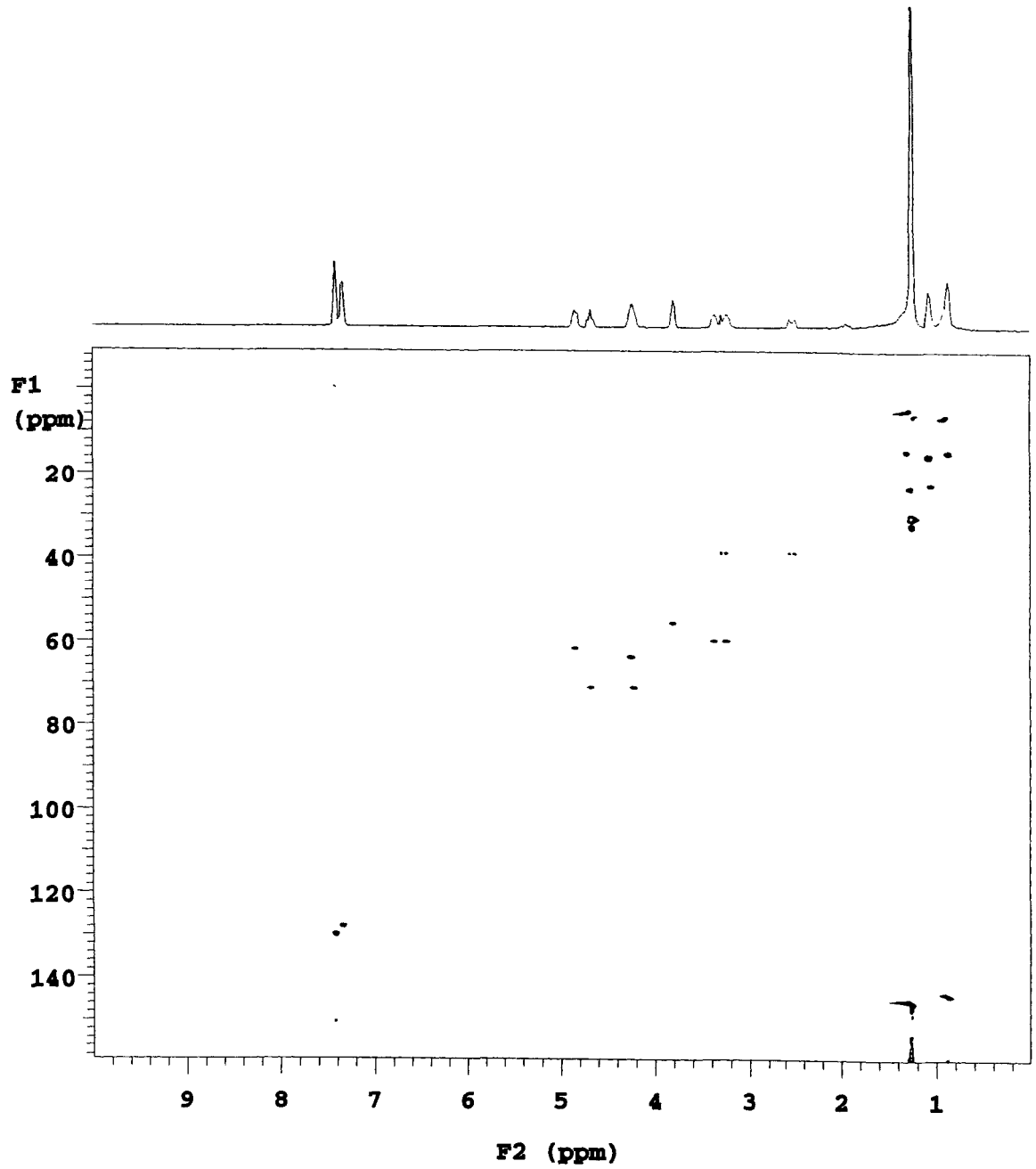

STANDARD 1H OBSERVE

Pulse Sequence: HMQC

Solvent: CDCl3
Ambient temperature
File: KLH_II_331_f19-27_HMQC
INOVA-500 "strmcld"

Relax. delay 1.000 sec
Acq. time 0.147 sec
Width 6982.6 Hz
2D Width 17105.0 Hz
8 repetitions
2 x 128 increments
OBSERVE H1, 400.1063260 MHz
DECOUPLE C13, 100.6143372 MHz
Power 38 dB
on during acquisition
off during delay
GARP-1 modulated
DATA PROCESSING
Gauss apodization 0.068 sec
F1 DATA PROCESSING
Gauss apodization 0.014 sec
FT size 2048 x 2048
Total time 40 min, 59 sec

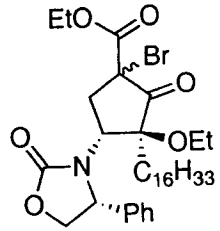

178

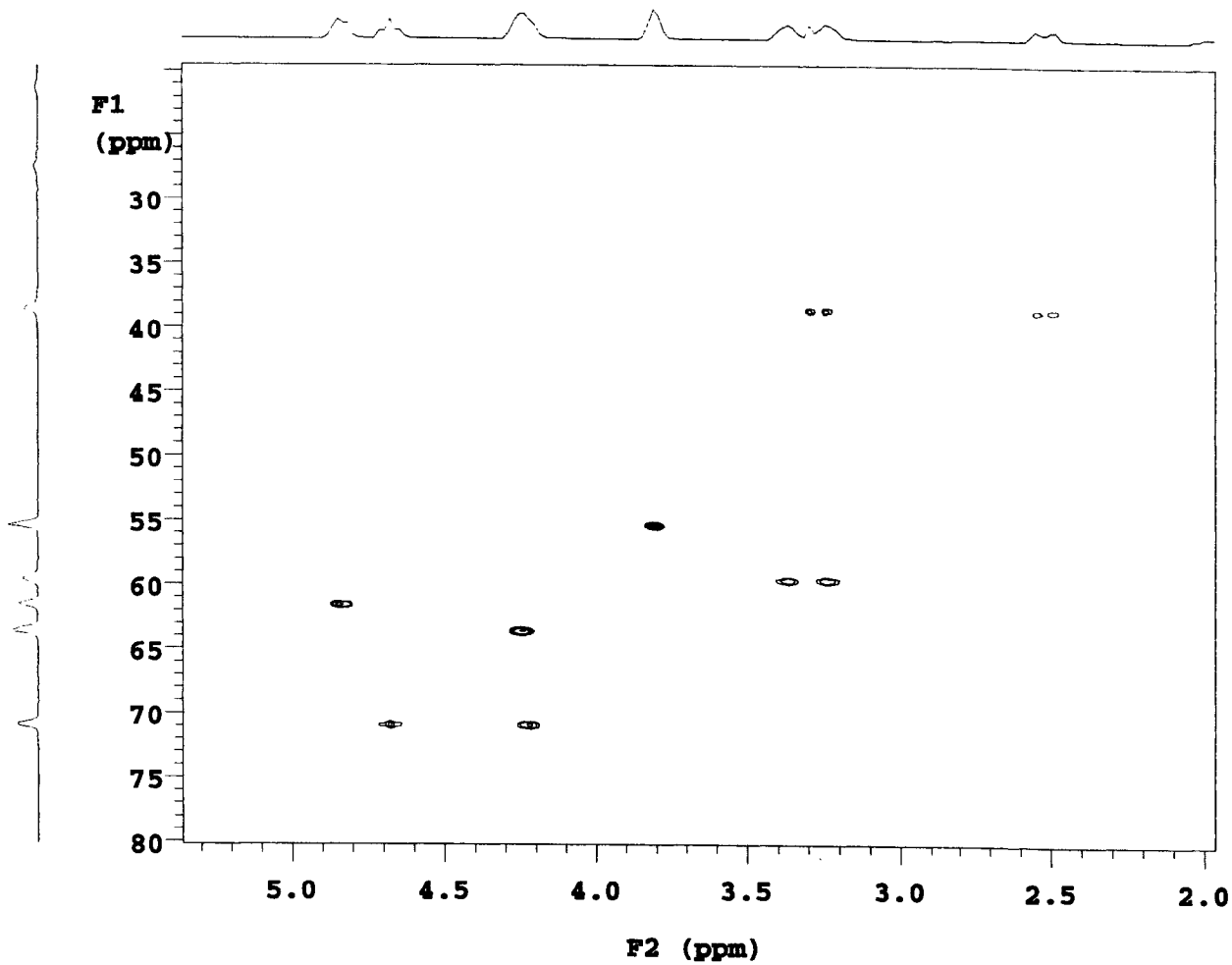

STANDARD 1H OBSERVE

Pulse Sequence: HMQC

Solvent: CDCl3
Ambient temperature
File: KLH_II_331_f19-27_HMQC
INOVA-500 "strmcld"

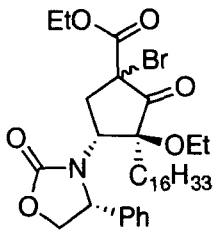

178

Relax. delay 1.000 sec
Acq. time 0.147 sec
Width 6982.6 Hz
2D Width 17105.0 Hz
8 repetitions
2 x 128 increments
OBSERVE H1, 400.1063260 MHz
DECOUPLE C13, 100.6143372 MHz
Power 38 dB
on during acquisition
off during delay
GARP-1 modulated
DATA PROCESSING
Gauss apodization 0.068 sec
F1 DATA PROCESSING
Gauss apodization 0.014 sec
FT size 2048 x 2048
Total time 40 min, 59 sec

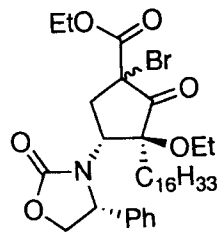

178

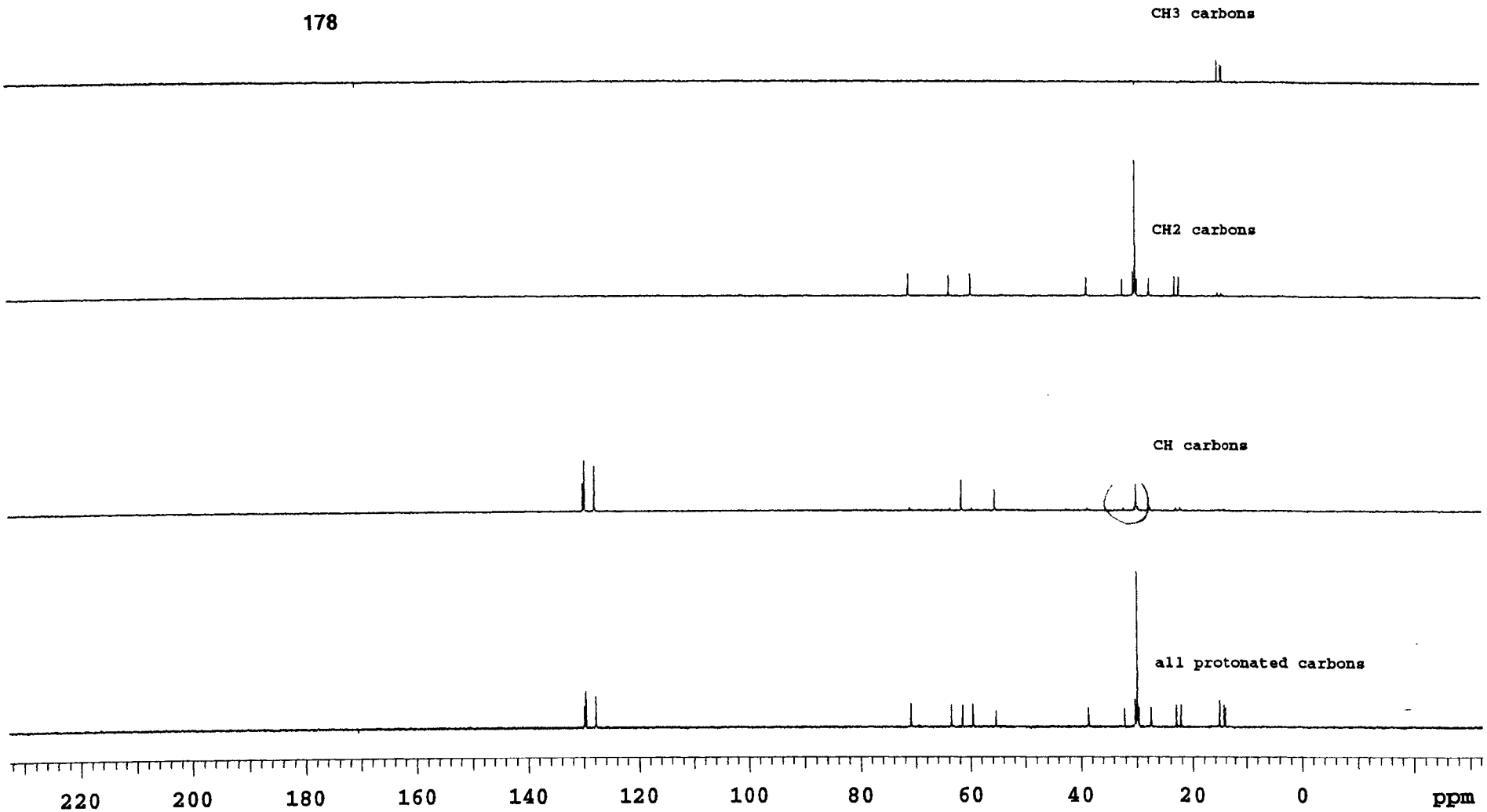

13C OBSERVE

Pulse Sequence: DEPT

Solvent: CDCl3
Ambient temperature
INOVA-300 "elfin"

Relax. delay 1.000 sec
Pulse 90.0 degrees
Acq. time 0.800 sec
Width 20000.0 Hz
64 repetitions
OBSERVE C13, 75.4639391 MHz
DECOUPLE H1, 300.1164227 MHz
Power 32 dB
on during acquisition
off during delay
WALTZ-16 modulated
DATA PROCESSING
Line broadening 1.0 Hz
FT size 32768
Total time 8 min, 15 sec

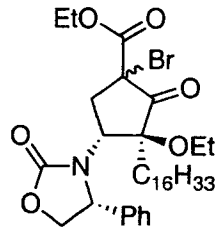

178

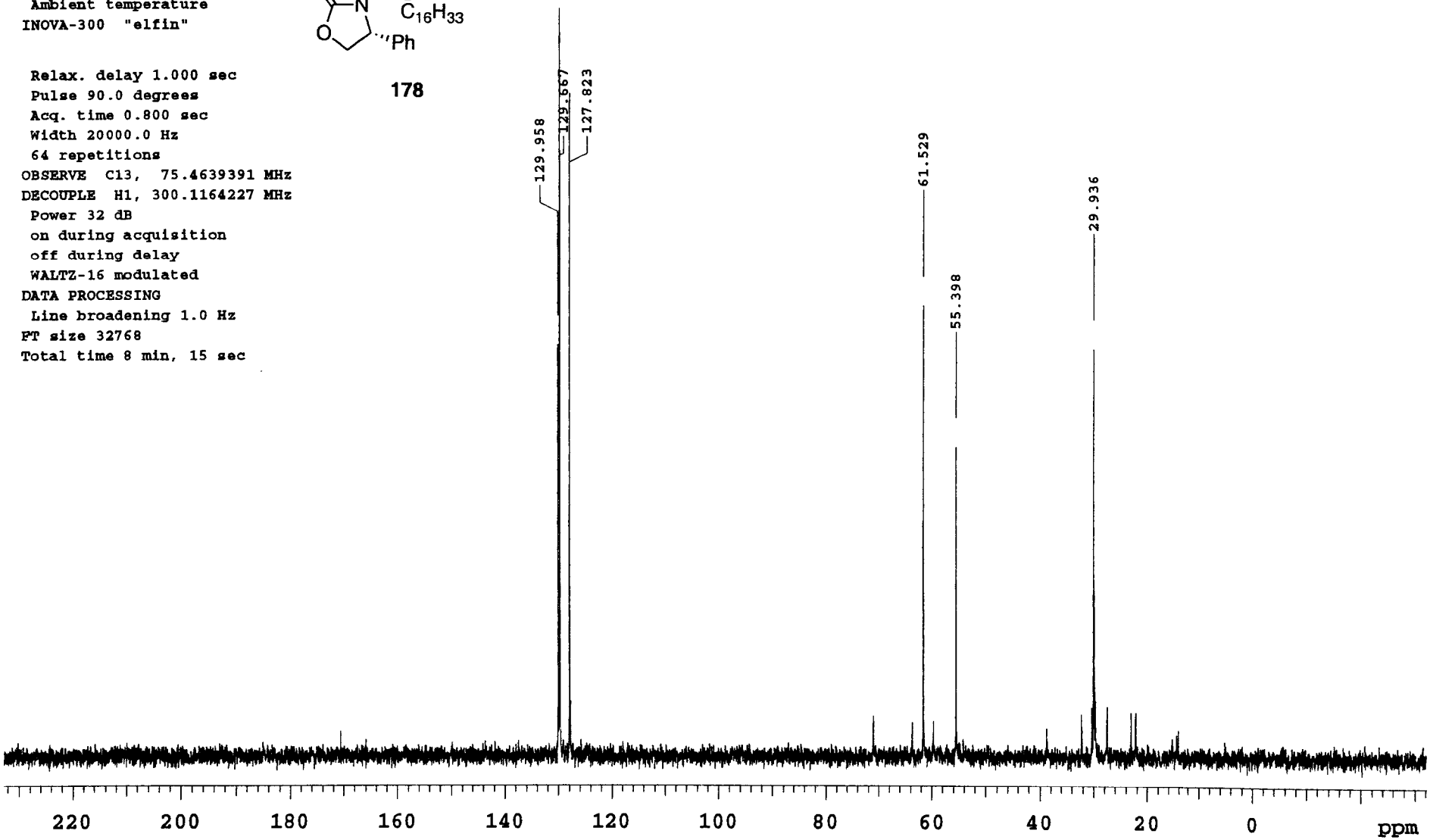

13C OBSERVE

Pulse Sequence: DEPT

Solvent: CDCl3
Ambient temperature
INOVA-300 "elfin"

Relax. delay 1.000 sec
Pulse 90.0 degrees
Acq. time 0.800 sec
Width 20000.0 Hz
64 repetitions
OBSERVE C13, 75.4639391 MHz
DECOUPLE H1, 300.1164227 MHz
Power 32 dB
on during acquisition
off during delay
WALTZ-16 modulated
DATA PROCESSING
Line broadening 1.0 Hz
FT size 32768
Total time 8 min, 15 sec

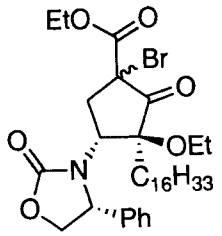

178

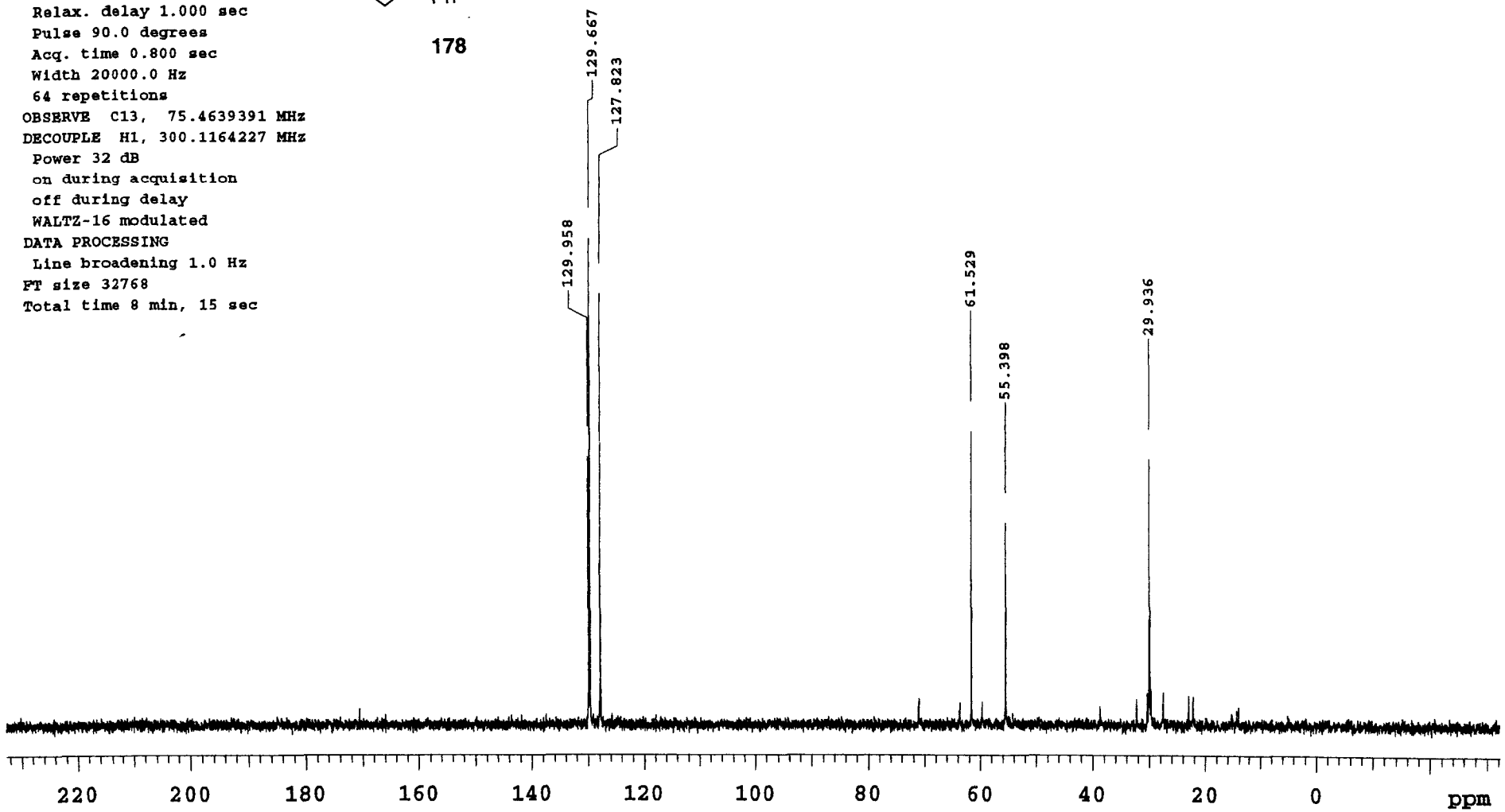

13C OBSERVE

Pulse Sequence: DEPT

Solvent: CDCl3
Ambient temperature
INOVA-300 "elfin"

Relax. delay 1.000 sec
Pulse 90.0 degrees
Acq. time 0.800 sec
Width 20000.0 Hz
64 repetitions
OBSERVE C13, 75.4639391 MHz
DECOUPLE H1, 300.1164227 MHz
Power 32 dB
on during acquisition
off during delay
WALTZ-16 modulated
DATA PROCESSING
Line broadening 1.0 Hz
FT size 32768
Total time 8 min, 15 sec

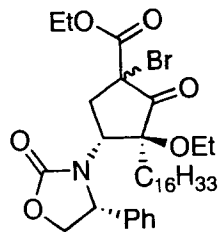

178

13C OBSERVE

Pulse Sequence: DEPT

Solvent: CDCl3
Ambient temperature
INOVA-300 "elfin"

Relax. delay 1.000 sec
Pulse 90.0 degrees
Acq. time 0.800 sec
Width 20000.0 Hz
64 repetitions
OBSERVE C13, 75.4639391 MHz
DECOUPLE H1, 300.1164227 MHz
Power 32 dB
on during acquisition
off during delay
WALTZ-16 modulated
DATA PROCESSING
Line broadening 1.0 Hz
FT size 32768
Total time 8 min, 15 sec

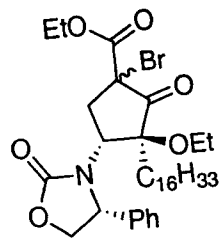

178

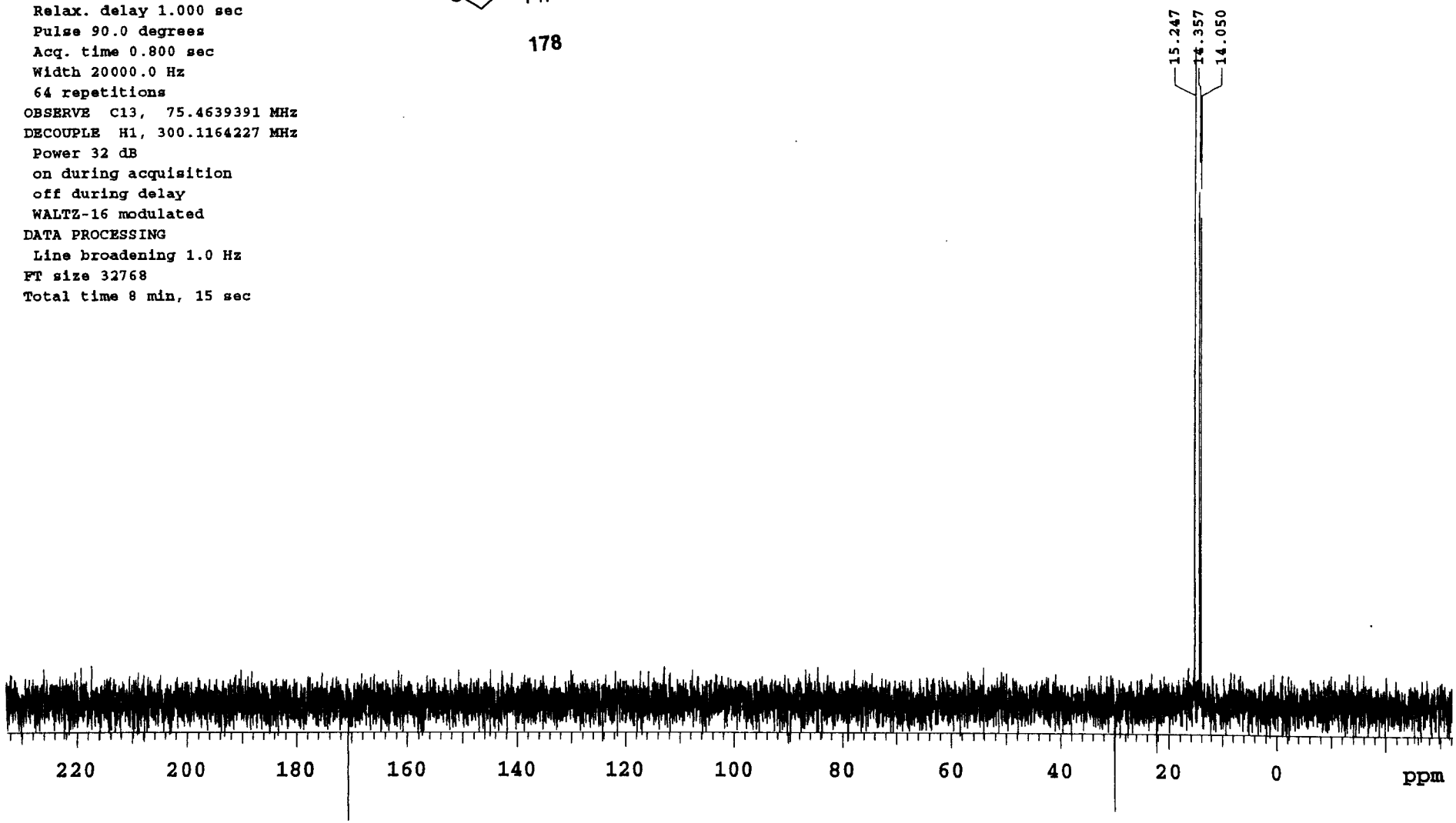

KLH_II_331_f19-27

Pulse Sequence: COSY

Solvent: CDCl3
Ambient temperature
File: KLH_II_331_f19-27_CSOY
INOVA-500 "strmcld"

Relax. delay 1.000 sec
Acq. time 0.147 sec
Width 6982.6 Hz
2D Width 6982.6 Hz
2 repetitions
128 increments
OBSERVE H1, 400.1063260 MHz
DATA PROCESSING
Sq. sine bell 0.073 sec
F1 DATA PROCESSING
Sq. sine bell 0.018 sec
FT size 2048 x 2048
Total time 5 min, 38 sec

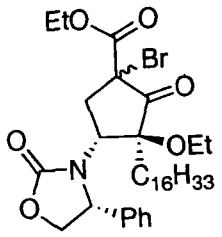

178

KLH_II_331_f19-27

Pulse Sequence: COSY

Solvent: CDCl3
Ambient temperature
File: KLH_II_331_f19-27_CSOY
INOVA-500 "strmcld"

Relax. delay 1.000 sec
Acq. time 0.147 sec
Width 6982.6 Hz
2D Width 6982.6 Hz
2 repetitions
128 increments
OBSERVE H1, 400.1063260 MHz
DATA PROCESSING
Sq. sine bell 0.073 sec
F1 DATA PROCESSING
Sq. sine bell 0.018 sec
FT size 2048 x 2048
Total time 5 min, 38 sec

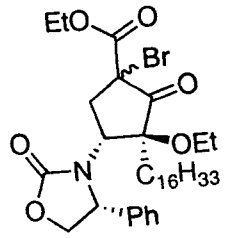

178

KLH_II_331_f19-27

Pulse Sequence: COSY

Solvent: CDCl3
Ambient temperature
File: KLH_II_331_f19-27_CSOY
INOVA-500 "strmcld"

Relax. delay 1.000 sec
Acq. time 0.147 sec
Width 6982.6 Hz
2D Width 6982.6 Hz
2 repetitions
128 increments
OBSERVE H1, 400.1063260 MHz
DATA PROCESSING
Sq. sine bell 0.073 sec
F1 DATA PROCESSING
Sq. sine bell 0.018 sec
FT size 2048 x 2048
Total time 5 min, 38 sec

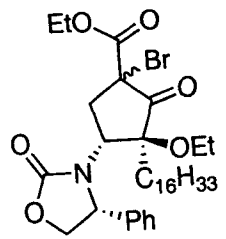

178

KLH_II_331_f19-27

Pulse Sequence: COSY

Solvent: CDCl3
Ambient temperature
File: KLH_II_331_f19-27_CSOY
INOVA-500 "strmcld"

Relax. delay 1.000 sec
Acq. time 0.147 sec
Width 6982.6 Hz
2D Width 6982.6 Hz
2 repetitions
128 increments
OBSERVE H1, 400.1063260 MHz
DATA PROCESSING
Sq. sine bell 0.073 sec
F1 DATA PROCESSING
Sq. sine bell 0.018 sec
FT size 2048 x 2048
Total time 5 min, 38 sec

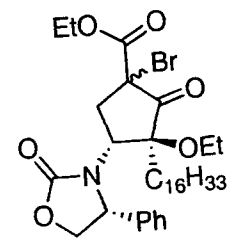

178

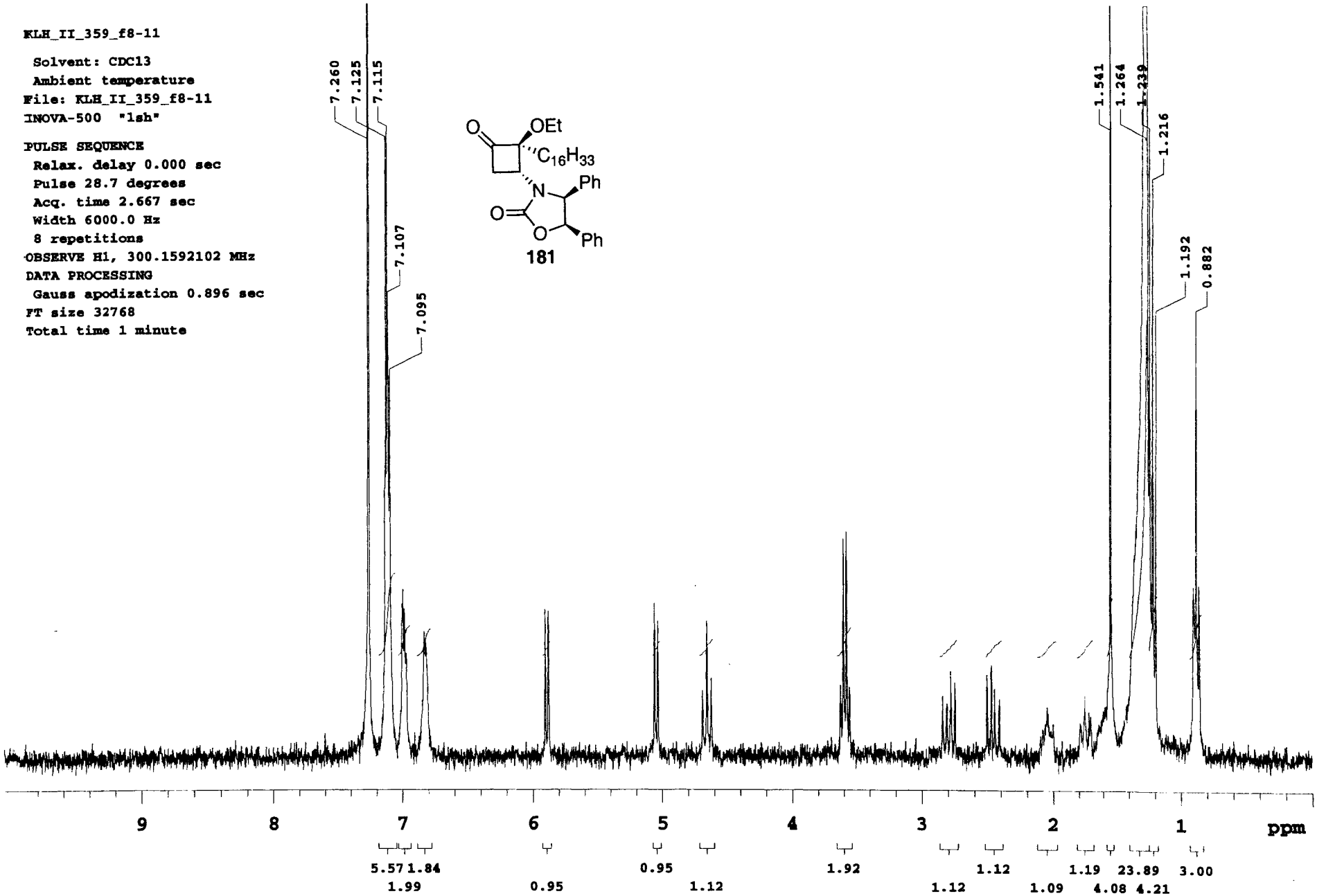

KLH_II_052804_diphenyl cyclobut

Pulse Sequence: s2pul

Solvent: CDCl3
Ambient temperature
INOVA-400 "narnia"

Relax. delay 1.700 sec
Pulse 44.5 degrees
Acq. time 0.533 sec
Width 30018.8 Hz
104 repetitions
OBSERVE C13, 100.6067917 MHz
DECOUPLE H1, 400.1083268 MHz
Power 42 dB
continuously on
WALTZ-16 modulated
DATA PROCESSING
Line broadening 2.0 Hz
FT size 32768
Total time 622730 hr, 10 min, 7 sec

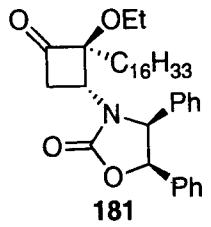

181

KLH_II_419_f18-22

Solvent: CDCl3
Ambient temperature
File: KLH_II_419_f18-22
INOVA-500 "lsh"

PULSE SEQUENCE
Relax. delay 0.000 sec
Pulse 28.7 degrees
Acq. time 2.667 sec
Width 6000.0 Hz
16 repetitions
OBSERVE H1, 300.1592102 MHz
DATA PROCESSING
Gauss apodization 0.896 sec
FT size 32768
Total time 1 minute

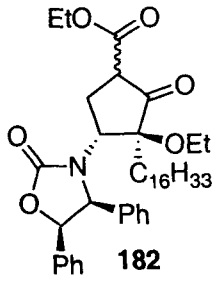

182

KLH_II_370_crude

Solvent: CDCl3
Ambient temperature
File: KLH_II_370_crude
INOVA-500 "lsh"

PULSE SEQUENCE
Relax. delay 0.000 sec
Pulse 28.7 degrees
Acq. time 2.667 sec
Width 6000.0 Hz
16 repetitions
OBSERVE H1, 300.1592102 MHz
DATA PROCESSING
Gauss apodization 0.896 sec
FT size 32768
Total time 1 minute

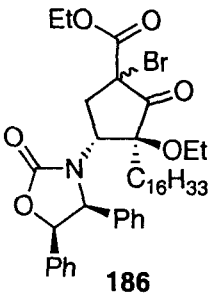

186

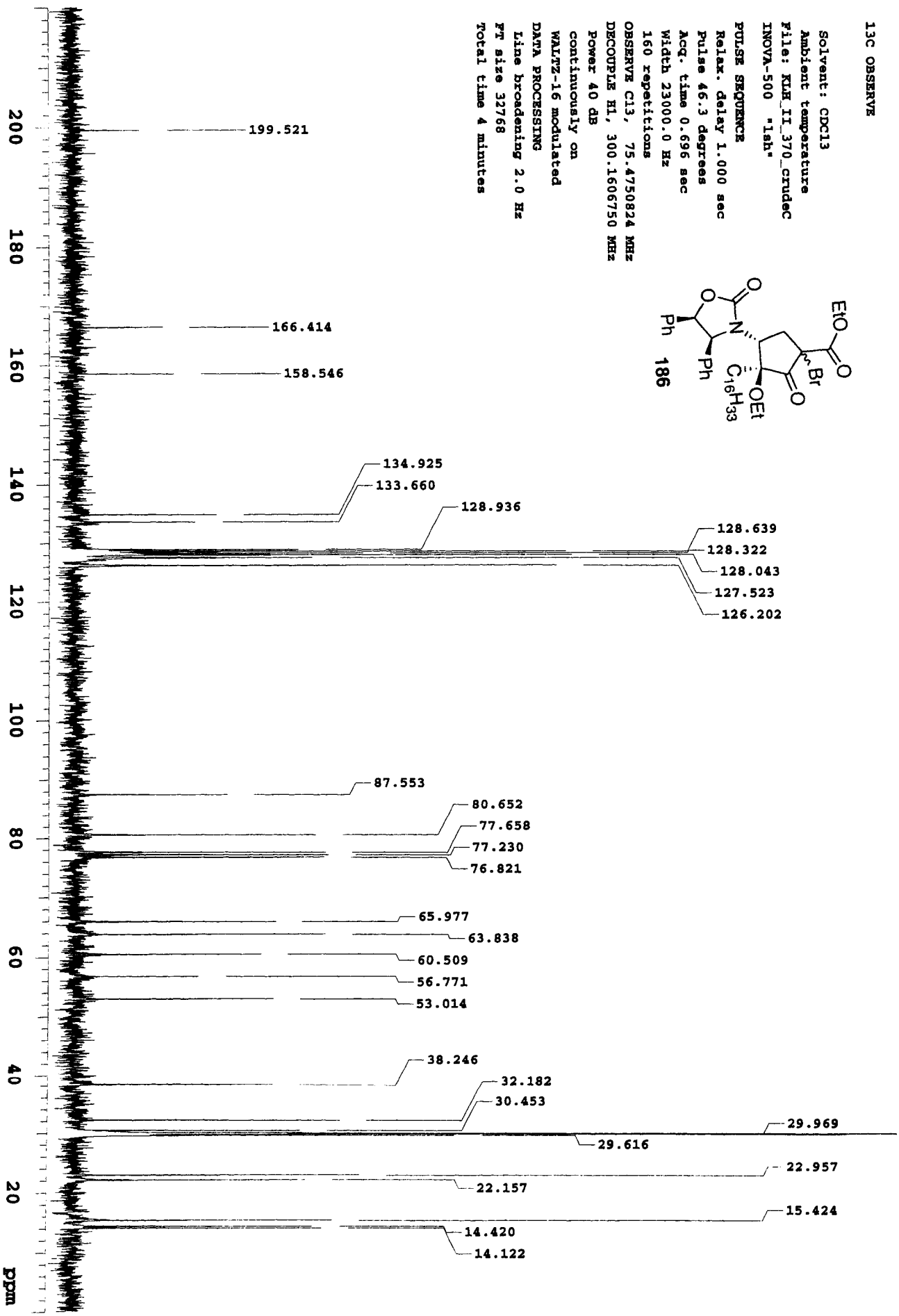

KLH_II_052904_brBKE

Pulse Sequence: HMQC

Solvent: CDCl3
Ambient temperature
File: KLH_II_Br_BKE_HMQC
INOVA-500 "strmcld"

Relax. delay 1.000 sec
Acq. time 0.171 sec
Width 6000.6 Hz
2D Width 12828.7 Hz
12 repetitions
2 x 128 increments
OBSERVE H1, 300.1149220 MHz
DECOUPLE C13, 75.4695989 MHz
Power 35 dB
on during acquisition
off during delay
GARP-1 modulated
DATA PROCESSING
Gauss apodization 0.079 sec
F1 DATA PROCESSING
Gauss apodization 0.018 sec
FT size 2048 x 2048
Total time 1 hr, 2 min, 27 sec

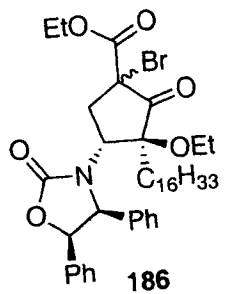

186

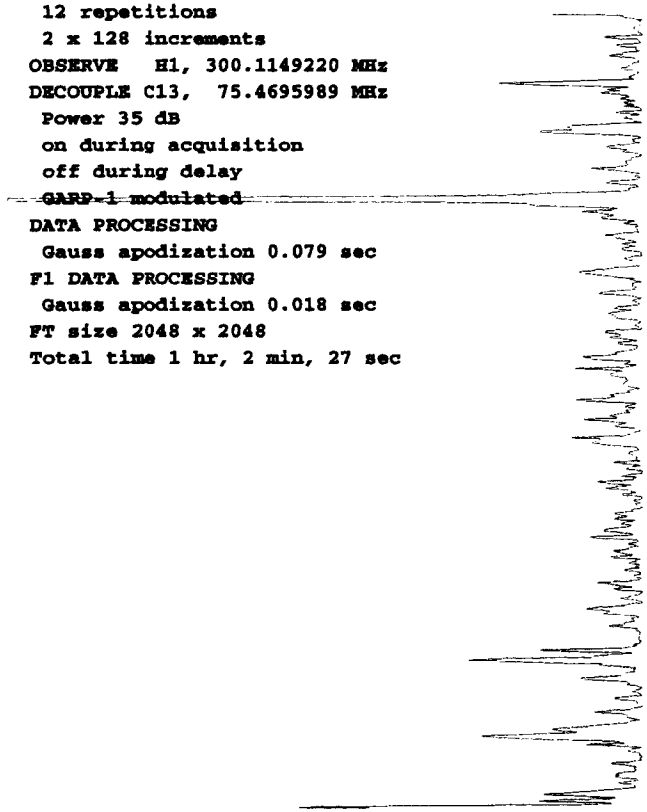

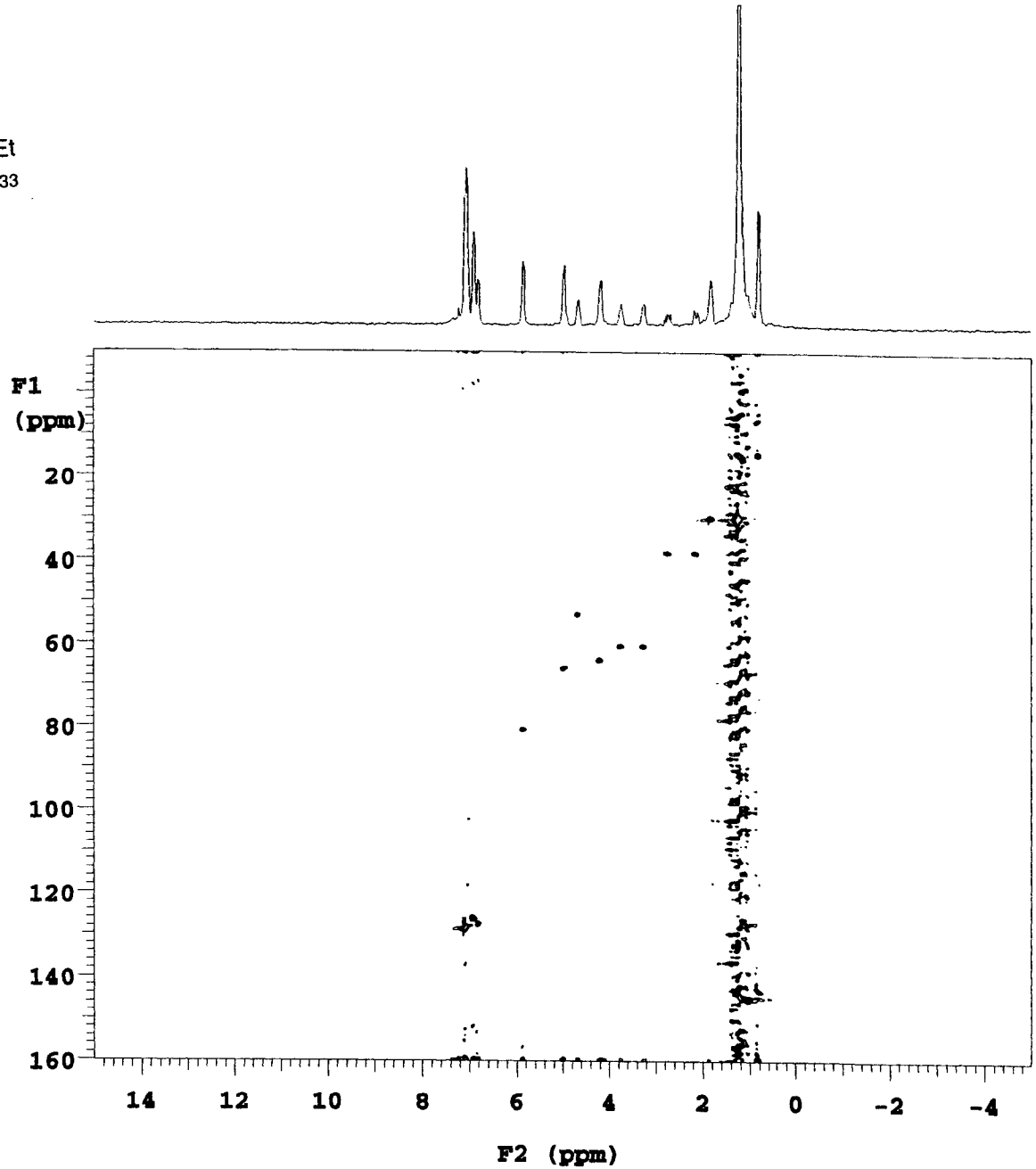

KLH_II_052904_brBKE

Pulse Sequence: HMQC

Solvent: CDCl3
Ambient temperature
File: KLH_II_Br_BKE_HMQC
INOVA-500 "strmcld"

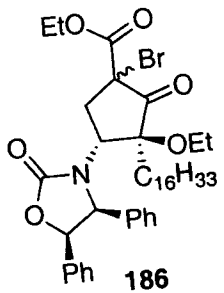

186

Relax. delay 1.000 sec
Acq. time 0.171 sec
Width 6000.6 Hz
2D Width 12828.7 Hz
12 repetitions
2 x 128 increments
OBSERVE H1, 300.1149220 MHz
DECOUPLE C13, 75.4695989 MHz
Power 35 dB
on during acquisition
off during delay
GARP-1 modulated
DATA PROCESSING
Gauss apodization 0.079 sec
F1 DATA PROCESSING
Gauss apodization 0.018 sec
FT size 2048 x 2048
Total time 1 hr, 2 min, 27 sec

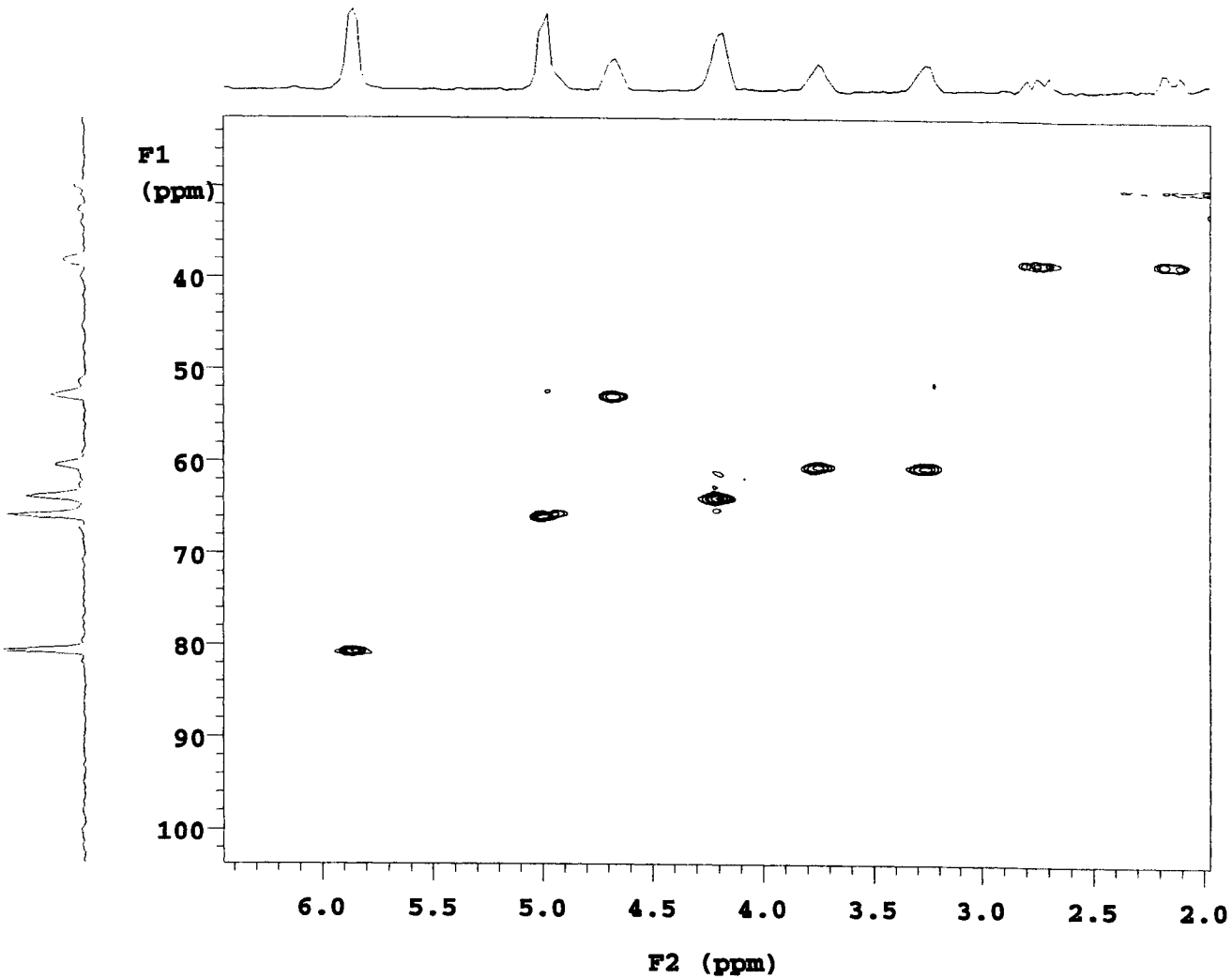

KLH_II_052904_brBKE

Pulse Sequence: HMQC

Solvent: CDCl3
Ambient temperature
File: KLH_II_Br_BKE_HMQC
INOVA-500 "strmcld"

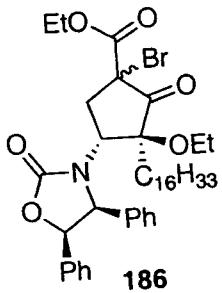

186

Relax. delay 1.000 sec
Acq. time 0.171 sec
Width 6000.6 Hz
2D Width 12828.7 Hz
12 repetitions
2 x 128 increments
OBSERVE H1, 300.1149220 MHz
DECOUPLE C13, 75.4695989 MHz
Power 35 dB
on during acquisition
off during delay
GARP-1 modulated
DATA PROCESSING
Gauss apodization 0.079 sec
F1 DATA PROCESSING
Gauss apodization 0.018 sec
FT size 2048 x 2048
Total time 1 hr, 2 min, 27 sec

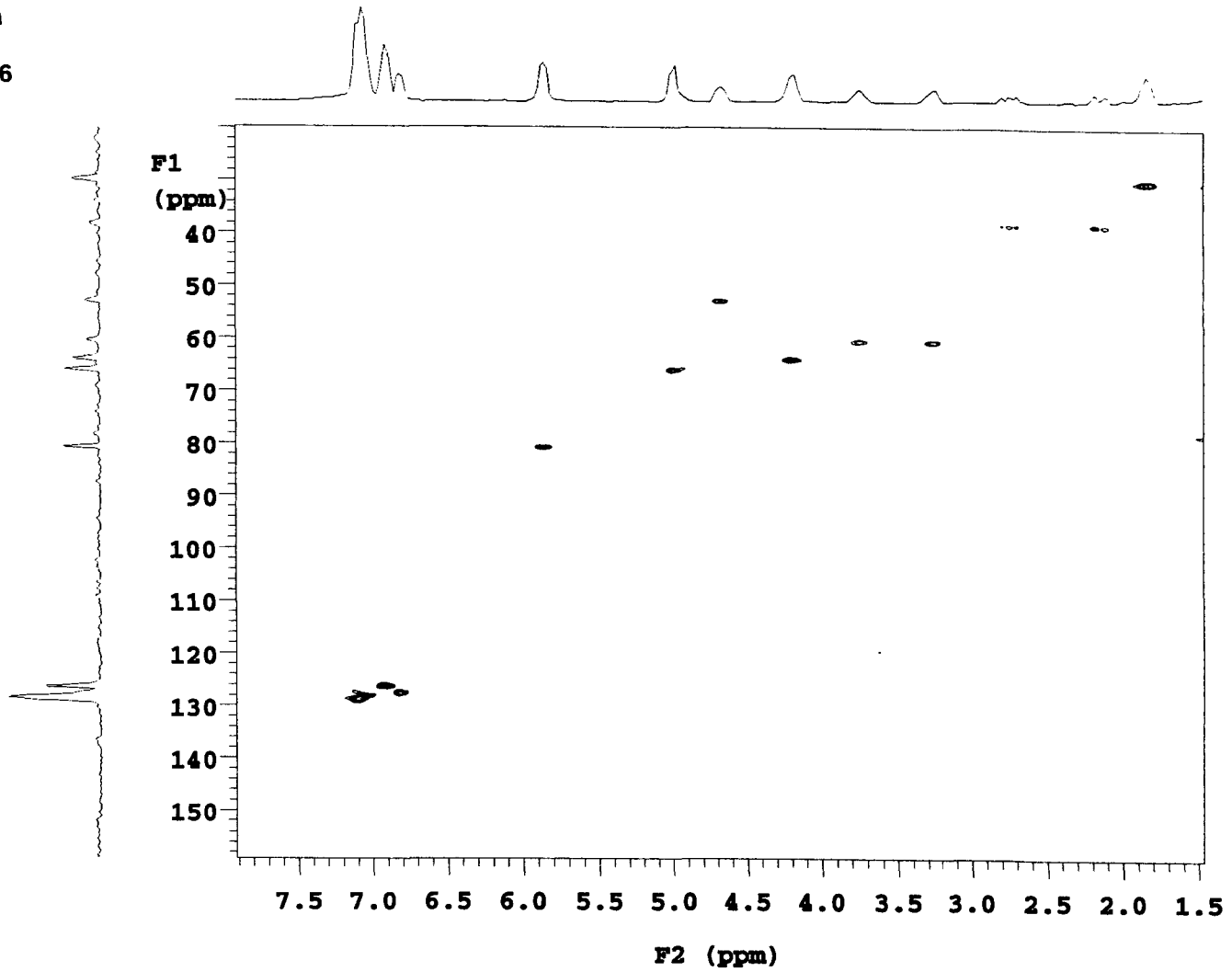

KLH_II_BromoAmineII

Solvent: CDCl3
Ambient temperature
File: KLH_II_BromoAmineII
INOVA-500 "lsh"

PULSE SEQUENCE
Pulse 30.8 degrees
Acq. time 2.291 sec
Width 6982.6 Hz
16 repetitions
OBSERVE H1, 400.1063232 MHz
DATA PROCESSING
Gauss apodization 0.971 sec
FT size 65536
Total time 1 minute

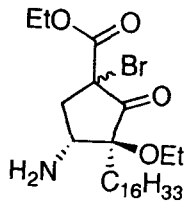

187

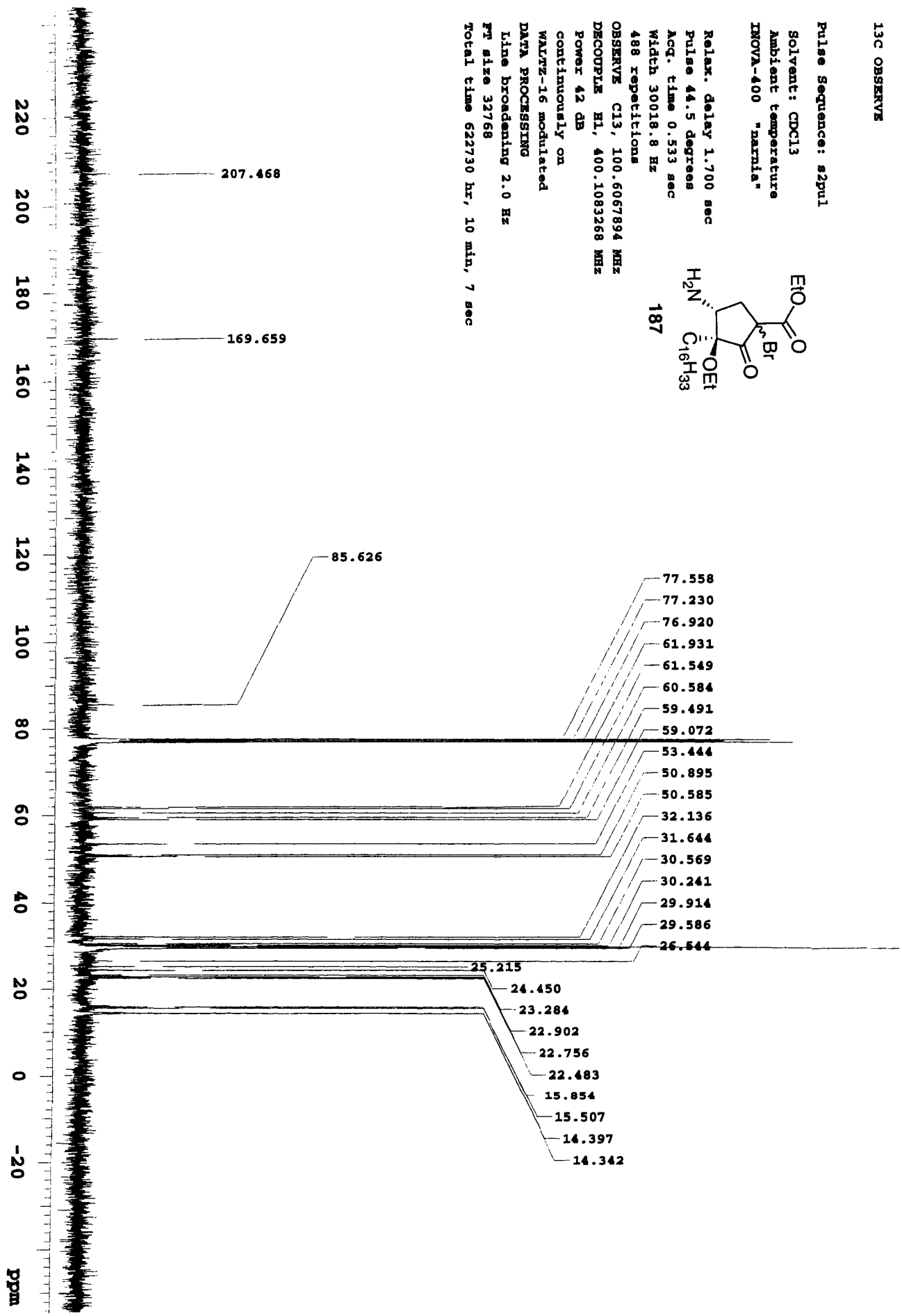

KLH_II_BromoAmineII

Pulse Sequence: COSY

Solvent: CDCl3
Ambient temperature
File: KLH_II_BromoAmineII_COSY
INOVA-500 "strmcld"

Relax. delay 1.000 sec
Acq. time 0.147 sec
Width 6982.6 Hz
2D Width 6982.6 Hz
2 repetitions
128 increments
OBSERVE H1, 400.1063260 MHz
DATA PROCESSING
Sq. sine bell 0.073 sec
F1 DATA PROCESSING
Sq. sine bell 0.018 sec
FT size 2048 x 2048
Total time 5 min, 38 sec

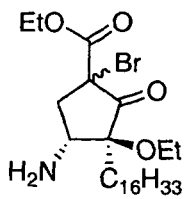

187

KLH_II_BromoAmineII

Pulse Sequence: COSY

Solvent: CDCl3
Ambient temperature
File: KLH_II_BromoAmineII_COSY
INOVA-500 "strmcld"

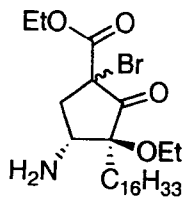

187

Relax. delay 1.000 sec
Acq. time 0.147 sec
Width 6982.6 Hz
2D Width 6982.6 Hz
2 repetitions
128 increments
OBSERVE H1, 400.1063260 MHz
DATA PROCESSING
Sq. sine bell 0.073 sec
F1 DATA PROCESSING
Sq. sine bell 0.018 sec
FT size 2048 x 2048
Total time 5 min, 38 sec

KLH_II_428_crude

Solvent: CDCl3
Ambient temperature
File: KLH_II_428_crude
INOVA-500 "lsh"

PULSE SEQUENCE
Relax. delay 0.000 sec
Pulse 28.7 degrees
Acq. time 2.667 sec
Width 6000.0 Hz
16 repetitions
OBSERVE H1, 300.1592102 MHz
DATA PROCESSING
Gauss apodization 0.896 sec
FT size 32768
Total time 1 minute

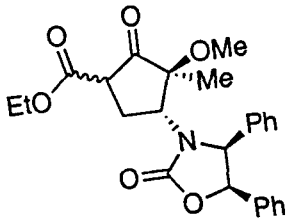

189

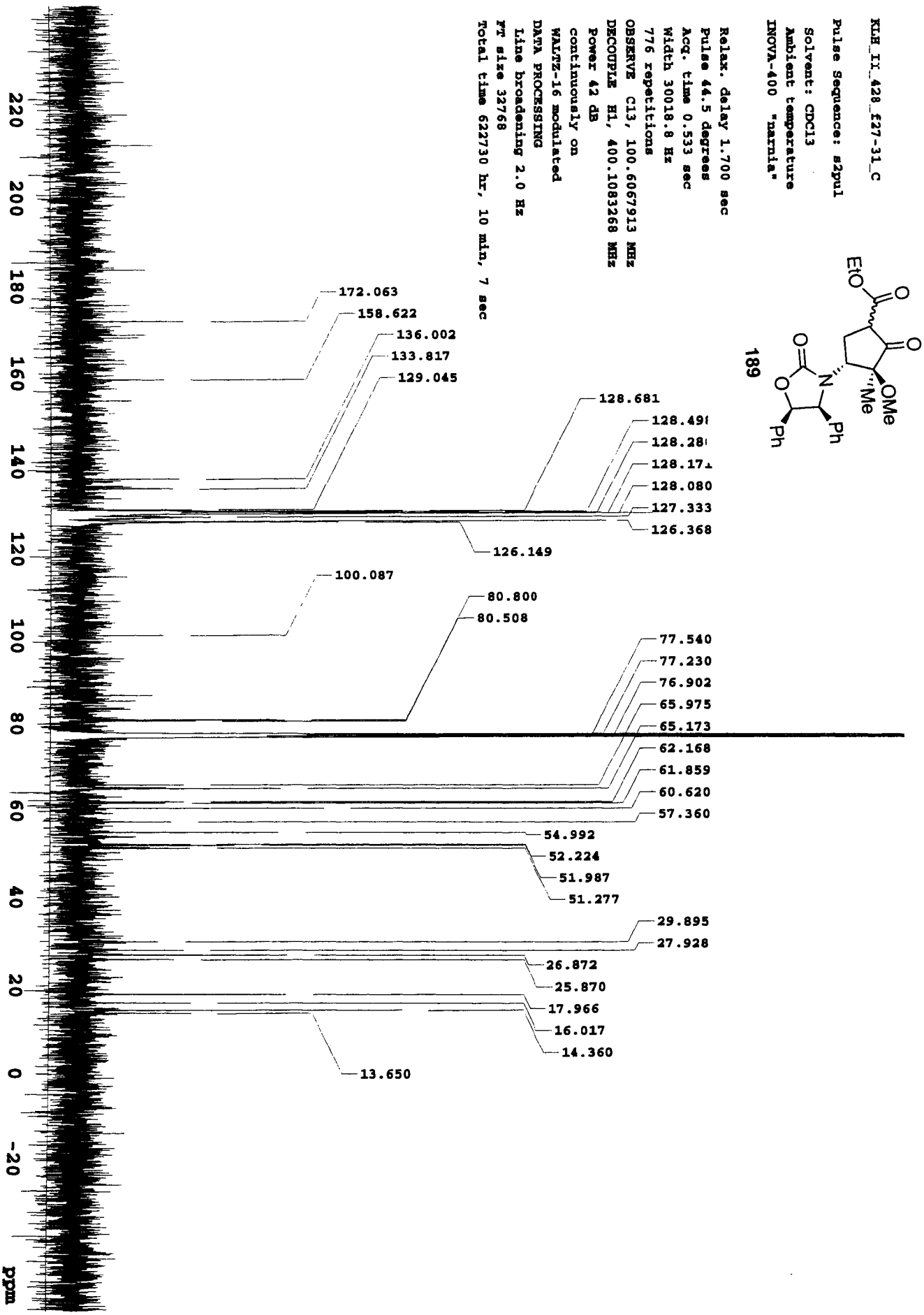

KLH_II_428_f27-31

Pulse Sequence: HMQC

Solvent: CDCl3
Ambient temperature
INOVA-400 "narnia"

Relax. delay 1.000 sec
Acq. time 0.147 sec
Width 6982.6 Hz
2D Width 17105.0 Hz
8 repetitions
2 x 128 increments
OBSERVE H1, 400.1063260 MHz
DECOUPLE C13, 100.6143372 MHz
Power 38 dB
on during acquisition
off during delay
GARP-1 modulated
DATA PROCESSING
Gauss apodization 0.068 sec
F1 DATA PROCESSING
Gauss apodization 0.014 sec
FT size 2048 x 2048
Total time 40 min, 59 sec

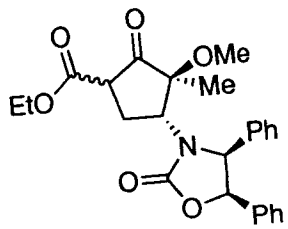

189

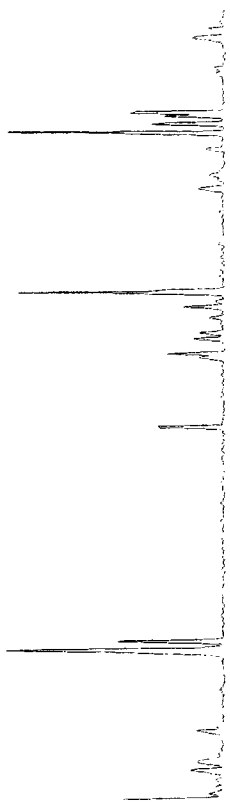

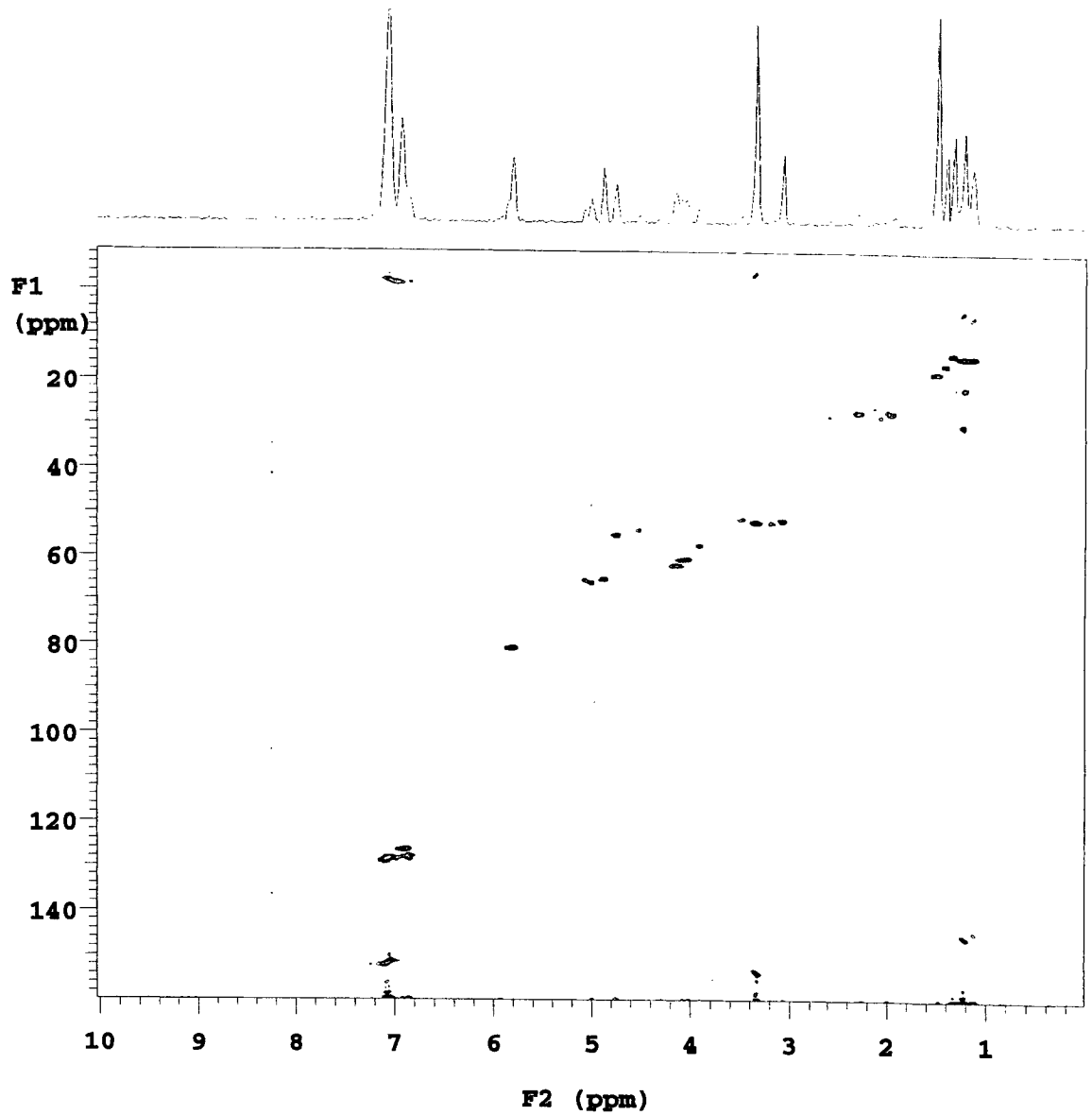

KLH_II_428_f27-31

Pulse Sequence: HMQC

Solvent: CDCl3
Ambient temperature
INOVA-400 "narnia"

Relax. delay 1.000 sec
Acq. time 0.147 sec
Width 6982.6 Hz
2D Width 17105.0 Hz
8 repetitions
2 x 128 increments
OBSERVE H1, 400.1063260 MHz
DECOUPLE C13, 100.6143372 MHz
Power 38 dB
on during acquisition
off during delay
GARP-1 modulated
DATA PROCESSING
Gauss apodization 0.068 sec
F1 DATA PROCESSING
Gauss apodization 0.014 sec
FT size 2048 x 2048
Total time 40 min, 59 sec

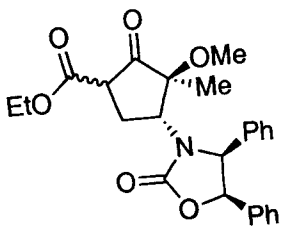

189

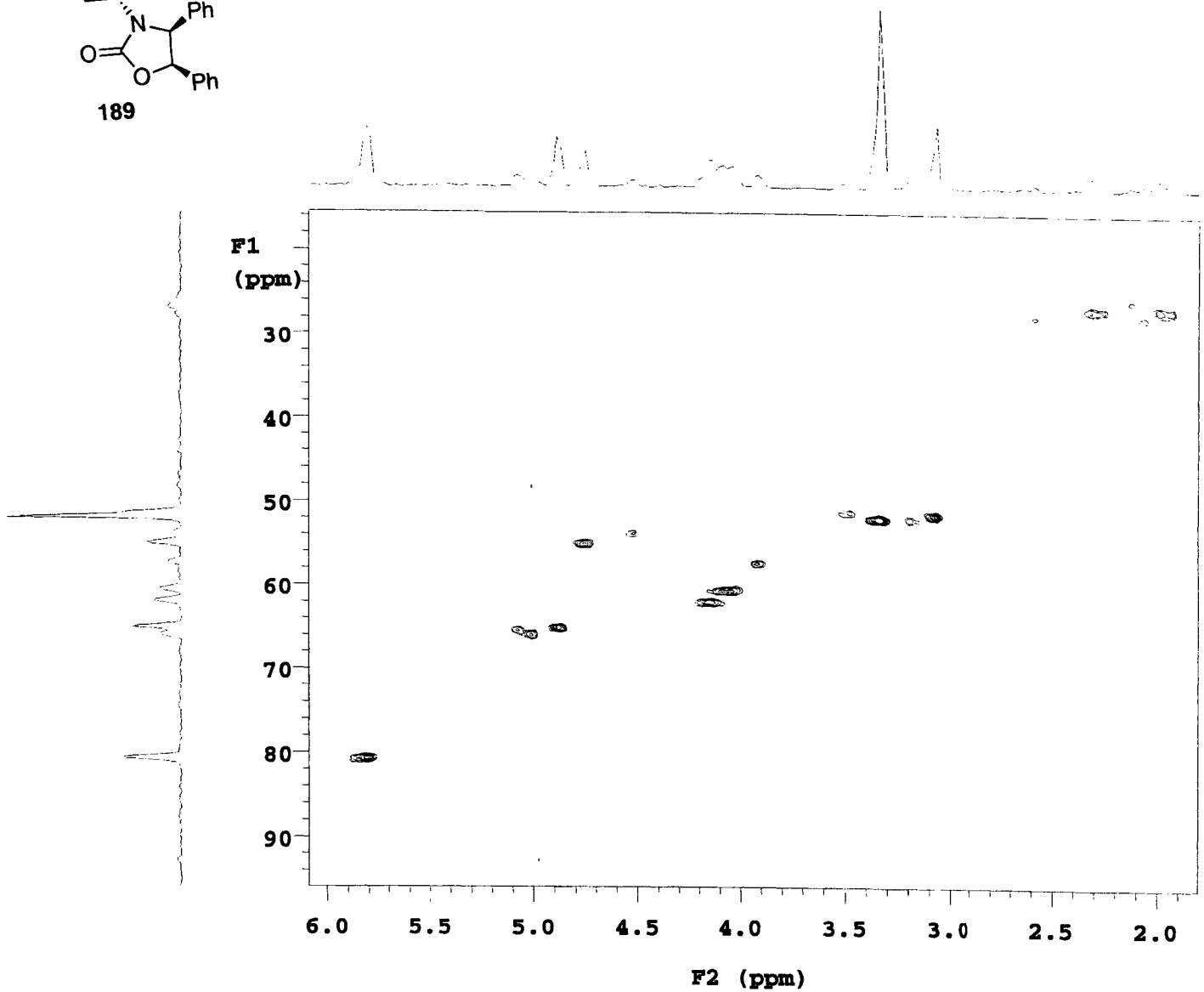

KLH_II_428_f27-31

Pulse Sequence: HMQC

Solvent: CDCl3
Ambient temperature
INOVA-400 "narnia"

Relax. delay 1.000 sec
Acq. time 0.147 sec
Width 6982.6 Hz
2D Width 17105.0 Hz
8 repetitions
2 x 128 increments
OBSERVE H1, 400.1063260 MHz
DECOUPLE C13, 100.6143372 MHz
Power 38 dB
on during acquisition
off during delay
GARP-1 modulated
DATA PROCESSING
Gauss apodization 0.068 sec
F1 DATA PROCESSING
Gauss apodization 0.014 sec
FT size 2048 x 2048
Total time 40 min, 59 sec

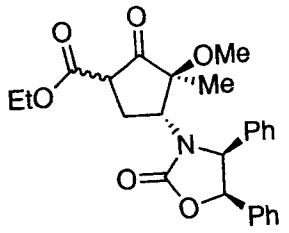

189

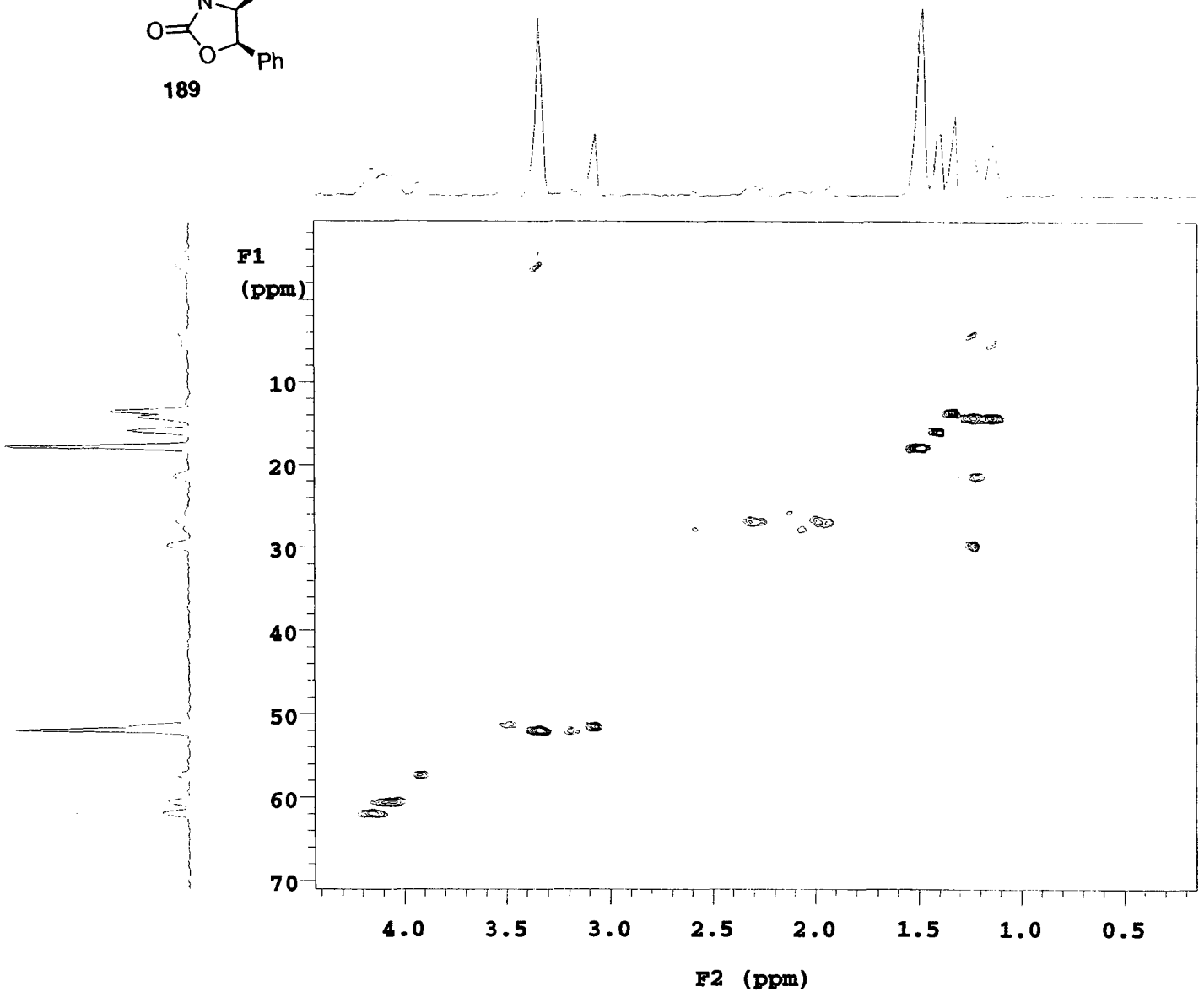

KLH_II_431_crude_i400

Pulse Sequence: s2pul

Solvent: CDCl3
Ambient temperature
File: KLH_II_431_crude_i400
INOVA-400 "narnia"

Pulse 30.8 degrees
Acq. time 2.291 sec
Width 6982.6 Hz
16 repetitions
OBSERVE H1, 400.1063117 MHz
DATA PROCESSING
Gauss apodization 0.971 sec
FT size 65536
Total time 0 min, 41 sec

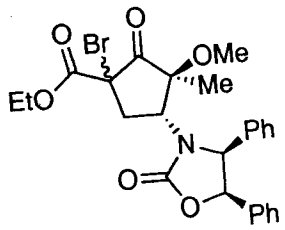

190

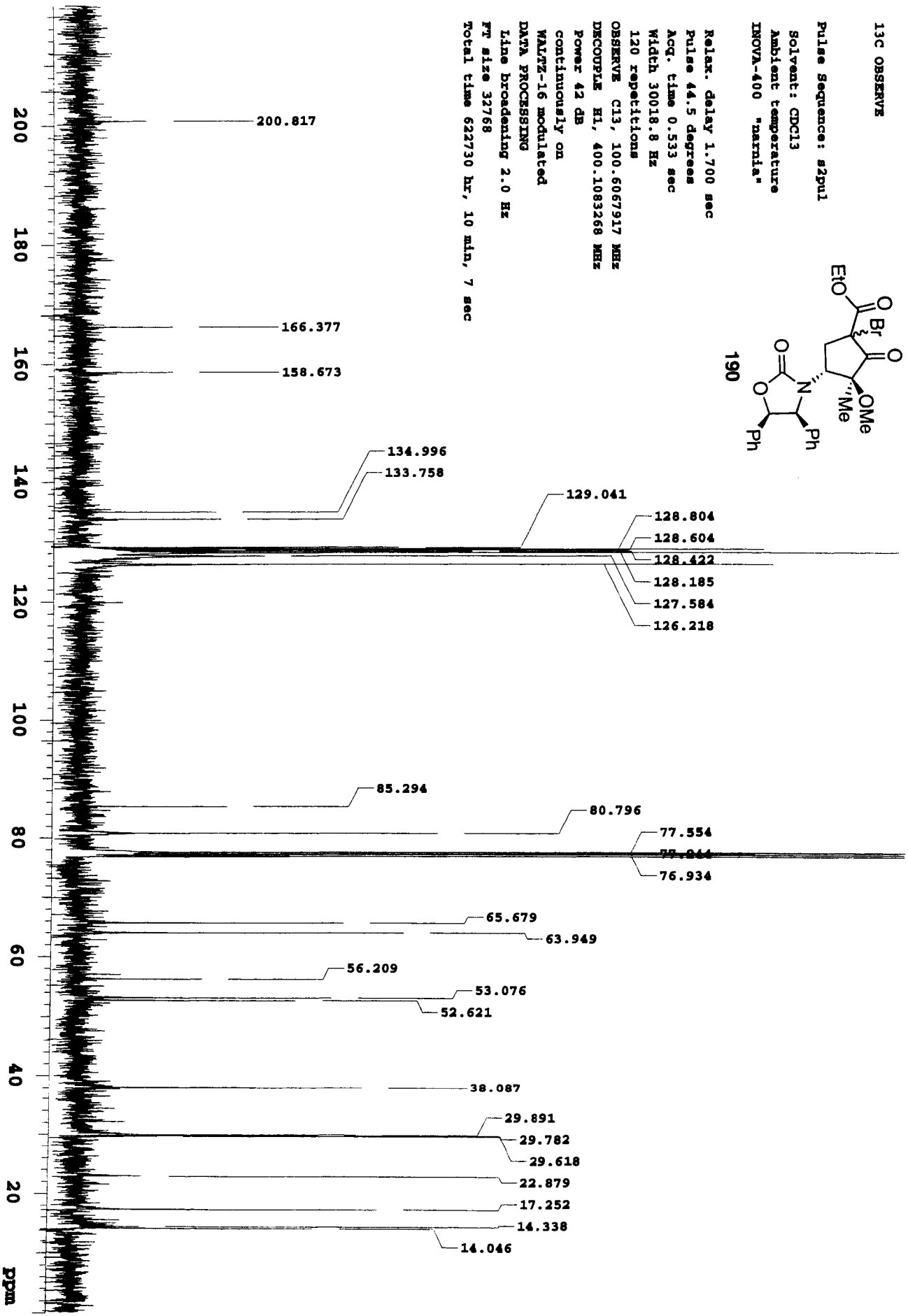

KLH_II_431_crude_i400

Pulse Sequence: HMQC

Solvent: CDCl3
Ambient temperature
File: KLH_II_431_crude_HMQC
INOVA-400 "narnia"

Relax. delay 1.000 sec
Acq. time 0.147 sec
Width 6982.6 Hz
2D Width 17105.0 Hz
8 repetitions
2 x 128 increments
OBSERVE H1, 400.1063260 MHz
DECOUPLE C13, 100.6143372 MHz
Power 38 dB
on during acquisition
off during delay
GARP-1 modulated
DATA PROCESSING
Gauss apodization 0.068 sec
F1 DATA PROCESSING
Gauss apodization 0.014 sec
FT size 2048 x 2048
Total time 40 min, 59 sec

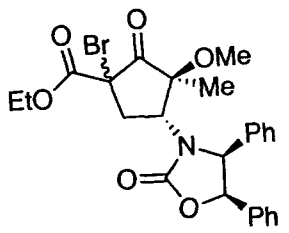

190

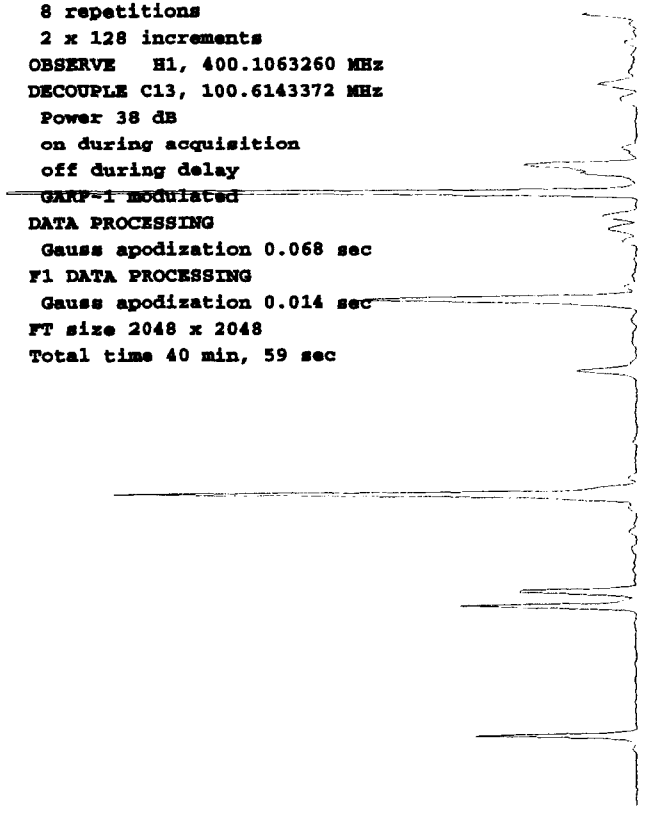

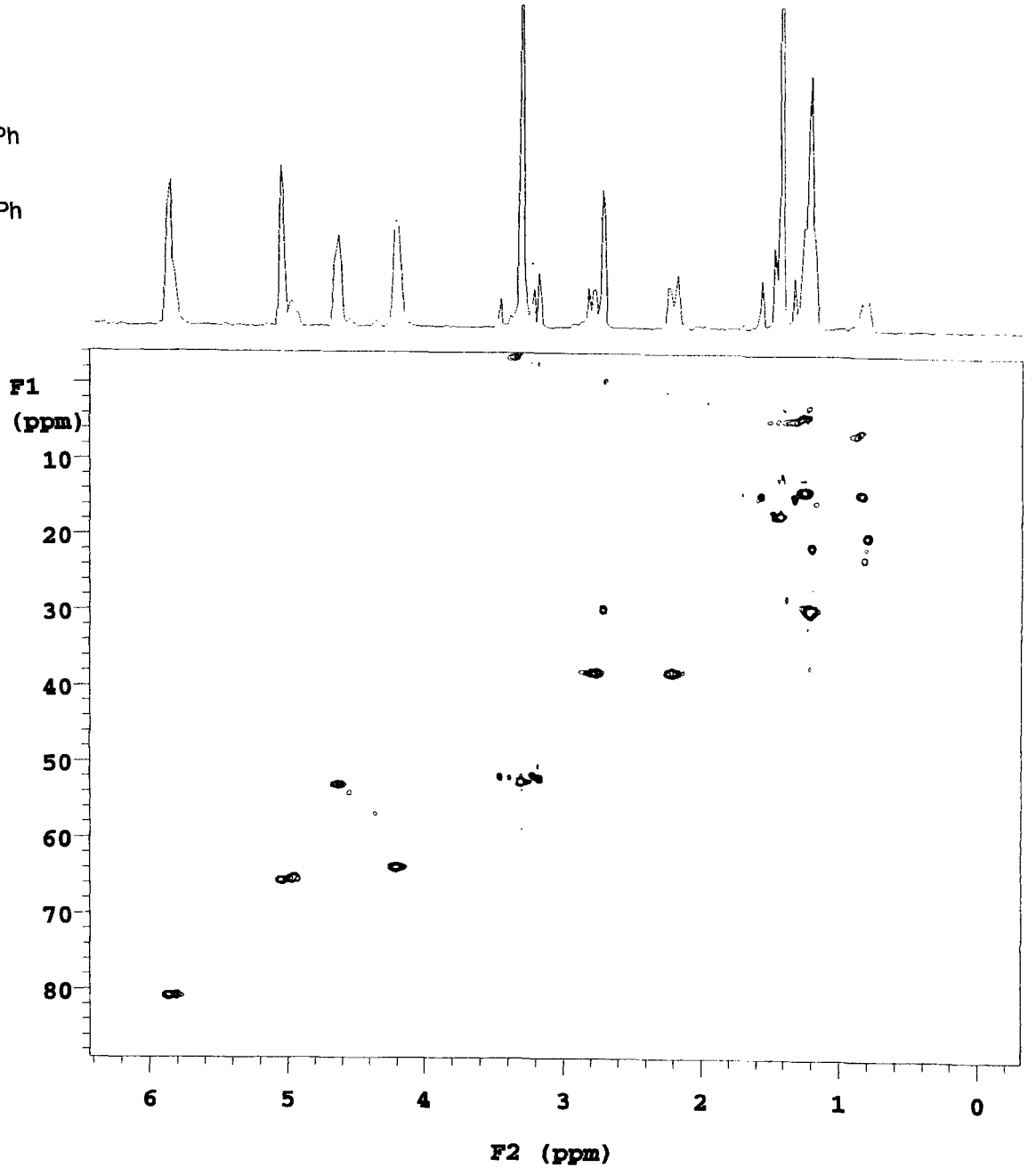

KLH_II_431_crude_i400

Pulse Sequence: HMQC

Solvent: CDCl3
Ambient temperature
File: KLH_II_431_crude_HMQC
INOVA-500 "strmcld"

Relax. delay 1.000 sec
Acq. time 0.147 sec
Width 6982.6 Hz
2D Width 17105.0 Hz
8 repetitions
2 x 128 increments
OBSERVE H1, 400.1063260 MHz
DECOUPLE C13, 100.6143372 MHz
Power 38 dB
on during acquisition
off during delay
GARP-1 modulated
DATA PROCESSING
Gauss apodization 0.068 sec
F1 DATA PROCESSING
Gauss apodization 0.014 sec
FT size 2048 x 2048
Total time 40 min, 59 sec

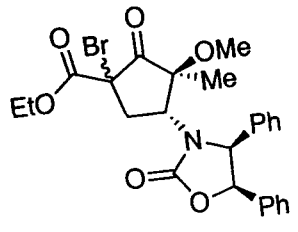

190

KLH_II_431_crude_i400

Pulse Sequence: HMQC

Solvent: CDCl3
Ambient temperature
File: KLH_II_431_crude_HMQC
INOVA-500 "strmcld"

Relax. delay 1.000 sec
Acq. time 0.147 sec
Width 6982.6 Hz
2D Width 17105.0 Hz
8 repetitions
2 x 128 increments
OBSERVE H1, 400.1063260 MHz
DECOUPLE C13, 100.6143372 MHz
Power 38 dB
on during acquisition
off during delay
GARP-1 modulated
DATA PROCESSING
Gauss apodization 0.068 sec
F1 DATA PROCESSING
Gauss apodization 0.014 sec
FT size 2048 x 2048
Total time 40 min, 59 sec

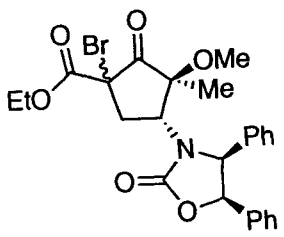

190

LKH_II_Peters_Bromo

Solvent: CDCl3
Ambient temperature
File: KLH_II_Peters_Bromo
INOVA-500 "1sh"

PULSE SEQUENCE
Pulse 30.8 degrees
Acq. time 2.291 sec
Width 6982.6 Hz
16 repetitions
OBSERVE H1, 400.1062622 MHz
DATA PROCESSING
Gauss apodization 0.971 sec
FT size 65536
Total time 1 minute

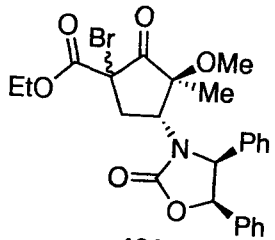

191

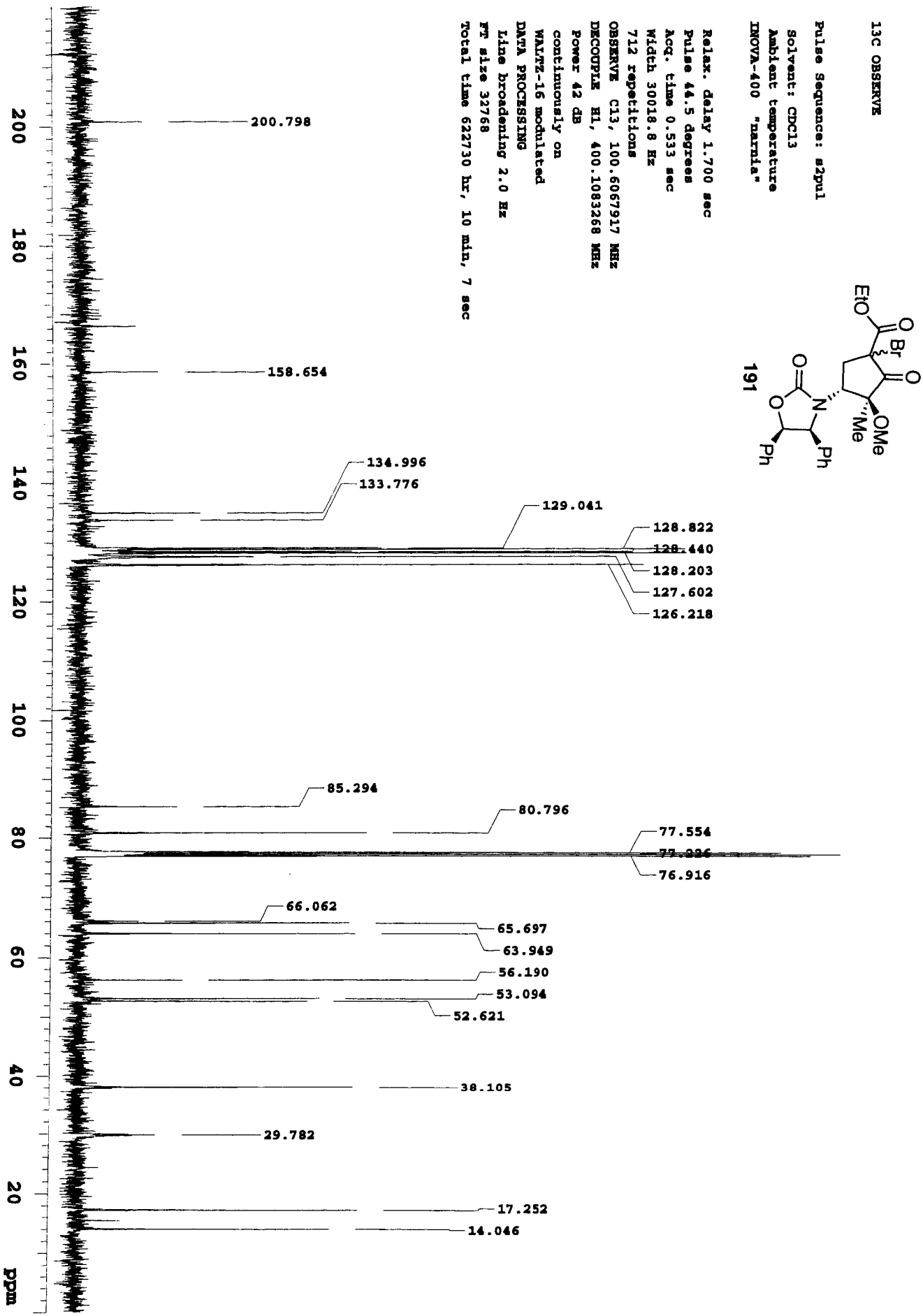

LKH_II_Peters_Bromo

Pulse Sequence: HMQC

Solvent: CDCl3
Ambient temperature
File: KLH_Peters_Bromo_HMQC
INOVA-500 "strmcld"

Relax. delay 1.000 sec
Acq. time 0.147 sec
Width 6982.6 Hz
2D Width 17105.0 Hz
8 repetitions
2 x 128 increments
OBSERVE H1, 400.1062665 MHz
DECOUPLE C13, 100.6143372 MHz
Power 38 dB
on during acquisition
off during delay
GARP-1 modulated
DATA PROCESSING
Gauss apodization 0.068 sec
F1 DATA PROCESSING
Gauss apodization 0.014 sec
FT size 2048 x 2048
Total time 40 min, 59 sec

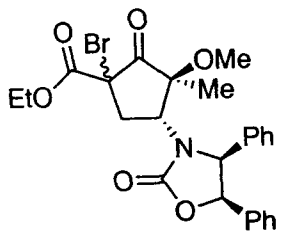

191

LKH_II_Peters_Bromo

Pulse Sequence: HMQC

Solvent: CDCl3
Ambient temperature
File: KLH_Peters_Bromo_HMQC
INOVA-500 "strmcld"

Relax. delay 1.000 sec
Acq. time 0.147 sec
Width 6982.6 Hz
2D Width 17105.0 Hz
8 repetitions
2 x 128 increments
OBSERVE H1, 400.1062665 MHz
DECOUPLE C13, 100.6143372 MHz
Power 38 dB
on during acquisition
off during delay
GARP-1 modulated
DATA PROCESSING
Gauss apodization 0.068 sec
F1 DATA PROCESSING
Gauss apodization 0.014 sec
FT size 2048 x 2048
Total time 40 min, 59 sec

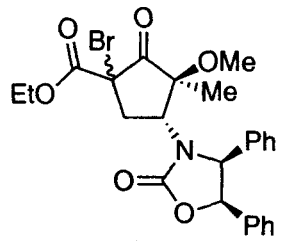

191